

Catalyst design for the transformation of CO₂ into value-added products.

THÈSE N° 8523(2018)

PRÉSENTÉE LE 15 JUIN 2018

À LA FACULTÉ DES SCIENCES DE BASE

LABORATOIRE DE CHIMIE ORGANOMÉTALLIQUE ET MÉDICINALE

PROGRAMME DOCTORAL EN CHIMIE ET GÉNIE CHIMIQUE

ÉCOLE POLYTECHNIQUE FÉDÉRALE DE LAUSANNE

POUR L'OBTENTION DU GRADE DE DOCTEUR ÈS SCIENCES

PAR

Felix Daniel BOBBINK

acceptée sur proposition du jury:

Prof. A. Züttel, président du jury
Prof. P. J. Dyson, directeur de thèse
Prof. J. Wilton-Ely, rapporteur
Dr J. Furrer, rapporteur
Prof. K. Severin, rapporteur



ÉCOLE POLYTECHNIQUE
FÉDÉRALE DE LAUSANNE

Suisse
2018

Acknowledgements

For the past four years I have been able to work on my PhD thesis under conditions that would probably be described as idyllic by many. For this, I am extremely grateful and have many people to thank.

I am extremely grateful to **Paul** (or Prof. **Paul J. Dyson**) for having accepted me in his lab, the Laboratory of Organometallic and Medicinal Chemistry, **LCOM**, as a PhD student. The enthusiasm with which new ideas were welcomed by Paul considerably contributed to the fun I had during my PhD. (Evidently, some other aspects of the PhD were less fun, but these have no business in the Acknowledgements section!) Moreover, the suggestions, supervision and constant help with drafts and manuscripts have helped me improve as a scientist.

I had previously worked in the LCOM lab during my master's degree, where I conducted my semester project under the supervision of **Fei**. **Fei** introduced me to the world of Ionic Liquids, and introduced me to the world of research. For that, I am very thankful. I am also thankful to **Fei** for having introduced me to *real* Chinese Tea, which is truly delicious!

I would like to acknowledge the members of the Jury, Prof. Andreas Züttel, Prof. James Wilton-Ely, Prof. Julien Furrer and Prof. Kay Severin for accepting to donate their time and energy for the evaluation of this thesis.

One important aspect that made my work at EPFL so enjoyable was also the atmosphere in the LCOM lab, and in particular in "my" lab, the BCH2412. I'd like to also thank **Ronald**, who was sitting right behind me for almost three years, and with whom we had many good discussions, both chemistry and non-chemistry related. A special thanks also goes to **Martin**, **Lucinda Kate**, and **Quentin** who are also important members of the BCH2412 lab!

Throughout the 4 year of thesis, part of the LCOM lab (**Mickael**, **Antoine** and myself) have collaborated very tightly with the LCS group. Unfortunately for science, the collaboration was strictly unprofessional and purely leisure, because every lunch time became a holiday because of our loud and (over?)-enthusiastic card games. Thanks to **Basile**, **Leonard** and **Floppy** for making the lunch breaks something to look forward too. **Florian** is specially acknowledged for his friendship and support throughout the thesis.

I would also like to dedicate a little paragraph for my family. First, my parents, "**Patat**" and "**Juf**", who have always supported me and were always of good advice. They have always been present and continue to be present whenever I need their help or support, and I would probably not have succeeded in going this far

without them! Second, thanks to my brothers **Erik, Paul** and **Patrick** who have contributed to the reaction of many people saying: “Wow, you have three brothers? Your poor mom!”.

A special paragraph also goes to **Eva**, my smart and cute soon-to-be-wife girlfriend who has been and still is able to continuously make me happy over the past seven+ years, and who is always able (not always purposely) to make me laugh. For all this, I thank you a (parking!) lot!

Lots of my results have been collected with the help of numerous students: master students, apprentices and internship students. I am thankful to **Joachim Weber, Bastien Roulier, Mylène Soudani, Florent Menoud, Sami Chamam, Johanna Buri, Wei-Tse Lee, Alexandre Redondo, Antoine Van Muyden, Weronika Gruszka**. Without them, my thesis would not have been as furnished, and for all their hard work and dedication, I am very thankful.

It would probably take a section equally as long as the entire thesis to mention and describe the positive impact of all the people I have spent enjoyable time with in the lab and in the building (LCOM lab, magasin, X-ray service, NMR service, Mass spec service, etc...). Therefore, this paragraph is for the people that are not directly mentioned but still relate to this section: thank you!

Abstract

The mass-utilization of fossil resources has led to a dramatic increase in carbon dioxide (CO₂) production, most of which is released directly into the Earth's atmosphere, resulting in global warming. Efforts to contain CO₂ emissions and to capture, store and use this molecule are required to reduce the rate at which the concentration of CO₂ increases in the atmosphere.

Valorizing CO₂ by chemical transformation is valuable as CO₂ is abundant, cheap, and considered as a waste molecule. Unfortunately, CO₂ is thermodynamically stable and chemically inert and therefore either high energy input or efficient catalysts are required to transform it.

This thesis details the design of catalytic systems for the transformation of CO₂ into value-added products. First, the consequences of high atmospheric CO₂ levels will be presented. Then, the catalytic systems that have been developed for CO₂ utilization are reviewed, with emphasis on fuel production and incorporation of CO₂ into organic scaffolds.

Next, our contributions to the ionic liquid (IL) catalyzed cycloaddition of CO₂ into epoxides (CCE reaction) to afford organic cyclic carbonates are compiled. Recent advances in the field of IL catalysts for the CCE reaction are summarized as an introduction to this chapter, followed by a mechanistic investigation on the imidazolium salt catalyzed CCE reaction. Then, the preparation and characterization of polymeric ILs based on a vinylbenzyl functionalized imidazolium salt are described. The ability of the materials to catalyze the CCE reaction is reported. Based on the knowledge gained throughout these studies, a catalytic CO₂ extraction reactor was developed containing a simple IL:epoxide mixture that is able to quantitatively extract CO₂ from an array of gas streams.

Subsequently, the utilization of carbene catalysts for the N-methylation and N-formylation of amines using CO₂ as the C1 source and hydrosilanes as the reducing agent is compiled in the form of a protocol. Then, an approach to produce organic cyclic carbonates employing diols rather than epoxides as the starting material is highlighted. The methodology relies on a carbene catalyst that was employed in combination with Cs₂CO₃ and an alkyl halide that was required to capture the water that is formed during the reaction. Afterwards, the concept of CO₂ and H₂ activation using an ionic frustrated Lewis pair composed of an IL and B(C₆F₅)₃ is presented. Finally, the knowledge obtained from the N-formylation reaction combined with the cyclic carbonate chemistry allowed us to develop a simple methodology relying on the cooperativity

between hydrosilanes and fluoride salts to transform cyclic carbonates into their corresponding diol and methanol. Formally, this methodology allows for the metal-free indirect reduction of CO₂ into methanol.

Together, our results show that CO₂ can effectively be used as a C1 source in an array of chemical reactions, some of which are of industrial importance. Utilizing CO₂ as a benign C1 source can lead to the replacement of existing methods that employ toxic and harmful chemicals.

Keywords

Carbon dioxide, ionic polymers, ionic liquids, catalysis, green chemistry, sustainable chemistry, organocatalysis

Résumé

L'utilisation massive de ressources fossiles a contribué à une augmentation rapide de la production de CO₂, dont la majeure partie est relâchée directement dans l'atmosphère terrestre. Cette gigantesque quantité de CO₂ (35 Gtonnes) dans l'atmosphère est partiellement responsable de l'effet de serre et du réchauffement climatique. Des efforts pour contenir les émissions, ainsi que pour capturer, stocker et utiliser cette molécule sont requis afin de limiter l'impact humain sur le réchauffement climatique.

L'utilisation et la valorisation du CO₂ est intéressante puisque cette molécule est abondante et peu chère. Malheureusement, le CO₂ est une molécule thermodynamiquement stable et cinétiquement inerte nécessitant soit une quantité importante d'énergie soit des catalyseurs efficaces pour être transformée.

Cette thèse décrit les systèmes catalytiques développés afin d'incorporer le CO₂ dans des molécules organiques. Tout d'abord les conséquences d'une concentration élevée de CO₂ dans l'atmosphère sur le climat seront abordées. Puis, les systèmes catalytiques utilisant le CO₂ comme substrat, en focalisant sur les carburants et sur l'incorporation du CO₂ dans des molécules organiques, seront décrits.

La thèse décrira ensuite notre contribution dans la production de carbonates cycliques par le couplage CO₂-époxyde, catalysée par des liquides ioniques (ILs). Tout d'abord, les avancées récentes dans le domaine des catalyseurs ioniques pour le couplage CO₂-époxyde seront résumées. Ensuite, une étude mécanistique de la réaction catalysée par des sels d'imidazolium sera développée. Puis, la préparation et la caractérisation de polymères ioniques comme catalyseurs dans la réaction sera décrite. Les connaissances acquises durant ces études nous a permis de construire un réacteur à flux continu contenant un mélange IL-époxyde capable d'extraire continuellement le CO₂ de diverses sources de gaz.

La seconde partie de la thèse se focalisera sur les méthodes synthétiques que nous avons développées. Premièrement, l'utilisation de carbènes comme catalyseurs pour la réaction de N-méthylation et N-formylation d'amines utilisant le CO₂ comme agent méthylant/formylant sera décrite sous la forme d'un protocole. Puis, la synthèse de carbonates cycliques à partir de diols plutôt que d'époxydes sera développée. La réaction se produit en présence d'un catalyseur carbène préparé *in situ* ainsi que de Cs₂CO₃ et d'un halogénure d'alkyle, ce dernier étant nécessaire à capturer l'eau qui est générée lors de la réaction. S'en suivra une étude sur la préparation d'une paire de Lewis frustrée ionique sera décrite. Finalement, les connaissances acquises sur les carbonates cycliques ainsi que sur l'activité des hydrosilanes nous a mené à étudier la réduction des carbonates cycliques en méthanol et en diols. Cette réaction est catalysée

par des sels de fluorure. Formellement, cette transformation consiste à réduire le CO₂ en méthanol via une molécule-relais, le carbonate cyclique.

Dans son ensemble, cette thèse démontre que des méthodes synthétiques utilisant le CO₂ comme substrat peuvent efficacement remplacer les méthodes existantes qui nécessitaient jusqu'ici des réactifs toxiques.

Mots-clés

Dioxyde de carbone, polymères ioniques, liquides ionique, catalyse, chimie renouvelable, organocatalyse

Table of Contents

Acknowledgements	iii
Abstract	v
Keywords	vi
Résumé	vii
Mots-clés	viii
Table of Contents	ix
List of Figures.....	xiii
List of Tables.....	xvii
List of Schemes	xix
Abbreviations	xx
1. Introduction.....	- 1 -
1.1. The CO ₂ problem	- 1 -
1.2. Current strategies for chemical CO ₂ valorization	- 2 -
1.2.1. Conversion of CO ₂ to fuels.....	- 3 -
1.2.2. Incorporation of CO ₂ into organic scaffolds	- 7 -
1.3. Ionic liquids as preferential catalysts for CO ₂ applications	- 9 -
1.4. Structure of the thesis.....	- 12 -
2. Synthesis of ionic poly(imidazolium) salts and their application in the cycloaddition of CO ₂ into epoxides	- 13 -
2.1. Ionic catalysts for the CCE reactions: state-of-the-art:	- 14 -
2.1.1. Properties and applications of cyclic carbonates	- 15 -
2.1.2. Mechanism of the CCE reaction	- 16 -
2.1.3. IL catalysts for the CCE reaction	- 17 -
2.1.4. Ammonium-based ILs.....	- 17 -
2.1.5. Imidazolium-based ILs	- 19 -
2.1.6. Phosphonium-based ILs and other ionic pairs	- 22 -
2.2. Intricacies of Cation-anion combination in imidazolium-salt catalyzed cycloaddition of CO ₂ into epoxides	- 27 -
2.2.1. Introduction.....	- 28 -
2.2.2. Results and Discussion.....	- 29 -
2.2.3. Conclusions.....	- 35 -
2.2.4. Experimental details.....	- 36 -

2.3.	Synthesis of linear ionic poly(styrenes) and their application as catalysts for the cycloaddition of CO ₂ and epoxides	- 41 -
2.3.1.	Results and Discussion.....	- 42 -
2.3.2.	Conclusions.....	- 49 -
2.3.3.	Experimental details.....	- 49 -
2.4.	Synthesis of cross-linked ionic poly(styrenes) and their application as catalysts for the cycloaddition of CO ₂ and epoxides.....	- 53 -
2.4.1.	Results and Discussion.....	- 54 -
2.4.2.	Conclusions.....	- 62 -
2.4.3.	Experimental details.....	- 62 -
2.5.	Synthesis of cross-linked poly(imidazolium) salts and their application in the CCE reaction .	- 69 -
2.5.1.	Results and Discussion.....	- 70 -
2.5.2.	Conclusions.....	- 79 -
2.5.3.	Experimental details.....	- 80 -
2.6.	Quantitative extraction of CO ₂ from air and other gas streams using simple IL:epoxide mixtures	- 83 -
2.6.1.	Introduction.....	- 84 -
2.6.2.	Results and Discussion.....	- 84 -
2.6.3.	Conclusions.....	- 88 -
2.6.4.	Experimental details.....	- 88 -
2.7.	General Conclusions	- 91 -
2.7.1.	Summary.....	- 91 -
2.7.2.	Further perspectives.....	- 92 -
3.	Catalytic methods for utilization of CO ₂ as a reactive synthon.....	- 93 -
3.1.	Reductive functionalization of amines with CO ₂ and hydrosilanes with carbene catalysts....	- 93 -
3.1.1.	Introduction:.....	- 94 -
3.1.2.	Comparison with other approaches.....	- 95 -
3.1.3.	Experimental design	- 97 -
3.1.4.	Materials.....	- 103 -
3.1.5.	Equipment setup	- 105 -
3.1.6.	Procedure	- 105 -
3.1.7.	N-formylation and N-methylation reactions.....	- 108 -
3.1.8.	Troubleshooting	- 113 -
3.1.9.	Anticipated results.....	- 116 -

3.2.	Metal-free catalyst for the synthesis of carbonates from diols and CO ₂	- 117 -
3.2.1.	Introduction.....	- 118 -
3.2.2.	Results and discussion.....	- 119 -
3.2.3.	Conclusions.....	- 123 -
3.2.4.	Experimental details.....	- 124 -
3.3.	Towards a frustrated Lewis pair-ionic liquid system.....	- 125 -
3.3.1.	Introduction.....	- 126 -
3.3.2.	Results and Discussion.....	- 126 -
3.3.3.	Conclusions.....	- 131 -
3.3.4.	Experimental details.....	- 131 -
3.4.	One-pot, two-step MeOH production from CO ₂ via cyclic carbonates under metal-free and atmospheric conditions.....	- 135 -
3.4.1.	Introduction.....	- 136 -
3.4.2.	Results and discussion.....	- 136 -
3.4.3.	Conclusions.....	- 141 -
3.4.4.	Experimental details.....	- 142 -
3.5.	General conclusions.....	- 143 -
3.5.1.	Summary.....	- 143 -
3.5.2.	Future perspectives.....	- 143 -
4.	Thesis conclusions.....	- 145 -
4.1.	Summary.....	- 145 -
4.2.	Outlook.....	- 147 -
4.3.	References.....	- 149 -
	Appendices.....	- 163 -
	Appendix Section 2.3.....	- 163 -
	Appendix Section 2.4.....	- 171 -
	Appendix Section 2.6.....	- 173 -
	Appendix Section 3.2.....	- 177 -
	Appendix Section 3.3.....	- 179 -
	Appendix Section 3.4.....	- 182 -
	Curriculum Vitae.....	- 185 -

List of Figures

Figure 1.2.1 Potential CO ₂ neutral synthetic gas production and utilization.	- 3 -
Figure 1.2.2 Example of CO ₂ reduction catalysts.	- 4 -
Figure 1.2.3. Fischer-Tropsch process to form alkanes and Monsanto process to form acetic acid.	- 5 -
Figure 1.2.4 Reduction of CO ₂ for H ₂ storage.....	- 6 -
Figure 1.2.5 Reactive applications of CO ₂	- 7 -
Figure 1.3.1 Examples of ILs.	- 10 -
Figure 1.3.2 Selected transformations in which simple ILs have been employed as catalysts. ^{33,91,92}	- 11 -
Figure 2.1.1 General structure of a cyclic carbonate (top) and selected examples (bottom).....	- 15 -
Figure 2.1.2 Examples of ammonium salt CCE catalysts. 1 tetrabutylammonium bromide (TBAB), 2 hydroxyethyltributylammonium bromide (HETBAB), 3 tris(hydroxyethyl)ethylammonium bromide (NEt(HE) ₃ Br), 4 N,N-dimethylglycine on polystyrene (PS-QNS) and 5 PEG-supported quaternary ammonium salt (PEG ₆₀₀₀ (NBu ₃ Br) ₂)..	- 18 -
Figure 2.1.3 Examples of imidazolium-based ILs used to catalyze the CCE reaction. 6 3-butyl-1-methylimidazolium chloride ([bmim]Cl), 7 3-octyl-1-methylimidazolium bromide ([omim]Br), 8 1-methylimidazolium bromide ([hmim]Br), 9 3-hydroxyethyl-1-methylimidazolium bromide ([hemim]Br, 10 bis-carboxylic acid functionalized imidazolium bromide, 11 3-(ethanoic acid)-1-methylimidazolium bromide, 12 2-hydroxymethyl-1-methyl-3-ethylimidazolium bromide, 13 1-(3-aminopropyl)-3-butylimidazolium iodide ([apbim]I) and 14 hydroxy-functionalized bisimidazolium bromide.....	- 20 -
Figure 2.1.4 Examples of supported imidazolium salts used to catalyze the CCE reaction. 15 3-(2-hydroxyethyl-ethyl)-1-(3-amino-propyl)imidazolium bromide grafted on a divinylbenzene polymer ([pdvb-heim]Br), 16 diol functionalized imidazolium salt grafted onto commercial polystyrene resin ([PS-DHPIM]Br), 17 alkyl imidazolium salt grafted onto commercial silica, 18 3-(2-hydroxyethyl)-1-propylimidazolium bromide immobilized on SBA-15 ([SBA-15-hepim]Br), 19 polymer grafted with functionalized di-cationic imidazolium IL ([P-FDILs]), 20 bis(1,3-vinylbenzyl)imidazolium chloride (poly[bvbim]Cl), 21 cross-linked polymer-supported IL (PSIL) and 22 3-ethyl-1-methylimidazolium bromide bound to chitosan ([CS-emim]Br).	- 21 -
Figure 2.1.5 Examples of N-based catalysts and phosphonium IL CCE catalysts. 23 1,8-diazabicyclo[5.4.0]undec-7-enium chloride ([hdbu]Cl), 24 dipyridylamine bridged with two pyrrolidinium moieties, 25 triazolium salt grafted onto mesoporous silica SBA-15, 26 choline chloride, 27 histidine derived IL (His-Mel), 28 hydroxyl functionalized tetramethyl guanidine ([hetmg]Br), 29 butyl-triphenylphosphonium iodide ([PPh ₃ Bu]I), 30 carboxylic acid functionalized phosphonium salt ([PPh ₃ C ₂ H ₄ COOH]I), 31 hydroxyl functionalized phosphonium salt ([hePPh ₃]Br), 32 phosphonium salt formed by reaction of tributylphosphine with chloromethylated polystyrene ([PS-QPS]), 33 organic-inorganic hybrid catalyst containing a phosphonium salt and 34 Polymer grafted with asymmetrical dicationic IL with imidazolium and phosphonium ([P-Im-C ₄ H ₈ Ph ₃ P]Br ₂).	- 23 -

Figure 2.2.1 Salt-based catalysts (1X – 4X , where X = Cl ⁻ , Br ⁻ or I ⁻) studied in this work.	29 -
Figure 2.2.2 Optimized geometries for the intermediates and transition states involved in the rate-limiting step for the cycloaddition of CO ₂ with PO catalyzed by 1Cl , computed at the B3PW91-D3/6-31G** level.	31 -
Figure 2.2.3 Optimized geometries for the intermediates and transition states involved in a possible reaction path for the cycloaddition of CO ₂ with PO catalyzed by 3Cl	32 -
Figure 2.2.4 Optimized geometries for the intermediates and transition states for C4-H-assisted ring-opening of the epoxide computed at the B3PW91-D3/6-31G** level.	33 -
Figure 2.3.1 Structures of imidazolium salts 1a – 6a and the corresponding polymers 1b – 6b (yields given in parenthesis).	43 -
Figure 2.3.2 ORTEP representations of the cation in 1a (top) and 2a (bottom). The counter anions have been omitted for clarity. Key bond lengths (Å) and angles (°) for 1a : N(1)-C(2): 1.331(5), N(1)-C(5): 1.392(6), C(2)-N(3): 1.330(5), N(3)-C(4): 1.387(6). N(1)-C(2)-H(2): 125.3, N(3)-C(2)-N(1): 109.3(4). Key bond lengths (Å) and angles (°) for 2a : N(1)-C(2): 1.337(15), N(1)-C(5): 1.400(15), C(2)-N(3): 1.341(15), N(3)-C(4): 1.390(14). N(1)-C(2)-H(2): 125.9, N(1)-C(2)-N(3): 108.2(10).	44 -
Figure 2.3.3 SEM image of 1b	44 -
Figure 2.3.4 Recycling studies with polymer catalyst 1b using epichlorohydrin, 7a , as the substrate.	49 -
Figure 2.4.1 Synthesis of vinyl-functionalized di-imidazolium salts m1a/b to m6a/b and their subsequent polymerization to form cross-linked polymers p1a/b to p6a/b	55 -
Figure 2.4.2 SEM images of polymer p1b (top and middle) and p5b (bottom).	56 -
Figure 2.4.3 TGA curves for selected polymers p1b , p2b and p5b	57 -
Figure 2.4.4 Recycling experiments using epichlorohydrin as a substrate under optimized conditions: p5b (24.9 mg, 0.5 mol%), epichlorohydrin (0.76 g, 8.3 mmol), CO ₂ (2.5 MPa), 130 °C, 15 h.	62 -
Figure 2.5.1 FT-IR spectra of IPs 1 – 4	71 -
Figure 2.5.2 Solid-state ¹³ C NMR spectra of the IPs 1 – 4 (from bottom)	71 -
Figure 2.5.3 TGA analysis of IPs 1 – 4 under nitrogen up to 600 °C at a heating rate of 40 °C/min.	72 -
Figure 2.5.4 SEM images of (a – c) IP 1 , (d – f) IP 2 , (g – i) IP 3 and (j – l) IP 4	73 -
Figure 2.5.5 XRD patterns of IPs 1 – 4	74 -
Figure 2.5.6 Postulated mechanism for the CCE reaction catalyzed by IP 3	77 -
Figure 2.5.7 Kinetic traces for catalyst IP 3 for the transformation of PO (red, circles for 10 atm., squares for 25 atm.) and SO (blue, circles for 10 atm, squares for 25 atm.). Conditions: IP 3 (5 mol%), SO or PO (0.83 mmol), CO ₂ (10 or 25 atm.). Yields determined by ¹ H NMR spectroscopy.	78 -
Figure 2.5.8 Recycling studies of catalyst IP 3 . Conditions: IP 3 (5 mol%), SO (0.83 mmol), CO ₂ (10 atm.), 15 h. Yields determined by ¹ H NMR spectroscopy.	79 -
Figure 2.5.9 FT-IR spectral variation of the catalyst (IP 3) after 10 catalytic cycles. The main additional peaks present may be attributed to the reaction product.	79 -

Figure 2.6.1 Generic cycloaddition of CO ₂ into epoxides to afford cyclic carbonates (CCE reaction).....	- 85 -
Figure 2.6.2 Proposed mechanism for the CCE catalyzed by imidazolium salts and rationale for catalyst decomposition and the formation of side-products. Alternative epoxides studied are shown below (see Appendix Section 2.6 for further details).	- 86 -
Figure 3.1.1 N-Formylation of phenylalanine ethyl ester. Cat: catalyst; DMAc: dimethylacetamide; PMHS: Poly(methylhydrosiloxane).	- 97 -
Figure 3.1.2 N-methylation of N-methylaniline. Cat: catalyst; DMF: N,N-dimethylformamide; Ph ₂ SiH ₂ : diphenylsilane.	- 98 -
Figure 3.1.3 N-Formylation and N-methylation of amines using NSC1 and PMHS. General conditions: amine, 0.5 mmol; NSC1, 7.5 mol%; PMHS, 200-300 μL; 50-100 °C; 24-48 h. Isolated yields following column chromatography using hexane and ethyl acetate with 1% added triethylamine are given in parenthesis. ²³³	- 100 -
Figure 3.1.4 Selected examples of N-methylation of amines using NHC1 and Ph ₂ SiH ₂ . General conditions: amine, 0.5 mmol; NHC1, 5 mol%; Ph ₂ SiH ₂ , 3 eq., 1.5 mmol, 278 μL; 50 °C, 24-48 h. Isolated yields following column chromatography on silica using hexane and ethyl acetate with 1% added triethylamine are given in parenthesis. ²³² EWG = Electron-withdrawing groups, EDG = Electron-donating groups.	- 100 -
Figure 3.1.5 Photograph of the four parallel reaction apparatus with the distillation distributor and distillation head. No cross-contamination was observed under these conditions.	- 107 -
Figure 3.1.6 Photographs illustrating steps 3, 4, 5 and 7. a) Color of NHC catalyst after 30 min stirring. b) 1 mL is removed with a N ₂ -purged syringe (note that extra N ₂ taken in the syringe). The catalytic solution is used for the reaction. c) 3 mL of catalytic solution is prepared. The remaining 1 mL is discarded and the tube can be washed with organic solvents or water, as it contains the salt by-product. Caution: Excess NaH reacts violently with water. It reacts also with acetone and ethanol, but the reaction is much less exothermic than it is with water.	- 107 -
Figure 3.1.7 Change in color of the catalyst upon exposure to air. a) t = 0 s, b) t = 30 s, c) when diluted in EtOH.	- 108 -
Figure 3.3.1 FLP-IL system designed for hydrogen activation	- 126 -
Figure 3.3.2 (top) ORTEP plot of the cation of the Lewis basic imidazolium cation in the crystal of [iPr ₂ N(CH ₂) ₂ mim][Tf ₂ N]. Key bond lengths (Å) and angles (°): N(1)-C(2) 1.331(2), N(2)-C(2) 1.328(2), C(3)-C(4) 1.351(3), N(2)-C(2)-N(1) 108.71(13), C(10)-N(3)-C(7) 117.05(12). (bottom) Crystal packing of [iPr ₂ N(CH ₂) ₂ mim][Tf ₂ N].	- 127 -
Figure 3.3.3 Optimized structures of the [iPr ₂ N(CH ₂) ₂ mim] ⁺ -B(C ₆ F ₅) ₃ (A) and [Tf ₂ N] ⁻ -B(C ₆ F ₅) ₃ (B) complexes. Fluorine and hydrogen atoms are omitted for clarity. A: B··N(i-Pr) ₂ distance = 4.35 Å. B: B··O distance = 1.66 Å.	- 128 -
Figure 3.3.4 Overlay of ¹¹ B NMR spectra of (B(C ₆ F ₅) ₃) (25 mol%) in [iPr ₂ N(CH ₂) ₂ mim][Tf ₂ N] under N ₂ , and in the presence of H ₂ (30 bars), CO ₂ (20 bars) and H ₂ /CO ₂ (P _{H₂} = 30 bars, P _{CO₂} = 20 bars).	- 129 -
Figure 3.3.5 Overlay of ¹³ C NMR spectra of (B(C ₆ F ₅) ₃) (25 mol%) in [iPr ₂ N(CH ₂) ₂ mim][Tf ₂ N] in the presence of H ₂ /CO ₂ (P _{H₂} = 30 bars, P _{CO₂} = 20 bars) and CO ₂ (20 bars, top).	- 131 -

Figure 3.4.1 Shell Omega process for PG production, and the method reported here for the simultaneous synthesis of MeOH and diols. - 136 -

List of Tables

Table 2.1.1 Examples of selected ammonium salt catalysts under optimized conditions.	19 -
Table 2.1.2 Examples of selected imidazolium salt catalysts under optimized conditions.	22 -
Table 2.1.3 Examples of selected ion-pair organocatalysts under optimized conditions.	25 -
Table 2.2.1 Influence of the cation and anion on the CCE reaction in the synthesis of epichlorohydrin carbonate.	30 -
Table 2.2.2 Effect of water on the reaction between epichlorohydrin and CO ₂ catalyzed by 1X and 4X	35 -
Table 2.2.3 Synthesis of the catalyst by reaction of the imidazole precursor and alkyl halide under solvent-free conditions.	37 -
Table 2.3.1 Optimization of the reaction conditions using catalyst 1b and styrene oxide as the substrate.	45 -
Table 2.3.2 Evaluation of ILs 1a – 6a and polymers 1b – 6b (in parenthesis) as catalysts in the cycloaddition of CO ₂ to styrene oxide.	46 -
Table 2.3.3 Evaluation of different epoxide substrates in the cycloaddition reaction with CO ₂ using catalyst 1b	48 -
Table 2.4.1. Evaluation of the polymers at catalysts for the synthesis of styrene carbonate	58 -
Table 2.4.2 Optimization of pressure and temperature employing p5b as the catalyst for the CCE reaction.	58 -
Table 2.4.3. Catalytic activity of m5b and p5b at a high loading.	59 -
Table 2.4.4. Investigation of the substrate scope of the CCE reaction using p5b as the catalyst under optimized conditions.	60 -
Table 2.5.1 Evaluation of IPs 1 – 4 in the CCE reaction using SO as the starting material.	75 -
Table 2.5.2 Substrate scope in the CCE reaction employing IPs 1 – 4	76 -
Table 2.5.3 CCE reaction under 10 atm. CO ₂ employing IPs 1 – 4	77 -
Table 2.6.1 Optimization of the reaction conditions for the transformation of SO into SC at atmospheric pressure. ...	85 -
Table 2.6.2 Results of the cycloaddition of CO ₂ into SO affording SC using air as the CO ₂ source.	87 -
Table 2.6.3 Evaluation of CO ₂ uptake under continuous flow conditions.	88 -
Table 3.1.1 Comparison between several methodologies for N-formylation and N-methylation.	95 -
Table 3.1.2 Benchmark reactions employing NSC-based catalysts for the N-formylation of phenylalanine ethyl ester.	98 -
Table 3.1.3 Benchmark reactions employing NSC-based catalysts for the N-methylation of N-methylaniline.	99 -
Table 3.2.1 Optimization of the reaction conditions for the transformation of 1-phenyl-1,2-ethanediol (1a) used as a model substrate.	120 -
Table 3.2.2 Reaction of various diols with CO ₂ under optimized conditions.	121 -
Table 3.4.1 Optimization of the reaction conditions for the transformation of PC to PG and MeOH.	138 -

List of Schemes

Scheme 2.1.1 Generic CCE reaction.	15 -
Scheme 2.1.2 General mechanism for the cycloaddition of CO ₂ to epoxides using ionic catalysts. (i) Ring-opening of epoxide by anion of the ion pair. (ii) Insertion of CO ₂ into the generated alkoxide. (iii) Release of product by ring-closing S _N 2.	17 -
Scheme 2.2.1 Accepted mechanism of the CCE reaction (top) and additional possible H-bonds between the epoxide and the acidic protons on the imidazolium ring (bottom).	29 -
Scheme 2.3.1 Synthesis of styrene-functionalized imidazolium salts and their corresponding polystyrene derivatives. R and X is defined in Figure 2.3.1.	42 -
Scheme 2.3.2 Side-products observed when water (1 eq.) is added to the reaction.	45 -
Scheme 2.3.3 Proposed mechanism for the CCE of epichlorohydrin catalyzed by 1b. The polystyrene part is omitted for clarity and represented by R. (i) Ring-opening of the oxirane by the bromide anion. (ii) Insertion of CO ₂ . (iii) Release of the product and catalyst. A proposed key intermediate, represented with 3b, is shown in the inset.	47 -
Scheme 2.4.1 Tentative mechanism for the CCE reaction catalyst employing p5b as the catalyst.	61 -
Scheme 2.5.1. Synthesis of IPs 1 – 4	70 -
Scheme 3.1.1 The four chemical reactions proposed in the Procedure hereafter.	102 -
Scheme 3.2.1 Tentative mechanism for the carbene-catalyzed reaction of diols and CO ₂ to form cyclic carbonates. The substituents of the catalyst are omitted for clarity.	122 -
Scheme 3.2.2 Proposed mechanism for the non-catalytic reaction of diols and CO ₂ to form cyclic carbonates. .	123 -
Scheme 3.3.1 Reaction of the [iPr ₂ N(CH ₂) ₂ mim][Tf ₂ N]-B(C ₆ F ₅) ₃ IL-FLP system without H ₂	130 -
Scheme 3.4.1 Epoxides used in the synthesis of glycols and MeOH from epoxides in a single pot reaction.	139 -
Scheme 3.4.2 Labelling experiments for the hydrosilylation/hydrolysis of propylene carbonate to produce labelled MeOH. * Yield estimated based on PG.	140 -
Scheme 3.4.3 Proposed mechanism for the transformation of propylene carbonate into MeOH and PG.	141 -

Abbreviations

[BMIm]: 1-butyl-3-methyl

AIBN: azobisisobutyronitrile

aIL: acidic ionic liquid

Atm.: atmosphere

BET: Brunauer-Emmett-Teller

CCE: cycloaddition of CO₂ into epoxides

CCS: carbon capture and storage

CCUS: carbon capture and utilization

CO₂: carbon dioxide

COP21: Conference of the Parties

DMAc: N,N-dimethylacetamide

DMF: N,N-dimethylformamide

DMSO: dimethylsulfoxide

EC: Ethylene carbonate

EMIm: 1-ethyl-3-methyl

Et₂O: diethyl ether

EtOAc: Ethyl acetate

EtOH: Ethanol

FA: Formic acid

FLP: Frustrated Lewis Pair

FT-IR: Fourier Transform-Infrared

GC-FID: Gas chromatography – flame ionization detector

GC-MS: Gas chromatography – mass spectrometry

Gton: gigaton

HEMIm: 1-hydroxyethyl-3-methylimidazolium

ILs: Ionic liquid(s)

IP: ionic polymer

ⁱPrOH: isopropanol

MeOH: Methanol

NaOH: sodium hydroxide

NHC: N-heterocyclic carbene

NMR: Nuclear magnetic resonance
OMIm: 1-octyl-3-methyl
P2G: Power-to-gas
PC: Propylene carbonate
pIL: polymeric ionic liquid
PO: propylene oxide
Ppm: part per million
Rpm: rate per minute
SC: Styrene carbonate
SEM: Scanning electronic microscope
sIL: supported ionic liquid
SO: Styrene oxide
TBA: tetrabutylammonium
Tf₂N: bis(trifluoromethylsulfonyl)imide
TGA: Thermogravimetric analysis
THF: tetrahydrofuran
VBI: 4-vinylbenzylimidazole
XRD: X-ray diffraction

1. Introduction

1.1. The CO₂ problem

Carbon dioxide (CO₂) is a molecule that is naturally present in the environment. It is involved and regulated by the natural carbon cycle. This carbon cycle includes capture, use and release of CO₂. Examples include biomass production (plants) and natural carbonization processes (ocean carbonification, seashells, etc.). Approximately 700 GTons of CO₂ are used in this cycle every year in the atmosphere alone.^{1,2} The total CO₂ reservoir is much larger (20 000 to 60 000 Tt in the lithosphere for example, amongst other sources) and the overall cycle has a fragile equilibrium.³

Human activities, especially in the past two centuries, have contributed to a dramatic increase of CO₂ emissions into the atmosphere. The discovery, intensive extraction and burning of fossil fuels (for example coal and oil) throughout the last 150 years has led to a concentration of CO₂ of 406 ppm in December 2017, when the concentration was approximately 290 ppm in the pre-industrial era (*i.e.* before 1860).⁴ In parallel, the energy demands have continuously increased and the majority is currently still met by burning fossil fuels.⁵

This large addition of CO₂ into the atmosphere combined with the growth of population and deforestation is leading to climate change and global warming that may potentially result in natural catastrophes, famines and wars.^{6,7} While CO₂ is not the only gas emitted by human activities and responsible for global warming, it is the one that is considered the most problematic.^{6,8}

There is an urgent necessity to reduce the emissions of CO₂ into the atmosphere and to step away from fossil fuels and petrochemicals in order to achieve the goals set by the COP21 in Paris.⁹ Simultaneously, developing chemical methodologies that take advantage of the abundance of CO₂, *i.e.* methodologies that consider it as a building block rather than a waste, will be helpful for the transition towards a more sustainable chemical industry.

CO₂ is a linear molecule composed of the highest oxidation state of carbon (+IV) and contains two polarized C=O bonds, but because it is linear and symmetric, it is non polar. Due to the highly oxidized form of carbon in the molecule, it is thermodynamically stable and kinetically inert. Nonetheless, in recent years, many soft approaches to functionalization using CO₂ have been developed, including methodologies that do not require a catalyst,¹⁰ indicating that the molecule does not necessarily require harsh conditions to be employed as a chemical reagent.¹¹

1.2. Current strategies for chemical CO₂ valorization

In this introduction, two main strategies for CO₂ utilization will be discussed. The first one is the direct reduction of CO₂ to fuels under catalytic conditions, which is not the target of this thesis, but will be briefly mentioned in this introduction since it is a crucial topic in CO₂ chemistry. The second one is the utilization of CO₂ as a C1 building block in synthesis, which will be the main target of this dissertation.

The rate at which this gas is emitted and the quantities involved are several orders of magnitude larger than the rates and quantities at which it can be chemically transformed. Reducing the CO₂ concentration will require all the possible strategies, and these involve also its capture and storage.¹² These fall in the concept of “carbon capture and storage” (CCS), which has been expanded to “carbon capture, storage and utilization” (CCSU).^{5,13} This thesis will only describe methods to chemically transform CO₂, which belongs to the category of “CO₂ utilization”, even if we can argue that CO₂ can also be captured catalytically, as will be presented in Section 2.6.

The main target molecules of CO₂ reduction are carbon monoxide, methanol, methane, formic acid and methodologies have been developed for the reduction of CO₂ directly to ethanol and lower alkanes/alcohols (see Figure 1.2.2).¹⁴ This is an important research area towards a CO₂-neutral energy consumption (Figure 1.2.1). Recently, to bypass the energy input necessary for direct CO₂ reduction, strategies have been described that first incorporate CO₂ into an organic scaffold, and subsequently hydrogenates the obtained molecule to produce MeOH.¹⁵ This approach will be discussed in more detail in Chapter 1.

There are many approaches that have been described to incorporate CO₂ into an organic scaffold, *i.e.* to use CO₂ as a valuable C1 source.¹⁶ In this approach, the oxidation state of CO₂ does not necessarily change and it can be incorporated in pure form (*i. e.*, the three atoms of CO₂ are conserved and remain covalently bound, but one or two additional bonds are generated, that covalently attach CO₂ to a pre-existing molecule). An example of a relevant reaction involves the preparation of cyclic carbonates from epoxides and CO₂. This reaction will be extensively detailed in Chapter 1 and has been the main focus of this thesis. Another reaction that will be detailed is the reductive functionalization using CO₂ as the C1 source, where successful examples are the N-Formylation and N-methylation of amines. Details about our studies on the topic will be given in Chapter 1. Other examples (not explained in this thesis but briefly mentioned in Section 1.2.2) of reactions that utilize CO₂ as a reactive synthon are the synthesis of quinazolidines, carboxylic acids, ureas, etc.⁵

1.2.1. Conversion of CO₂ to fuels

The complete combustion (oxidation) of hydrocarbons (for example fuels) yields H₂O and CO₂ and supplies energy. Reducing the resulting CO₂ back to hydrocarbons for energy storage would allow for a CO₂-neutral cycle if the required energy for the reaction is gathered from a renewable source (*e.g.* sun) and that efficient catalytic systems are available. For example, the hypothetical cycle depicted in Figure 1.2.1 shows a schematic CO₂-neutral cycle for synthetic natural gas utilization. This cycle is commonly referred to as “power-to-gas” (P2G) in Switzerland.

Utilization of renewable Energy
(hydro, sun, wind, ...)

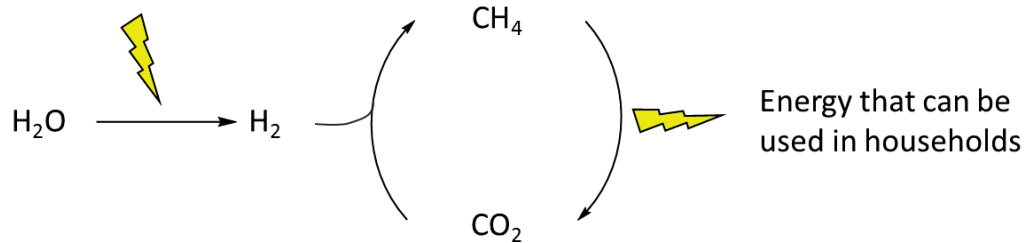
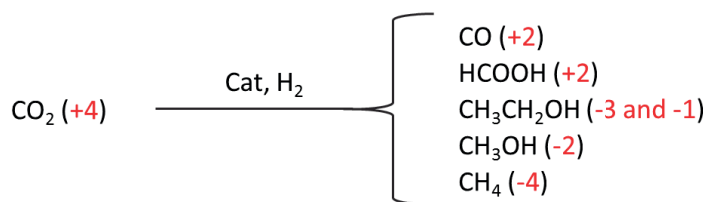


Figure 1.2.1 Potential CO₂ neutral synthetic gas production and utilization.

Figure 1.2.2 shows possible products and their oxidation states that can be formed during the reduction of CO₂ in the presence of a reducing agent (typically H₂) and a catalyst. A few catalysts are presented in the figure. It is not the scope of this thesis to review all the existing systems, and reviews have been written on the topic.^{17–20}



Selected catalysts and generated product:



^{ind} = industrially employed catalyst

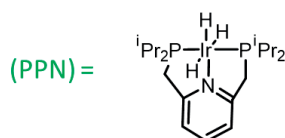


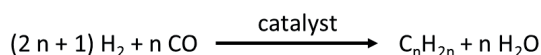
Figure 1.2.2 Example of CO₂ reduction catalysts.

Methanation of CO₂ is important because of the utility of methane as a fuel, as stated above (example of P2G). However, the reduction of CO₂ to CH₄ concomitantly leads to the formation of water (Sabatier reaction) that hinders catalytic activity, which is why catalyst development is ongoing. Typical catalysts comprise an active metal such as Rh or Ru on a support (for example aluminum oxide or titanium oxide).^{21,22} Using Rh supported on $\gamma\text{-Al}_2\text{O}_3$, the reaction proceeds at temperatures between 50 and 150 °C and a total pressure of 2 bars. The Ru/TiO₂ catalyst presented in Figure 1.2.2 produced 100% yield of CH₄ at 160 °C under continuous flow reactions.²¹ Reviews on catalytic methanation of CO₂ can be found throughout literature.^{23–25}

Another gas that can be formed from CO₂ reduction is CO, which finds numerous industrial applications despite its toxicity.²⁶ Example include the Monsanto process or the Fischer Tropsch reaction, where several MTons are used annually (See Figure 1.2.3).^{27,28} CO finds also other applications such as in lasers or in meat coloring.^{29,30} The reaction of CO₂ with H₂ to form CO and H₂O is the reverse water gas shift reaction (RWGS).²⁴ In particular, heterogeneous copper catalysts and bimetallic catalysts containing copper and another metal are very popular for this reaction.³¹ The abstraction of one oxygen atom from CO₂ is energy demanding, which is why this reaction is also often conducted under electrocatalytic conditions.³² Recently, it was found that ionic liquids dramatically decrease the working overpotential when used in combination

of a silver cathode.³³ This led to the evaluation of many new classes of co-catalysts for this reaction, that are working cooperatively with the cathode of the electrochemical cell.^{34–36}

Fischer Tropsch process:



Monsanto process:

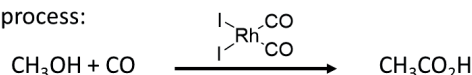


Figure 1.2.3. Fischer-Tropsch process to form alkanes and Monsanto process to form acetic acid.

Reducing CO₂ into methanol is attractive because unlike CH₄ or CO, methanol is liquid under ambient conditions, which makes its transport convenient. On an industrial scale, MeOH is often produced from CO and H₂, with a few percent of CO₂ in the chemical mixture.³⁷ Directly reducing CO₂ into MeOH remains challenging, but progress is being made and examples of catalysts are presented in Figure 1.2.2.^{38,39} Typical conditions using a CuZnGa catalyst produce MeOH under 45 bars of pressure at 250 °C, with a selectivity of approx. 50%, which is in the range of conditions used for industrial Cu/ZnO/Al₂O₃ catalysts. A Ni₅Ga₃ catalyst was discovered *via* a descriptor-based analysis of the reaction.³⁸ This catalyst is capable of producing MeOH at conditions close to standard type catalyst, *i.e.* a temperature of 200 °C under only 1 bar of pressure in a tubular fixed-bed reactor and shows that other type of materials could be used rather than the usual Cu/Zn mixtures. An example of a homogeneous catalytic system is comprised of a catalytic triade consisting of a scandium salt and two ruthenium catalysts. Using this catalytic system, MeOH was obtained at 135 °C, which is a much lower temperature than under heterogeneous conditions. However, the system lacked stability and resulted in low TONs.⁴⁰

The reaction of CO₂ with 1 equivalent of H₂ can lead to formic acid (FA) and allows, similarly to methanol, a form of H₂ storage under liquid form. In this context, CO₂ is used as a relay molecule to store the energy in chemical bonds. The ideal catalytic cycle for hydrogen storage *via* formic acid (but also generalized to other reduced forms of CO₂) is presented in Figure 1.2.4.^{41,42} Typical reaction conditions require a 1:1 ratio of CO₂ and H₂. Interestingly, the FA production reaction is reversible and the hydrogenation or dehydrogenation reaction can be catalyzed by the same catalyst and simply depend on the reaction conditions. The production of FA requires high pressures and low temperatures, while the dehydrogenation of FA will occur if the system is heated with no initial pressure.^{43,44} One example of another potent catalyst is depicted in Figure 1.2.2 and relies on an iridium centre in presence of a base.

This example achieved an extremely high TOF of $73\,000\text{ h}^{-1}$ and TON of $3\,500\,000$ and represents a state-of-the-art catalyst for CO_2 reduction to FA.⁴⁵

CO_2 reduction is not limited to the production of C1 chemicals, and molecules such as ethanol or lower alkanes can be produced. A recent example of CO_2 reduction to ethanol was achieved under electrocatalytic conditions. The system was composed of copper nanoparticles embedded on a N-doped graphene electrode and operated under aqueous conditions with good selectivity for EtOH.⁴⁶

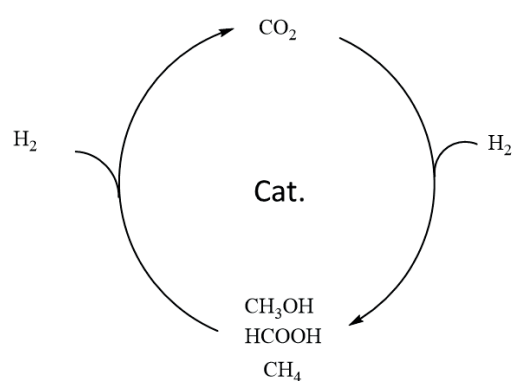


Figure 1.2.4 Reduction of CO_2 for H_2 storage.

1.2.2. Incorporation of CO₂ into organic scaffolds

CO₂ can be used as a C1 source to build chemical complexity, and can be incorporated in various oxidation states, as seen in the previous part. Figure 1.2.5 gives a non-exhaustive overview of reactions that employ CO₂ as a chemical building block. Reaction (1) and (2) are the reductive functionalization of amines using CO₂ as the C1 source. It is possible to prepare either a methylated or formylated amine using CO₂ as the carbon source and an external reducing agent. Examples relying on homogeneous metal catalysts (Ru, Fe, Co) in combination with hydrogen have been reported.^{47,48} Metal-free catalysts have been developed that are used in combination with a hydrosilane or hydroborane.⁴⁹⁻⁵¹ The field of catalytic N-functionalization has been reviewed recently.⁵² This reaction will be detailed in Chapter 3.

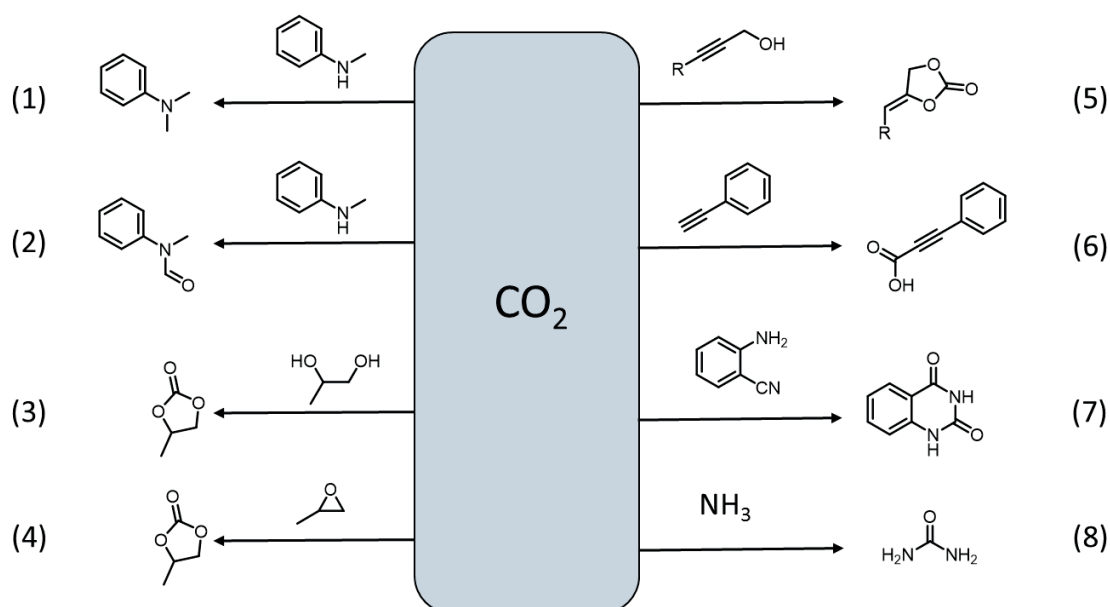


Figure 1.2.5 Reactive applications of CO₂.

Reactions (3) and (4) afford a cyclic carbonate product. Reaction (3) uses a diol as a starting material, which is advantageous over epoxides because of their lower toxicity and availability. However, the reaction results in elimination of a water molecule, which hinders catalytic development.^{53,54} The results achieved with diols as starting materials are moderate, and additives such as alkyl halides are often necessary to increase the yields.^{55,56} Our results on the topic will be described in Section 3.2. The reaction between an epoxide and CO₂ (reaction (4)) to afford the cyclic carbonates will be the target of Chapter 2. Another important reaction employs the same reagents as that of the cycloaddition reaction (epoxides and CO₂), but yields a polycarbonate product. The reaction relies on metal catalysts, with homogeneous cobalt or aluminum catalysts being very active.^{57,58} Other examples of reactivity highlight the library of different

products that can be built from CO₂. Examples are the preparation of carbonates from propargylic alcohols (reaction (5)) the carboxylation of alkynes (reaction (6)),^{59,60} the synthesis of quinazolidines (reaction (7))^{61,62} or the production of ureas from the reaction of CO₂ with ammonia (reaction (8)).⁶³ Several other transformations use CO₂ as a chemical building blocks, and excellent reviews summarize the latest advances.¹¹ Interestingly, many of the transformations presented in Figure 1.2.5 can be catalyzed by ILs, which can be seen as “preferential” catalysts for CO₂ applications.

1.3. Ionic liquids as preferential catalysts for CO₂ applications

This introduction was published as: ChemPlusChem, 2018, 83, 7-18.

List of authors: Pavel Izák, **Felix D. Bobbink**, Martin Hulla, Martina Klepic, Karel Friess, Štěpán Hovorka, Paul J. Dyson

Statement of contribution: the selected part of the published review that has been copied in this thesis has been co-written by Felix D. Bobbink.

Ionic Liquids (ILs) are somewhat arbitrarily defined as salts with a melting point below 100 °C.⁶⁴ Due to a number of key features of these salts, including low toxicity, negligible vapor pressure under ambient conditions and high electrical conductivity, ILs have received considerable interest in a wide and diverse range of applications.⁶⁵⁻⁶⁷ A near infinite number of cations and anions could potentially combine to form ILs, which facilitates the design of ILs with specific properties for targeted applications,⁶⁸ with the most commonly studied ILs based on imidazolium-, ammonium-, phosphonium- and pyridinium cations (Figure 1.3.1, structures **1-4**).⁶⁹ Since some ILs are liquid at room temperature and have negligible vapor pressure, they are considered as *green* alternatives to volatile organic solvents.⁷⁰ However, due to their intriguing properties ILs have been explored in many applications,⁷¹ notably as electrolytes⁷² and catalysis.^{66,73} Some ILs are used commercially, as propellant in satellites, as lubricants, etc.^{74,75}

ILs can be classified according to the functional group(s) present on the cation or the anion. For example, Brønsted acidic ILs (aILs, Figure 1.3.1, structures **5-8**), which are frequently employed as dual solvent-catalyst systems in acid-catalyzed reactions.^{76,77} If a polymerizable group is present, the ILs are referred to as polymerizable ionic liquids and their polymeric analogues are classified as polymeric ionic liquids or poly-ionic liquids (pILs). Both the cation and anion may possess a polymerizable group, for example vinyl or vinylbenzyl,⁷⁸ and once polymerized the materials possess vastly different physical properties to the monomer (lower affinity for water, lower solubility, higher thermal stability, etc.). PILs based on phosphonium, imidazolium and ammonium cations have been particularly well studied (Figure 1.3.1, structures **9-13** shows examples of imidazolium-based polymers).^{79,80} Notably, pILs have found applications in membrane technologies (see below) as well as in heterogeneous catalysis. Supported ILs (sILs) comprise a similar class of solid materials in which ILs are covalently attached to a surface (Figure 1.3.1, structures **14-17**).^{81,82} Commonly used supports include polystyrene,⁸³ silica,⁸⁴ polyethylene glycol,⁸⁵ and ferromagnetic beads.⁸⁶ The resulting materials have been employed as heterogeneous catalysts⁸⁷ and

as anti-microbial materials.⁸⁸ Some excellent reviews highlight recent advances in the field of pILs/sILs including the synthesis of these materials.^{79,89}

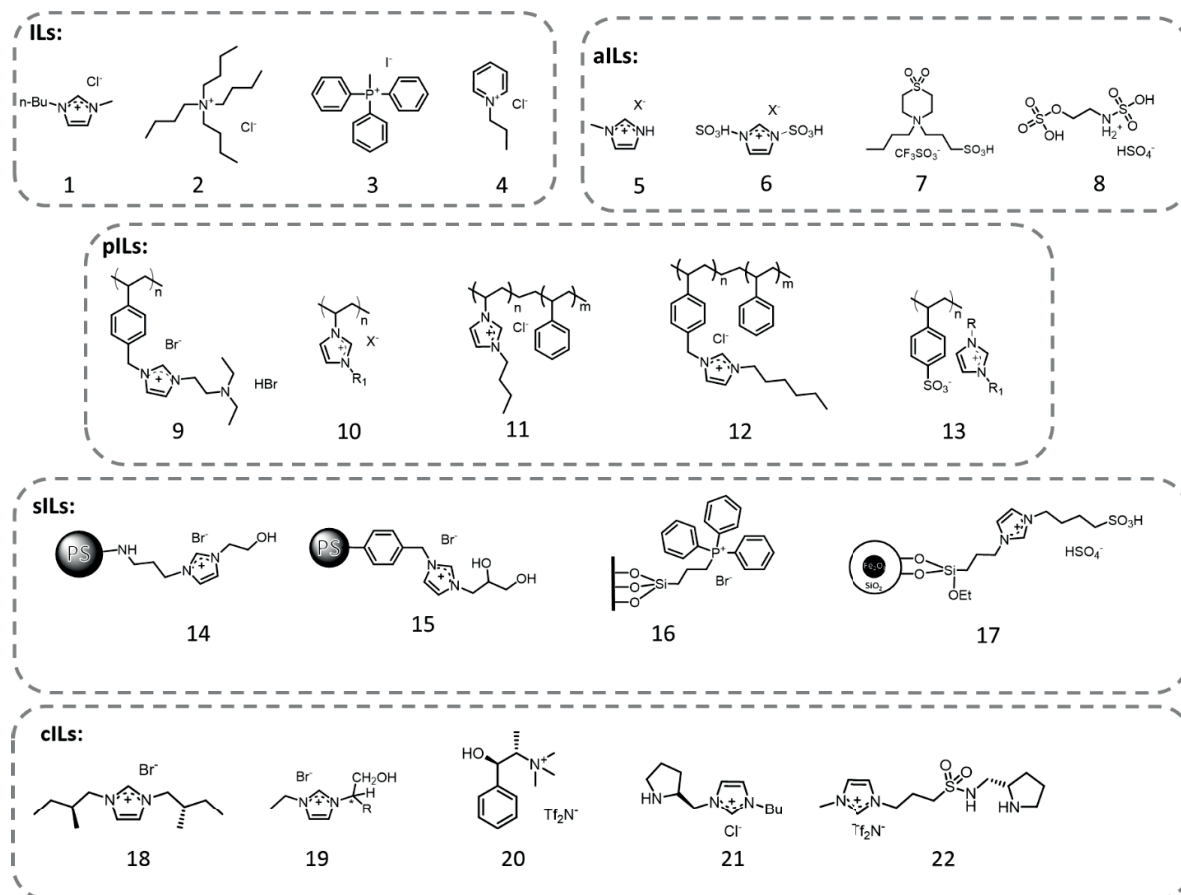


Figure 1.3.1 Examples of ILs.

ILs are highly versatile catalysts and have been evaluated in a wide range of transformations including C-C, C-O and C-N bond forming reactions (Figure 1.3.2). ILs have been intensively investigated for applications in sustainable chemistry such as CO₂ transformations and biomass processing.⁹⁰ For example, the simple alkyimidazolium salts, 1-butyl-3-methylimidazolium chloride ([BMIm]Cl) and 1-ethyl-3-methylimidazolium chloride ([EMIm]Cl), demonstrate catalytic activity in a range of CO₂ transformations (Figure 1.3.2) and subsequent modifications to the cation has led to the development of highly active ILs optimized for specific reactions.

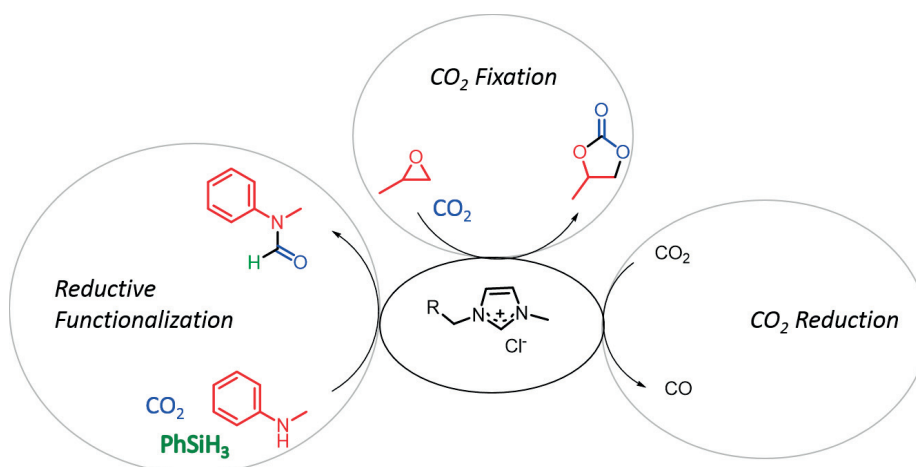


Figure 1.3.2 Selected transformations in which simple ILs have been employed as catalysts.^{33,91,92}

[BMIm]Cl has been employed as a catalyst in the synthesis of cyclic carbonates from the cycloaddition reaction of CO₂ to epoxides (CCE reaction), a reaction performed on an industrial scale.⁸⁷ Subsequently, a large number of modified imidazolium salts and other ILs and pILs have been explored as catalysts for the CCE reaction. The CCE reaction has, to some extent, become a benchmark reaction for IL-catalysis in CO₂ transformations⁹³ and catalyst design has led to the development of pILs catalysts capable of catalyzing the CCE reaction under very mild conditions.⁹⁴ These insoluble pILs facilitate product extraction and catalyst recycling, with specific functional groups attached to the IL monomers enhancing catalytic activity. Recent studies have focused on the preparation of structurally defined mesoporous and nanoporous pILs which show high catalytic activity in the CCE reaction and operate under mild conditions.^{16,95} The utilization of ILs and pILs as catalysts for the CCE reaction will be further detailed in Sections 2.1 to 2.6.

[BMIm]Cl also catalyzes the reductive N-functionalization of amines with CO₂ as a C1-source and hydrosilane reducing agents.⁹² The products, N-formylamines and N-methylamines, are important building blocks for pharmaceuticals and agrochemicals.^{96,97} Indeed, the use of CO₂ in these transformations is relatively recent,⁵⁰ and the use of IL catalysts makes these reactions cheap and simple to conduct. Mechanistic studies of the N-formylation reaction led to the discovery that N-tetrabutylammonium fluoride (TBAF), a simple ammonium-based salt, catalyzes the reaction under ambient conditions.⁹⁸ The reaction proceeds *via* activation of the hydrosilane reducing agent by nucleophilic anions resulting in a hypervalent silicon species able to directly reduce CO₂. The N-methylation and N-formylation reaction will be presented in more details in Section 3.1.

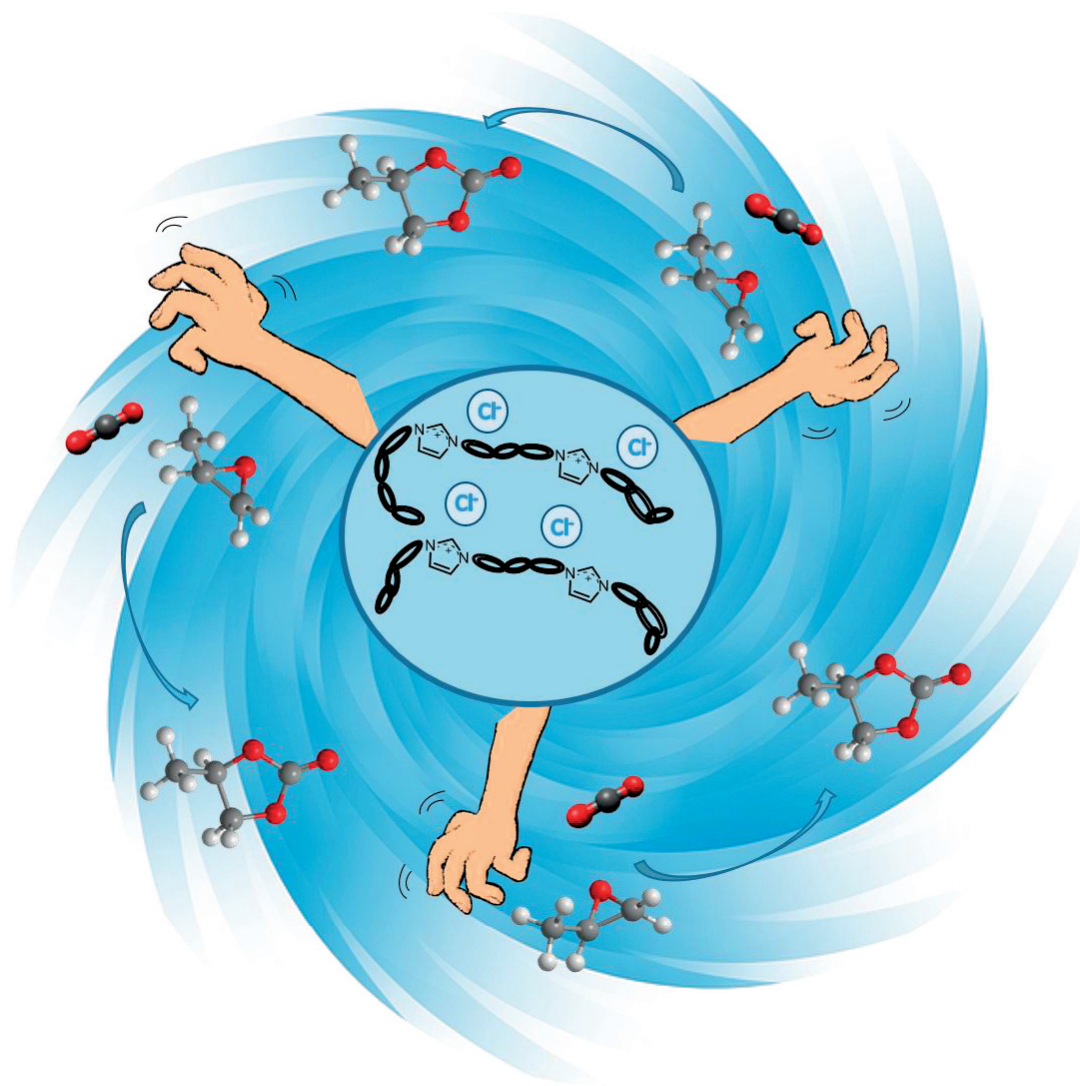
1.4. Structure of the thesis

The first chapter of the thesis will focus on the synthesis, characterization and utilization of novel ionic polymer catalysts for the cycloaddition reaction between CO₂ and epoxides (CCE reaction), resulting in cyclic carbonates. Despite the fact that this reaction was first described more than fifty years ago, it continues to attract attention. This is due to the fact that propylene carbonate, one of the target products of the reaction, is a platform chemical prepared on multiton scale. Moreover, the reaction is an example of industrialized process employing CO₂ as a reagent.

The state-of-the-art IL catalysts for the CCE reaction is reviewed (Section 2.1) as well as details on the mechanism of the transformation. A more complete mechanistic study is provided in Section 2.2. Then, details are provided on the synthesis and utilization of linear ionic (poly)styrenes in the reaction (Section 2.3). Following this, the preparation of cross-linked ionic (poly)styrenes that were employed as heterogeneous catalysts (Section 2.4) is discussed. Subsequently, the preparation of cross-linked polymers that were directly prepared from the condensation reaction between a substituted imidazole and an organohalide compound (Section 2.5) are summarized. Finally, based on the knowledge gained from the transformation, a prototype reactor containing an IL:epoxide capable of quantitatively capturing CO₂ from air and related gas streams was developed (Section 2.6).

The second part of the thesis (Chapter 3) describes the contributions made to the field of soft approaches for functionalization employing CO₂ as the C1 source. The N-methylation and N-formylation of amines using CO₂ as the carbon source and a hydrosilane as the reducing agent is discussed in the form of a protocol (Section 3.1). Then, the cyclic carbonate synthesis from diols and CO₂ (Section 3.2) under metal-free catalysis is detailed. Section 3.3 discusses the synthesis of an ionic liquid bearing a tertiary amine that was utilized in combination of tris(pentafluorophenyl)borane to activate and reduce CO₂. The initial design proposed this combination to produce an ionic frustrated Lewis pair, but finally a boron-nitrogen adduct was formed. Section 3.4 details the work on methanol synthesis from cyclic carbonates, which can be derived directly from epoxides and CO₂. Formally, this reaction reduces CO₂ to methanol in two-steps using a simple metal-free ammonium catalytic system that is able to catalyze both steps.

2. Synthesis of ionic poly(imidazolium) salts and their application in the cycloaddition of CO₂ into epoxides



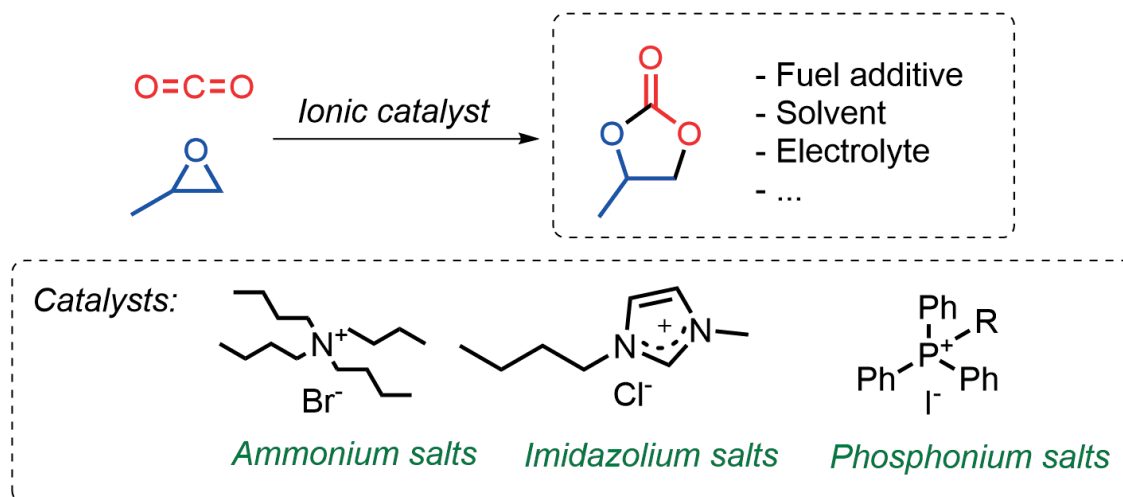
Cover picture for the article *ChemSusChem*, **2017**, *10*, 2728–2735.

2.1. Ionic catalysts for the CCE reactions: state-of-the-art:

This introduction is published as a review article in *J. Catal.* **2016**, *343*, 52-61.

List of authors: **Felix D. Bobbink**, Paul J. Dyson.

Graphical abstract:



2.1.1. Properties and applications of cyclic carbonates

Five-membered cyclic carbonates (Figure 2.1.1) have many diverse applications⁹⁹ and are produced industrially on multiton scales.¹⁰⁰ Small cyclic carbonates (ethylene carbonate, EC, and propylene carbonate, PC) may be prepared from the cycloaddition of CO₂ with the corresponding epoxide (Scheme 2.1.1), typically using alkylammonium halide catalysts.¹⁰¹ Other routes for carbonate production tend to be less attractive because they require the use of toxic reagents such as phosgene.¹⁰²

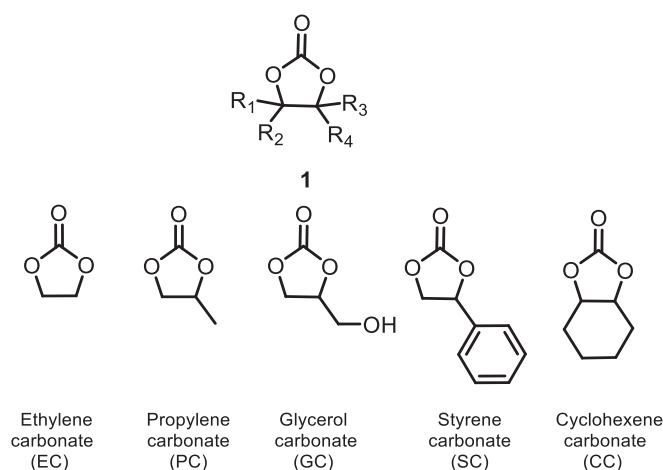
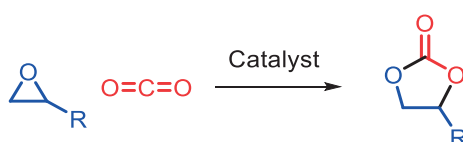


Figure 2.1.1 General structure of a cyclic carbonate (top) and selected examples (bottom).

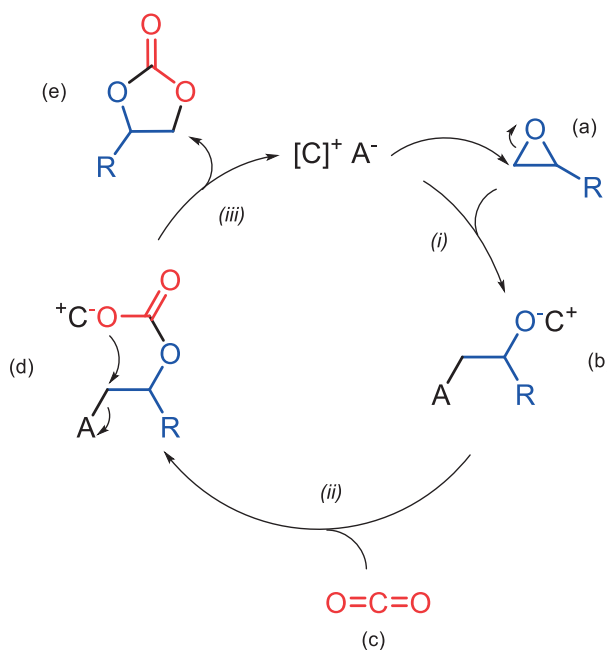


Scheme 2.1.1 Generic CCE reaction.

Ethylene carbonate (EC) and propylene carbonate (PC) are widely used as solvents,¹⁰³ are used in biomass liquefaction,¹⁰⁴ and may be converted in dimethyl carbonate which is a fuel additive¹⁰¹ and methylating agent.¹⁰⁵ EC and PC are also used in lithium batteries,¹⁰⁶ and PC is found in cosmetics products as it is non-toxic.¹⁰⁷ Glycerol carbonate (GC) can be obtained from glycerol (a bio-based product),¹⁰⁸ and is used as a solvent,¹⁰⁹ in cosmetics¹¹⁰ and in batteries.¹¹¹ Styrene carbonate (SC) and bicyclic cyclohexene carbonate (CC) can be converted to polycarbonates and subsequently to polyurethanes.¹¹² Recently, Bayer announced an industrial process for polycarbonate synthesis incorporating 20% CO₂ for the production of polyurethanes,¹¹³ which have many applications as materials.¹¹⁴

2.1.2. Mechanism of the CCE reaction

The mechanism of the CCE reaction catalyzed by salts is depicted in Scheme 2.1.2. In the first step the epoxide (**a** in the scheme) is opened *via* nucleophilic attack of the anion of the catalytic ion pair (step *i*). Consequently, strong nucleophiles such as halide ions are often used for this reaction.¹¹⁵ This ring opening step is facilitated if the catalyst is able to further activate the oxygen of the three membered ring, for example by H-bonding, typically with an alcohol functional group tethered to the cation as shown in the scheme (intermediate **b**).¹¹⁶ The obtained alkoxide is stabilized by the cation in order to facilitate the insertion of CO₂ (species **c**) which takes place in the next step (*i.e.* step *ii*). This prerequisite rationalizes why simple salts such as NaCl are inefficient catalysts for the CCE reaction unless they are strongly solvated and associated with an organic solvent such as N-methylpyrrolidine.¹¹⁷ With imidazolium salts the alkoxide can potentially deprotonate the acidic C2 proton to generate the corresponding N-heterocyclic carbene (NHC). However, it has been demonstrated that this reaction does not appear to take place when the C2 proton is substituted by a methyl group, *i.e.* the reaction rates of the two imidazolium salts are essentially the same.¹¹⁸ After insertion of CO₂ a 5-membered ring is obtained by elimination of the anion of the ion pair, *via* a S_N2-type mechanism (Scheme 2.1.2, step *iii*). Thus, the anion should be both a good nucleophile and a good leaving group, whereas the cation should provide favorable interactions to stabilize the intermediates.¹¹⁹ In such a process, the interactions between the anion and cation in the catalyst are critical and should be optimized to maximize the catalytic process. Several computational studies have been performed that provide further mechanistic insights into the reaction. It has been shown that there is a difference of >20 kcal/mol in the rate-determining step in the presence or absence of a catalyst,¹²⁰ and that the rate-determining step comprises the ring-opening of the epoxide. These predictions were subsequently confirmed using ammonium salt catalysts in the DFT simulation.¹²¹ Recent experimental results from our laboratory explored the influence of the C4- and C5 proton of the imidazolium ring, and studied the cation-anion intricacies of the reaction. Details are provided in Section 2.2.



Scheme 2.1.2 General mechanism for the cycloaddition of CO₂ to epoxides using ionic catalysts. (i) Ring-opening of epoxide by anion of the ion pair. (ii) Insertion of CO₂ into the generated alkoxide. (iii) Release of product by ring-closing S_N2.

2.1.3. IL catalysts for the CCE reaction

Many classes of ILs have been reported and many have been used to catalyze the CCE reaction, including ILs based on imidazolium,¹²² ammonium,¹²³ phosphonium and pyridinium¹²⁴ salts. A wide range of anions have also been explored with halides generally leading to best activities.⁷¹ It should be noted that in other types of reactions ILs have been designed to improve catalytic processes (see introduction Section 1.3).^{90,125} Although ILs are considered green alternatives to volatile organic solvents, primarily due to their low vapor pressure¹²⁶ and high stability,¹²⁷ it should be noted that some ILs are unstable¹²⁸ and some are not readily biodegradable.^{129,130}

2.1.4. Ammonium-based ILs

Certain ammonium-based salts may be classified as ILs (examples are given in Figure 2.1.2) and have been used to catalyze the CCE reaction. These salts are usually prepared from tertiary amines by reaction with appropriate alkyl halides and, when necessary, the anion can be exchanged by reaction with a suitable acid or Group 1 metal salt,¹³¹ although complete removal of halide impurity can be challenging.¹³² It would appear that the first examples of a metal-free catalyst for the CCE reaction employed ammonium salts.¹³³ For example, tetrabutylammonium chloride catalyzes the formation of PC under relatively mild

conditions,²⁴ and a mixture of tetrabutylammonium bromide and iodide (TBAB (**1**) and TBAI) may also be used to catalyze the reaction.¹²³

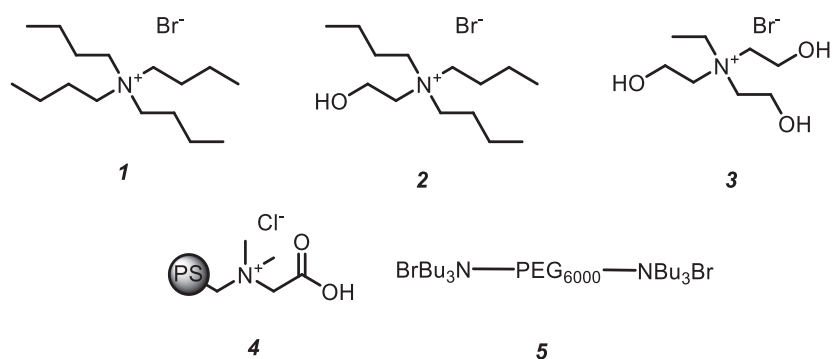


Figure 2.1.2 Examples of ammonium salt CCE catalysts. **1** tetrabutylammonium bromide (TBAB), **2** hydroxyethyltributylammonium bromide (HETBAB), **3** tris(hydroxyethyl)ethylammonium bromide (NET(HE)₃Br), **4** N,N-dimethylglycine on polystyrene (PS-QNS) and **5** PEG-supported quaternary ammonium salt (PEG₆₀₀₀(NBu₃Br)₂).

Various studies were undertaken to optimize the ion pairs employed in the CCE reaction, which support the mechanism described above. Ammonium salts with short alkyl chains are less efficient than longer chain alkyl ammonium salts, and the reactivity of the catalyst also decreases when fluoride is used as the counter anion.¹³⁴ As mentioned above, a cation that stabilizes the alkoxide intermediate *via* H-bonding could potentially enhance the activity of the catalyst and, for this reason, hydroxyl-functionalized ammonium salts emerged as potent catalysts for the CCE reaction. The effect of hydroxyl functionalized ammonium salts was studied with the highest activities obtained when three hydroxyl groups are present (Figure 2.1.2, **3**). Interestingly, under the experimental conditions, the authors showed that tetrahydroxyethyl ammonium salts provided lower activities.¹³⁵ Microreactor technology in combination with **2** was used to produce PC in 99% yield under 35 bars of CO₂ at a residence time of only 14 seconds.¹³⁶ Other ways to improve the processing properties of quaternary ammonium salt catalysts involve grafting the cation onto polystyrene¹³⁷ or polyethylene glycol supports⁸⁵ (Figure 2.1.2, **4-5**), providing solid catalysts that are easily recovered and reused. Quaternary ammonium salts were also attached covalently to carbon nanotubes, but the resulting catalyst is significantly less active than the polystyrene and polyethylene glycol supported systems.¹³⁸ Table 2.1.1 lists some catalysts and conditions employed in the CCE reaction. The Table highlights the differences between a simple ammonium salt, an alcohol-functionalized ammonium salt, and a supported functionalized and non-functionalized ammonium salts, although care must be taken when comparing the data in the Table as the conditions employed differ.

Table 2.1.1 Examples of selected ammonium salt catalysts under optimized conditions.

Catalyst ([mol%])	Epoxide	Temp [°C]	Pressure [bar]	Time [h]	Yield [%]	Ref.
1 (1)	PO	100	30	2	56	121
3 (1)	PO	130	15	1	97	135
4 (1.1)	PO	140	80	8	96	137
5 (0.5)	PO	120	80	6	98	85

2.1.5. Imidazolium-based ILs

The capacity of imidazolium salts to form hydrogen bonds with all three ring protons potentially makes them particularly attractive as catalysts for CCE reactions. The acidic C2 proton is not essential for catalytic activity,¹¹⁸ as the other two ring protons are able to form hydrogen bonds.¹³⁹ Routes to prepare imidazolium salts are very well documented and described throughout literature.¹⁴⁰ Simple ILs can be prepared from 1-methylimidazole as the N-atom is nucleophilic and readily reacts with suitable organohalides to generate an imidazolium salt (1-methylimidazole is obtained from the Radziszewski reaction).¹⁴¹ Sodium imidazolidate may be used as a precursor to generate compounds with two different substituents onto the imidazolium ring.¹⁴² Reactions are often conducted in the absence of solvent, but care should be taken as the reaction is exothermic¹⁴³, the viscosity can be high¹⁴⁴ and the resulting IL may be very hygroscopic.¹⁴⁵

Following the first report of CCE reactions catalyzed by imidazolium salts in 2001,⁹³ a plethora of related catalysts have been reported. Initially, the 1-methyl-3-butylimidazolium cation ([Bmim]⁺) was evaluated for catalytic activity with various anions (Figure 2.1.3, **1**). With BF₄⁻, a yield of 90.3% of PC was obtained after 6 hours at 110 °C under 25 bars of pressure. In more recent reports it has been shown that BF₄⁻ salts are less active than Cl⁻ salts.

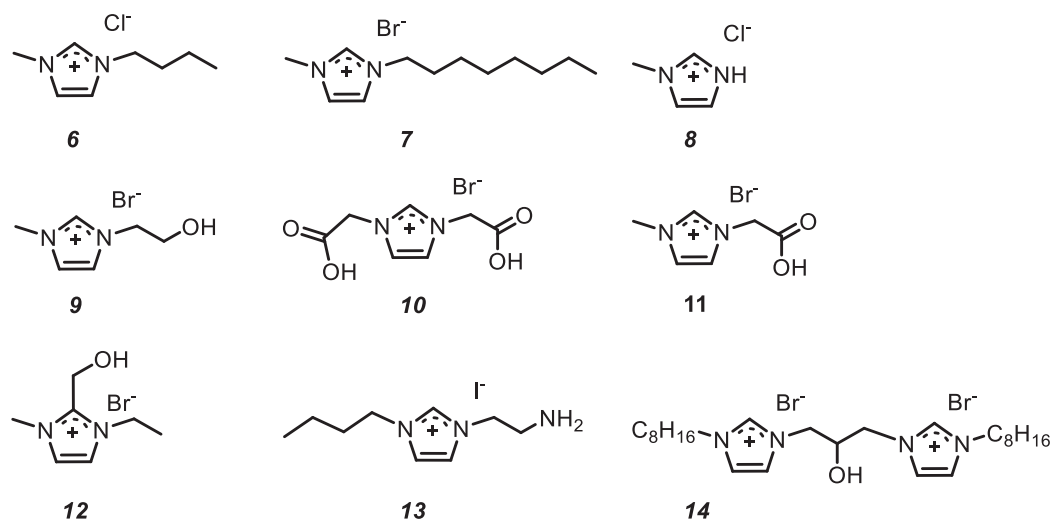


Figure 2.1.3 Examples of imidazolium-based ILs used to catalyze the CCE reaction. **6** 3-butyl-1-methylimidazolium chloride ([bmim]Cl), **7** 3-octyl-1-methylimidazolium bromide ([omim]Br), **8** 1-methylimidazolium bromide ([hmim]Br), **9** 3-hydroxyethyl-1-methylimidazolium bromide ([hemim]Br, **10** bis-carboxylic acid functionalized imidazolium bromide, **11** 3-(ethanoic acid)-1-methylimidazolium bromide, **12** 2-hydroxymethyl-1-methyl-3-ethylimidazolium bromide, **13** 1-(3-aminopropyl)-3-butylimidazolium iodide ([apbim]I) and **14** hydroxy-functionalized bisimidazolium bromide.

Similar to that observed for ammonium salts, the introduction of a hydroxyl group in **9** enhances catalytic activity, with yields of PO of 99% obtained under 20 bars of CO₂ at 125 °C in 1 hour.¹¹⁶ If the hydroxyl group is placed at the C2 position of the ring (Figure 2.1.3, **12**) the activity of the resulting catalyst is very similar.¹⁴⁶ A series of Brønsted acidic imidazolium salts (Figure 2.1.3, **10-11**) are efficient CCE catalysts,¹⁴⁷ with the catalytic activity correlated to the pKa of the acidic moiety attached to the imidazolium ring. Presumably, the acidic proton facilitates ring-opening of the epoxide.¹⁴⁸ Several other carboxylic acid functionalized ILs were reported and show comparable activities.^{149,150} A dicationic imidazolium salt (Figure 2.1.3, **14**) with a hydroxyl group operates under relative mild conditions (70 °C and 4 bars of CO₂) albeit at high catalyst loadings (5 mol%) and long reaction times, thus making direct comparisons difficult. However, under the optimized conditions, PC is obtained in 95% yield, whereas **9** affords PC in 32% under the same conditions.¹⁵¹ Longer alkyl chain imidazolium salts such as **7** show enhanced activities compared to the short chain ILs.¹⁵² These results are consistent with the ammonium salts where longer alkyl chains also gave higher yields.

A series of amino-functionalized imidazolium salts (Figure 2.1.3, **13**) were evaluated in the CCE reaction,¹⁵³ with the best amine-functionalized IL yielding PC in 94% compared to 53% in [Emim]Br under the same

conditions. Simple protic ILs such as **8**, in which the H-donor is directly attached to the imidazolium ring, were also used to catalyze the CCE reaction in high yield.¹⁵⁴

As in the case of ammonium salts, efforts have been made to heterogenize imidazolium salts, and several approaches were studied. Heterogeneous catalysts incorporating a hydroxyl-functionalized imidazolium salt were prepared *via* copolymerization of vinyl-functionalized imidazoliums with divinylbenzene (Figure 2.1.4, **21**).^{155,156} In a slightly different approach imidazolium salts have been anchored to a polystyrene resin.⁸³ The catalyst also incorporates a diol unit (Figure 2.1.4, **16**), which is able to form favorable interactions with reaction intermediates, leading to high catalytic activities.

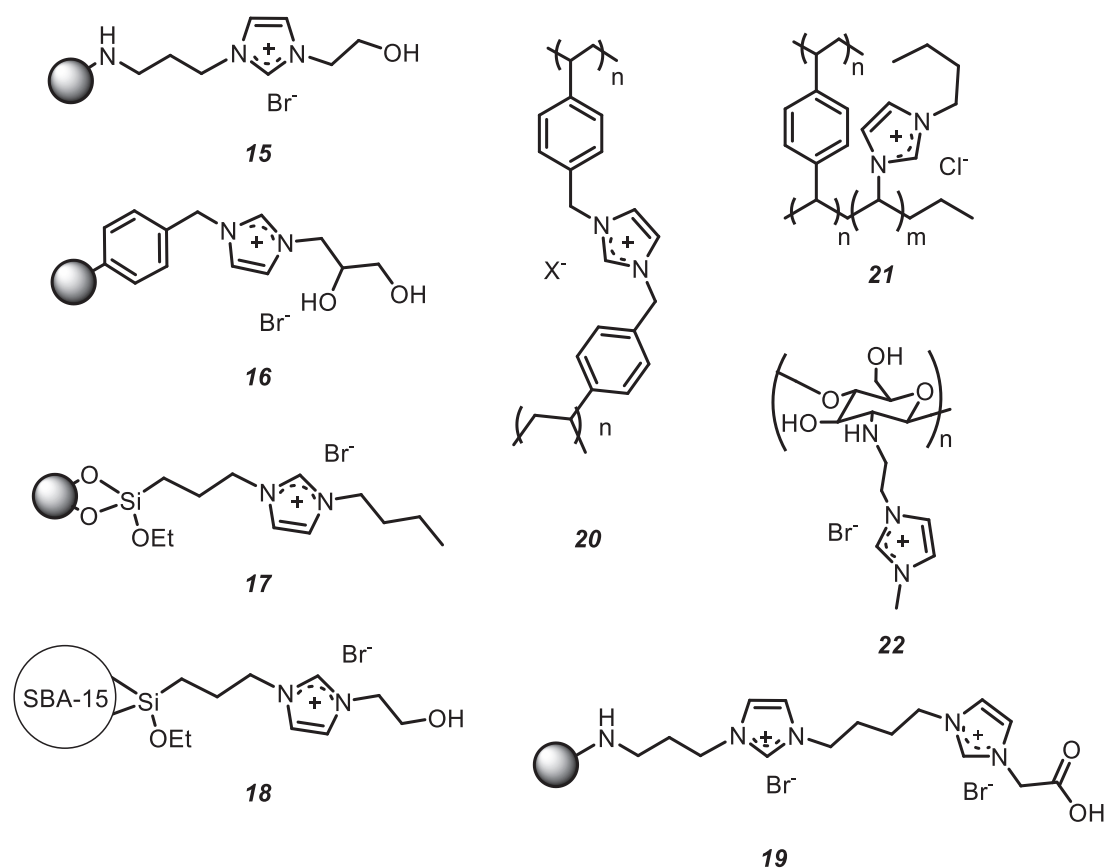


Figure 2.1.4 Examples of supported imidazolium salts used to catalyze the CCE reaction. **15** 3-(2-hydroxyethyl)-ethyl-1-(3-amino-propyl)imidazolium bromide grafted on a divinylbenzene polymer ([pdvb-heim]Br), **16** diol functionalized imidazolium salt grafted onto commercial polystyrene resin ([PS-DHPIM]Br), **17** alkyl imidazolium salt grafted onto commercial silica, **18** 3-(2-hydroxyethyl)-1-propylimidazolium bromide immobilized on SBA-15 ([SBA-15-hepim]Br), **19** polymer grafted with functionalized di-cationic imidazolium IL ([P-FDILs]), **20** bis(1,3-vinylbenzyl)imidazolium chloride (poly[bvbim]Cl), **21** cross-linked polymer-supported IL (PSIL) and **22** 3-ethyl-1-methylimidazolium bromide bound to chitosan ([CS-emim]Br).

Other supports used to immobilize imidazolium cations include cross-linked polymers (Figure 2.1.4, **15**),⁸² functionalized ferromagnetic beads,⁸⁶ and functionalized chitosan (Figure 2.1.4, **22**),¹⁵⁷ and other biopolymers.¹⁵⁸ Since chitosan is the second most abundant bio-polymer after cellulose,¹⁵⁹ and possesses several hydroxyl groups, it is ideal for this application.

Cross-linked polymers obtained from an imidazolium salt with two styrene groups (Figure 2.1.4, **20**)⁹¹ or the reaction of vinyl imidazolium with divinylbenzene,¹⁶⁰ or with acrylates,¹⁶¹ have been evaluated in CCE reactions, as have imidazolium salts grafted on different types of silica (Figure 2.1.4, **17**).^{162,163} In these latter types of materials the imidazolium cations are easily functionalized (Figure 2.1.4, **18**).¹⁶⁴ Furthermore, a supported dicationic species with a carboxylic acid functional group was synthesized and its catalytic activity evaluated (Figure 2.1.4, **19**).¹⁶⁵ All the aforementioned heterogeneous systems are reasonably good catalysts for the CCE reaction, with the main advantage over simple ILs corresponding to more facile product recovery and catalyst recycling. Table 2.1.2 summarizes some conditions employed in the CCE reaction using various catalysts which highlights the difference between different imidazolium salts.

Table 2.1.2 Examples of selected imidazolium salt catalysts under optimized conditions.

Catalyst ([mol%])	Epoxide	Temp [°C]	Pressure [bar]	Time [h]	Yield [%]	Ref.
6 (1.5)	PO	110	20	6	63.8	93
9 (1.6)	PO	125	20	0.7	99.2	116
15 (0.44)	PO	140	20	4	97.6	82
20 (1)	Epichlorohydrin	140	50	3	98	91

2.1.6. Phosphonium-based ILs and other ionic pairs

A series of Lewis basic ILs catalysts derived from DBU were evaluated in the CCE reaction with **23** being the most potent catalyst of the series.¹⁶⁶ While DBU is essentially inactive, [DBUH]Cl affords PC in 97% yield at 140 °C, 10 bars of CO₂ after 2 hours with catalyst loading of 1 mol%. In comparison [BMIm]Br affords only 54% and [OMIm]Br 85% under the same conditions.

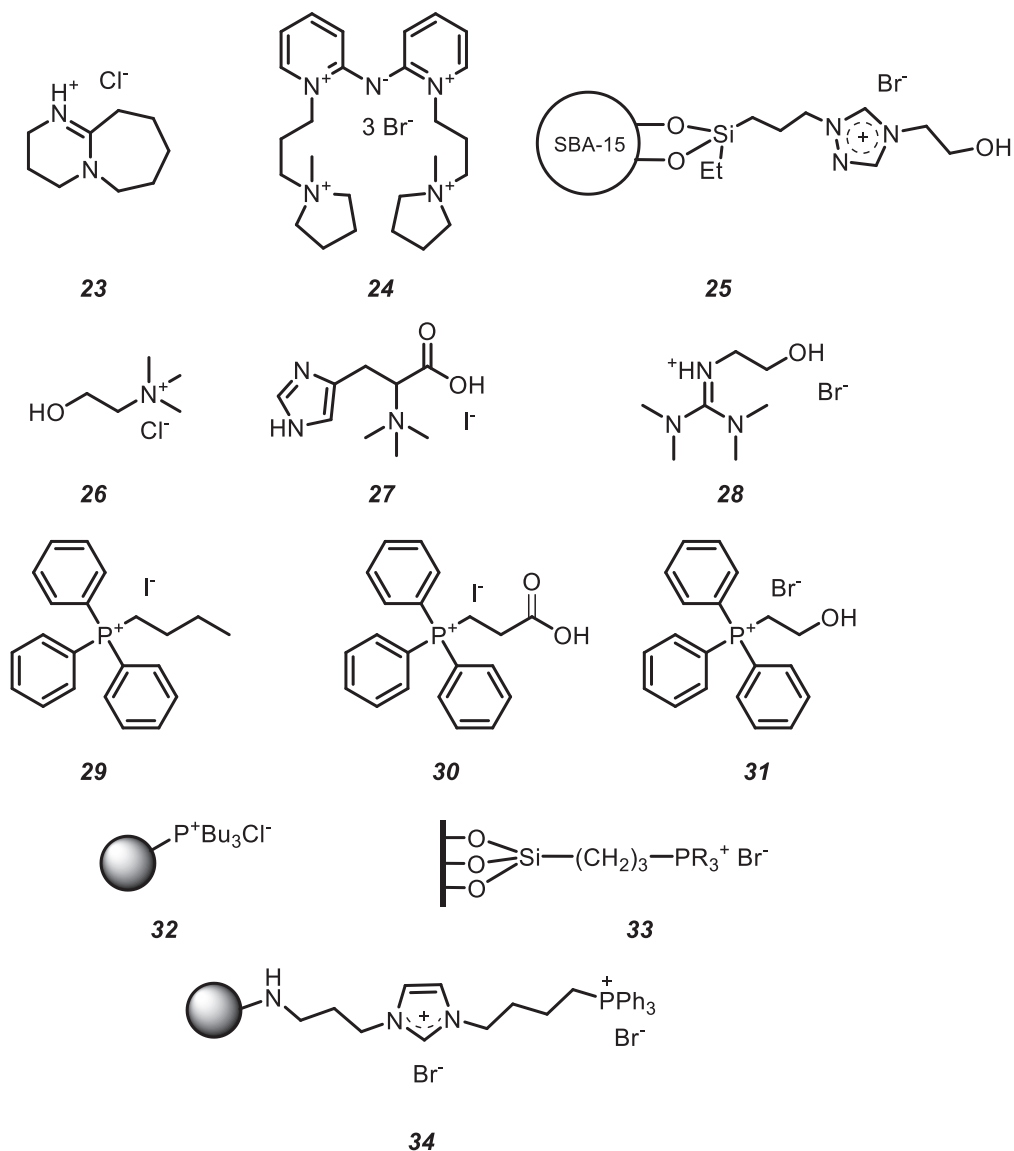


Figure 2.1.5 Examples of N-based catalysts and phosphonium IL CCE catalysts. **23** 1,8-diazabicyclo[5.4.0]undec-7-enium chloride ([hdbu]Cl), **24** dipyriddyamine bridged with two pyrrolidinium moieties, **25** triazolium salt grafted onto mesoporous silica SBA-15, **26** choline chloride, **27** histidine derived IL (His-Mel), **28** hydroxyl functionalized tetramethyl guanidine ([hetmg]Br), **29** butyl-triphenylphosphonium iodide ([PPh₃Bu]I), **30** carboxylic acid functionalized phosphonium salt ([PPh₃C₂H₄COOH]I), **31** hydroxyl functionalized phosphonium salt ([hePPh₃]Br), **32** phosphonium salt formed by reaction of tributylphosphine with chloromethylated polystyrene ([PS-QPS]), **33** organic-inorganic hybrid catalyst containing a phosphonium salt and **34** Polymer grafted with asymmetrical dicationic IL with imidazolium and phosphonium ([P-Im-C₄H₈Ph₃P]Br₂).

Somewhat more elaborate tricationic species (Figure 2.1.5, **24**) containing pyridinium and pyrrolidinium cations have also been reported to catalyze the CCE reaction in the presence of 2 wt% water.¹²⁴ Interestingly, while most reports make efforts to exclude water from the experimental setup, with this catalyst it was necessary to add 2 wt% water to give an active catalyst solution. Related pyridinium salts were evaluated using computational methods, indicating that most functional groups attached on the nitrogen of the pyridine would not enhance the catalytic activity, with the exception of carboxylic acids.¹⁶⁷ In contrast to imidazolium and ammonium salts, hydroxyl functional groups on a pyridinium salt is expected to lower the catalytic potential of the salt, suggesting that the mechanism of the CCE reaction catalyzed by pyridinium ions is slightly different compared to the mechanism with imidazolium salts.

Triazolium salts are structurally related to imidazolium salts, but exhibit vastly different reactivities. A triazolium IL grafted onto a series of SBA-15 molecular sieves (Figure 2.1.5, **25**) led to only moderately active catalysts, even though the triazolium was functionalized with a hydroxyl functional group.¹⁶⁸ Choline chloride (Figure 2.1.5, **26**) combined with urea was also used to catalyze the CCE reaction.¹⁶⁹ When mixed, these two reagents form a deep eutectic solvent,¹⁷⁰ and the IL mixture could be incorporated in molecular sieves which allows easy recycling. Under optimized conditions PC is formed in 99% yield after 5 hours at 110 °C with a 1 mol% catalyst loading, whereas when choline chloride was used alone PC was obtained in only 85% yield, showing that the formation of the deep eutectic solvent also provided favorable interactions for the CCE reaction. ILs derived from natural amino acids (Figure 2.1.5, **27**) afford catalysts with activities comparable to **9**.¹⁷¹ Guanidinium-based ILs (Figure 2.1.5, **28**) are highly active catalysts affording PC in 95% yield under conditions in which **9** affords PC in 58% yield,¹⁷² presumably with the basicity of the guanidinium being responsible for the high activity. Phosphonium-type ILs have also been evaluated in the CCE reaction and the simple salt **29** is a potent catalyst when used in combination with water and, in this system, the water was proposed to facilitate opening of the epoxy ring.¹¹⁵ Functionalized phosphonium salts have also been evaluated, with hydroxyl and carboxyl derivatives showing excellent activities (Figure 2.1.5, **30-31**).¹⁷³ Compared to triphenylphosphonium salts **30** and **31**, less sterically hindered tributylphosphonium salts were also evaluated as bifunctional catalysts, demonstrating the importance of dual activation in the CCE reaction.^{174,175} Halide-free phosphonium salts were evaluated in the CCE reaction, but the yields are modest.¹⁷⁶ Similarly to the ammonium and imidazolium salts, phosphonium-based ILs have also been anchored to polymer supports by reaction of the suitable phosphine with chloromethylpolystyrene.¹⁷⁷ A hybrid organic-inorganic material comprising a phosphonium salt grafted onto silica was also shown to be an efficient and recyclable catalyst (Figure 2.1.5, **32-33**).⁸¹ Both these heterogeneous phosphonium salts show good activities, but comparisons with a

simple salt such as **1** or **9** were not reported. A more unique catalyst comprises a dicationic species with both an imidazolium and a phosphonium unit (Figure 2.1.5, **34**), subsequently grafted onto a poly(divinylbenzene). The dicationic species yielded 95% PC after 4 hours reaction at 130 °C and 25 bars of CO₂ with a catalyst loading of 0.38 mol%. The [bmim]Br salt anchored onto the same polymer affords PC in only 75% under similar reaction conditions. The dual catalyst is more effective than both the imidazolium and phosphonium salt used separately,¹⁷⁸ possible due to simultaneous interactions of the substrates with both the imidazolium and phosphonium units. Table 2.1.3 collates some conditions employed in the CCE reaction using various catalyst based on different cations combined with halide anions. Note that the conditions employed vary making direct comparisons problematic.

Table 2.1.3 Examples of selected ion-pair organocatalysts under optimized conditions.

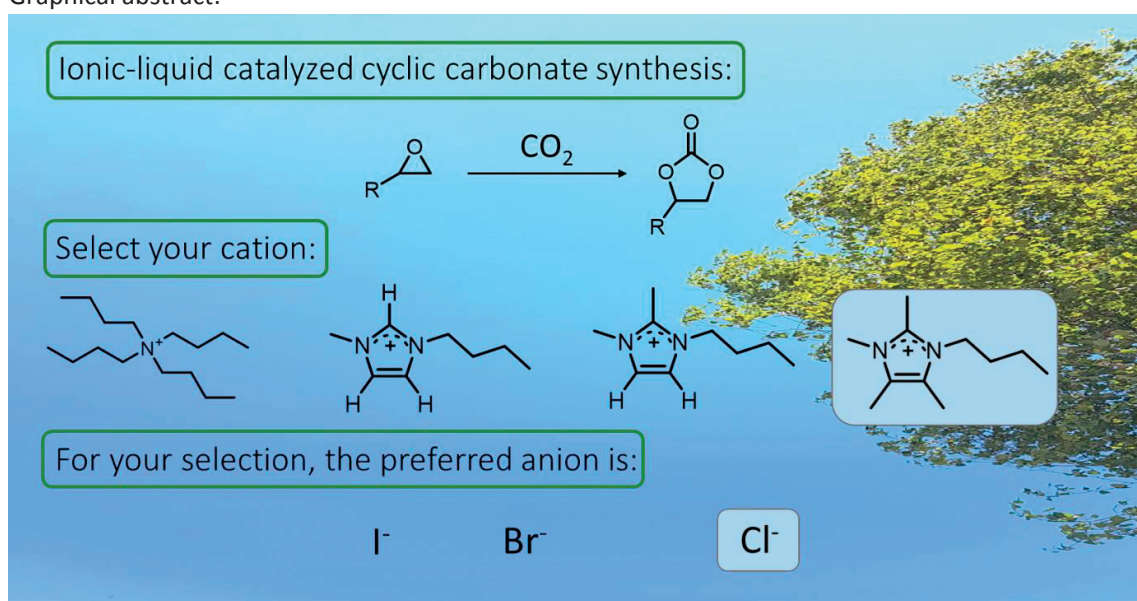
Catalyst ([mol%])	Epoxide	Temp [°C]	Pressure [bar]	Time [h]	Yield [%]	Ref.
23 (1)	PO	140	10	2	97	166
24 (50)	PO	80	40	3	99	124
29 (0.5)	PO	125	20	1	95	115
31 (0.5)	PO	130	25	3	96.5	173

2.2. Intricacies of Cation-anion combination in imidazolium-salt catalyzed cycloaddition of CO₂ into epoxides

This section is published as an article in *ACS Catal.* **2018**, *8*, 2589–2594

List of authors: **Felix D. Bobbink**, Dmitry Vasilyev, Martin Hulla, Sami Chamam, Florent Menoud, Gábor Laurenczy, Sergey Katsyuba, and Paul J. Dyson.

Graphical abstract:



2.2.1. Introduction

As presented in the previous sections, many ionic catalysts have been developed for the CCE reaction. In the case of imidazolium salts, the transformation is proposed to take place in three-steps: (i) ring-opening of the epoxide by the nucleophilic anion of the salt, (ii) insertion of CO₂ into the C2-proton-stabilized alkoxide and (iii) release of the anion *via* an intramolecular S_N2 reaction.¹²⁰ The C2-proton of the imidazolium ring is considered key due to favorable H-bonding interactions with the substrate as well as the alkoxide transition state,¹¹⁹ and both DFT and experimental data have been used to highlight its importance.^{120,179} For example, it was shown that H-bonding could activate the epoxide and decrease the energy barrier of the ring opening step.¹²⁰ Most studies, however, overlook the acidity of the C4 and C5 protons of the imidazolium ring despite their acidity being comparable to that of the C2 proton.¹⁸⁰ Furthermore, when the C2 position is blocked, the halide strongly interacts with the C4 proton in the solid state,¹⁸¹ which could affect the ability of the anion to open the epoxide ring. Moreover, tetraalkylammonium, phosphonium or pyrrolidinium salts do not possess acidic protons capable of forming pronounced H-bonds with the epoxide substrate or the alkoxide transition state, and yet they are potent catalysts for the transformation.¹⁸² Unfortunately, direct comparison between catalysts is hindered by the lack of benchmark conditions⁵⁷ and, since almost every study is “unique”, it is difficult to assess whether true progress is made. Catalyst development is then frequently dependent on quantum calculations, which are often difficult to verify experimentally due to poor solubility of many of these salts, leading to pseudo-heterogeneous conditions.¹⁸³

Hence, we decided to systematically investigate and clarify the role of the acidic C2, C4 and C5 protons of the imidazolium ring, evaluate the influence of the cation on the counter-anion and establish the key differences between the imidazolium and ammonium catalyzed reactions under homogeneous (standardized) reaction conditions. For this purpose, we prepared a series of imidazolium salts with varying number of ring substituents and different halide counter-ions and evaluated them in the CCE reaction using epichlorohydrin as the substrate (Figure 2.2.1 and Table 2.2.1). The activity of these catalysts was compared to that of N-tetrabutylammonium halides and key aspects of the transformation were elucidated with the aid of DFT calculations.

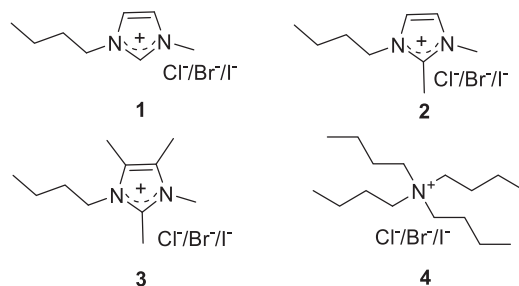
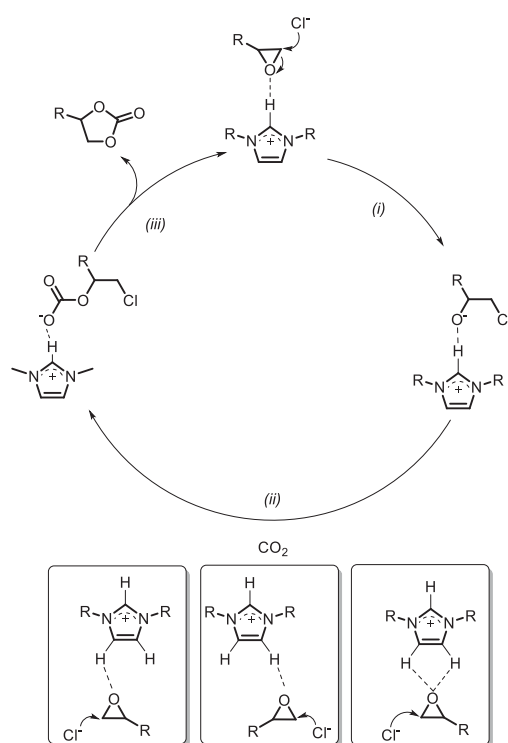


Figure 2.2.1 Salt-based catalysts (**1X** – **4X**, where X = Cl⁻, Br⁻ or I⁻) studied in this work.



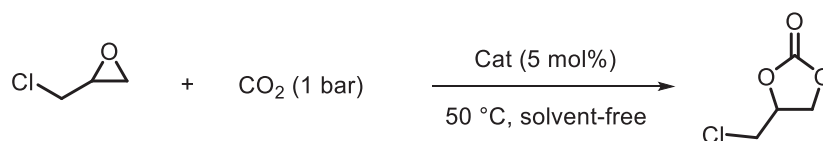
Scheme 2.2.1 Accepted mechanism of the CCE reaction (top) and additional possible H-bonds between the epoxide and the acidic protons on the imidazolium ring (bottom).

2.2.2. Results and Discussion

The salt catalysts, **1X** – **4X** (Figure 2.2.1) were evaluated under a kinetic regime in the cycloaddition reaction between epichlorohydrin and CO₂ at atmospheric pressure without a co-solvent (Table 2.2.1). Note that a similar analysis is not possible with propylene oxide (the most widely used epoxide) at atmospheric pressure as the catalysts are not completely soluble in the substrate, which appears to be frequently overlooked in the literature. Under these standardized reaction conditions, the most common imidazolium

salt, [BMIm]Cl **1Cl**, yielded the product in a 52% yield (Table 2.2.1, entry 1). Methylation of the C2-position, *i.e.* catalyst **2Cl**, resulted in a slightly lower yield of 49 % (Table 2.2.1, entry 2) compared to that obtained with **1Cl** as previously reported,¹¹⁸ indicating that the H-bonding between the epoxide ring or the reaction intermediates with the C2 proton could play a role in the reaction. The relatively small difference between **1Cl** and **2Cl** could possibly be attributed to the H-bonding ability of **2Cl** *via* its C4 and C5 protons. However, the fully substituted imidazolium salt **3Cl**, which cannot form strong H-bonds at any position, resulted in a comparable yield to **1Cl** of 51 % (Table 2.2.1, entry 3). In addition, N-tetrabutylammonium chloride, **4Cl**, is even more active than **1Cl** yielding the product in 56%. (Table 2.2.1, entry 4). These results rule out the possibility that a carbene, formed *via* the deprotonation of the C2 proton or the more rare C4 or C5¹⁸⁴ positions of the imidazolium ring by the alkoxide intermediate (Scheme 2.2.1, step *i*), is the key active catalytic species.^{118,119} In addition, H-bonding does not appear crucial for the catalysis either as the yields are comparable for all the imidazolium salts and the tetrabutylammonium catalyst (52 %, 49 %, 51 % and 56 % for **1Cl** - **4Cl**, respectively), irrespective of whether they can form H-bonds or not.

Table 2.2.1 Influence of the cation and anion on the CCE reaction in the synthesis of epichlorohydrin carbonate.



Entry	Catalyst	Yield (%)
1	1Cl	52
2	2Cl	49
3	3Cl	51
4	4Cl	56
5	1Br	53
6	2Br	46
7	3Br	60
8	4Br	45
9	1I	62
10	2I	50
11	3I	53
12	4I	36

Reaction conditions: epichlorohydrin (1 g, 10.8 mmol), catalyst (5 mol%), CO₂ (1 bar), 50°C, 3 h, average yield from three runs run in parallel to ensure reproducibility (vertical shift error of +/- 3%).

Although the experimental results suggest that H-bonding *via* the ring protons does not play a vital role in the reaction, the substantial computational evidence that suggests otherwise cannot be disregarded, especially with respect to the rate-limiting epoxide ring opening step (Scheme 2.2.1, step *i*).^{179,185} Note,

when additional or external H-bond donors are present, computational findings suggest that the rate-determining step can be, but is not limited to, epoxide ring-opening.^{149,186} Hence, we decided to perform calculations on the energy barrier for the epoxide ring opening with the three imidazolium catalysts **1Cl**–**3Cl**. In addition, we expanded these calculations to include the possibility of the epoxide ring opening *via* participation of the C4 and C5 protons, which were previously not considered.^{118–120,179,187} The strength of C2H...O, C4H...O and C5H...O H-bonds in imidazolium ILs is quite similar,¹⁸⁰ and our DFT computations on the stabilization of the alkoxide show that an energy barrier for the ring-opening step *via* participation of the C4 proton (27.3 kcal·mol⁻¹, Figure 2.2.4) is only marginally higher than the barrier for that of the C2 proton participation (25.9 kcal·mol⁻¹, Figure 2.2.2).

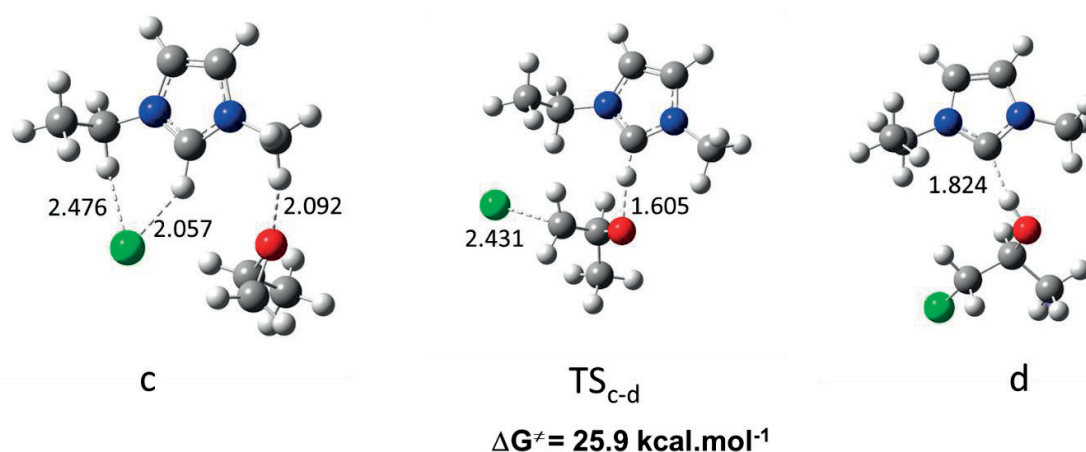


Figure 2.2.2 Optimized geometries for the intermediates and transition states involved in the rate-limiting step for the cycloaddition of CO₂ with PO catalyzed by **1Cl**, computed at the B3PW91-D3/6-31G** level.

The calculations for the ring-opening step with the fully-substituted imidazolium cation, **3Cl**, which does not contain a strong H-bonding donor, give an energy barrier of 23.0 kcal·mol⁻¹, even lower than that of **1Cl** or **2Cl** (Figure 2.2.3).

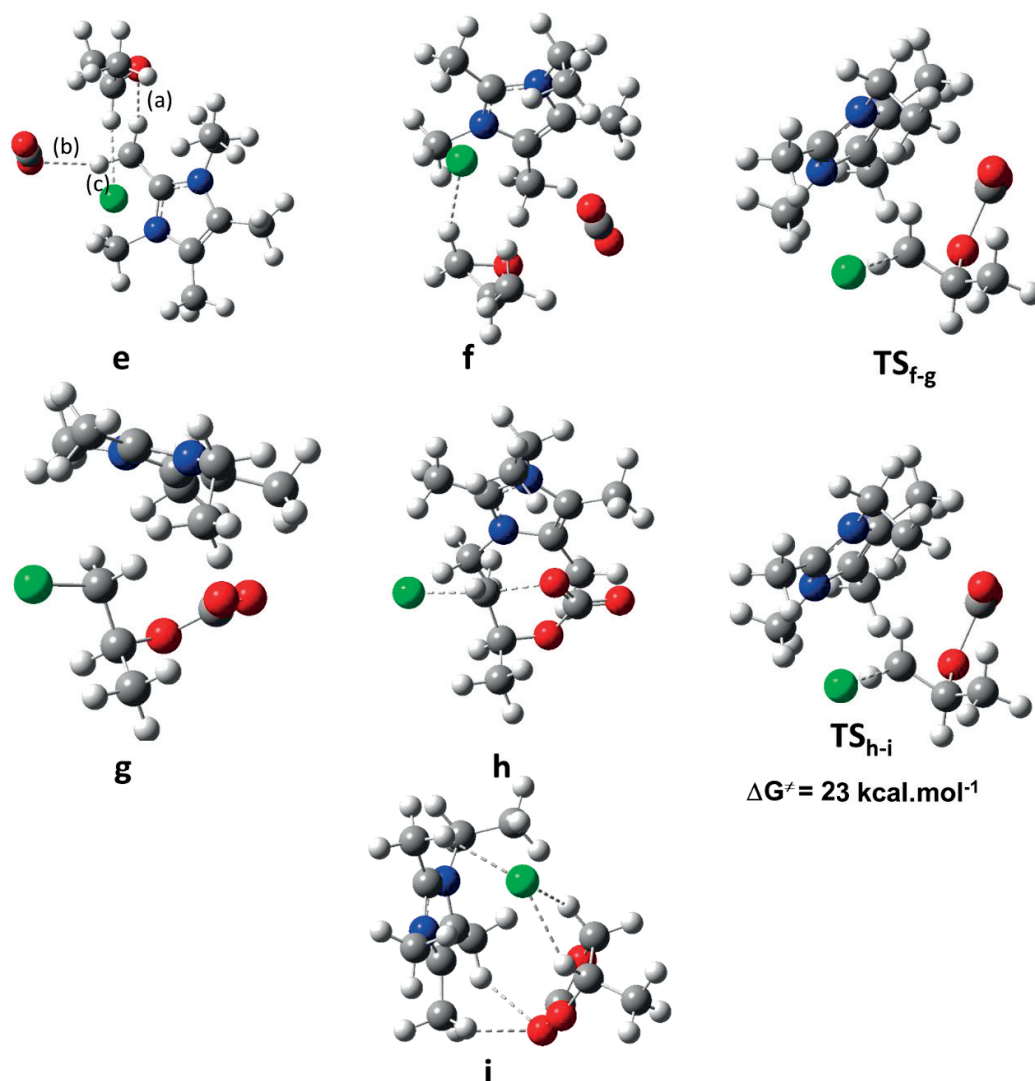


Figure 2.2.3 Optimized geometries for the intermediates and transition states involved in a possible reaction path for the cycloaddition of CO₂ with PO catalyzed by 3Cl.

These results indicate that even if H-bonds are able to activate epoxides towards ring opening, they do not play a key role in the ring opening of the epoxide, and that another underlying feature or a combination of features of the catalyst must control the observed reaction rate. Note that an ethyl group was used for the calculations instead of a butyl group (Figure 2.2.4, 3Cl), as it was previously demonstrated that the side chain does not affect the computational results in the gas phase.¹²⁰ However, experimentally smaller alkyl chains reduce the solubility of the catalyst in the epoxide, leading to lower yields.¹⁵²

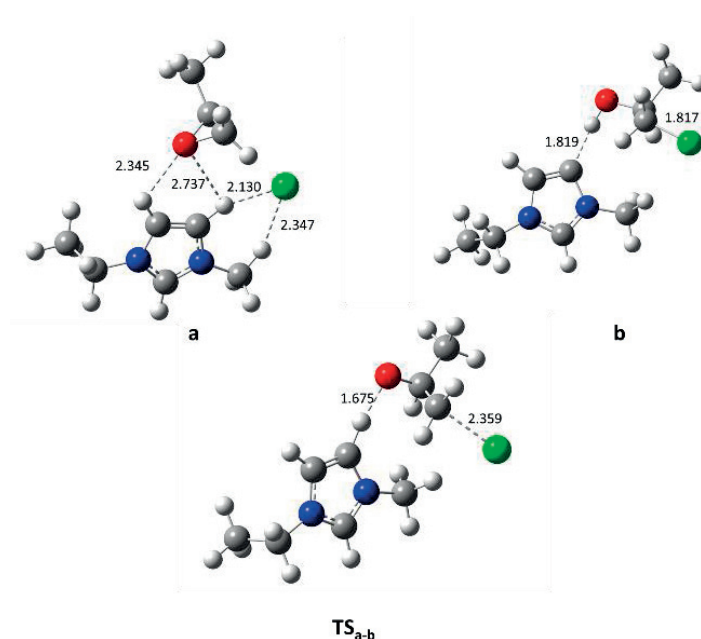


Figure 2.2.4 Optimized geometries for the intermediates and transition states for C4-H-assisted ring-opening of the epoxide computed at the B3PW91-D3/6-31G** level.

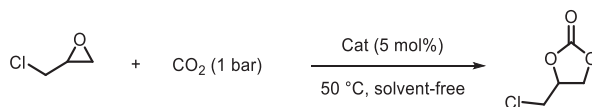
The role of the imidazolium ring protons has only been associated with the activation of the epoxide *via* H-bonding. However, they may also interact with the anion of the salt, leading to a reduction in the nucleophilicity of the anion and its ability to open the epoxide ring. To understand the relationship between cation-anion interactions in the CCE reaction, the effect of the halide anion was also investigated using the salts **1X**, **2X**, **3X** and **4X** (where X = Cl⁻, Br⁻ or I⁻). Numerous studies have confirmed the importance of the halide on the catalytic activity with the trend for imidazolium cations usually being, I⁻ > Br⁻ > Cl⁻, which is attributed to the nucleophilic character of the anion under the catalytic conditions. Interestingly, for **1X**, containing 3 acidic protons, the order is I⁻ > Br⁻ ≈ Cl⁻ (62, 53 and 52 %, respectively, Table 2.2.1, entries 1, 7 and 13). For **2X**, with a methyl group at the C2 position, the trend differs, with the chloride salt being more active than the bromide salt, *i.e.* I⁻ ≈ Cl⁻ > Br⁻ (50, 49 and 46 %, respectively, Table 2.2.1, entries 2, 8 and 14). For **3X**, which is fully substituted, the order differs again, *i.e.* Br⁻ > Cl⁻ ≈ I⁻ (60, 53 and 51 %, respectively, Table 2.2.1, entries 5, 11 and 17). Finally, for **4X**, the benchmark tetrabutylammonium salt, the trend is completely reversed to that of the **1X** series, with Cl⁻ > Br⁻ > I⁻ (56, 45 and 36 %, respectively), which concurs with a previous study.¹²¹

To rationalize the trends observed for the different catalysts with various halide anions DFT calculations were performed and experiments were conducted with water added to the reaction (employed as H-bond promoter). In order to quantify the nucleophilicity of the anion using DFT calculations, we employed a probe molecule, MeOH, and calculated the length of the H-bond between the anion of the catalyst with

the probe. As expected, the computations demonstrate that the Cl⁻ anion of the **3Cl** ion pair forms a shorter (*i.e.* stronger) H-bond with MeOH than the Cl⁻ anion of the **1Cl** ion pair (2.050 Å vs 2.108 Å, respectively). Thus, the ability of the anion in **3Cl** to donate its lone pair to the hydrogen atom of the -OH group is stronger than that of the same anion in **1Cl**. Most probably, the same is the case with respect to the relative capacity of the anions in **3Cl** and **1Cl** to donate their lone pairs to the carbon atom of the epoxide ring, indicating that H-bonds are potentially detrimental to the reaction, and that **3Cl** should be a better catalyst than **1Cl**. However experimentally, this is not the case as both **1Cl** and **3Cl** demonstrated practically equivalent activity.

The addition of water as an external H-bond source was previously demonstrated to promote the CCE reaction when employed in ca. 30 mol%, regardless of the cation-anion combination in the **1X** and **4X** catalyst series. However, higher concentrations (100 mol% and above) are detrimental to the reaction and lead to unwanted side-reactions.¹¹⁵ We therefore decided to test the effect of a catalytic quantity of water (*i.e.* 5 mol%, the same concentration as the catalyst) as an external H-bond donor and its effect on the reaction to further probe the H-bond interactions between the epoxide, the halide anion and the H-bond donor (water and/or the acidic protons in the imidazolium cation). Catalytic quantities of water (5 mol%) were added to the reactions employing the series of **1X** and **4X** halide catalysts (Table 2.2.2). The trend for the imidazolium salts **1X** remained largely unchanged with only a slight increase in yield obtained with **1Br** (from 53 % to 57 %) and **1I** (from 62 % to 65 %) and a slight decrease with **1Cl** (from 52 % to 46 %). However, the order for the ammonium salt series **4X** was reversed in the presence of 5 mol% water with the order being **4I** > **4Br** > **4Cl**. The yield also increases significantly with **4I** from 36 % in the absence of water to 68 % with 5 mol% of water present (Table 2.2.1, entry 12, Table 2.2.2, entries 6). A higher yield was also obtained with **4Br** in the presence of 5 mol% of water (from 45 to 59 %), whereas a slight detrimental effect was observed with the catalyst **4Cl** (from 56 to 50 %).

Table 2.2.2 Effect of water on the reaction between epichlorohydrin and CO₂ catalyzed by **1X** and **4X**.



Entry	Catalyst	Water mol %	Yield (%)
1	1Cl	5%	46
2	1Br	5%	57
3	1I	5%	65
4	4Cl	5%	50
5	4Br	5%	59
6	4I	5%	68

Reaction conditions: epichlorohydrin (1 g, 10.8 mmol), catalyst (5 mol%), CO₂ (1 bar), 50 °C, 3 h. Yield determined by ¹H NMR spectroscopy.

The difference in the magnitude of the change in the yield when water is present between the catalysts may be attributed to the different H-bonding strengths of the cation and solvation of the anion. With the tetrabutylammonium cation which cannot form a H-bond with the substrate, the impact on the addition of water, which can form a H-bond with the substrate is much more profound. With the imidazolium cation the impact of water is counter-balanced by the acidic ring protons on the cation. Additionally, the solvation enthalpy of the halide by water is important, and follows the order chloride > bromide > iodide. Thus, the nucleophilicity of the anions is reduced, as discussed above, resulting in the decrease of reaction rate for all catalysts, and the effect being most pronounced for the chloride anion. The overall catalytic activity is therefore dependent on the balance between the nucleophilicity of the anion, which is reduced following solvation by water,¹⁸⁸ and the H-bond induced activation of the epoxide ring, which promotes the reaction. Hence, highest yields are obtained with iodide anions in the presence of H-bonding donors as iodide is least strongly solvated by water and benefits the most from H-bond induced epoxide activation.

2.2.3. Conclusions

In summary, we have demonstrated that methyl groups on the cation of simple imidazolium salts do not significantly affect the efficacy of the CCE reaction. When acidic protons are present in the imidazolium ring of the cation (C2, C4, C5 or combination thereof), the acidic protons simultaneously activate the epoxide (as demonstrated previously),¹¹⁸ but interact with the halide ion to reduce its nucleophilicity (as we have shown here). In the absence of acidic protons (**3X** and **4X**), the epoxide is presumably less well activated, but the nucleophilicity of the halide is higher due to weaker cation-anion pairing, leading to higher activities and the preferred anion is strongly cation-dependent. The experimental data demonstrate that higher nucleophilicity (*i.e.* lower interactions between the anion and the cation) governs the activity of the catalyst. When H-bonding interactions between the cation and substrate are available, they are

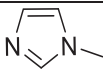
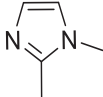
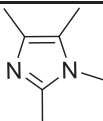
mostly counterbalanced by a decrease in nucleophilicity of the anion in the case of Cl^- and Br^- (both of which can interact with the H-bond donor). External H-bond donors can be used if they do not interact negatively with the anion (Cl^- is deactivated by water as it is strongly solvated and therefore is less nucleophilic) and if they do not hinder the overall solubility of the catalyst into the epoxide.¹⁸⁵ Further catalyst development should therefore strive to increase the nucleophilicity of the anion, by minimizing ion pairing interactions (e.g. having a buried or highly delocalized charge),¹⁸⁹ as well as ensuring that the cation ensures high solubility of the salt in the epoxide (e.g. inclusion of hydrophobic groups), rather than incorporating additional H-bond donors which has been the most widely employed strategy so far and usually leads to an overall lower solubility of the catalyst. Finally, this study also demonstrates that one of the first ILs reported to catalyze the CCE reaction is considerably more active than previously thought when applied under homogeneous conditions (*i.e.* with epichlorohydrin rather than propylene oxide), thus highlighting the need for benchmark conditions for the CCE reaction.^{57,93}

2.2.4. Experimental details

2.2.4.1. General Remarks

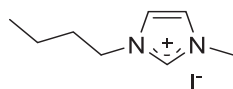
All chemicals were purchased from commercial sources and used as received. Catalysts **1Cl**, **1Br**, **2Cl**, **4Cl**, **4Br**, **4I** were purchased from commercial suppliers and used as received. Catalysts **1I**, **2Br**, **2I**, **3Cl**, **3Br**, **3I** were synthesized according to a general procedure that involves reacting the appropriate imidazole precursor with an excess of the appropriate alkyl halide (1-5 eq.) in a microwave vial.⁷¹ Typically, the imidazole precursor (15 mmol) was charged in a microwave vial equipped with a magnetic stirrer. The microwave vial was sealed with a septum. Then, the alkyl halide (45-75 mmol) was added to the closed microwave vial *via* the septum. The reaction was heated to 60-100 °C depending on the alkyl halide (see Table 2.3.1) for 18 h and monitored *via* ^1H NMR spectroscopy until the imidazole was completely consumed. After reaction the ILs were extensively washed with diethyl ether and dried *in vacuo* at 60 °C for 24 h prior to use. The catalysts were characterized by ^1H and ^{13}C NMR spectroscopy on a Bruker 400 MHz instrument.

Table 2.2.3 Synthesis of the catalyst by reaction of the imidazole precursor and alkyl halide under solvent-free conditions.

Catalyst	Imidazole	Alkyl halide (eq.)	T [°C]	t [h]	Yield [%]
1I		Bu-I (1)	60	18	95
2Br		Bu-Br (5)	100	18	98
2I		Bu-I (5)	100	18	96
3Cl		Bu-Cl (5)	100	48	75
3Br		Bu-Br (5)	100	48	80
3I		Bu-I (5)	100	24	75

Conditions: imidazole (0.5 g), alkyl halide (1-5 eq.), solvent-free. The yield refers to the isolated catalyst.

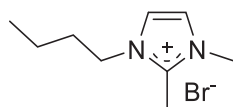
2.2.4.2. Characterization



1-butyl-3-methylimidazolium iodide

^1H NMR (400 MHz, $\text{DMSO-}d_6$) δ 9.14 (s, 1H), 7.79 (s, 1H), 7.72 (s, 1H), 4.17 (t, $J = 7.2$ Hz, 2H), 3.86 (s, 3H), 1.83 – 1.71 (m, 2H), 1.28 (m, 2H), 0.90 (t, $J = 7.4$ Hz, 3H).

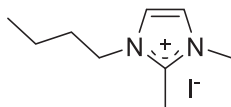
^{13}C NMR (101 MHz, $\text{DMSO-}d_6$) δ 136.95, 124.07, 122.73, 48.97, 36.29, 31.82, 19.24, 13.76.



1-butyl-2,3-dimethylimidazolium bromide

^1H NMR (400 MHz, $\text{DMSO-}d_6$) δ 7.66 (s, 1H), 7.63 (s, 1H), 4.11 (t, $J = 7.3$ Hz, 2H), 3.75 (s, 3H), 2.59 (s, 3H), 1.74 – 1.59 (m, 2H), 1.29 (m, 2H), 0.91 (t, $J = 7.4$ Hz, 3H).

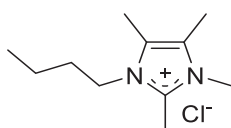
^{13}C NMR (101 MHz, $\text{DMSO-}d_6$) δ 144.69, 122.77, 121.34, 47.74, 35.16, 31.66, 19.35, 13.88, 9.65.



1-butyl-2,3-dimethylimidazolium iodide

^1H NMR (400 MHz, Chloroform-*d*) δ 7.49 (s, 1H), 7.32 (s, 1H), 4.11 (t, J = 7.5 Hz, 2H), 3.93 (s, 3H), 2.76 (s, 3H), 1.83 – 1.69 (m, 2H), 1.36 (m, 2H), 0.92 (t, J = 7.3 Hz, 3H).

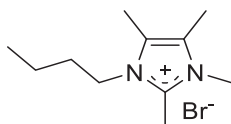
^{13}C NMR (101 MHz, DMSO-*d*₆) δ 144.69, 122.76, 121.33, 47.75, 35.19, 31.66, 19.35, 13.88, 9.70.



1-butyl-2,3,4,5-tetramethylimidazolium chloride

^1H NMR (400 MHz, Chloroform-*d*) δ 4.16 – 4.05 (m, 2H), 3.86 (s, 3H), 2.88 (s, 3H), 2.26 (m, 6H), 1.74 – 1.62 (m, 2H), 1.40 (m, 2H), 0.98 (t, J = 7.3 Hz, 3H).

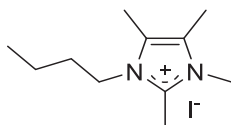
^{13}C NMR (101 MHz, Chloroform-*d*) δ 126.12, 124.78, 45.72, 32.96, 31.81, 19.85, 13.56, 11.47, 8.98, 8.82.



1-butyl-2,3,4,5-tetramethylimidazolium bromide

^1H NMR (400 MHz, DMSO-*d*₆) δ 4.08 (t, J = 7.7 Hz, 2H), 3.62 (s, 3H), 2.62 (s, 3H), 2.23 (d, J = 11.0 Hz, 6H), 1.59 (p, J = 7.7 Hz, 2H), 1.33 (h, J = 7.3 Hz, 2H), 0.92 (t, J = 7.3 Hz, 3H).

^{13}C NMR (101 MHz, DMSO-*d*₆) δ 142.92, 125.95, 124.81, 44.87, 32.25, 31.50, 19.55, 13.95, 10.32, 8.64, 8.49.



1-butyl-2,3,4,5-tetramethylimidazolium iodide

^1H NMR (400 MHz, $\text{DMSO-}d_6$) δ 4.13 – 3.98 (m, 2H), 3.61 (s, 3H), 2.60 (s, 3H), 2.31 – 2.18 (m, 6H), 1.65 – 1.51 (m, 2H), 1.32 (m, 2H), 0.92 (t, $J = 7.3$ Hz, 3H).

^{13}C NMR (101 MHz, $\text{DMSO-}d_6$) δ 142.89, 125.95, 124.81, 44.86, 32.22, 31.48, 19.55, 13.94, 10.28, 8.62, 8.48.

2.2.4.3. Catalytic reactions

Four reactions were run simultaneously using a literature procedure.¹⁹⁰ The catalyst (5 mol%) and the appropriate epoxide (0.83 mmol) were charged in a 10 mL two-neck flask that was connected to a distillation separator. The flasks were connected to a Schlenk line *via* an adaptor, and equipped with a CO₂-filled balloon. After three vacuum-CO₂ cycles, the mixture was brought to the required temperature in a pre-heated oil bath. After the appropriate time, the mixture was allowed to cool to room temperature, and CDCl₃ (1 mL) was added to the mixture. The yield of the reaction product was determined by ¹H NMR spectroscopy using D1 = 3 sec.

2.2.4.4. Computational details

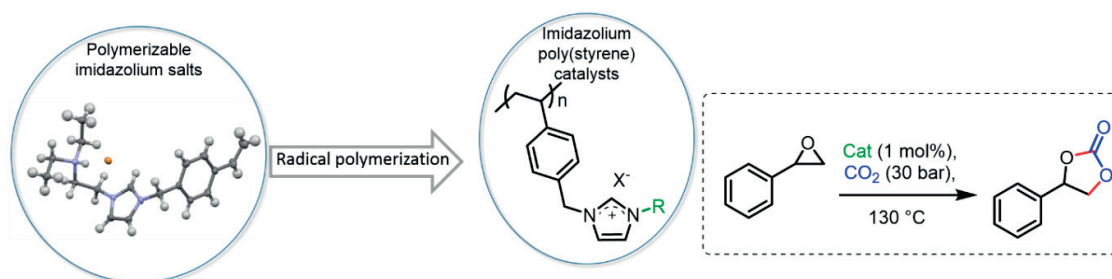
All quantum chemical calculations were carried out using the ORCA program, version 3.0.¹⁹¹ All geometries for the reactants, products, intermediates and transition states were fully optimized by density functional theory (DFT), corresponding to the Becke's three-parameter exchange functional¹⁹² in combination with the Perdew and Wang 1991 gradient-corrected correlation functional (B3PW91)¹⁹³ and 6-31G** basis set. Following full geometry optimizations, harmonic vibrational frequencies were calculated at the same level to identify the nature of all the stationary points (local minimum or first-order saddle point). The intrinsic reaction coordinate (IRC)¹⁹⁴ pathways were traced in order to verify that each saddle point links two desired minima. In non-covalently bound systems, the correct treatment of nonlocal London dispersion interactions is mandatory for accurate geometries and binding energies.¹⁹⁵ These interactions are not included in any semi local density functional and require dispersion corrections.¹⁹⁶ We used the D3 London dispersion correction in the Becke-Johnson sampling scheme (indicated by "-D3" appended to the functional name).^{197,198}

2.3. Synthesis of linear ionic poly(styrenes) and their application as catalysts for the cycloaddition of CO₂ and epoxides

This section is published as an article in *Helv. Chim. Acta*, 2016, **99**, 821–829.

List of authors: **Felix D. Bobbink**, Zhaofu Fei, Rosario Scopelliti, Shoubhik Das, Paul J. Dyson

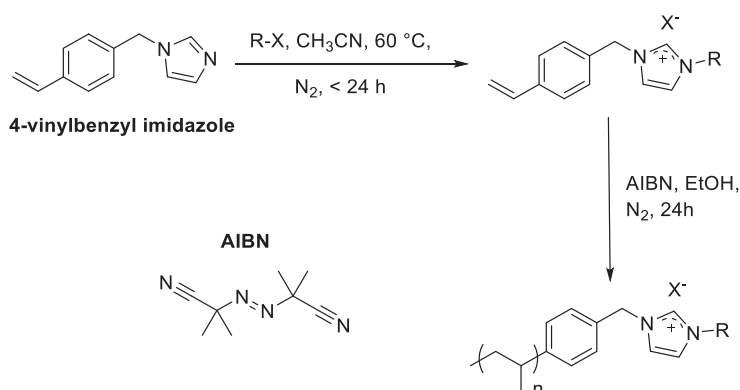
Graphical abstract:



2.3.1. Results and Discussion

The route used to prepare the imidazolium salts is shown in Scheme 2.3.1, commencing with styrene-derived imidazole (4-vinylbenzylimidazole), which was prepared according to a literature procedure.¹⁹⁹ Quaternization of the imidazole is achieved by reaction with the appropriate organohalide in acetonitrile at 60 °C. Under the reaction conditions the styrene unit is stable and does not polymerize. The imidazolium halides (**1a** – **6a**, Figure 2.3.1) were purified by precipitation with ethyl acetate or diethyl ether, followed by washing/sonicating in diethyl ether. The reaction occurs smoothly for organohalides with both electron donating groups (fast, < 3 h), and electron withdrawing groups (slower, but < 24 h). Compounds **1a**, **2a**, **5a** and **6a** were obtained as white powders in excellent yield (up to 97%). In the case of **3a** and **4a** the salt was isolated as a hygroscopic, off-white gel in slightly lower yield.

Salts **1a** – **6a** were polymerized by radical polymerization in ethanol (or acetonitrile for the more hygroscopic salts), heated under reflux in the presence of the initiator azobisisobutyronitrile (AIBN).



Scheme 2.3.1 Synthesis of styrene-functionalized imidazolium salts and their corresponding polystyrene derivatives. R and X is defined in Figure 2.3.1.

Spectroscopic features of ILs **1a** – **6a** are essentially as expected. The ¹H NMR spectra of **1a** – **6a** in deuterated DMSO features a characteristic peak at ca. 9 ppm, distinctive of the acidic proton at the 2-position of the ring. The positive ion electrospray ionization (ESI) mass spectra of **1a** – **6a** contain a peak corresponding to the intact imidazolium cation together with a peak at m/z = 117 corresponding to cleavage of the substituent, which takes place during the ionization process. ILs **1a** – **6a** are soluble in polar solvents including methanol, ethanol, acetonitrile and DMSO and are insoluble in non-polar solvents such as ethyl acetate, pentane and diethyl ether. The polymers are slightly soluble in DMSO and ethanol, and

insoluble in all other organic solvents tested. NMR (in DMSO-d₆) and IR spectroscopy confirm that the vinyl bonds have undergone polymerization (See Appendix Section 2.3).

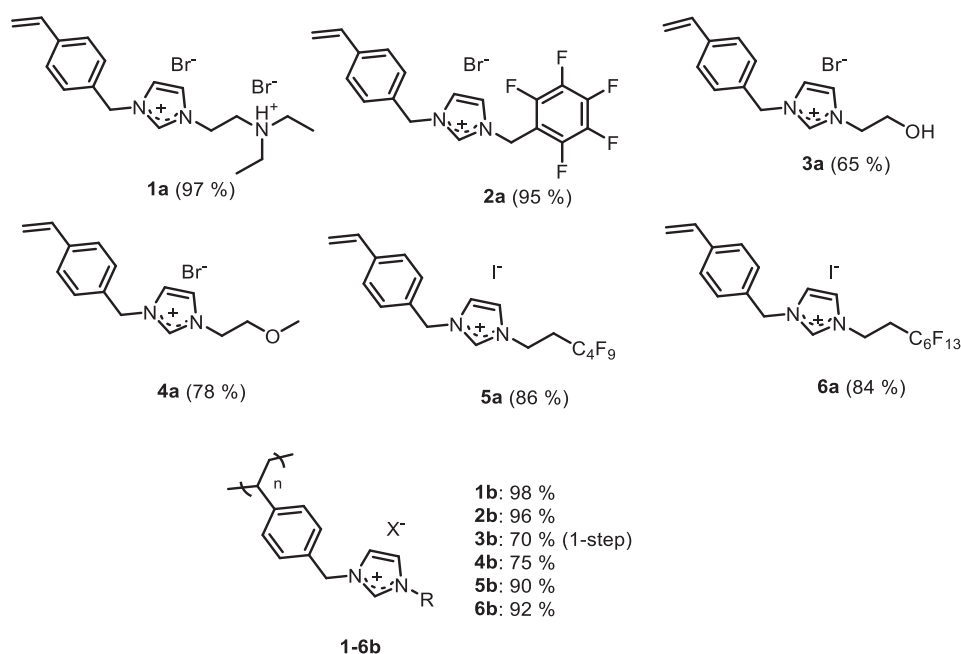


Figure 2.3.1 Structures of imidazolium salts **1a** – **6a** and the corresponding polymers **1b** – **6b** (yields given in parenthesis).

Crystals of **1a** and **2a** were obtained by slow diffusion of diethyl ether into a concentrated solution of the IL in ethanol. Their structures were solved by X-ray diffraction analysis, and are shown in Figure 2.3.2, with key bond lengths and angles given in the caption. Structural parameters of **1a** and **2a** resemble the values found in literature for other imidazolium salts.²⁰⁰ In particular, both imidazolium rings are almost planar and their bond lengths vary between 1.330(5) and 1.400(15) Å. The angles of both rings vary from 106.4(10) to 126.6(4)°. In **1a** the bromide closest to the ammonium group interacts with N(17) via hydrogen bonding, $d(\text{N}(17)\text{-Br}(2)) = 3.249(4)$ Å.

The polymers derived from the **1a** – **6a** exhibit excellent thermal stability up to 250 °C, based on thermogravimetric analysis (See Appendix Section 2.3). The more hygroscopic polymer **4b** shows significant weight loss at 100 °C due to loss of water. SEM images of the polymers indicate that the different functional groups of the imidazolium salts only marginally influence the morphology of the materials (Figure 2.3.3). Moreover, BET analysis shows that the polymers are essentially non-porous.

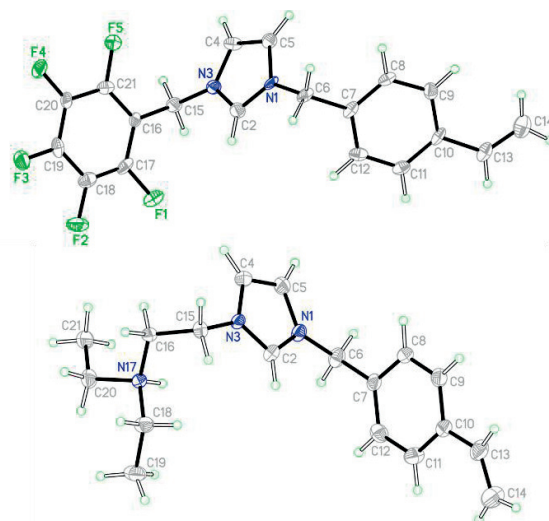


Figure 2.3.2 ORTEP representations of the cation in **1a** (top) and **2a** (bottom). The counter anions have been omitted for clarity. Key bond lengths (Å) and angles (°) for **1a**: N(1)-C(2): 1.331(5), N(1)-C(5): 1.392(6), C(2)-N(3): 1.330(5), N(3)-C(4): 1.387(6). N(1)-C(2)-H(2): 125.3, N(3)-C(2)-N(1): 109.3(4). Key bond lengths (Å) and angles (°) for **2a**: N(1)-C(2): 1.337(15), N(1)-C(5): 1.400(15), C(2)-N(3): 1.341(15), N(3)-C(4): 1.390(14). N(1)-C(2)-H(2): 125.9, N(1)-C(2)-N(3): 108.2(10).

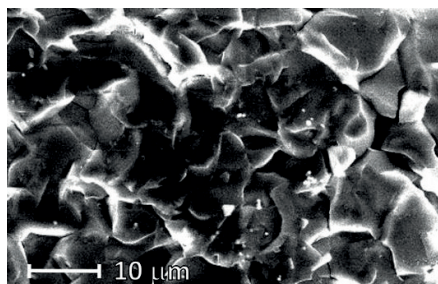
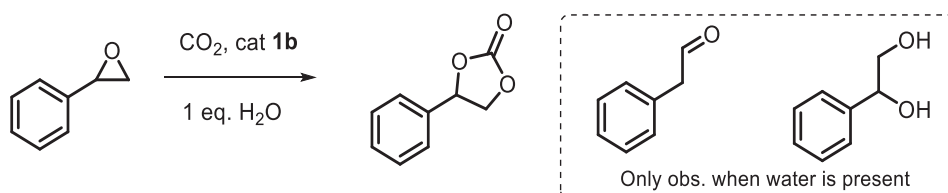


Figure 2.3.3 SEM image of **1b**.

The imidazolium salts were screened as catalysts in the CCE reaction (Scheme 2.1.1). Initially, the reaction conditions were optimized using **1b** as the catalyst and styrene oxide as a model substrate (Table 2.3.1). Styrene oxide was selected as model substrate because it is less reactive than propylene oxide and epichlorohydrin and the corresponding carbonate is easily isolated and characterized by GC-MS/FID and NMR spectroscopy. Moreover, the epoxide is non-volatile and easy to handle. Variation of the temperature and pressure of CO₂ showed the optimum conditions to be 130 °C and 30 bar, respectively. At lower temperatures and higher pressures the yield of the styrene carbonate product is reduced.

The selectivity of the reaction is high, *i.e.* no side-products were detected under the optimized conditions. However, in the presence of 1 equivalent of water (Table 2.3.1, entry **6**), the yield decreases to 80% and

side-products such as 2-phenylacetaldehyde and 1-phenylethane-1,2-diol were identified. These products arise from the nucleophilic ring opening of the epoxide by water (Scheme 2.3.2).



Scheme 2.3.2 Side-products observed when water (1 eq.) is added to the reaction.

Table 2.3.1 Optimization of the reaction conditions using catalyst **1b** and styrene oxide as the substrate.

Entry	T [°C]	P [Bar]	Yield [%]
1	100	30	65
2	130	30	95
3	150	30	94
4	130	10	72
5	130	50	55
6^a	130	30	80

Conditions: Styrene oxide (1 g, 8.3 mmol), catalyst **1b** (1 mol%), 15 h. Yields were determined by GC using n-decane as an internal standard. ^a100 mol% water was added. In 1-5, there was no side products.

Catalysts **1a – 6a** and **1b – 6b**, in addition to commercially available 1-butyl-3-methylimidazolium chloride ([BMIm]Cl) were evaluated in the cycloaddition of styrene oxide under the optimized reaction conditions (Table 2.3.2). The monomeric imidazolium salts (**1a – 6a**) are slightly more efficient catalysts than the corresponding ionic polymers (**1b – 6b**), presumably due to slightly less efficient mass transfer of the styrene oxide substrate with the polymer catalysts. The catalyst that provides the highest yield of styrene carbonate is **1a/1b** that contain the ammonium moiety, with yields of 98 and 95% obtained with the IL and polymer catalysts, respectively. The alcohol-functionalized salts **3a** and **3b** are also efficient catalysts. It has previously been shown that the alcohol functional group can enhanced reactivity of organocatalysts for the cycloaddition of carbon dioxide to epoxides *via* H-bonding interactions.^{116,201} Conversely, the ether-functionalized salts **4a-b** are less active than **3a-b**. Although a fluororous containing polymer was previously shown to be a very active catalyst for this reaction,²⁰² catalysts **2a/2b**, **5a/5b** and **6a/6b**, which containing a fluororous side-group, were markedly less active than **1a/1b**. The ammonium group in **1a/1b** increases the efficiency of the reaction to a greater extent than any of the other functional groups employed. In this context, simple ammonium salts are known to catalyze the cycloaddition of CO₂ to epoxides.¹²³ It should

be noted that **1a/1b** can be used in similar loadings than simple imidazolium salts, but, notably, polymer **1b** has the added advantage of facile product separation and reuse.

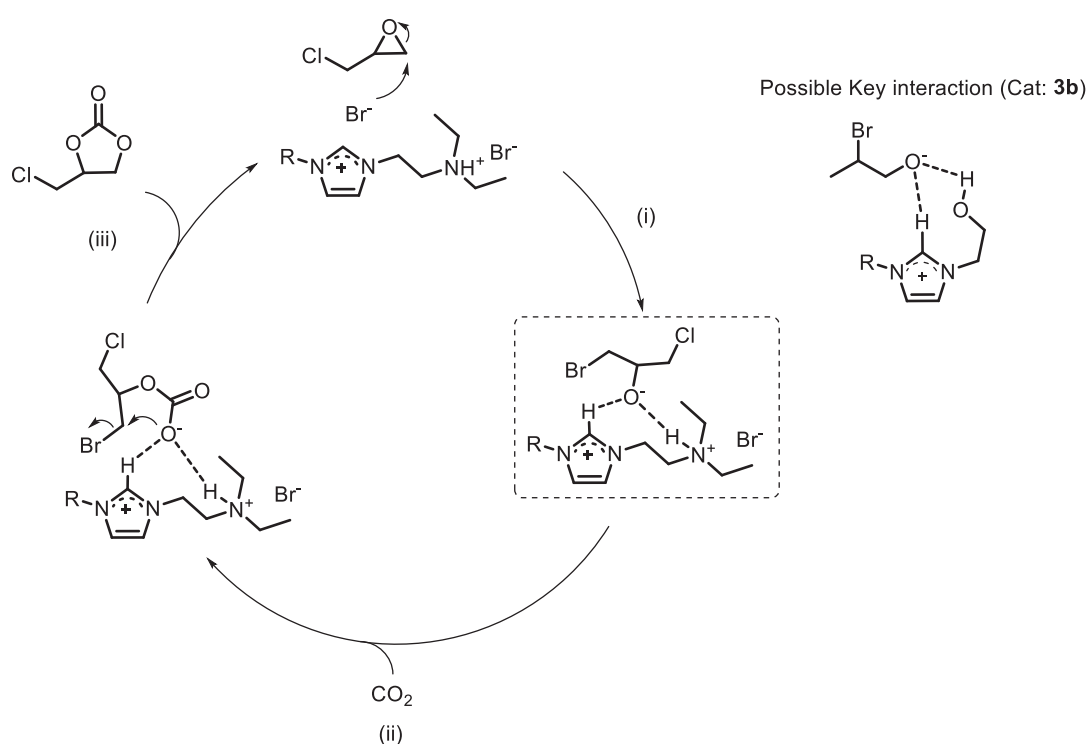
Table 2.3.2 Evaluation of ILs **1a – 6a** and polymers **1b – 6b** (in parenthesis) as catalysts in the cycloaddition of CO₂ to styrene oxide.

Catalyst	Yield [%]
[BMim]Cl	94
1a (1b)	<u>98 (95)</u>
2a (2b)	60 (45)
3a (3b)	90 (82)
4a (4b)	78 (59)
5a (5b)	87 (73)
6a (6b)	76 (65)

Conditions: Styrene oxide (1 g, 8.32 mmol), catalyst (1 mol%), CO₂ (30 bars), 130 °C, 15 h. Yields were determined by GC using n-decane as internal standard.

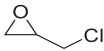
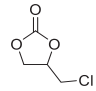
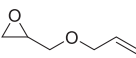
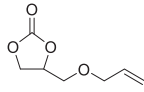
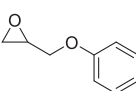
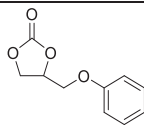
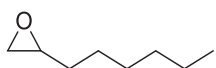
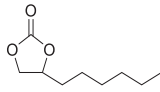
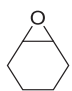
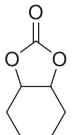
The scope of the reaction was investigated using catalyst **1b** (Table 2.3.3). With the exception of the sterically hindered cyclic oxide substrate **11a**, all the epoxides were transformed into carbonates in excellent yield. In particular, epichlorohydrin, **7a**, is transformed in quantitative yield and the product can be isolated by filtration. Less reactive/deactivated epoxides (**8a**, **9a**) are converted to carbonates in high yield, 95% for **8a** and 91% for **9a**. Substrate **10a** also reacts in near-quantitative yield, but only after a longer reaction time of 48 hours.

The mechanism of the CCE reaction catalyzed by imidazolium ILs has been investigated,²⁰³ and based on these studies a mechanism for the formation of **1b** is proposed in Scheme 2.3.3. The nucleophilic ring opening by the bromide anion that is in close proximity to the imidazolium ring is likely, although it is not unreasonable that the bromide from the ammonium could also perform the ring-opening reaction. The H-donor functional group may stabilize the obtained intermediate, to facilitate CO₂ insertion. In the final step the carbonate product is realized *via* an intramolecular S_N2-type reaction. The high yield obtained with **3b** suggests an interaction between the side-chain and the substrate *via* H-bonding.



Scheme 2.3.3 Proposed mechanism for the CCE of epichlorohydrin catalyzed by **1b**. The polystyrene part is omitted for clarity and represented by R. (i) Ring-opening of the oxirane by the bromide anion. (ii) Insertion of CO₂. (iii) Release of the product and catalyst. A proposed key intermediate, represented with **3b**, is shown in the inset.

Table 2.3.3 Evaluation of different epoxide substrates in the cycloaddition reaction with CO₂ using catalyst **1b**.

Substrate	Product/yield
 7a	 7b, >99%^a
 8a	 8b, 95%
 9a	 9b, 91%
 10a	 10b, >99%^b
 11a	 11b, 50%^c

Conditions: epoxide (8.32 mmol), **1b** (1 mol%), CO₂ (30 bars), 130°C, 15 h. ^a: 3 h. ^b 48 h. ^c: 72 h. All yields are isolated yields.

Recycling of polymer **1b** was evaluated in the cycloaddition reaction with epichlorohydrin and, following five runs, no loss of activity was observed (Figure 2.3.4). The catalyst was removed by filtration to afford the pure carbonate product **7b**. Then, the polymer catalyst was washed with diethyl ether and ethyl acetate, dried prior to use in the next batch. Although the polymer exhibited some solubility in polar solvents such as DMSO and ethanol, the NMR spectrum of the carbonate after recycling did not contain signs of leaching.

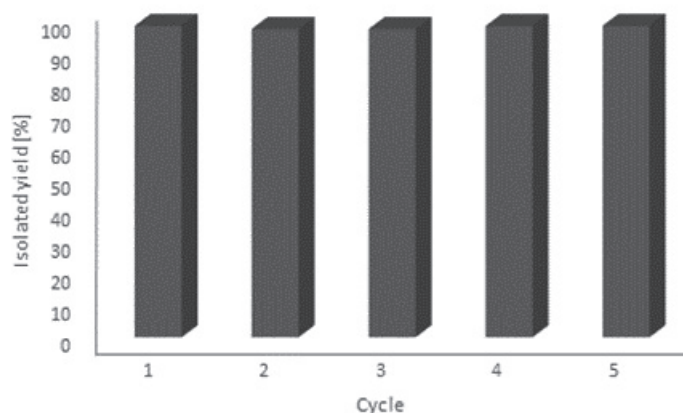


Figure 2.3.4 Recycling studies with polymer catalyst **1b** using epichlorohydrin, **7a**, as the substrate.

2.3.2. Conclusions

A series of functionalized imidazolium-salts and polymers were prepared and evaluated as catalysts in the cycloaddition of epoxides with CO₂ to form carbonates. The nature of the functional group strongly influences the activity of the catalyst with the ammonium containing system showing superior activity in this reaction. Notably, isolation of the carbonate product is very simple with the polymer catalysts and the polymer may be recycled and reused without loss of activity.

2.3.3. Experimental details

2.3.3.1. General Remarks

All starting materials were purchased from commercial providers and used as received. 4-Vinylbenzylimidazole was prepared using a literature procedure.¹⁹⁹ GC-FID were recorded on a Varian Chrompack CP-3380 Gas Chromatograph equipped with a capillary column from Agilent (l x d x f: 25 m x 0.25 mm x 0.25 μm) using N₂ as carrier gas. ¹H and ¹³C NMR spectra were recorded on a Bruker 400 MHz instrument and electrospray ionization mass spectra were obtained on a LTQ-Orbitrap Elite instrument (ThermoFisher) operated in positive ionization mode. Elemental analysis was determined on a Flash 2000 Organic Elemental Analyzer. IR spectra were recorded on a Perkin-Elmer FT-IR 2000 instrument. TGA was carried out on a Perkin-Elmer TGA 4000 with a heating rate of 40 °C.min⁻¹. Scanning electron microscopy (SEM) was performed on a FEI XLF30- FEG with Schottky field emission gun operated between 1 - 30 kv.

2.3.3.2. Typical procedure for the synthesis of 1a – 6a:

To a 10 mL two-neck flask equipped with a magnetic stirrer, 4-vinylbenzylimidazole (1 g, 5.43 mmol) and the corresponding organohalide (4.89 mmol) were added (4-vinylbenzylimidazole was added in slight excess, 1.1:1). After purging three times with N₂, dry acetonitrile (5 mL) was added. The reaction mixture was heated to 60 °C and stirred for 24 h. After reaction, the solution was concentrated under reduced pressure and ethyl acetate (30 mL) was added, causing the imidazolium salt to precipitate. The mixture was sonicated for 1 h. The solid was collected by filtration, washed with diethyl ether (3 x 20 mL) and dried.

2.3.3.3. Characterization of products

1-(2-(diethylamino)ethyl)-3-(4-vinylbenzyl)-1H-imidazol-3-ium 1a: White powder, 97% yield. ¹H NMR (400 MHz, DMSO-d₆) δ 9.83 (s, 1H), 9.47 (s, 1H), 7.98 (s, 1H), 7.88 (s, 1H), 7.55 (d, J = 8.0 Hz, 2H), 7.46 (d, J = 8.0 Hz, 2H), 6.76 (dd, J = 17.7, 10.9 Hz, 1H), 5.89 (d, J = 17.7 Hz, 1H), 5.46 (s, 2H), 5.32 (d, J = 10.9 Hz, 1H), 4.78 – 4.63 (m, 2H), 3.67 (s, 2H), 3.23 (s, 4H), 1.24 (s, 6H). ¹³C NMR (101 MHz, DMSO-d₆) δ 138.1, 137.6, 136.4, 134.4, 129.4, 127.1, 123.4, 123.2, 115.8, 52.3, 49.8, 47.4, 43.7, 8.9. HRMS (ESI) for C₁₈H₂₆N₃ [M⁺]: calc.: 284.2121 Found: 284.2108 Anal. Calcd for C₁₈H₂₇Br₂N₃: C, 48.56; H, 6.11; N, 9.44. Found: C, 48.57; H, 6.07; N, 9.12.

1-((perfluorophenyl)methyl)-3-(4-vinylbenzyl)-1H-imidazol-3-ium bromide 2a: White powder, 95% yield. ¹H NMR (400 MHz, DMSO-d₆) δ 9.50 (s, 1H), 7.90 (d, J = 14.8 Hz, 2H), 7.61 (d, J = 8.2 Hz, 2H), 7.48 (d, J = 7.9 Hz, 2H), 6.83 (dd, J = 17.7, 11.0 Hz, 1H), 5.96 (d, J = 17.7 Hz, 1H), 5.73 (s, 2H), 5.48 (s, 2H), 5.39 (d, J = 11.0 Hz, 1H). ¹³C NMR (101 MHz, DMSO-d₆) δ 138.1, 137.4, 136.4, 134.5, 129.2, 127.1, 123.6, 123.3, 115.8, 52.3. HRMS (ESI) for C₁₉H₁₄F₅N₂ [M⁺]: calc.: 365.1077 Found: 365.1081. Anal. Calcd for C₁₉H₁₄BrF₅N₂: C, 51.26; H, 3.17; N, 6.29. Found: C, 51.05; H, 3.30; N, 6.04.

1-(2-hydroxyethyl)-3-(4-vinylbenzyl)-1H-imidazol-3-ium bromide 3a: Hygroscopic off-white solid, 65% yield. ¹H NMR (400 MHz, DMSO-d₆) δ 9.30 (s, 1H), 7.91 – 7.73 (m, 2H), 7.54 (d, J = 7.9 Hz, 2H), 7.42 (d, J = 8.0 Hz, 2H), 6.75 (dd, J = 17.7, 10.8 Hz, 1H), 5.88 (d, J = 17.6 Hz, 1H), 5.45 (s, 2H), 5.31 (d, J = 10.9 Hz, 1H), 5.18 (t, J = 5.1 Hz, 1H), 4.24 (t, J = 4.24 Hz, 2H), 3.74 (q, J = 4.9 Hz, 2H). ¹³C NMR (101 MHz, DMSO-d₆) δ 138.0, 136.9, 136.4, 134.8, 129.1, 127.1, 123.6, 122.7, 115.8, 59.7, 52.3, 52.0. HRMS (ESI) for C₁₄H₁₇N₂O [M⁺]: calc.: 229.1335 Found: 229.1330.

1-(2-methoxyethyl)-3-(4-vinylbenzyl)-1H-imidazol-3-ium bromide 4a: Hygroscopic off-white solid, 78% yield. ¹H NMR (400 MHz, DMSO-d₆) δ 9.31 (s, 1H), 7.83 (s, 1H), 7.79 (s, 1H), 7.54 (d, J = 8.0 Hz, 2H), 7.41 (d, J = 8.1 Hz, 2H), 6.75 (dd, J = 17.7, 10.9 Hz, 1H), 5.88 (d, J = 17.7 Hz, 1H), 5.45 (s, 2H), 5.31 (d, J = 10.9 Hz,

1H), 4.38 (t, J = 4.9 Hz, 2H), 3.70 (t, J = 4.9 Hz, 2H), 3.27 (s, 3H). ¹³C NMR (101 MHz, DMSO-d6) δ 138.1, 137.0, 136.4, 134.8, 129.1, 127.2, 123.6, 122.8, 115.8, 70.0, 58.6, 52.1. HRMS (ESI) for C₁₄H₁₇N₂O [M⁺]: calc.: 229.1341 Found: 229.1358. Anal. Calcd for C₁₅H₁₉BrN₂O: C, 55.74; H, 5.93; N, 8.67. Found: C, 54.15; H, 5.95; N, 8.07.

3-(3,3,4,4,5,5,6,6,6-nonafluorohexyl)-1-(4-vinylbenzyl)-1H-imidazol-3-ium iodide 5a: White powder, 85% yield. ¹H NMR (400 MHz, DMSO-d6) δ 9.43 – 9.12 (br, 1H), 7.88 (s, 1H), 7.76 (s, 1H), 7.57 – 7.32 (m, 4H), 6.75 (dd, J = 17.7, 10.9 Hz, 1H), 5.88 (d, J = 17.7 Hz, 1H), 5.43 (s, 2H), 5.31 (d, J = 10.9 Hz, 2H), 4.58 (t, J = 7.1 Hz, 2H), 3.12 – 2.95 (m, 2H). ¹³C NMR (101 MHz, DMSO-d6) δ 138.1, 137.3, 136.4, 134.5, 129.2, 129.0, 127.1, 123.5, 123.1, 115.8, 52.3, 30.3. HRMS (ESI) for C₁₈H₁₆F₉N₂ [M⁺]: calc.: 431.1164 Found: 431.1170 Anal. Calcd for C₁₈H₁₆F₉I N₃: C, 38.73; H, 2.89; N, 5.02. Found: C, 39.74; H, 3.05; N, 5.75.

3-(3,3,4,4,5,5,6,6,7,7,8,8,8-tridecafluorooctyl)-1-(4-vinylbenzyl)-1H-imidazol-3-ium iodide 6a: White powder, 84% yield. ¹H NMR (400 MHz, DMSO-d6) δ 9.35 (s, 1H), 7.93 (s, 1H), 7.84 (s, 1H), 7.62 – 7.29 (m, 4H), 6.75 (dd, J = 17.8, 11.0 Hz, 1H), 5.88 (d, J = 17.7 Hz, 1H), 5.42 (s, 2H), 5.31 (d, J = 10.9 Hz, 1H), 4.58 (t, J = 7.1 Hz, 1H), 3.15 – 2.95 (m, 2H). ¹³C NMR (101 MHz, DMSO-d6) δ 138.1, 137.3, 136.4, 134.5, 129.2, 128.9, 127.1, 123.5, 123.1, 115.8, 52.3, 51.6, 41.9, 30.4. HRMS (ESI) for C₂₀H₁₆F₁₃N₂ [M⁺]: calc.: 531.1100 Found: 531.1075. Anal. Calcd for C₂₀H₁₆F₁₃I N₂: C, 36.49; H, 2.45; N, 4.26. Found: C, 37.42; H, 1.77; N, 4.82.

Structure determination in the solid-state:

Single crystals of **1a** and **2a** were obtained by slow evaporation of diethyl ether into a concentrated solution of the salt in ethanol. Diffraction data were measured using Mo K α radiation on a Bruker APEX II CCD diffractometer equipped with a kappa geometry goniometer. The datasets were reduced by EvalCCD²⁰⁴ and then corrected for absorption.²⁰⁵ The solutions and refinements were performed by SHELX.²⁰⁶ The crystal structures were refined using full-matrix least-squares based on F² with all non-hydrogen atoms anisotropically defined. Hydrogen atoms were placed in calculated positions by means of the “riding” model. CCDC-1411530 (**1a**), CCDC-1411531 (**2a**) contains the supplementary crystallographic data for this paper. These data can be obtained free of charge from The Cambridge Crystallographic Data Centre *via* www.ccdc.cam.ac.uk/data_request/cif.

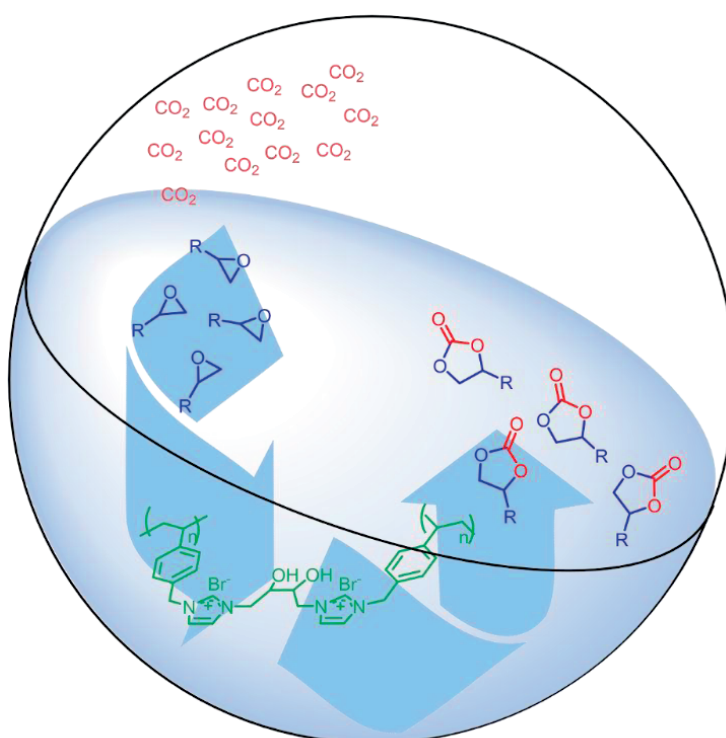
2.4. Synthesis of cross-linked ionic poly(styrenes) and their application as catalysts for the cycloaddition of CO₂ and epoxides

This section is published as an article in *ChemPlusChem*, **2017**, *82*, 144–151.

List of authors: **Felix D Bobbink***, Antoine P Van Muyden*, Aswin Gopakumar, Zhaofu Fei, Paul J Dyson

* = equal contribution

Graphical abstract:



2.4.1. Results and Discussion

The synthetic route used to prepare the vinyl-functionalized di-imidazolium salt monomers **m1a/b** to **m6a/b** and subsequent polymers **p1a/b** to **p6a/b** is depicted in Figure 2.4.1. In the first step the styryl-functionalized di-imidazolium salts are prepared from 4-vinylbenzylimidazole (**VBIm**) (prepared according to a literature procedure¹⁹⁹) by reaction with the appropriate spacer precursor (organobromide or organochloride). For the more reactive organobromides, it was possible to react the bromo-functionalized spacer directly with **VBIm**. The reaction was monitored by ¹H NMR spectroscopy and it was found that a slight excess of **VBIm** avoids any contamination from the mono-quaternization product. The reaction was terminated when a single peak corresponding to the C2-imidazolium ring proton was observed at ca. 9.4 ppm in the ¹H NMR spectrum indicative of a single species in solution. All the reactions with the organobromides went to completion, however, with organochlorides long reaction times were required to obtain the di-substituted monomers in high yield. For spacers **m4** and **m5**, which contain hydroxyl groups (Figure 2.4.1), the reaction did not proceed with the dichloride starting materials. However, monomers **m4a** and **m5a** may be obtained *via* an alternative synthetic route. The route involves reaction of the spacer with imidazole in presence of NaOH. In a second step, the chloride imidazolium salt is obtained from the reaction of the di-imidazole with 4-vinylbenzylchloride (See Appendix Section 2.4).

The ¹H NMR spectra of the monomers are as expected with the imidazolium-proton observed at ca. 9.4 ppm (See representative example in Appendix 2.4). Note, the spectra of **m1a** (the only salt that was reported previously) is consistent with the one reported in the literature.²⁰⁷ In the electrospray ionization mass spectra of the monomers peaks corresponding to the intact di-cation with one counter-anion are observed.

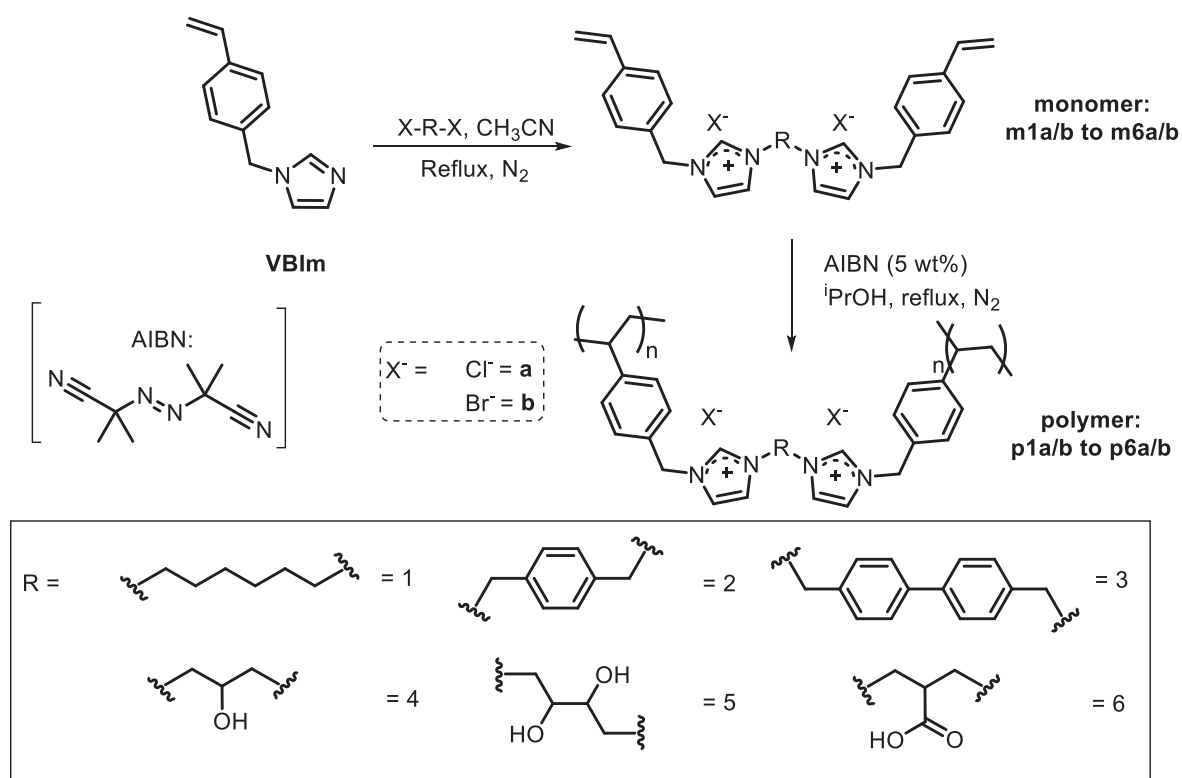


Figure 2.4.1 Synthesis of vinyl-functionalized di-imidazolium salts **m1a/b** to **m6a/b** and their subsequent polymerization to form cross-linked polymers **p1a/b** to **p6a/b**.

All the monomers were readily polymerized in *i*PrOH using 5 wt% AIBN as a radical initiator (Figure 2.4.1) yielding the polymer as a white powder. In contrast to the hygroscopic monomers, *i.e.* **m1a/b**, **m4a/b**, **m5a/b** and **m6a**, all the polymers could be stored on the bench without absorbing ambient moisture. The polymer with the hexyl spacer was reported previously and evaluated as membrane, but with Tf₂N as counter-anion.²⁰⁸ In their work an alternative synthetic route was used to prepare the monomer, *i.e.*, they prepared the bridged di-imidazole first, and reacted it with 4-vinylbenzyl chloride. Polymers **p1a/b** - **p6a/b** were characterized by IR spectroscopy, thermogravimetric analysis (TGA), Brunauer-Emmett-Teller (BET) and scanning electron microscopy (SEM) (See Appendix Section 2.4. for representative examples). Notably, the polymers are insoluble in water, CH₃CN, DMSO, DMF and EtOAc. Comparison of the IR spectra of the monomers with the analogous polymers demonstrates that the vinyl moiety (ca. 1620 cm⁻¹ and 920 cm⁻¹) has been polymerized. BET measurements (Table A.2.4.1) on the dried polymer show that the polymers exhibit only modest porosities, and the spacer seems to have only a marginal effect on surface area. Compared to previously reported linear ionic poly(styrenes) that exhibited no porosity,²⁰⁹ the cross-linked polymers show small surface areas. The SEM images of selected polymers give further insights on the overall morphological structure in the solid-state (Figure 2.4.2). For example, polymer **p1b** with a hexyl-

spacer presents a smoother surface than **p5b** containing a diol group whereas the particle size of **p5b** appears to be more homogeneous than that of **p1b**.

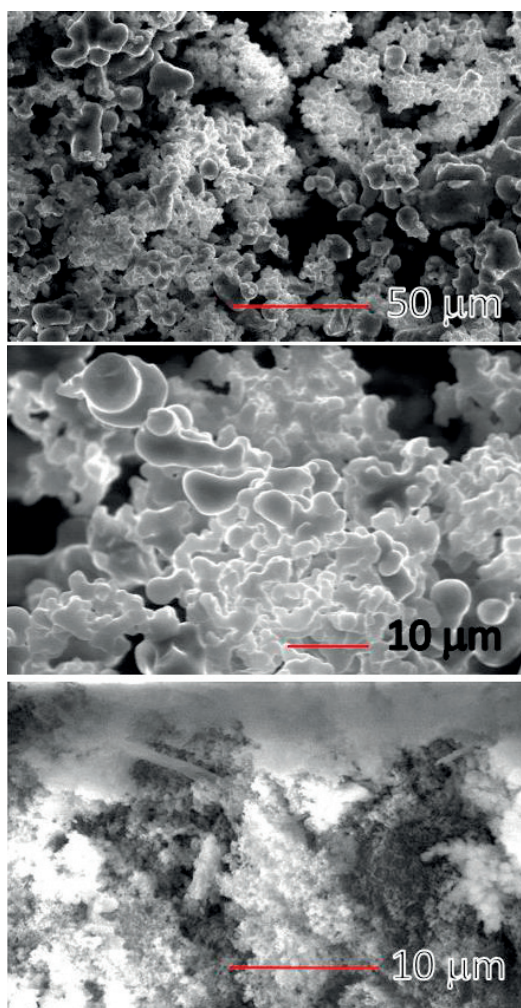


Figure 2.4.2 SEM images of polymer **p1b** (top and middle) and **p5b** (bottom).

TGA analysis of the dried polymers showed that the polymers are stable in the range 250 to 350 °C (Figure 2.4.3), with an average of 5 wt% loss associated with trace solvent evaporation. The materials with hexyl and benzyl spacers are stable up until 350 °C, whereas the polymers containing H-donor spacers show mass losses at around 250 °C, which is associated with slightly lower stability of the spacer containing an alcohol, diol or acid compared to the more stable hexyl, benzyl and dibenzyl spacers.

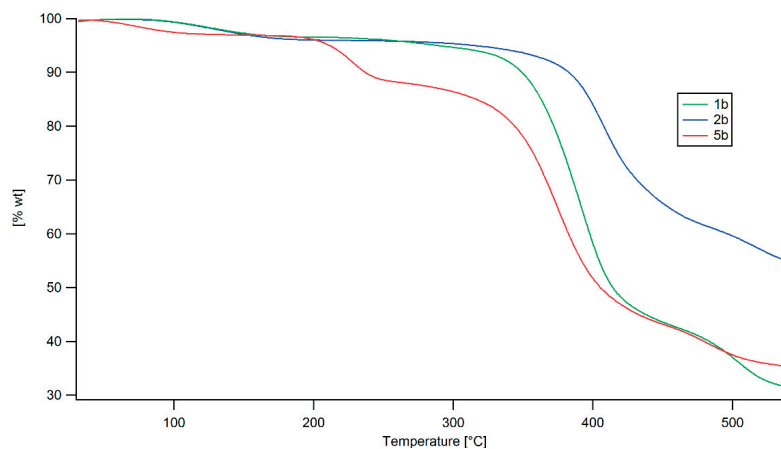


Figure 2.4.3 TGA curves for selected polymers **p1b**, **p2b** and **p5b**.

All the polymers were evaluated as catalysts in the cycloaddition of CO₂ to epoxides using styrene oxide (SO) to afford styrene carbonate (SC). Table 2.4.1 shows the yields of SC obtained under standard conditions for the polymers in order to identify the most potent catalyst. The anion is important for activity and in general bromide containing salts are more active than their chloride counterparts⁹³. However, for the ionic polymers with benzyl and dibenzyl spacers the catalytic activity of the bromide and chloride salts are essentially the same (Table 2.4.1, entries 3-4 and 5-6). As expected, the nature of the spacer has a marked influence on the reaction: simple spacers like hexyl, benzyl or dibenzyl lead to significantly less active catalysts than those incorporating a H-donor, *i.e.* **p4b**, **p5b** and **p6b** (Table 2.4.1, entries 8-10-11). The most active catalyst is **p5b** which contains a diol spacer. Imidazolium salts modified with similar functional groups to those described here have been evaluated as catalysts for the CCE reaction.^{151,210} However, for processing purposes, the polymer-based catalysts facilitate product separation. In this context, an example of a diol-functionalized imidazolium cation grafted onto polystyrene has also been evaluated in the CCE reaction.⁸³ A carboxylic acid functionalized imidazolium cation has also been grafted onto silica,²¹¹ and a hydroxyl-functionalized imidazolium cation grafted onto a cross-linked polymer⁸² to afford heterogeneous CCE catalysts.

Table 2.4.1. Evaluation of the polymers at catalysts for the synthesis of styrene carbonate.

Entry	Catalyst	Yield [%] ^[a]
1	p1a	12
2	p1b	25
3	p2a	14
4	p2b	15
5	p3a	14
6	p3b	15
7	p4a	16
8	p4b	48
9	p5a	17
10	p5b	62
11	p6b	37

Conditions: catalyst (0.5 mol%), SO (1 g, 8.33 mmol), CO₂ (25 bars), 100 °C, 15 h, neat. [a] Determined by GC-FID using n-decane as internal standard. All selectivities >99%.

Using the most efficient catalyst, *i.e.* **p5b**, the reaction conditions (pressure and temperature) were further optimized with a catalyst loading of 0.5 mol% (Table 2.4.2). The diol-containing polymer **p5b** afforded SC in near-quantitative yield at 130 °C under 2.5 MPa of CO₂ and the SC product was obtained by simply removing the catalyst by filtration (Table 2.4.2, entry 2). At a lower temperature of 80 °C the catalyst is active and SC is obtained in 41 % yield is obtained after 15 hours reaction (Table 2.4.2, entry 3).

Table 2.4.2 Optimization of pressure and temperature employing **p5b** as the catalyst for the CCE reaction.

Entry	P [bars]	T [°C]	Yield [%] ^[a]
1	10	130	62
2	25	130	99
3	25	80	41
4	25	100	62

Conditions: **p5b** (0.5 mol%), SO (1 g, 8.33 mmol), CO₂, 100 °C, 15 h. [a] Determined by GC-FID using n-decane as internal standard.

The activity of **p5b** is at least as good as other heterogeneous, supported catalysts which tend to require a co-catalyst and employ much higher catalyst loadings.^{212,213} Since a structurally-related homogeneous imidazolium salt containing a hydroxyl functional group fully converts styrene oxide at 80 °C and 4 bars of CO₂ after 24 hours at 5 mol% loading¹⁵¹, we were interested to see whether the catalyst presented herein would achieve high yields at a similar catalyst loading. Table 2.4.3 compares the activity of the monomer and the corresponding polymer under milder conditions than for **m/p5b** (note that for these experiments, 5 mol% cat. was used instead of 0.5 mol% used in Table 2.4.1 and Table 2.4.2). Interestingly, full conversion is obtained under these conditions after 24 hours, which is in contrast with the low yield of 41 % obtained at 80 °C and 2.5 MPa of CO₂ obtained with 0.5 mol% catalyst (Table 2.4.3, entries 1 and 2, and Table 2.4.2, entry 3). Moreover, SC was obtained in 94 % yield under atmospheric CO₂ pressure (balloon) at 120 °C

(Table 2.4.3, entry 5); at lower temperatures the yield is somewhat reduced (Table 2.4.3, entries 3-4). These results demonstrate the importance of benchmark conditions for the CCE reaction, because direct comparison between studies is difficult when more than one parameter differs.

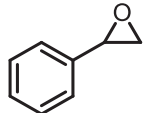
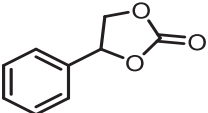
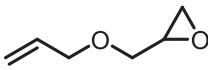
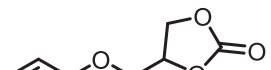
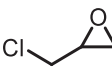
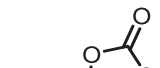
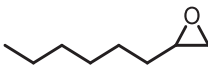


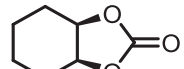
Table 2.4.3. Catalytic activity of **m5b** and **p5b** at a high loading.

Entry	Cat	T [°C]	P [bars]	Yield [%] ^[a]
1	m5b	80	4	>99
2	p5b	80	4	>99
3	p5b	80	1	68
4	p5b	100	1	78
5	p5b	120	1	94

Conditions: **cat.** (5 mol%), SO (0.1 g, 0.83 mmol), CO₂, 24 h. [a] Determined by ¹H NMR.

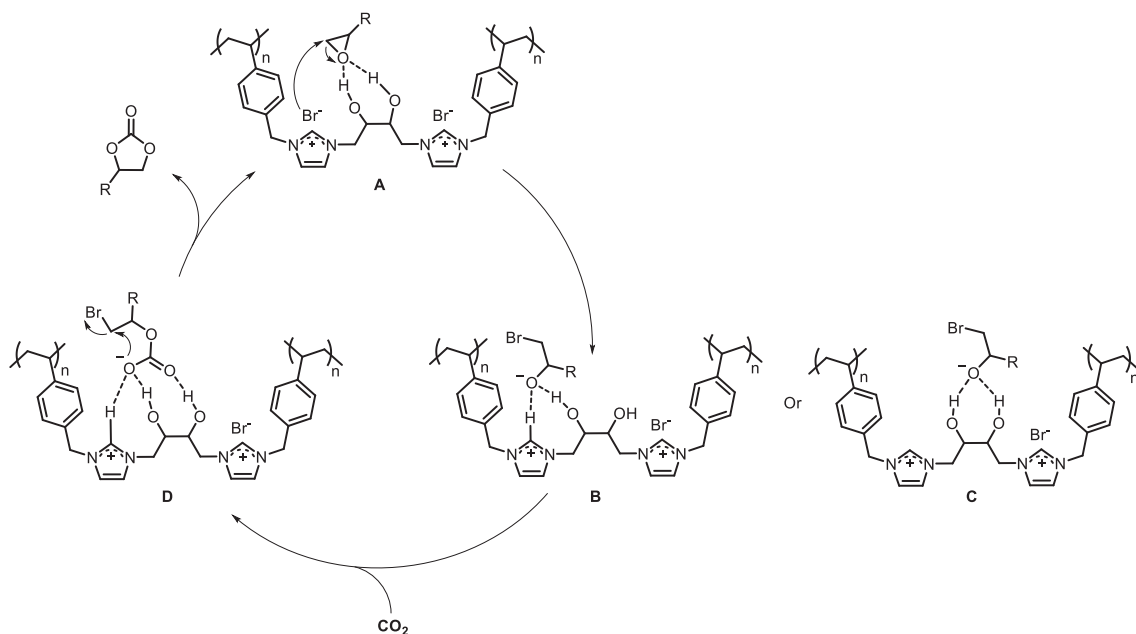
The scope of the CCE reaction was investigated with **p5b** using the optimized conditions with a low catalyst loading (0.5 mol%, Table 2.4.2 entry 2), and it was found to selectively incorporate CO₂ into a range of epoxides (Table 2.4.4, entries 1-4) in high yield, including cyclohexene oxide under more forcing conditions (140 °C, 86 hours, Table 2.4.4, entry 5), as the bicyclic structure of cyclohexene oxide leads to a much less reactive substrate.¹¹⁸ Polymers **p4b** and **p5b** are structurally related to a recently reported and highly active functionalized-imidazolium salt catalyst,¹⁵¹ which owe the high activity to the formation of favorable H-bonding interactions with the substrate, see below.

Table 2.4.4. Investigation of the substrate scope of the CCE reaction using **p5b** as the catalyst under optimized conditions.

Entry	Substrate	Product	Yield [%] ^[a]	Selectivity [%]
1			98	> 99
2			94	> 99
3			99	> 99
4			98 ^[b]	> 99
5			98 ^[c]	> 99

Conditions: **p5b** (25 mg, 0.5% mol), epoxides (8.3 mmol), CO₂ (25 bars), 130 °C, 15 h, neat. [a] Isolated yield. [b] Conditions: 48 h, 140 °C. [c] Conditions: 86 h, 140 °C.

The mechanism of the CCE reaction catalyzed by ion pairs has been proposed with the anion initially opening the oxirane which, in turn, facilitates CO₂ insertion. The catalytic cycle is concluded with a ring-closing SN₂ reaction also regenerating the catalyst. DFT calculations have been used to confirm this mechanism for both ammonium and imidazolium salts.^{120,121} Following this mechanism (See Sections 2.1.2 and 2.2 for more details on the mechanism), we hypothesize that the key interactions shown in the catalytic cycle (Scheme 2.4.1) result in the high activity of the diol containing polymer **p5b**. Since the rate-determining step is usually the ring-opening of the epoxide (at least in the case of imidazolium salts),¹²⁰ the H-bonding interactions between the diol and epoxide O-atom presumably help to reduce the activation energy of this step. This is consistent with previous studies which show that catalysts can be improved by incorporating a H-bonding functionalities.⁸⁷ While the polymers possess two imidazolium centers, it is uncertain whether this has a catalytic advantage. However, this di-cationic structure makes the catalyst robust and insoluble, presumably due to the highly cross-linked nature of the material. Note that with other catalysts such as polyphenols or aluminum complexes, the mechanism and in particular the rate-determining step can be different (See also Sections 2.1 and 2.2).^{214,215}



Scheme 2.4.1 Tentative mechanism for the CCE reaction catalyst employing **p5b** as the catalyst.

Although diol containing ILs are generally hygroscopic, polymer **p5b** is not noticeably hygroscopic and is bench-stable for months. The cross-linked nature of **p5b** provides a robust and easily handled catalyst ideal for recycling and reuse. The catalyst was recycled three times (Figure 2.4.4) without any loss of activity with epichlorohydrin as the starting material. After each reaction the mixture was diluted in ethyl acetate and the product was recovered by filtration without the need for any additional purification steps. The ^1H NMR spectrum of the product after the third recycling indicates that the product is pure and is not contaminated by the catalyst and is free from unreacted starting material. It should be noted that the catalyst turns from white to brown after several runs, although this has no influence on catalytic activity.

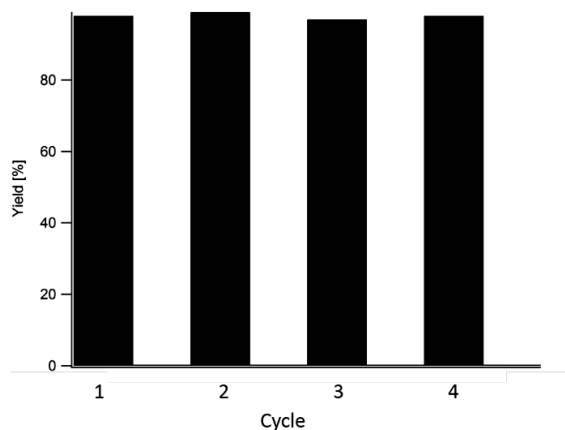


Figure 2.4.4 Recycling experiments using epichlorohydrin as a substrate under optimized conditions: **p5b** (24.9 mg, 0.5 mol%), epichlorohydrin (0.76 g, 8.3 mmol), CO₂ (25 bars), 130 °C, 15 h.

2.4.2. Conclusions

Herein, we described a series of cross-linked di-cationic ionic imidazolium polymers with different functionalized spacers between the imidazolium rings. Cationic polymers resembling **p1** have been employed in membranes with TF₂N⁻ as the counter-anion, however, these materials as well as the new polymers **p2a/b** to **p6a/b** were not used in catalysis. Consequently, we evaluated the polymers as catalysts for the industrially important CCE reaction, as previous studies had shown that imidazolium salts are efficient catalysts for this reaction, especially when H-donor functional groups such as alcohols or diols are in proximity to the ring. The diol-functionalized solid-phase organocatalyst reported here is highly active and operates under high CO₂ pressures or, at higher loadings, under ambient conditions so that the use of autoclaves can be avoided. The most active polymer catalyst of the series, *i.e.* **p5b**, the di-cationic polymer containing a diol-functionalized spacer, can incorporate CO₂ selectively in a range of epoxides including cyclohexene oxide, and can be recycled without a marked decrease in activity.

2.4.3. Experimental details

2.4.3.1. General Remarks

All starting materials were purchased from commercial providers and used as received. Reaction solvents were of absolute purity (according to Acros® brand). The solvents used for washing of the catalysts and for carbonate extraction were of technical grade. All the monomers and polymers were prepared under a N₂ atmosphere using standard Schlenk techniques. 4-Vinylbenzylimidazole was prepared using a literature procedure.¹⁹⁹ GC-MS were carried out on a Gas Chromatograph Agilent 7890B equipped with a Agilent 7000C MS triple quad detector and a capillary column from Agilent (l x d x f: 30 m x 0.25 mm x 0.25 μm)

using N₂ as carrier gas. ¹H and ¹³C NMR spectra were recorded on a Bruker 400 MHz instrument and electrospray ionization mass spectra were obtained on a LTQ-Orbitrap Elite instrument (ThermoFisher) operated in positive ionization mode using a literature method.²¹⁶ Elemental analysis was determined on a Flash 2000 Organic Elemental Analyzer. IR spectra were recorded on a Perkin-Elmer FT-IR 2000 instrument. TGA was carried out on a Perkin-Elmer TGA 4000. BET experiments were obtained on a Quantachrome Autosorb-IQ/MP-XR with N₂ as gas for analyte. SEM pictures were obtained on a FEI XLF30-FEG with Schottky field emission gun operated between 1 - 30 kv.

2.4.3.2. Typical procedure for ionic monomer synthesis, m1a-b to m6a-b

4-Vinylbenzylimidazole (4.2 mmol), the appropriate spacer (2 mmol) and CH₃CN (10 mL) were loaded into a 25 mL two-neck flask. The mixture was heated to 80 °C for 12 – 168 h depending on the spacer. The reaction was monitored by ¹H NMR spectroscopy and when the reaction was complete (*i.e.*, all the mono-quaternization product disappeared), the reaction mixture was cooled down to r.t and transferred to a 100 mL round bottom flask. The product was precipitated with EtOAc (50 mL) and sonicated for 10 min, after which the white solid was left to settle. The liquid phase was carefully removed, and the washing procedure was repeated twice with EtOAc (2 x 50 mL), and twice with 50 mL Et₂O. Then, the white solid product was dried under vacuum overnight.

3,3'-(hexane-1,6-diyl)bis(1-(4-vinylbenzyl)-1H-imidazol-3-ium) chloride was isolated as a white hygroscopic powder. Reaction time: 12 h. Yield 98 %. ¹H NMR (400 MHz, DMSO-*d*₆) δ 9.46 (s, 2H), 7.84 (s, 4H), 7.53 (d, 4H), 7.42 (d, *J* = 7.8 Hz, 4H), 6.75 (dd, *J* = 17.6, 11.0 Hz, 2H), 5.88 (d, *J* = 17.7 Hz, 2H), 5.43 (s, 4H), 5.31 (d, *J* = 10.9 Hz, 2H), 4.17 (t, *J* = 7.2 Hz, 4H), 1.79 (t, *J* = 7.2 Hz, 5H), 1.25 (tt, *J* = 8.1, 3.4 Hz, 4H). ¹³C NMR (101 MHz, DMSO-*d*₆) δ 138.1, 136.7, 136.38, 134.77, 129.16, 127.13, 123.00, 115.78, 52.14, 49.27, 29.46, 25.33. Yield: 99%. Anal. Calc. for C₃₀H₃₆Cl₂N₄: C 68.82, H 6.93, N 10.7; Found: C 67.82, H 7.56, N 10.79. HRMs Calc. for C₂₁H₂₇N₄²⁺: 335.2225; Found: 335.2254.

3,3'-(hexane-1,6-diyl)bis(1-(4-vinylbenzyl)-1H-imidazol-3-ium) bromide was isolated as a white solid. Reaction time: 12 h. Yield: 98 %. ¹H NMR (400 MHz, Methanol-*d*₄) δ 9.26 – 9.13 (m, 2H), 7.76 – 7.63 (m, 4H), 7.59 – 7.50 (m, 4H), 7.50 – 7.40 (m, 4H), 6.85 – 6.69 (m, 2H), 5.84 (dd, *J* = 17.7, 0.9 Hz, 2H), 5.44 (d, *J* = 4.8 Hz, 4H), 5.31 (dd, *J* = 11.0, 0.9 Hz, 2H), 4.27 (q, *J* = 7.4 Hz, 5H), 4.12 (q, *J* = 7.1 Hz, 1H), 3.46 (td, *J* = 6.7, 5.2 Hz, 6H), 2.00 – 1.84 (m, 5H), 1.51 – 1.37 (m, 5H), 1.26 (t, *J* = 7.2 Hz, 2H). ¹³C NMR (101 MHz, MeOD) δ 138.73, 135.84, 133.15, 128.58, 126.70, 122.68, 122.43, 114.12, 60.11, 52.52, 49.40, 29.36, 25.12, 13.04. Anal. Calc. for C₃₀H₃₆Br₂N₄: C 58.83, H 5.93, N 9.15; Found: C 54.20, H 5.88, N 8.64.

3,3'-(1,4-phenylenebis(methylene))bis(1-(4-vinylbenzyl)-1H-imidazol-3-ium) chloride was isolated as a white powder. Reaction time: 12 h. Yield 96 %. ¹H NMR (400 MHz, DMSO-*d*₆) δ 9.53 (s, 2H), 7.85 (h, *J* = 2.1 Hz, 4H), 7.53 (d, *J* = 8.0 Hz, 4H), 7.50 (d, *J* = 6.4 Hz, 4H), 7.42 (d, *J* = 8.0 Hz, 4H), 6.75 (dd, *J* = 17.7, 11.0 Hz, 2H), 5.88 (d, *J* = 17.7 Hz, 2H), 5.44 (d, *J* = 7.5 Hz, 8H), 5.32 (d, *J* = 11.0 Hz, 2H). ¹³C NMR (101 MHz, DMSO-*d*₆) δ 138.1, 136.8, 136.4, 135.8, 134.6, 129.5, 129.3, 127.2, 123.4, 115.8, 52.3. Anal. Calc. for C₃₂H₃₂Cl₂N₄: C 70.71, H 5.93, N 10.31; Found: C 70.50, H 6.11, N 10.42. HMRs Calc. for C₂₃H₂₃N₄²⁺: 355.1912; Found: 355.1939.

3,3'-(1,4-phenylenebis(methylene))bis(1-(4-vinylbenzyl)-1H-imidazol-3-ium) bromide was isolated as a white hygroscopic powder. Reaction time: 12 h. Yield 97 %. ¹H NMR (400 MHz, DMSO-*d*₆) δ 9.44 (s, 1H), 7.90 – 7.80 (m, 2H), 7.54 (d, *J* = 8.0 Hz, 4H), 7.48 (s, 2H), 7.42 (d, *J* = 8.1 Hz, 2H), 6.76 (dd, *J* = 17.7, 10.9 Hz, 1H), 5.89 (d, *J* = 17.7 Hz, 1H), 5.44 (d, *J* = 8.1 Hz, 4H), 5.32 (d, *J* = 10.9 Hz, 1H). ¹³C NMR (101 MHz, DMSO-*d*₆) δ 138.1, 136.8, 136.4, 135.8, 134.6, 129.5, 129.3, 127.2, 123.4, 115.8, 52.2. Anal. Calc. for C₃₂H₃₂Br₂N₄: C 60.77, H 5.1, M 8.86; Found: C 59.07, H 5.32, N 8.83. HMRs Calc. for C₂₃H₂₃N₄²⁺: 355.1912; Found: 355.1947.

3,3'-([1,1'-biphenyl]-4,4'-diylbis(methylene))bis(1-(4-vinylbenzyl)-1H-imidazol-3-ium) chloride was isolated as a white powder. Reaction time: 12 h. Yield: 95 %. ¹H NMR (400 MHz, DMSO-*d*₆) δ 9.62 – 9.49 (m, 1H), 8.06 (s, 2H), 7.89 (dq, *J* = 10.7, 2.0 Hz, 2H), 7.80 – 7.65 (m, 3H), 7.54 (d, *J* = 7.8 Hz, 5H), 7.44 (dd, *J* = 6.5, 4.4 Hz, 2H), 6.76 (ddd, *J* = 17.7, 10.9, 3.3 Hz, 1H), 5.89 (dd, *J* = 17.8, 3.3 Hz, 1H), 5.48 (dd, *J* = 18.6, 3.6 Hz, 5H), 5.32 (dd, *J* = 10.9, 3.5 Hz, 1H). ¹³C NMR (101 MHz, MeOD) δ 171.55, 138.74, 135.85, 128.57, 128.41, 126.71, 126.69, 123.27, 122.48, 114.12, 60.11, 52.63, 19.44, 13.05. Anal. calc. for C₃₈H₃₈Cl₂N₄: C 73.42, H 6.16, N 9.01; Found: C 71.45, H 6.31, N 8.58. HMRs Calc. for C₁₉H₁₈N₂⁺: 274.1465; Found 274.1470.

3,3'-([1,1'-biphenyl]-4,4'-diylbis(methylene))bis(1-(4-vinylbenzyl)-1H-imidazol-3-ium) bromide was isolated as a white powder. Reaction time: 12 h. Yield: 98 %. ¹H NMR (400 MHz, DMSO-*d*₆) δ 9.49 (s, 2H), 7.87 (dt, *J* = 9.7, 1.9 Hz, 4H), 7.82 – 7.71 (m, 5H), 7.59 – 7.50 (m, 9H), 7.43 (d, *J* = 8.2 Hz, 4H), 6.75 (dd, *J* = 17.7, 11.0 Hz, 2H), 5.88 (dd, *J* = 17.7, 0.9 Hz, 2H), 5.47 (d, *J* = 19.4 Hz, 9H), 5.32 (dd, *J* = 10.9, 0.9 Hz, 2H). ¹³C NMR (101 MHz, DMSO) δ 138.1, 136.8, 136.4, 134.7, 134.6, 129.5, 129.3, 127.8, 127.2, 123.4, 115.8, 52.3, 52.2. Anal. calc. for C₃₈H₃₈Br₂N₄: C 64.42, H 5.12, N 7.91; Found: C 63.35, H 5.15, N 7.71.

3,3'-(2-carboxypropane-1,3-diyl)bis(1-(4-vinylbenzyl)-1H-imidazol-3-ium) bromide was isolated as a yellowish hygroscopic powder. Reaction time: 24 h. Yield 85 %. ¹H NMR (400 MHz, Methanol-*d*₄) δ 9.16 (dt, *J* = 74.5, 1.6 Hz, 2H), 7.79 (t, *J* = 1.8 Hz, 1H), 7.66 (dq, *J* = 5.1, 1.9 Hz, 2H), 7.52 (dt, *J* = 8.5, 1.9 Hz, 4H), 7.44 – 7.35 (m, 4H), 6.86 – 6.69 (m, 2H), 5.85 (dt, *J* = 17.6, 0.9 Hz, 2H), 5.46 (d, *J* = 3.6 Hz, 3H), 5.31 (dd, *J* = 10.9, 0.8 Hz, 2H), 4.12 (q, *J* = 7.1 Hz, 2H), 1.23 (dt, *J* = 24.3, 7.1 Hz, 4H). ¹³C NMR (101 MHz, MeOD) δ 171.6, 138.7, 135.9, 128.6, 128.4, 126.7, 126.7, 123.3, 122.5, 114.1, 60.1, 52.6, 19.4, 13.1. Anal. Calcd for C₂₈H₃₂Br₂N₄O₂: C 54.56, H 5.23, N 9.09; Found: C 54.24, H 5.47, N 9.09. HRMs Calc. for C₂₈H₂₉N₄O₂⁺: 453.2285; Found 453.2288.

3,3'-(2-hydroxypropane-1,3-diyl)bis(1-(4-vinylbenzyl)-1H-imidazol-3-ium) bromide was isolated as a white hygroscopic powder. Reaction time: 168 h. Yield 93 %. ¹H NMR (400 MHz, DMSO-*d*₆) δ 9.33 (s, 1H), 7.83 (d, *J* = 23.1 Hz, 2H), 7.53 (d, *J* = 50.0 Hz, 4H), 7.43 (d, *J* = 8.1 Hz, 4H), 6.75 (dd, *J* = 17.6, 11.0 Hz, 2H), 5.98 (d, *J* = 5.6 Hz, 1H), 5.88 (d, *J* = 17.7 Hz, 2H), 5.47 (s, 4H), 5.31 (d, *J* = 10.9 Hz, 2H), 4.45 (dd, *J* = 13.3, 2.4 Hz, 2H), 4.31 – 4.10 (m, 2H). ¹³C NMR (101 MHz, DMSO-*d*₆) δ 138.0, 137.3, 136.4, 134.7, 129.2, 127.1, 123.9, 122.8, 115.8, 67.9, 65.4, 52.6, 52.1. Anal. Calcd for C₂₇H₃₀Br₂N₄O: C 55.31, H 5.16, N 9.55; Found: C 54.65, H 5.58, N 9.26. HRMs Calc. for C₂₇H₃₀BrN₄O⁺: 505.1603; Found 505.1593.

3,3'-(2,3-dihydroxybutane-1,4-diyl)bis(1-(4-vinylbenzyl)-1H-imidazol-3-ium) bromide was isolated as a white hygroscopic powder. Reaction time: 168 h. Yield 78 %. ¹H NMR (400 MHz, DMSO-*d*₆) δ 9.27 (s, 3H), 7.79 (d, *J* = 24.2 Hz, 6H), 7.54 (d, *J* = 8.1 Hz, 6H), 7.41 (d, *J* = 8.1 Hz, 6H), 6.76 (dd, *J* = 17.6, 11.0 Hz, 3H), 5.89 (d, *J* = 17.7 Hz, 3H), 5.57 (d, *J* = 6.6 Hz, 3H), 5.45 (s, 5H), 5.32 (d, *J* = 10.6 Hz, 3H), 4.38 – 4.28 (m, 3H), 4.25 – 4.14 (m, 3H), 3.84 – 3.79 (m, 3H). ¹³C NMR (101 MHz, DMSO-*d*₆) δ 138.0, 137.2, 136.4, 134.7, 129.1, 127.1, 124.0, 115.8, 70.3, 52.1. Anal. Calc. for C₂₈H₃₂Br₂N₄O₂: C 54.56, H 5.23, N 9.09; Found: C 52.60, H 5.15, 8.82. HRMs Calc. for C₂₈H₃₂N₄O₂Br⁺: 535.1708, 537.1693; Found 535.1705, 537.1689.

2.4.3.3. Alternative procedure for the synthesis of ionic monomers m4a and m5a

Imidazole (1.64 g, 24 mmol, 3 eq) and NaOH (0.96 g, 24 mmol, 3 eq) and CH₃CN (10 mL) were loaded into a 25 mL two-neck flask. To the suspension the appropriate organohalide (8 mmol) was added dropwise. The mixture was heated to 60 °C for 15 h. After reaction, the mixture was cooled to r.t. and diluted in DCM (ca. 20 mL), and the resulting white solid was collected. An aqueous work-up was not possible as the product is soluble in water. The solid was washed with EtOH to solubilize the target compound. The insoluble solid was discarded, and the EtOH evaporated to afford the di-imidazole product. In a second step, the di-imidazole compound (1.34 g, 7 mmol, 1 eq) and CH₃CN (10 mL) were loaded in a 25 mL two-

neck flask. Then, 4-vinylbenzyl chloride (2.48 g, 14.7 mmol, 2.1 eq) was added dropwise to the solution. The mixture was heated to 80 °C for 15 h. After reaction, the mixture was cooled to r.t. and transferred to a 250 mL flask. The imidazolium salt was purified by precipitation in EtOAc and diethyl ether using the procedure described above.

3,3'-(2-hydroxypropane-1,3-diyl)bis(1-(4-vinylbenzyl)-1H-imidazol-3-ium) chloride was isolated as a white hygroscopic powder. Yield 50%. ¹H NMR (400 MHz, DMSO-*d*₆) δ 9.51 – 9.30 (m, 2H), 7.84 (s, 4H), 7.65 (s, 2H), 7.60 – 7.48 (m, 6H), 7.42 (t, *J* = 7.0 Hz, 5H), 6.75 (dd, *J* = 17.6, 11.0 Hz, 3H), 5.88 (d, *J* = 17.7, 1.3 Hz, 3H), 5.45 (d, 4H), 5.31 (d, *J* = 10.9 Hz, 3H), 4.43 (t, *J* = 12.2, 11.2 Hz, 2H), 4.30 – 4.13 (m, 2H). ¹³C NMR (101 MHz, DMSO) δ 138.1, 137.3, 136.4, 134.7, 129.2, 128.8, 127.1, 127.0, 123.9, 122.8, 115.8, 68.6, 67.9, 65.4, 52.5, 52.1, 36.4, 15.7. Anal. Calcd for C₂₇H₃₀Cl₂N₄O: C 65.19, H 6.08, N 11.26; Found: C 59.24, H 6.25, N 11.83.

3,3'-(2,3-dihydroxybutane-1,4-diyl)bis(1-(4-vinylbenzyl)-1H-imidazol-3-ium) chloride was isolated as a white powder. Yield 58%. ¹H NMR (400 MHz, DMSO-*d*₆) δ 9.27 (s, 2H), 7.79 (d, *J* = 24.3, 1.8 Hz, 4H), 7.54 (d, 4H), 7.41 (d, 4H), 6.76 (dd, *J* = 17.7, 11.0 Hz, 2H), 5.88 (d, *J* = 17.7, 1.0 Hz, 2H), 5.57 (d, *J* = 6.6 Hz, 2H), 5.44 (s, 2H), 5.32 (d, 2H), 4.33 (d, *J* = 13.8, 3.0 Hz, 2H), 4.25 – 4.12 (m, 2H). ¹³C NMR (101 MHz, DMSO-*d*₆) δ 138.0, 136.4, 134.7, 129.3, 129.2, 127.2, 127.1, 123.9, 123.3, 115.8, 70.3, 52.1.

2.4.3.4. Typical polymerization procedure

The monomer (0.2 g), azobisisobutyronitrile (AIBN) (5 wt%) and isopropanol (40 mL) were placed into a 100 mL two neck flask equipped with a condenser. The mixture was heated to 90 °C for 15 h. After reaction, the reaction mixture was cooled down to r.t., and the white precipitate was transferred to a 250 mL round bottom flask. 100 mL of diethyl ether was added. The precipitate was sonicated for 15 minutes. This procedure was repeated three times and the white product was dried under vacuum overnight.

2.4.3.5. Typical catalytic experiment (at high pressure)

The epoxide (8.3 mmol) and the catalyst (0.5 mol%) are loaded into a 45 mL stainless steel autoclave. CO₂ is added to the desired pressure. The autoclave was purged 3 times with CO₂ to ensure that no air remained in the system. The autoclave was heated in an oil bath set to the appropriate temperature. To quench the reaction, the autoclave is cooled down in an ice cold water bath and slowly de-pressurized. 5 mL of EtOAc were added to dilute the reaction mixture. After decane was added as internal standard, the yields were determined by GC-MS. For the scope, all the carbonate products were obtained in pure form after either a column-chromatography or by simple filtration of the solid catalyst.

2.4.3.6. Typical catalytic experiment (at atmospheric pressure)

The catalyst (5 mol%) and the epoxide (0.83 mmol) were loaded in a 10 mL two-neck flask equipped with a stirring bar. The flask was connected to a Schlenk line and a CO₂ balloon. After 3 vacuum-CO₂ cycles, the flask was brought to the desired temperature in an oil bath for the appropriate time. After reaction, the mixture was cooled to RT. CDCl₃ (1 mL) was added to the flask, as the product was in solid phase, to extract the epoxide/carbonate mixture. The yield was determined by ¹H NMR (D1 = 3 sec).

2.4.3.7. Typical recycling experiment

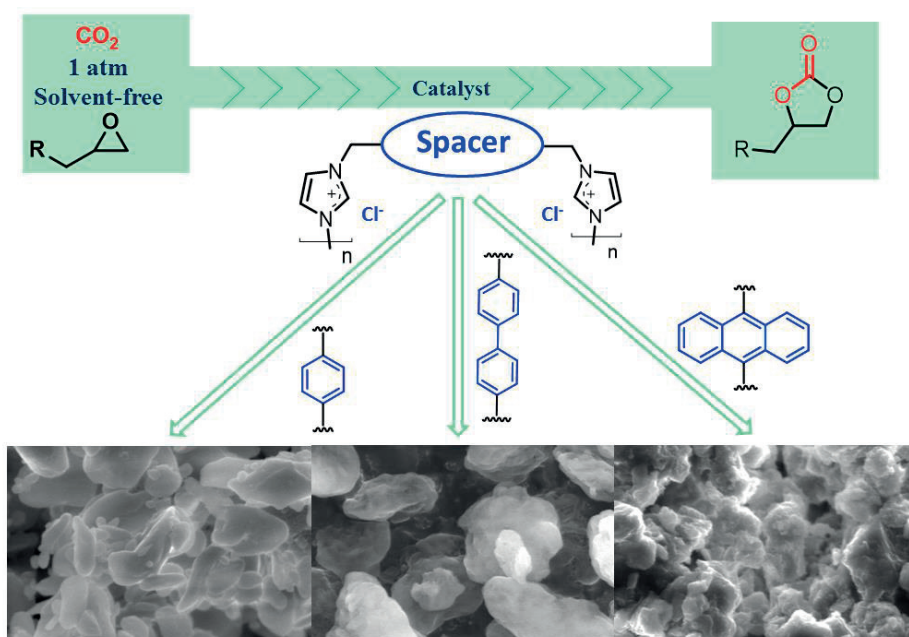
The recycling experiment was performed with epichlorohydrin as a starting material. After reaction, 5 mL ethyl acetate was added to the mixture, and the liquid phase was carefully removed with a pipette. This washing was done 3 times. The catalyst was then dried under vacuum and reused in the next catalytic experiment.

2.5. Synthesis of cross-linked poly(imidazolium) salts and their application in the CCE reaction

This section is published as an article in *ChemSusChem*, **2017**, 10, 2728–2735.

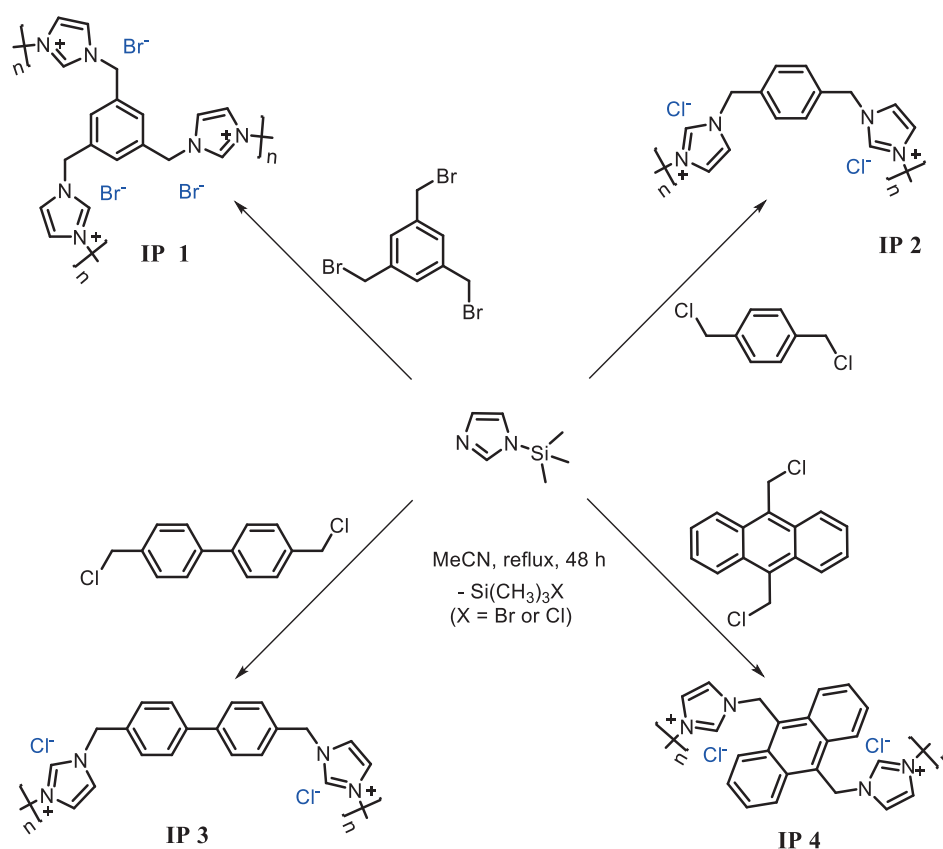
List of authors: **Felix D. Bobbink***, Wei Zhong*, Zhaofu Fei, Paul J Dyson, * = equal contribution.

Graphical abstract:



2.5.1. Results and Discussion

Polyimidazolium salts, **IPs 1 – 4**, were prepared from the reaction of trimethylsilylimidazole with the appropriate alkyl halide in a 3:2 ratio for **IP 1** or a 1:1 ratio for **IPs 2 – 4** (Scheme 2.5.1). The reaction requires only gently heating under catalyst-free conditions and the volatile by-product, *i.e.* trimethylsilyl bromide or trimethylsilyl chloride, is easily removed under vacuum. The **IPs 1 – 4** are obtained as solids in near-quantitative yield by filtration and subsequent washing with acetonitrile and ethyl ether. All the IPs are insoluble in organic solvents and water, and are highly hydrophobic and may be stored on the bench without capturing ambient moisture from the air.



Scheme 2.5.1. Synthesis of **IPs 1 – 4**.

The presence of the imidazolium rings in **IPs 1 – 4** was confirmed by IR spectroscopy from the characteristic bands centered around 1150 ($\text{C}=\text{N}^+$), 1560 ($\text{C}=\text{C}$) and 1625 ($\text{C}=\text{N}$) cm^{-1} (Figure 2.5.1).²¹⁷ The solid-state cross-polarization magic angle spinning (CP-MAS) ^{13}C NMR spectra of the IPs further confirm their composition (Figure 2.5.2), with signals at ca. 132 and 40 ppm assigned to the ring 2-carbon and methylene carbon atoms, respectively, as described previously.^{91,218} The thermal properties of **IPs 1 – 4** were

investigated under nitrogen using thermal gravimetric analysis (TGA) at a heating rate of 40 °C/min. Following the initial mass losses assigned to the desorption of trapped solvent at lower temperatures, the IPs are thermally stable up to 300 °C (Figure 2.5.3) and, notably, **IP 2** and **IP 3** are stable to almost 400 °C, which is higher than that observed for other imidazolium-containing polymers including those discussed in Chapter 2.3 and 2.4.^{207,219}

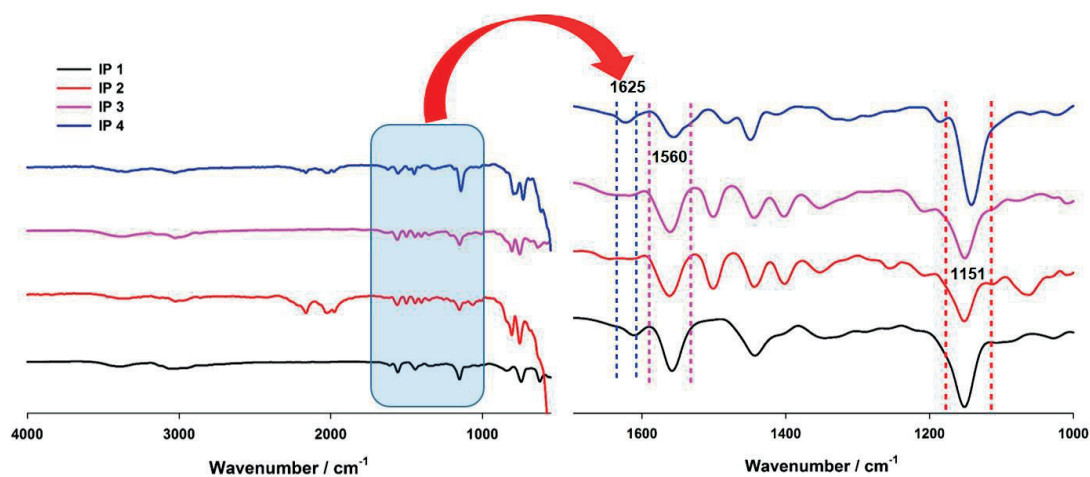


Figure 2.5.1 FT-IR spectra of IPs 1 – 4.

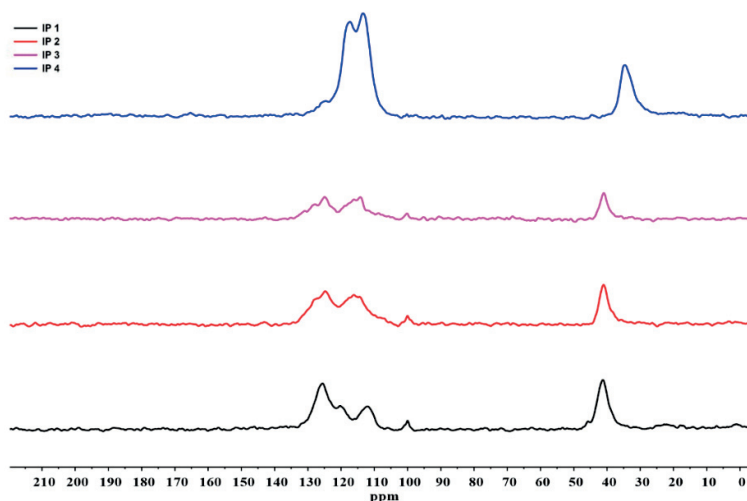


Figure 2.5.2 Solid-state ¹³C NMR spectra of the IPs 1 – 4 (from bottom).

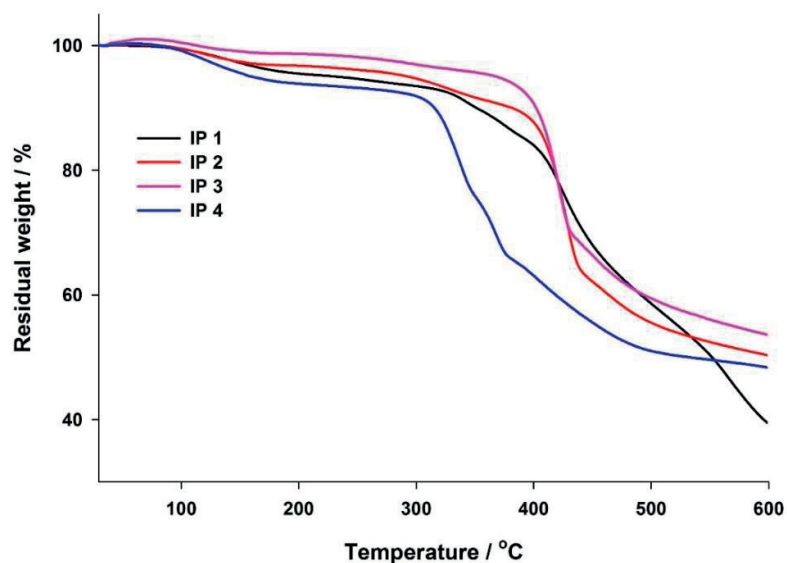


Figure 2.5.3 TGA analysis of **IPs 1 – 4** under nitrogen up to 600 °C at a heating rate of 40 °C/min.

The specific Brunauer–Emmett–Teller (BET) surface area of the IPs reveals slight differences between the polymers. Low BET values of 10.55 and 10.62 m²/g for **IP 1** and **IP 2**, respectively, are indicative of tight cross-linking (aggregation), confirming a condensed structure with a low empty volume. In contrast, **IP 3** and **IP 4** have larger spacers which form somewhat more porous structures have higher BET values of 91.56 and 68.34 m²/g, respectively.

The morphology of **IPs 1 – 4** was assessed by scanning electron microscopy (SEM) to reveal a composition of aggregated particles with irregular shapes and sizes (Figure 2.5.4). **IPs 3** and **4** display a sponge-like morphology and appear to have slightly rougher surfaces than **IP 1** and **IP 2**, consistent with the BET analysis. The powder X-ray diffraction (XRD) of **IPs 1 – 4** exhibit a broad reflection around 22°, which suggests they are largely amorphous (Figure 2.5.5), which is consistent with the SEM images.

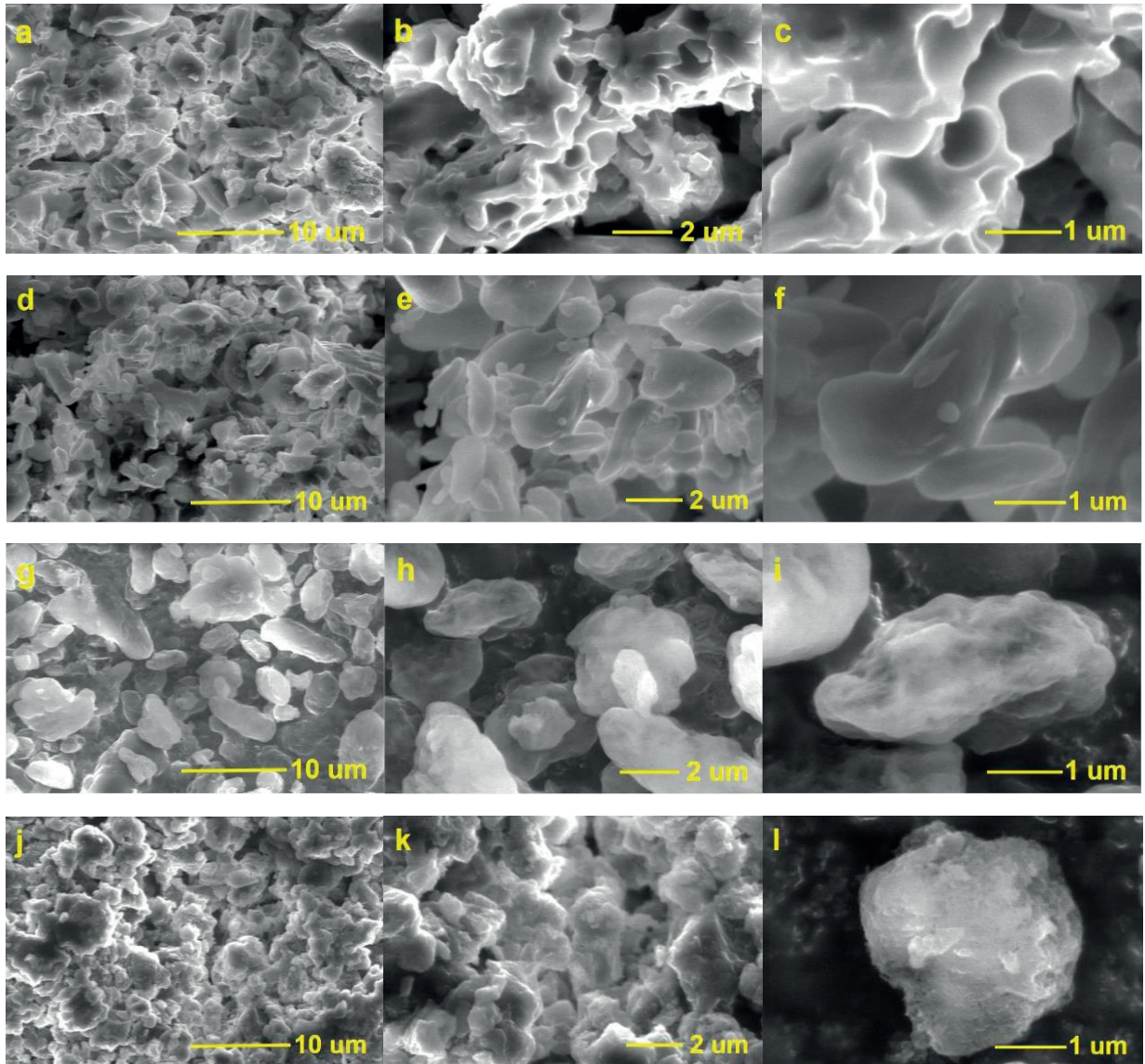


Figure 2.5.4 SEM images of (a – c) IP 1, (d – f) IP 2, (g – i) IP 3 and (j – l) IP 4

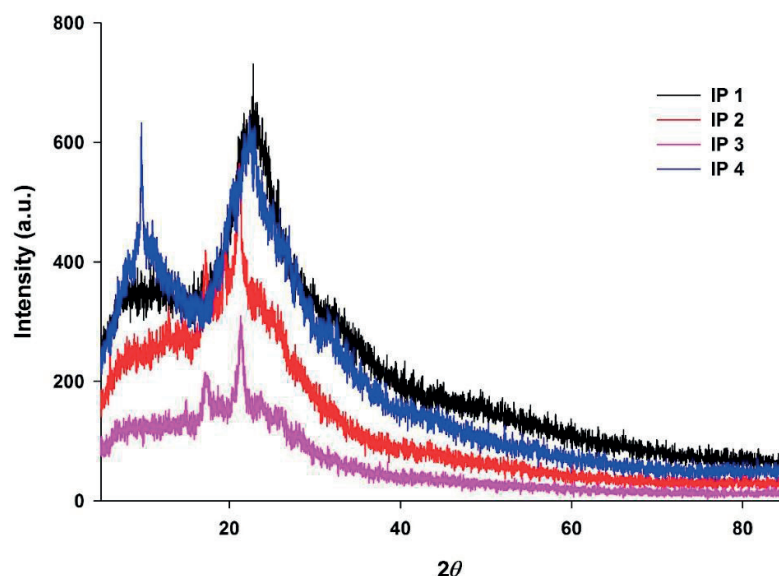


Figure 2.5.5 XRD patterns of IPs 1 – 4.

Since water can be detrimental to the cycloaddition of CO₂ to epoxides to afford cyclic carbonates (the CCE reaction) and these **IPs 1 – 4** are highly hydrophobic, they were evaluated as catalysts for the CCE reaction, an industrially relevant reaction that has been intensively investigated in recent years.^{87,220} The reaction was optimized for styrene oxide (**SO**) using 5 mol% of the polymer catalysts under 1 atmosphere of CO₂ and solvent-free conditions (Table 2.5.1).

All four **IPs** catalyze the cycloaddition of CO₂ with **SO** to afford styrene carbonate (**SC**), with **IP 2** and **3** being the most active (Table 2.5.1, entries 6 and 7), resulting in yields of 84 and 87 %, respectively, after 24 h at 100 °C and 1 atm. of CO₂. Catalysts employed in this reaction that operate at atmospheric pressure tend to rely on the synergies between cationic and anionic components of the catalyst and non-covalent interactions to provide the activity,²²¹ whereas our results demonstrate that simple **IPs** are also efficient at atmospheric pressure, consistent with recent studies on structurally-related **IPs** and our recent mechanistic study (See Chapter 2.2).^{95,220} **IP 1** is the least active of the series, with **SC** formed in 71 % yield after 24 h (Table 2.5.1, entries 1 and 5). The activity of **IP 4** decreases with time (Table 2.5.1, entries 4 and 8) due to a decomposition process observed during reaction. It is unlikely that the differences in catalytic activity is exclusively due to the different surface areas of the polymers. Instead catalyst stability and the nature of the counter anion appear to play critical roles. The difference in activity between **IP 1** and **IPs 2** and **3** is presumably due to the different counter anions present, with **IP 1** based on bromide and **IPs 2** and **3** containing chloride. **IP 4** is unstable under the reaction conditions, which presumably leads to the low

catalytic activity. Attempts to increase the catalytic activity of **IP 3** by the addition of a solvent (both polar and non-polar solvents were evaluated, see Table 2.5.1, entries 13–16) only led to lower activities compared to the reaction conducted under solvent-free conditions.

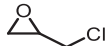
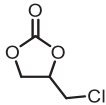
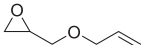
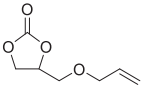
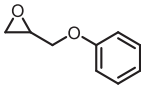
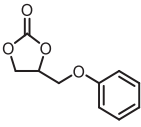
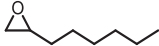
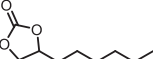
Table 2.5.1 Evaluation of **IPs 1 – 4** in the CCE reaction using **SO** as the starting material.

Entry	Catalyst	Solvent	P [atm.]	T [°C]	Time [h]	Yield [%]
1	IP 1	-	1	100	4	14
2	IP 2	-	1	100	4	23
3	IP 3	-	1	100	4	22
4	IP 4	-	1	100	4	44
5	IP 1	-	1	100	24	71
6	IP 2	-	1	100	24	84
7	IP 3	-	1	100	24	87
8	IP 4	-	1	100	24	73
9	-	-	1	120	24	0
10	IP 3	-	1	120	24	80
11	IP 3 (1 mol%)	-	1	120	24	40
12	IP 3	-	1	25	24	0
13	IP 3	DMF	1	100	24	39
14	IP 3	DMSO	1	100	24	76
15	IP 3	DMA	1	100	24	40
16	IP 3	Toluene	1	100	24	65

Conditions: Catalyst (5 mol%, based on monomer), **SO** (100 mg, 0.83 mmol), CO₂ (balloon). Yields determined by ¹H NMR spectroscopy.

Although **IP 3** is the most active catalyst, all the **IPs** were evaluated for catalytic activity under the optimized reaction conditions for a range of epoxide substrates (Table 2.5.2) with yields determined at 4 and 24 hours. Previously, it was reported that under certain conditions, catalytic activity is substrate size-dependant,²²² and since **IPs 1 – 4** differ in size of the spacer, and consequently porosity, several substrates were screened. Notably, **IP 1** results in the lowest activity for all the employed epoxides (see Table 2.5.2). **IP 2** and **IP 3** resulted in almost similar activities for all the tested substrates, with the exception of allyl glycidyl ether that was transformed more efficiently with **IP 3** (Table 2.5.2, entry 2, 76% for **IP 3** and 56% for **IP 2**). Notably, **IP 4** results in lower yields than that **IP 2** and **IP 3** with the exception of allyl glycidyl ether, which was converted in 79%, and for the slightly larger phenyl glycidyl ether or 1,2-epoxyoctane substrates (Table 2.5.2, entries 3 and 4), full conversion was not achieved within 24 hours. In the case of phenyl glycidyl ether a reaction time of 48 hours afforded the product in 87% yield using **IP 3** as the catalyst (Table 2.5.2, entry 3), whereas prolonging the reaction time did not improve the yield of 1,2-epoxyoctane. This might be attributable to the size of the substrate, which could hinder substrate-catalyst interactions within the polymer pores, but is probably also due to the intrinsic lower reactivity of the 1,2-epoxyoctane substrate.

Table 2.5.2 Substrate scope in the CCE reaction employing **IPs 1 – 4**.

Entry	Substrate	Product	Catalyst	Yield(%)
1			IP 1 IP 2 IP 3 IP 4	19 63 63 (99) 59
2			IP 1 IP 2 IP 3 IP 4	45 56 76 (99) 79
3			IP 1 IP 2 IP 3 IP 4	6 38 37 (78, 87) 36
4			IP 1 IP 2 IP 3 IP 4	1 10 4 (90) 6

Conditions: Catalyst (5 mol%), epoxide (0.83 mmol), CO₂ (balloon), 100 °C, 4 h. Yields determined by ¹H NMR spectroscopy. Yields in bracket are after 24 h and 48 h reaction, respectively.

Although the polymer catalysts are active at atmospheric pressure the volatility of propylene oxide (**PO**) necessitates the use of higher pressures to ensure good conversions. The reactivity of **PO**, arguably the most important epoxide substrate due to the importance of the corresponding carbonate,¹⁰⁵ was evaluated using a stainless steel autoclave under elevated pressures. After 15 hours at 115 °C under 10 atm. of CO₂ pressure, all the catalysts afforded propylene carbonate (**PC**) in 95 – 98 % yield (Table 2.5.3, entries 1-4, see Experimental for full details). At 100 °C, **IP 3** resulted in a yield of 93% of **PC** whereas a yield of only 60% was obtained for the reaction of **SO** (Table 2.5.3, entries 5 and 6). A quantitative yield was obtained when **SO** was reacted at 115 °C under 10 atm. of CO₂ (Table 2.5.3, entry 7). Under our experimental conditions, the use of higher pressures of CO₂ enables the reaction to reach completion, which was not achieved at atmospheric pressure (Table 2.5.1).

Table 2.5.3 CCE reaction under 10 atm. CO₂ employing **IPs 1 – 4**.

Entry	Catalyst	Epoxide	T [°C]	Yield [%]
1	IP 1	PO	115	98
2	IP 2	PO	115	98
3	IP 3	PO	115	95
4	IP 4	PO	115	96
5	IP 3	PO	100	93
6	IP 3	SO	100	60
7	IP 3	SO	115	>99

Conditions: Catalyst (5 mol%), epoxide (0.83 mmol), CO₂ (10 atm.), 15 h. Yields were determined by ¹H NMR spectroscopy.

The mechanism of the cycloaddition reaction employing imidazolium salt catalysts has been previously proposed and is supported by calculations (See also Section 2.1.2 and 2.2).^{120,179} It is not unreasonable to assume that **IPs 1-4** operate *via* a similar mechanism, *i.e.* in which the anion of the polymer opens the epoxide ring which enables insertion of CO₂ and a subsequent ring-closing S_N2 reaction (see Figure 2.5.6).

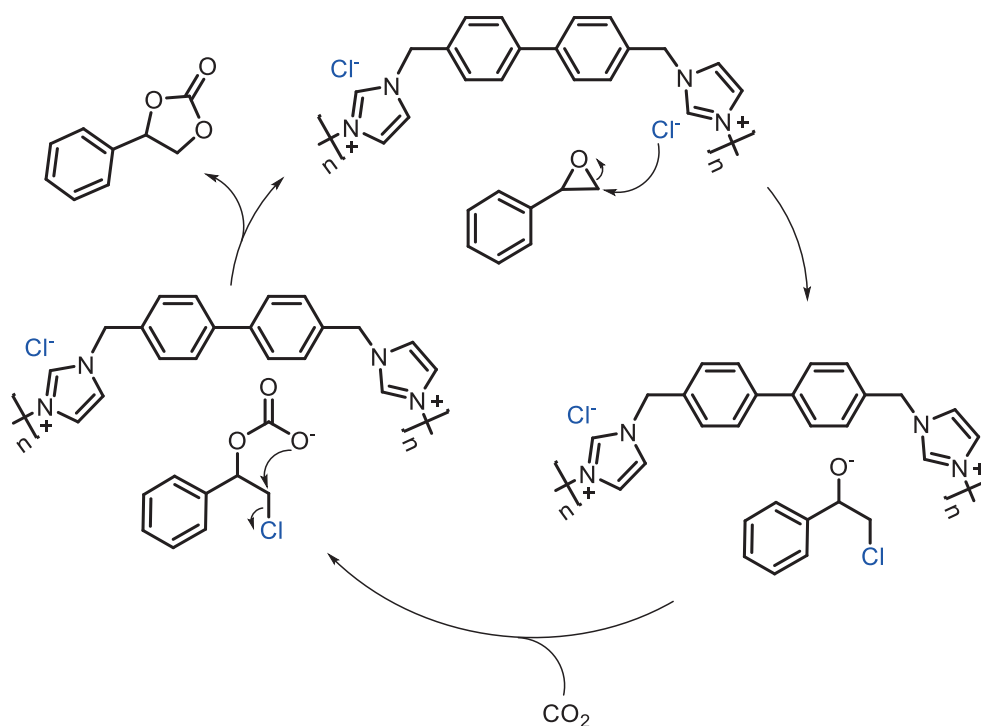


Figure 2.5.6 Postulated mechanism for the CCE reaction catalyzed by **IP 3**.

It has previously been shown that the CO₂ pressure influences the reaction rate and, therefore, **IP 3** was evaluated in the conversion of **PO** and **SO** at two different pressures (Figure 2.5.7). **PO** is transformed more rapidly than **SO** under similar conditions (Fig. 8, the red lines correspond to the formation of **PC** and the blue lines to **SC**, at different pressures). Moreover, at 10 atm. of pressure the reaction rate was faster than at 25 atm. of pressure for both epoxides (Figure 2.5.7), *i.e.* the yield of **PC** was 31 and 18% at 10 and 25 atm. of CO₂, respectively. This inverse relationship has been noted previously and is attributed to the formation of detrimental CO₂-PO interactions at higher pressures, that hinder contact with the catalyst and lead to lower reaction rates.^{164,223} However, after 6 h of reaction, the yields are almost similar for PC whereas the difference is more marked for SC (77 vs 82% and 62.5 vs 45% at 10 and 25 atm., respectively).

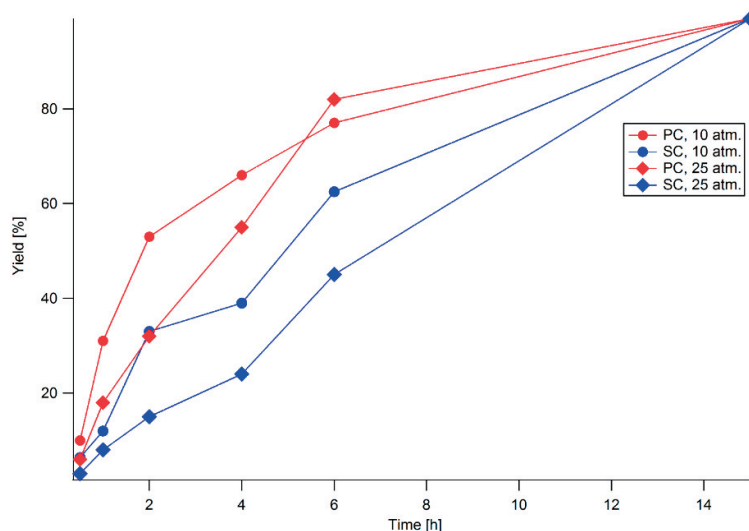


Figure 2.5.7 Kinetic traces for catalyst **IP 3** for the transformation of **PO** (red, circles for 10 atm., squares for 25 atm.) and **SO** (blue, circles for 10 atm, squares for 25 atm.). Conditions: **IP 3** (5 mol%), SO or PO (0.83 mmol), CO₂ (10 or 25 atm.). Yields determined by ¹H NMR spectroscopy.

The ability to recycle catalyst **IP 3** was investigated using **SO** as the substrate under 10 atm. of CO₂ at 115 °C in an autoclave. After each reaction, the product was extracted with Et₂O and the catalyst was dried and reused. It was possible to reuse the catalyst 10 times without a marked loss of activity (Figure 2.5.8), indicative of good structural stability of the catalyst. This is also supported by a comparison of the FT-IR spectra of the spent catalyst (Figure 2.5.9), which shows that the characteristic peaks around 1150 (C=N⁺) and 1560 (C=C) cm⁻¹, remain unperturbed after 10 reaction cycles. Such consistent reactivity suggests that the heterogeneous catalyst could be adapted to continuous flow reaction conditions.

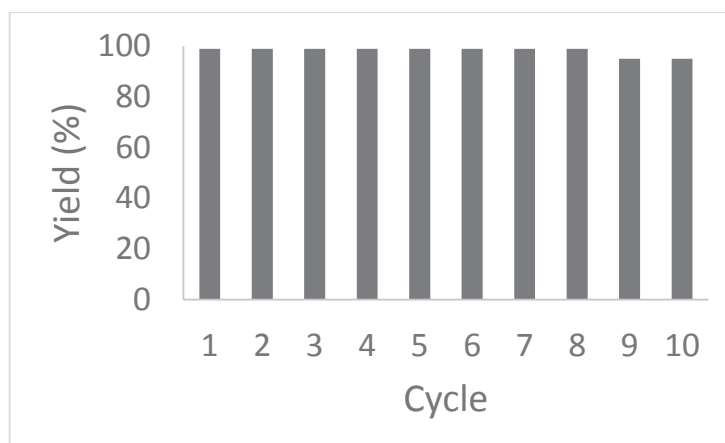


Figure 2.5.8 Recycling studies of catalyst **IP 3**. Conditions: **IP 3** (5 mol%), **SO** (0.83 mmol), CO₂ (10 atm.), 15 h. Yields determined by ¹H NMR spectroscopy.

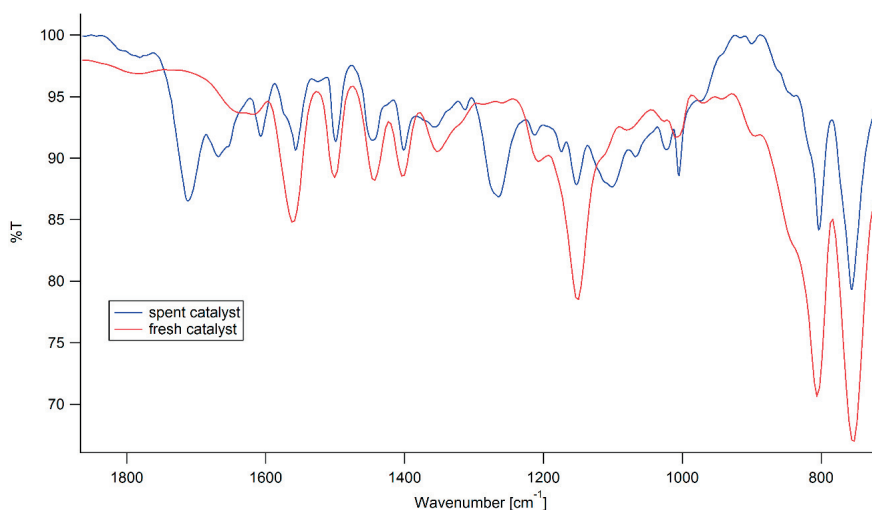


Figure 2.5.9 FT-IR spectral variation of the catalyst (**IP 3**) after 10 catalytic cycles. The main additional peaks present may be attributed to the reaction product.

2.5.2. Conclusions

A series of imidazolium-based IPs with different spacers were prepared in a facile manner from commercial starting materials in near-quantitative yields in which the porosity of the polymer is dependent upon the size of the spacer used in the starting material. The IPs are thermally stable and two of them, *i.e.* **IPs 2** and **3**, containing the phenyl and biphenyl spacer, are efficient heterogeneous organocatalysts for the cycloaddition of CO₂ to epoxides operating under solvent-free conditions. Catalyst **IP 3** could be reused multiple times without an appreciable loss of activity. We believe that these polymers could pave the way

toward more sustainable, non-toxic catalysts for the transformation of CO₂ and other substrates under ambient conditions. Moreover, they could find additional applications as membranes for the simultaneous extraction and transformation of CO₂.

2.5.3. Experimental details

2.5.3.1. General Remarks

Reagents were obtained from commercial sources and used as received. IR spectra were recorded on a Perkin-Elmer FT-IR 2000 instrument. Solid-state ¹³C NMR spectra were acquired using a Bruker Avance-II spectrometer equipped with a wide-bore 9.4 T magnet operating at a Larmor frequencies $\omega_0/2\pi = 100.6$ MHz for ¹³C. TGA analysis was carried out using a TGA/SDTA851 thermal analyzer with a heating rate of 40 °C/min under nitrogen. The BET area was recorded using a 30% v/v N₂/He flow using a Micromeritics Autochem II unit. Powder XRD measurements were determined on an X'Pert Philips diffractometer in Bragg-Brentano geometry with monochromatic CuK α _{1,2} radiation and a fast Si-PIN multi strip detector (0.1540 nm). Scanning electron microscopy (SEM) was performed on a Zeiss Nvision 40 CrossBeam instrument with dual beam FIB/SEM based on GEMINI[®] column. Elemental analysis was carried out on a Thermo Scientific Flash 2000 Organic Elemental Analyzer.

2.5.3.2. Synthesis of the IPs 1 – 4

1,3,5-Tris(bromomethyl)benzene (3.56 g, 10 mmol) and 1-(trimethylsilyl)imidazole (2.11 g, 15 mmol) were dissolved in acetonitrile (40 mL) in a 100 mL Schlenk-flask. The mixture was heated at refluxing for 48 h. The solvent and side-product was removed under vacuum and the white solid removed by filtration and washed with acetonitrile (3 × 30 mL) and diethyl ether (5 × 50 mL). The solid was collected as **IP 1** and dried under vacuum for 24 h. Yield: 3.35 g (99.1%). Elemental analysis calcd (%) for (C₂₇H₂₇N₆Br₃)_n: C, 48.03, H, 4.03, N, 12.45; found: C, 43.92, H, 4.13, N, 11.45.

IPs 2 – 4 were prepared using the same procedure employed for the preparation of **1**, but replacing 1,3,5-tris(bromomethyl)benzene with the appropriate alkyl dihalides (1,4-bis(chloromethyl)benzene for **IP 2**, 4,4'-bis(chloromethyl)-1,1'-biphenyl for **IP 3** and 9,10-bis(chloromethyl)anthracene for **IP 4**) and changing the molar ratio of the reactants from 2:3 into 1:1. Elemental analysis for **2** (white solid, 4.09 g, 98.8%, initially with 20 mmol) calcd (%) for (C₂₂H₂₂N₄Cl₂)_n: C, 63.93, H, 5.36, N, 13.55; found: C, 61.95, H, 5.36, N, 12.56. Elemental analysis for **3** (white solid, 5.62 g, 99.3%, initially with 20 mmol) calcd (%) for (C₃₄H₃₀N₄Cl₂)_n: C, 72.21, H, 5.35, N, 9.91; found: C, 67.76, H, 5.46, N, 9.49. Elemental analysis for **IP 4** (yellow solid, 3.02 g, 98.4%, initially with 10 mmol) calcd (%) for (C₃₈H₃₀N₄Cl₂)_n: C, 74.39, H, 4.93, N, 9.13; found: C, 68.69, H, 4.96, N, 8.14.

2.5.3.3. Catalytic studies

2.5.3.3.1. At atmospheric pressure:

Cycloaddition of CO₂ with epoxides was carried out in a 10 mL two-neck flask with vigorous stirring. In a typical catalytic reaction, the **IP** (5 mol%) and styrene oxide (100 mg, 0.83 mmol) were added to the flask without any solvent. The flask was equipped with a CO₂ balloon and the atmosphere was replaced by CO₂ using three vacuum-CO₂ cycles. The mixture was brought to the appropriate reaction temperature. After the appropriate time, the flask was cooled to room temperature, and CDCl₃ (1 mL) was added to the mixture. The reaction mixture was then filtered to discard the solid catalyst and the yield of the product was determined by ¹H NMR spectroscopy.

2.5.3.3.2. At elevated pressure:

In a typical catalytic reaction under pressure, the **IP** (1-5 mol%) and the epoxide (0.83 mmol) were added to a GC-vial without any solvent. The GC vial was sealed and pierced with a syringe and inserted in the stainless steel autoclave (100 mL capacity). Up to 4 GC vials could be inserted simultaneously to the autoclave. The reactor was sealed and pressurized to the appropriate pressure. The autoclave was heated to the appropriate temperature in an oil bath. After the appropriate time, the autoclave was cooled to 0 °C in an ice bath and the autoclave was depressurized. CDCl₃ (0.5 – 1 mL) was added to each GC vial *via* the septum, and the liquid phase was filtered to discard the solid catalyst and the yield of the product was determined by ¹H NMR spectroscopy.

2.5.3.3.3. Kinetic studies:

IP 3 (5 mol%, 16 mg) and the epoxide (**PO** or **SO**, 0.83 mmol) were weighed in a GC vial. The GC vial was sealed and pierced with a syringe and inserted in a stainless steel autoclave (100 mL capacity). Two vials were run at the same time, one containing **PO** and the other **SO**, to ensure the conditions were similar for the two epoxides. The autoclave was heated in a pre-heated oil bath at 115 °C. After the appropriate time (30 min to 15 h), the autoclave was cooled to 0 °C in an ice bath and the autoclave was depressurized. CDCl₃ (0.5 – 1 mL) was added to each GC vial *via* the septum, and the liquid phase was filtered to discard the solid catalyst and the yield of the product was determined by ¹H NMR spectroscopy.

2.5.3.3.4. Recycling studies:

IP 3 (5 mol%, 16 mg) and **SO** (0.83 mmol, 100 mg) were weighed in a GC vial, and the reaction was run as described in the previous section. After reaction, the autoclave was cooled to 0 °C, depressurized, and Et₂O (1 mL) was added to the GC vial for extraction. The catalyst was left to settle at the bottom of the vial and

the liquid phase was collected. The extraction was performed three times. The liquid phase contained the pure product which crystalized upon removal of the solvent. The catalyst was dried inside the vial on a rotary evaporator (by inserting the vial in a 10 mL flask). Then, fresh **SO** was added to the vial and the reaction was run again. The yield of the product was determined by ^1H NMR spectroscopy.

2.6. Quantitative extraction of CO₂ from air and other gas streams using simple

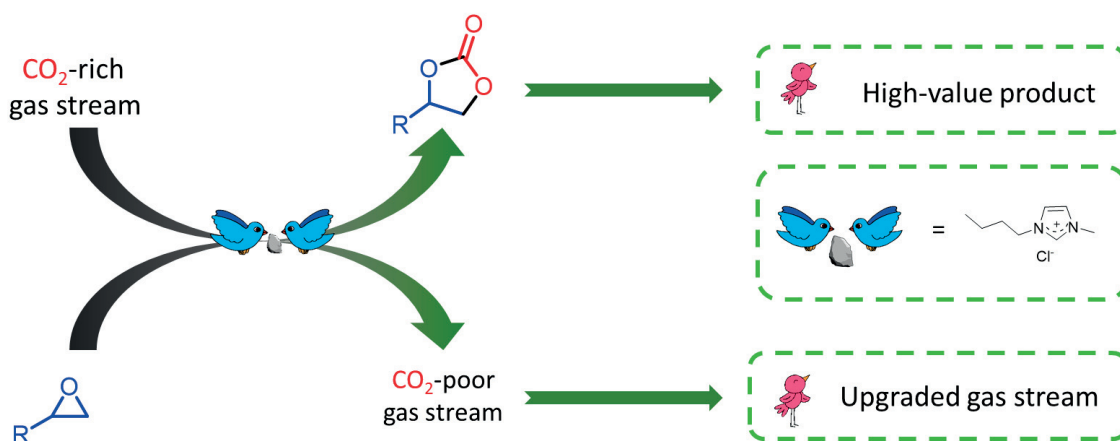
IL:epoxide mixtures

Manuscript in preparation.

List of authors: **Felix D. Bobbink**, Oliver A. Beswick, Sami Chamam, Liubov Kiwi-Munster, Gábor

Laurencyzy, Paul J. Dyson

Graphical abstract:



2.6.1. Introduction

The direct transformation of CO₂ from ambient air would be advantageous in an industrial setting as it would negate the costs associated with purifying air, and the additional costs involved in pressurizing the pure CO₂. In order to achieve this goal a reaction is required in which the co-substrate is highly activated and in this context the cycloaddition of CO₂ with epoxides is ideal as epoxides contain a highly strained and reactive three-membered ring. Moreover, the cycloaddition of CO₂ into epoxides (CCE) reaction has been thoroughly investigated in recent years because of the increasing importance of cyclic carbonate products, e.g. they are used as electrolytes in lithium batteries, as solvents or in the manufacture of CO₂-containing (poly)carbonates used as plastics in bottles and containers.^{100,103,224} These products are routinely prepared from the catalytic incorporation of CO₂ into appropriate epoxides (Figure 2.6.1), highlighting a successful industrial application involving CO₂ (see Chapter 2.1).¹¹ To the best of our knowledge, two catalytic processes employ air as a CO₂ source. The first one is for the preparation of oxazolidinones, and in this reaction a large excess of 1,8-Diazabicyclo[5.4.0]undec-7-ene, DBU is consumed, thus diminishing the benefits of the process. The second reaction is the electro-chemical reduction of CO₂ contained in air to oxalates *via* a copper-catalyst.²²⁵

2.6.2. Results and Discussion

Reaction conditions were initially optimized using pure CO₂ at 1 atm. employing a high loading of the cheap, commercial [BMIm]Cl catalyst, since the ultimate goal is to use air (average 400 ppm CO₂) in place of pure CO₂. With a catalyst loading of 5 mol%, at 100 °C full conversion was obtained after 20 h of reaction (Table 2.6.1, entry 1), demonstrating that simple imidazolium salts are much more potent than previously reported (this was confirmed in Chapter 2.2).⁹³ Increasing the catalyst loading results in a quantitative yield of the styrene carbonate (**SC**) product after only 5 h at a lower temperature of 80 °C (Table 2.6.1, entries 2 and 3). Decreasing the temperature to 60 °C resulted in a lower yield, but the reaction nonetheless proceeded (Table 2.6.1, entry 4), and even at room temperature small amounts of **SC** were formed (see Table A.2.6.1 in Appendix Chapter 2.6). Importantly, the selectivity of the reaction remains high under the reactions conditions evaluated. As expected, when the reaction is conducted in a stainless steel autoclave at 10 atm., the reaction proceeds faster than at atmospheric pressure (Table 2.6.1, cf. entries 10 and 5).¹⁵³ Interestingly, it has previously been reported that incorporating H-bonding groups on the cation of the catalyst enhances activity,^{82,116} such enhancements were not observed under our experimental conditions (Table 2.6.1, entries 5, 6, 7 and 8). Finally, the reaction also proceeds using a stoichiometric amount of dry ice and, to some extent, using breath (see Table A.2.6.2 in Appendix Chapter 2.6 for details).

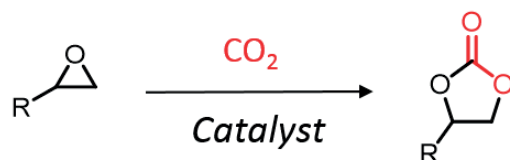


Figure 2.6.1 Generic cycloaddition of CO₂ into epoxides to afford cyclic carbonates (CCE reaction).

Table 2.6.1 Optimization of the reaction conditions for the transformation of **SO** into **SC** at atmospheric pressure.

Entry	Catalyst (mol%)	Time [h]	T (°C)	Yield (%)
1	[BMIm]Cl (5)	20	100	>99
2	[BMIm]Cl (50)	20	80	>99
3	[BMIm]Cl (50)	5	80	>99
4	[BMIm]Cl (50)	5	60	58
5	[BMIm]Cl (50)	1	80	23
6	[BMIm]Cl (5)	1	80	15
7	[HEMIm]Cl (50)	1	80	13.3
8	[HEMIm]Cl (5)	1	80	2.6
9^a	[BMIm]Cl (50)	1	80	25
10^b	[BMIm]Cl (50)	1	80	49

Reaction conditions: catalyst, **SO** (100 mg, 0.83 mmol), CO₂ (1 atm.). ^a 1 mL DMSO-d₆ was used as a solvent. ^b 10 atm. of CO₂ in an autoclave.

Several epoxides including phenyl glycidyl ether (**PGE**), allyl glycidyl ether (**AGE**) and epichlorohydrin (**EC**), are all smoothly converted to their respective carbonate product under a pure CO₂ atmosphere (Figure 2.6.2 and Table A.2.6.1 in Appendix Chapter 2.6). Bisphenol A diglycidyl ether (**BPAGO**) was converted in good yield (see Table A.2.6.1 in Appendix Chapter 2.6), and would potentially be a good epoxide candidate for reactions with air, owing to its low volatility, and the resulting carbonate product is a key compound for production of polycarbonates used as packaging materials.³⁴

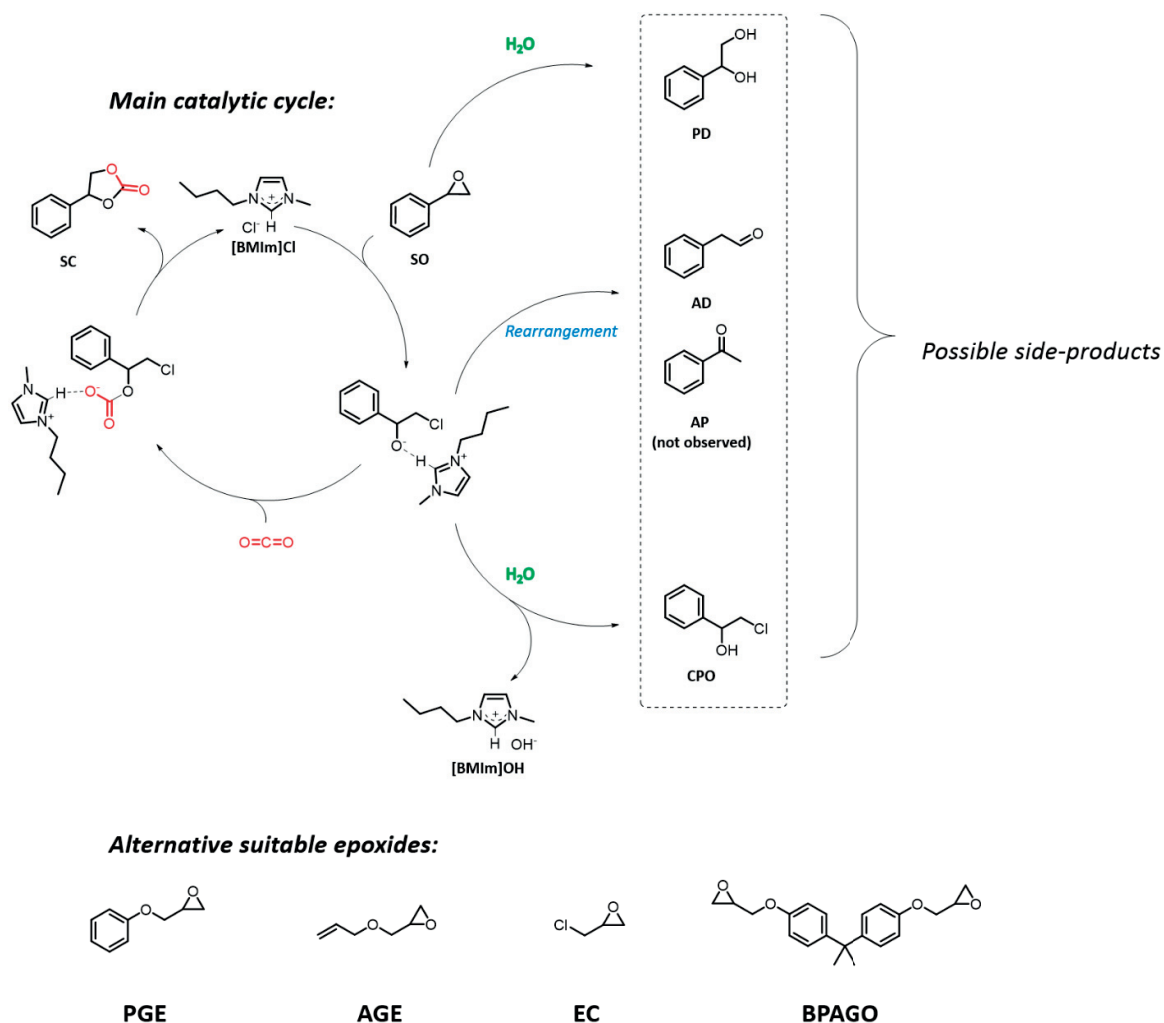


Figure 2.6.2 Proposed mechanism for the CCE catalyzed by imidazolium salts and rationale for catalyst decomposition and the formation of side-products. Alternative epoxides studied are shown below (see Appendix Section 2.6 for further details).

Following the optimization of the reaction using pure CO₂ at atmospheric pressure we studied the use of air as the CO₂ source and **SO** as the epoxide. The reaction mixture turned dark when air was bubbled through the mixture due to moisture that is not well tolerated under the reaction conditions. To clarify the impact of water on the reaction several control experiments were conducted and it was found that addition of water to the reaction system leads to side products such as 2-chloro-1-phenylethan-1-ol (**CPO**) and 1-phenylethane-1,2-diol (**PD**) (see Figure 2.6.2 for details). **CPO** presumably originates from the protonation of the alkoxide intermediate by water and concomitant formation of [BMIm]OH. Further control experiments demonstrate that small amounts of aldehyde may also form during the reaction,

possibly through a Meinwald rearrangement, which has been reported previously for the CCE reaction catalyzed by phosphonium salts.³⁵

Water was removed from the air by passing it through a desiccant (97% H₂SO₄ followed by silica beads) prior to entering the reaction flask. To maximize the surface area of the bubbles the dried air was blown through a frit filter prior its entrance in the reaction flask (Table 2.6.2, entries 2-4). Under these conditions the reaction proceeded with catalyst loadings of 5, 25 and 50 mol% employing **SO** as a starting material (25 g scale reaction, see Table 2). The reaction mixture could be kept on-stream for at least 14 days (see Fig. S3 for a representative example of a 5-day reaction). To avoid evaporation of the **SO** substrate, a reflux condenser was used, due to the high gas flow-rates (c.a. 20 l/min). Using 50 mol% catalyst the average uptake of CO₂ was 30 % (determined by GC and ¹H NMR spectroscopy, Table 2, entry 4).

Table 2.6.2 Results of the cycloaddition of CO₂ into **SO** affording **SC** using air as the CO₂ source.

Entry	Catalyst (mol%)	Time (days)	CO ₂ uptake (%)	T (°C)	Yield (%)
1 ^a	[BMIm]Cl (5)	-	-	80	n.d.*
2	[BMIm]Cl (5)	7	15	80	7
3	[BMIm]Cl (25)	7 (14)	20	80	9.2 (15)
4	[BMIm]Cl (50)	7	30	80	11

Reaction conditions: [BMIm]Cl (5-50 mol%), **SO** (25 g, 0.83 mmol), CO₂ (air pumped through system). ^a The air was pumped in the system *via* a needle, no drying. *: the selectivity dropped preventing quantification.

Following these investigations we progressed to continuous operation using a semi-batch stirred reactor (150 cm³ stainless steel autoclave) equipped with baffles and modified to allow a gas stream to flow through (see Experimental). For quantification purposes, defined gas mixtures were used as models for industrial flue gases or air. Initial reaction conditions were selected according to the previous results, namely 49.5 g **SO**, 5 mol% [BMIm]Cl, and an operating temperature of 75 °C. To ensure that the reaction was not limited by mass transfer, the stirrer speed was varied, with the reaction rate remaining constant at stirrer speeds of 500 to 2000 rpm, indicating adequate liquid-gas contact under the reaction conditions. In subsequent experiments a speed of 2000 rpm was used. Using a gas mixture of CO₂:O₂:N₂ (0.04:20.0:79.6 – as a model for air, c.a. 400 ppm) and a flow rate of 20 mL/min very slow reaction rates were obtained and kinetic parameters could not be obtained. Using a CO₂:N₂ mixture (5:95 – as a model for industrial flue gas), quantitative uptake of CO₂ was achieved at a catalyst loading of 5 mol% (see Table 2.6.3). Notably, when pure CO₂ is passed through the system, the uptake is also quantitative at a flow rate of 20 mL/min, confirming the ability of the system to efficiently scavenge CO₂.

Table 2.6.3 Evaluation of CO₂ uptake under continuous flow conditions.

Entry	Catalyst (mol%)	CO ₂ :O ₂ :N ₂	Flow-rate [mL/min]	T [°C]	CO ₂ uptake [%]
1	[BMIm]Cl (5)	0.04:20.0:79.6	20	75	>99
2	[BMIm]Cl (5)	100:0:0	20	75	>99
3	[BMIm]Cl (5)	100:0:0	20	60	50
4	[BMIm]Cl (5)	5:0:95	20	60	>99

Conditions: [BMIm]Cl (3.6 g, 0.02 mol, 5 mol%), **SO** (49.5 g, 0.40 mol), CO₂ (from gas cylinder).

2.6.3. Conclusions

Cyclic carbonates have many applications and are currently prepared on an industrial scale from the reaction of epoxides and pure, pressurized CO₂, with the purification and pressurization steps adding significantly to the cost of the process. Herein, we have described an alternative concept that bridges CO₂ capture and CO₂ utilization, *i.e.* simultaneous removal of CO₂ from air with the concomitant formation of a value-added product, negating the costs associated with the use of pure CO₂. We have shown that under continuous flow conditions using a semi-batch stirred reactor quantitative removal of CO₂ can be achieved with gas streaming ranging from ca. 400 ppm CO₂, corresponding to air, through to pure CO₂ gas streams.

2.6.4. Experimental details

2.6.4.1. General remarks

All chemicals were purchased from commercial sources and used as received, with exception of 1-hydroxyethyl-3-methylimidazolium chloride ([HEMIm]Cl), which was synthesized by reacting 2-chloroethanol with 1-methylimidazole according to a reported method. 1-butyl-3-methylimidazolium chloride, Bisphenol A diglycidyl ether, styrene oxide, Allyl glycidyl ether and phenyl glycidyl ether were purchased from Sigma-Aldrich. Epichlorohydrin and CDCl₃ were purchased from Acros.

2.6.4.2. Instrumentation:

Gas chromatography-mass spectrometry (GC-MS) were recorded on a Gas Chromatograph Agilent 7890B equipped with an Agilent 7000C MS triple quad detector and a capillary column from Agilent (l x d x f: 30 m x 0.25 mm x 0.25 μm) using N₂ as carrier gas. GC of gas samples were analyzed on a Gas Chromatograph 7890A from Agilent equipped with a CP-CarboPlot P7 GC column from Agilent (27.5 m x 0.53 mm x 25 μm). ¹H and ¹³C NMR spectra were recorded on a Bruker 400 MHz instrument.

2.6.4.3. Catalytic procedures:

2.6.4.3.1. Using pure CO₂ at atmospheric pressure:

A 10 mL two-neck flask was charged with the catalyst (5-100 mol%) and the appropriate epoxide (0.83 mmol). The flask was connected to a Schlenk line *via* an adaptor, and equipped with a CO₂-filled balloon. After three vacuum-CO₂ cycles, the mixture was brought to the appropriate temperature in a pre-heated oil bath. After reaction for the appropriate time, the mixture was allowed to cool to room temperature, and CDCl₃ (1 mL) was added to the mixture. The yield of the reaction product was determined by NMR spectroscopy using D1 = 3 sec. Note that when dry ice or exhaust breath was used, the same set-up was employed.

2.6.4.3.2. Using air as the CO₂ source:

A 25 mL three-neck flask was charged with the catalyst (5-50 mol%) and the appropriate epoxide (25 g, 0.208 mol, note that the scale of this reaction is 50-250 times larger than that with a CO₂ balloon). The flask was equipped with a septum and a condenser. The air was bubbled through a frit in the system with a flow rate of approx. 22 l/h. To remove moisture from the air-flow, the stream was first bubbled through concentrated H₂SO₄ (97%), and then silica beads. Every 24 h, one drop of the reaction mixture was removed and analysed by ¹H NMR spectroscopy using a D1 = 3 sec. for quantification.

2.6.4.3.3. Using synthetic air, 5% CO₂ or pure CO₂:

reactions with a stationary liquid phase and a continuous gas flow (semi-batch operation) were carried out in a commercial stainless steel reactor (150 cm³ Büchi AG, Uster, Switzerland) equipped with 6 wall baffles. A mass-flow controller (Bronkhorst AG, Switzerland) was used to deliver a controlled flow rate of gas to the reactor from the gas cylinders (the pressure was reduced to c.a. 8 bar before reaching the MFC). The reaction temperature was controlled using a heating circulator Colora K4 (Lorch, Germany) connected to the reactor jacket. A 6-blade disk turbine impeller ensured intensive mixing. The stirrer was driven by a magnetic drive and equipped with a speed controller (cyclone 075/cc 075, Büchi AG, Uster, Switzerland). The reactor temperature, pressure and stirring rate were monitored and recorded *via* a control unit (bpc 6002/bds mc, Büchi AG, Uster, Switzerland).

Prior to the start of each experiment the reactor was charged with [BMim]Cl (3.6 g, 0.02 mol, 5 mol%) and 49.5 g of styrene oxide (0.40 mol) in order to reach of total volume of 50 mL. After flushing the reactor with N₂ (3 times) to remove ambient air, the reactor was heated (333–348 K) and equilibrated for 5 min. The introduction of a synthetic, diluted or pure CO₂ flow through the reactor defined the start of the reaction. A typical reaction was performed with a gas flow of 20 mL/min and a stirring rate of 2000 rpm.

Every 30 min during the reaction, 0.1 mL of the reaction mixture was withdrawn using a 1 mL syringe (Codan Medical AG) connected to the sampling valve and one drop of it was analysed by ^1H NMR spectroscopy.

2.7. General Conclusions

2.7.1. Summary

The chapter started with a review of ionic catalysts for the CCE reaction in Section 2.1, and was followed by a detailed mechanistic study on the reaction in Section 2.2. Previous studies have shed light on mechanistic aspects of the imidazolium catalyzed reaction with respect to the acidic C2 hydrogen. Here, the effect of the C4 and C5 hydrogens of the imidazolium ring was studied, and it was found that these hydrogens can participate in the reaction in a similar way than the C2 hydrogen, leading to novel activation modes and transition states. Further, several cations with different degrees of methylation were evaluated, and the effect of the cation on the anion was studied. The prerequisites for a good catalyst are as follows. First, there must be sufficiently small cation-anion interactions. In other words, the anion is more available for catalysis if it does not strongly interact with the H-atoms of the imidazolium ring. Secondly, a further activation mode *via* H-bonding to the O-atom of the epoxide can be valuable if the H-bond does not simultaneously weaken the anion of the catalyst. The anion must be highly nucleophilic in order to minimize the RDS for imidazolium salts, which is the ring-opening of the epoxide by the halide anion. Sections 2.3 to 2.5 detailed our results on the CCE reaction catalyzed by heterogeneous ionic polymers based on (poly)styrene. Three generations of catalysts were prepared, characterized and systematically evaluated as catalysts for the reaction. The first generation of catalyst contains one vinylbenzyl functional group which leads to linear polymers, while the catalysts presented in Sections 2.4 and 2.5 were prepared from precursors containing respectively two vinylbenzyl groups or from a condensation strategy, both methods leading to highly cross-linked networks (*i.e.* insoluble materials that did not swell upon addition of solvent). It was found that the cross-linked polymers (Sections 2.4 and 2.5) resulted in higher thermal stability and facilitated product extraction with comparison to the linear polymers (Section 2.3). The cross-linked nature of the polymers presented in Section 2.4 and 2.5 resulted in completely heterogeneous materials that did not dissolve in any organic solvent, while the linear polymers presented in Section 2.3 were slightly soluble in polar solvents, presumably leading to less facile product extraction. While additional H-bonding aided in catalysis through interactions with the O-atom of the epoxide (Sections 2.3 and 2.4), Section 2.5 also emphasized that simple polymeric salts were also potent catalysts for the transformation, as the catalysts were prepared in one step from available reagents. Finally, based on the knowledge gained throughout the work, a continuous flow-reactor containing a mixture of simple ILs and epoxides was developed as an efficient CO₂ scavenger from gas streams including air. We demonstrated that all the CO₂ can be extracted from virtually any gas stream using simple IL:epoxide mixtures. This opens

up the possibility to upgrade gas streams contaminated by CO₂ (for example exhaust from sewage) and simultaneously producing a value-added chemical incorporating CO₂.

2.7.2. Further perspectives

Different ionic polymers (IPs) were evaluated as catalysts for the CCE reaction, a benchmark CO₂ utilization reaction. Preliminary results using simple homogeneous IL catalysts demonstrated that 100 % of CO₂ could be extracted from a continuous gas flow containing CO₂ (air, flue gas or pure CO₂). Utilizing the materials presented in Sections 2.3 to 2.5 as heterogeneous CO₂-extractor catalysts using the reactor described in Section 2.6 can allow for a clean production of cyclic carbonates from waste CO₂ sources. In this paradigm, CO₂ capture becomes profitable rather than adding to the cost of the scrubbing. Further work will consist in evaluating a catalogue of different epoxides and catalysts that are suitable for operation under continuous-flow conditions, as well as optimizing the reaction parameters that will lead to optimized gas residence times and CO₂ extraction rates as well as product yield and selectivity.

Further, we envision that the materials that were prepared and characterized can find widespread applications and are not restricted to use as catalysts. As mentioned in Section 1.3, ILs are preferential catalysts for CO₂ applications, but in fact ILs are very versatile materials that have gained interest in different areas of chemistry. For example, ionic polymers based on (poly)styrenes have been evaluated as CO₂ separation membranes, as mentioned briefly in Section 2.4, and there is a high chance that structures presented herein, especially the cross-linked, functionalized polymers detailed in Section 2.4 would display at least moderate activity as membranes.^{208,226,227} IPs have also been successfully used in perovskites and in photochemical processes,²²⁸ and since our polymers can be tuned (*i.e.* they can be linear, or cross-linked, functionalized with H-bond donor groups or non-functionalized), they are potential candidates for applications in these areas.²²⁹ IPs have also been used as anti-bacterial agents²³⁰ and the materials presented herein share certain similarities to common antibacterial agents. For example, polyhexamethylene guanidine hydrochloride is an antimicrobial agent that is a polymeric guanidinium salt with a chloride anion,²³¹ and one of the polymers presented in Section 2.3 is a linear polymer encompassing an ammonium salt, which could presumably display some disinfectant properties.

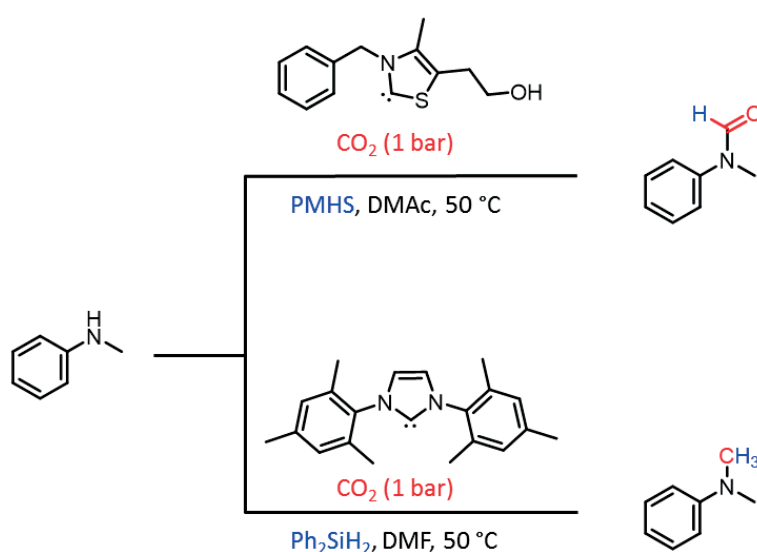
3. Catalytic methods for utilization of CO₂ as a reactive synthon

3.1. Reductive functionalization of amines with CO₂ and hydrosilanes with carbene catalysts

This section is published as a protocol in *Nat. Protoc.*, 2017, **12**, 417–428.

List of authors: **Felix D. Bobbink**, Shoubhik Das, Paul J. Dyson

Graphical abstract:



Our laboratory has published 4 articles on the topic of N-methylation and N-formylation of amines where I was involved as first or second author. After the two first papers in *Angew. Chemie, Int. Ed.*²³² And *Chem. Commun.*,²³³ a complete protocol was written based on the two papers and was published in *Nature Protocols*. The protocol summarized and reviewed recent advances in the N-methylation and N-formylation reactions. The fourth article was published in *ChemCatChem*⁹⁸ and relied on the cooperativity between TBAF and hydrosilanes. The *Protocol* was used as basis for this chapter.

3.1.1. Introduction:

In recent years, carbon dioxide (CO₂) has emerged, as an environmentally benign reagent in the synthesis of fine chemicals as has been highlighted in the introduction of this thesis (chapter 0). Given that this compound is an abundant (and growing) greenhouse gas, its use as a synthetic substrate can be also viewed as complementing carbon capture and storage approaches. Of the various reactions reported,¹¹ the reductive functionalization of amines with CO₂ has emerged as a highly viable approach. For example, Beller *et al.*^{48,234} and Leitner *et al.*²³⁵ have reported well-defined metal catalysts (*i.e.* a catalyst containing a metal-center and ligands that is fully characterized) that employ hydrogen as the reducing agent to afford N-methylated products. Although these catalysts operate at low loadings, the requirement for high pressures of CO₂ and hydrogen (20–60 atm.) makes the use of stainless-steel autoclaves necessary. In 2012, Cantat *et al.* described the highly selective N-formylation of amines, imines and other substrates using an N-heterocyclic carbene (NHC)-type catalyst, in the presence of CO₂ (1 atm.) and polymethylhydrosiloxane (PMHS), the latter being a non-toxic by-product of the silicone industry.⁵⁰ Cantat extended this approach to N-methylation using CO₂ with phenylsilane (a more reactive silane than PMHS) as the reductant, in the presence of a zinc-NHC catalyst.²³⁶ Notably, DFT calculations revealed that the reaction mechanism involves the partial activation of the silanes by the NHC-type catalyst,^{237,238} and hence, the nature of the silane can be used to control the reaction, at least in part.

In 2014, we reported conditions in which a metal-free NHC catalyst is able to N-methylate primary and secondary amines using CO₂ at atmospheric pressure in the presence of silanes.²³² Subsequently, in 2016, we reported the use of a considerably cheaper thiazolium carbene-type (NSC) catalyst related to vitamin B1 for the N-formylation and N-methylation of amines using PMHS as the reducing agent.²³³ Since the N-formylated product is an intermediate of the N-methylated product, the catalytic system can be tuned to afford either of these products by varying the temperature and/or the stoichiometry of the reducing agent. For example, the NSC catalyst can be used for formylation at 50 °C and for methylation at 100 °C. During this two-year period, a plethora of catalytic systems, both metal-based and metal-free, were developed for the N-formylation and N-methylation of amines using CO₂ as the carbon source, and excellent overviews have been published on the topic.^{96,49} Potent catalysts include nickel-phosphine complexes,⁴⁷ diazaphospholenes,²³⁹ and even heterogeneous NHC catalysts.²⁴⁰ Moreover, it was demonstrated that simple imidazolium salts catalyze the reaction, albeit at elevated CO₂ pressures,⁹² and the reaction conditions may be tuned to generate amins from amines and CO₂.²⁴¹ Recently, another mechanism was proposed, in which a copper-based catalyst activates (solely) the silane, which in turns reacts with CO₂. The formylation then proceeds essentially in a non-catalytic way. This contrasts with the carbene

mechanism, where silane, CO₂ and amine may be activated.²⁴² Moreover, inorganic bases have been used as catalysts²⁴³, and a catalyst-free approach was also proposed for the N-formylation of amines.¹⁰ The key mechanistic steps of the N-formylation reaction have been proposed.²³⁷

3.1.2. Comparison with other approaches

The use of CO₂ as a C1 building block is not only advantageous in that CO₂ is an abundant and inexpensive source of carbon, but that, with respect to 'classical' N-formylation and N-methylation reactions, it replaces toxic agents, such as formaldehyde and methyl iodide. Additionally, the vitamin B1-type thiazolium carbene catalyst is very cheap and, in combination with appropriate silanes, it operates under mild conditions, making this system both more cost-effective and safer than other methods. An overview of the pros and cons of our method as well as other recent methods employing CO₂ are summarized in Table 3.1.1.

Table 3.1.1 Comparison between several methodologies for N-formylation and N-methylation.

Reaction	Catalyst	Scope	Pros	Cons
N-methylation	This protocol (NHC, silane, 50 °C, CO ₂ = 1 atm.)	Tolerates many functional groups. Excellent chemo selectivity towards reducible groups (keto, nitrile, nitro)s	-Easy to implement. -High yields -Commercially available catalyst - No autoclaves or pressure-resistant systems necessary -Easy purification because side-products flushed out very fast off the column	-Requires inert conditions -not atom-economical -mono-methylation of primary amines is not possible -Requires CO ₂ cylinder to fill up the balloons
	Beller (Ruthenium centre, phosphine ligand, H ₂ , total pressure = 80 atm., 140 °C) [ref 2]	Broad scope, tolerates esters. No keto or nitrile group reported	-Uses H ₂ (high atom-economy) -Commercially available catalyst and ligand	-Requires high-pressure autoclaves -mono-methylation of primary amines is not possible -Requires precious metal catalyst and high-molecular weight ligand
	Beller(Ruthenium centre, phosphine ligane, silane, CO ₂ = 30 atm.) [Ref 3]	Broad scope. Excellent chemoselectivity.	-Commercially available reagents	-Requires high-pressure autoclaves -Requires precious metal catalyst

	Leitner (Ruthenium center, phosphine ligand, total pressure = 80 atm.) [Ref 4]	Low chemoselectivity, but can sequentially hydrogenate/formylate certain substrates (for example acetanilidine)	-High yields	Reducible groups may be reduced (for example indole) Requires precious metal catalyst
	Cantat (Zinc salt + NHC, silane, CO ₂ = 1 atm.) [Ref 5]	Moderate, substrates result in mixtures of formylation and methylation products	-Commercially available catalyst -easy to implement	Moderate yields Results in mixture of products
	Fu (Boron center, silane, formic acid as C1 source) [Ref 23]	Wide scope, tolerates some reducible groups	-Commercially available catalyst -Good alternative for methylation if no CO ₂ cylinder is available.	Some chemoselectivity issues Mono-methylation of primary amines is not achievable
N-Formylation	This protocol (NSC, PMHS, CO ₂ = 1 atm., 50 °C)	Tolerates many functional groups. Electron withdrawing groups are not well tolerated (results in mixtures of methylated and formylated product)	-Cheap -Commercially available catalyst -High yields -Easy purification	-Depending on the substrate, it is hard to achieve full selectivity towards the formylated product (e.g. very EWG substrates require high temperature and get methylated) -Not atom-economical (high PMHS amount)
	Cantat (NHC, PMHS, CO ₂ = 1 atm., 25 °C) [Ref 6]	Wide scope, in particular tolerates imines, hydrazones and heterocycles (imidazole for example)	-Commercially available catalyst -High yields	-No electron deficient amines were proposed in the scope
	Liu (Ionic liquid, silane, CO ₂ = 10 atm., 30 °C) [Ref 16]	- Good scope, no reducible ends were proposed in the scope.	-Cheap commercial ionic liquid catalyst	-Requires high-pressure autoclave -Electron-withdrawing groups not tolerated

For practical reasons (for example if CO₂ cylinders can't be stored safely), it may be convenient to use formic acid as the C1 source (which can be derived from direct catalytic reduction of CO₂⁴⁴) rather than CO₂ itself. Beller *et al.*²⁴⁴ and Fu *et al.*²⁴⁵ have developed efficient methodologies for N-methylation of amines using formic acid as a C1 source. In particular, the boron-centered catalyst reported by Fu *et al.* produces N-methylated products under mild conditions in yields similar to those presented in this protocol.

3.1.3. Experimental design

Herein, we describe the detailed preparation of the catalyst solution and its use for the N-formylation and N-methylation of amines. The present robust methodology tolerates a wide range of functional groups, and no side-reactions occur even in presence of reducible functional groups in the substrate, such as keto or nitrile groups. It should be noted, however, that the solvent used is crucial for the NHC or NSC-catalyzed reaction and, in general, the reaction proceeds most efficiently in N,N-dimethylformamide (DMF), N,N-dimethylacetamide (DMAc) or dimethylsulfoxide (DMSO). No reaction is observed in solvents such as dioxane, THF or toluene, although these solvents have been applied in related reactions employing slightly different catalysts. Importantly, the reactivity of silanes, which is described in literature, follows the trend phenylsilane (PhSiH_3) > diphenylsilane (Ph_2SiH_2) > PMHS. An essential parameter to control in these synthetic procedures is the concentration of silane in the reaction mixture. Since N-formylated product is an intermediate in the formation of the N-methylated one, smaller quantities of silane must be used if the goal is to isolate the N-formylated compound than if the target product is N-methylated. Data from the optimization of the catalytic conditions in the benchmark reaction employing either phenylalanine ethyl ester or N-methylaniline as the substrates are reported in Table 3.1.2 and Table 3.1.3 (see also Figure 3.1.1 and Figure 3.1.2).

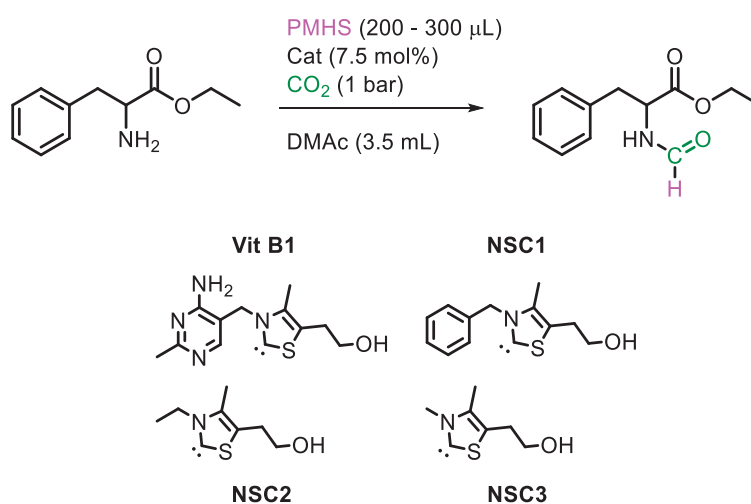


Figure 3.1.1 N-Formylation of phenylalanine ethyl ester. Cat: catalyst; DMAc: dimethylacetamide; PMHS: Poly(methylhydrosiloxane).

Notably, for the N-formylation reaction, a less reactive silane (PMHS) and a less active NSC were employed, whereas larger amounts of a more potent silane (Ph_2SiH_2), a more potent catalyst and a higher reaction temperature are required for N-methylation. It should be noted that primary amines can selectively be N-formylated to the mono-formylated product, whereas with N-methylation only the di-methylated product can be obtained with a high selectivity, if the reaction is conducted in the presence of an excess of hydrosilane.

Table 3.1.2 Benchmark reactions employing NSC-based catalysts for the N-formylation of phenylalanine ethyl ester.

Entry	Catalyst	Solvent	Yield [%]
1	Vit. B1	DMAc	58
2	NSC1	DMAc	95
3	NSC2	DMAc	63
4	NSC3	DMAc	43
5	NSC1	DMF	77
6	NSC1	CH_3CN	0
7	NSC1	Toluene	0
8	NSC1	THF	0

Reaction conditions: catalyst, 7.5 mol%; amine, 0.5 mmol; PMHS, 200 μL ; CO_2 , 1 bar; solvent, 3.5 mL; 50 $^\circ\text{C}$; 24 h. Yields determined by GC-FID using n-decane as internal standard.

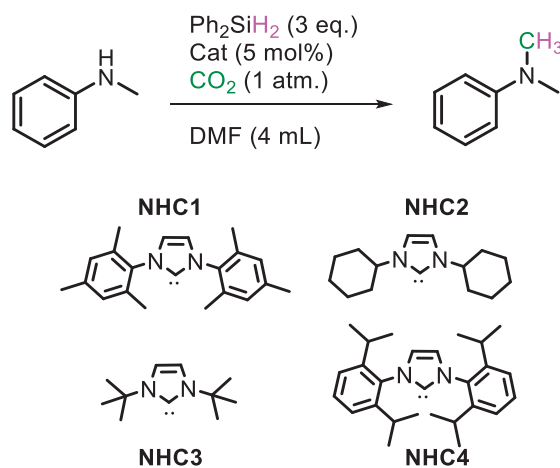


Figure 3.1.2 N-methylation of N-methylaniline. Cat: catalyst; DMF: N,N-dimethylformamide; Ph_2SiH_2 : diphenylsilane.

Table 3.1.3 Benchmark reactions employing NSC-based catalysts for the N-methylation of N-methylaniline.

Entry	Catalyst	Silane	Solvent	Yield [%]
1	NHC1	Ph ₂ SiH ₂	DMF	91
2	NHC2	Ph ₂ SiH ₂	DMF	25
3	NHC3	Ph ₂ SiH ₂	DMF	78
4	NHC4	Ph ₂ SiH ₂	DMF	79
5	NHC1	PMHS	DMF	48
6	NHC1	1,1,3,3-tetramethyldisiloxane	DMF	32
7	NHC1	Ph ₂ SiH ₂	CH ₃ CN	87
8	NHC1	Ph ₂ SiH ₂	Toluene	0

Reaction conditions: catalyst, 5 mol%; amine, 0.5 mmol; silane, 3 eq; CO₂, 1 bar; solvent, 4 mL; 50 °C; 24 h. Yields determined by GC-FID using n-decane as internal standard.

Figure 3.1.3 and Figure 3.1.4 summarize the scope of both the NHC-type and NSC-type catalysts. Reactions were performed on a scale of 0.5 mmol substrate, although the reaction may be scaled up to at least 10 mmol without taking any additional precautions. Importantly, the reaction does not proceed in the presence of air and moisture, so it is imperative that care is taken during the preparation and use of the catalyst to avoid all contact with air and moisture, in other words, use of glovebox and Schlenk techniques are required.

Figure 3.1.3 illustrates data from the N-formylation of several amino acid ester derivatives, which demonstrate the versatility of the NSC catalyst with a range of other substrates. Although very similar in structure, NSCs are slightly less active than NHC catalysts, a characteristic that results in very high selectivity for the N-formylated product. Figure 3.1.4 highlights data on the N-methylation of several pharmacological compounds using the NHC catalyst, as well as several model substrates with both electron-donating and electron-withdrawing groups, which can be isolated in pure form in high yields following column chromatography. It should be noted that drug substrates are important because secondary and tertiary amines often exhibit different biological activities, for example in structure-activity or in bio-availability. Please note that high selectivity towards secondary amines cannot be achieved under the conditions presented herein. In our laboratory, primary amines are treated with 4 eq. of Ph₂SiH₂ to produce the corresponding tertiary amine.

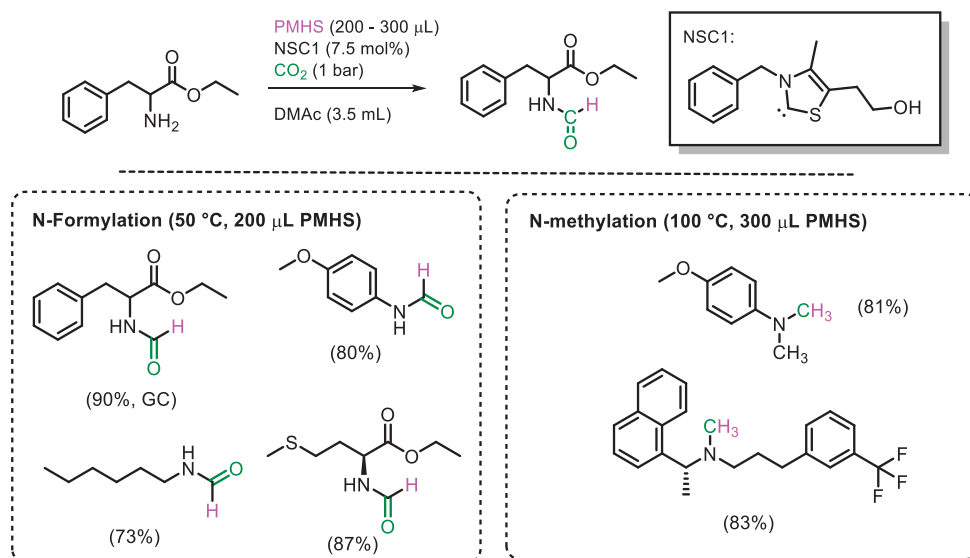


Figure 3.1.3 N-Formylation and N-methylation of amines using NSC1 and PMHS. General conditions: amine, 0.5 mmol; NSC1, 7.5 mol%; PMHS, 200-300 μL; 50-100 °C; 24-48 h. Isolated yields following column chromatography using hexane and ethyl acetate with 1% added triethylamine are given in parenthesis.²³³

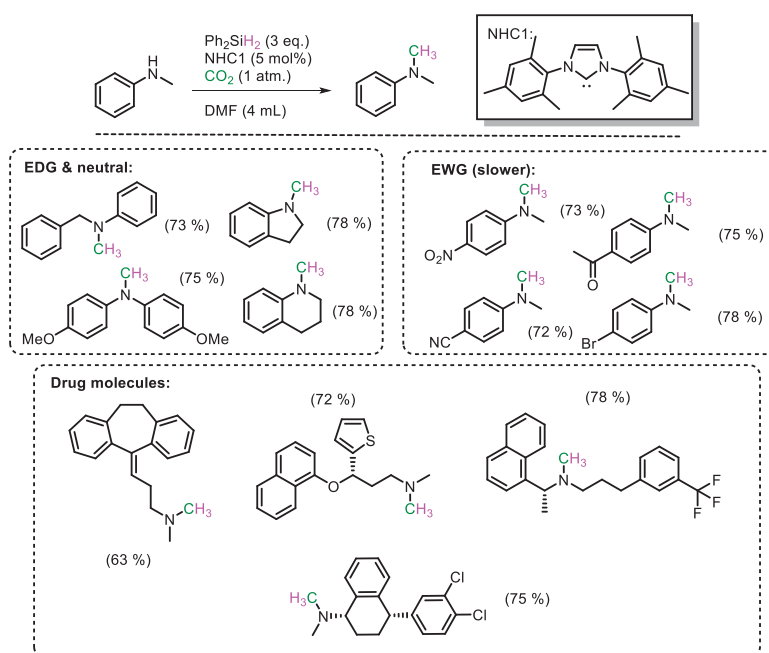
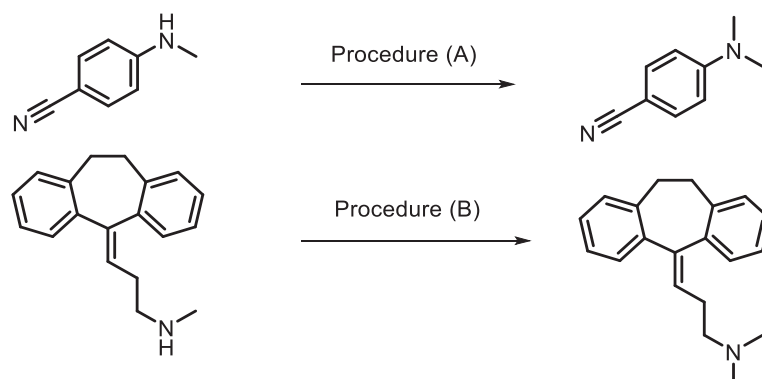


Figure 3.1.4 Selected examples of N-methylation of amines using NHC1 and Ph₂SiH₂. General conditions: amine, 0.5 mmol; NHC1, 5 mol%; Ph₂SiH₂, 3 eq., 1.5 mmol, 278 μL; 50 °C, 24-48 h. Isolated yields following column chromatography on silica using hexane and ethyl acetate with 1% added triethylamine are given in parenthesis.²³² EWG = Electron-withdrawing groups, EDG = Electron-donating groups.

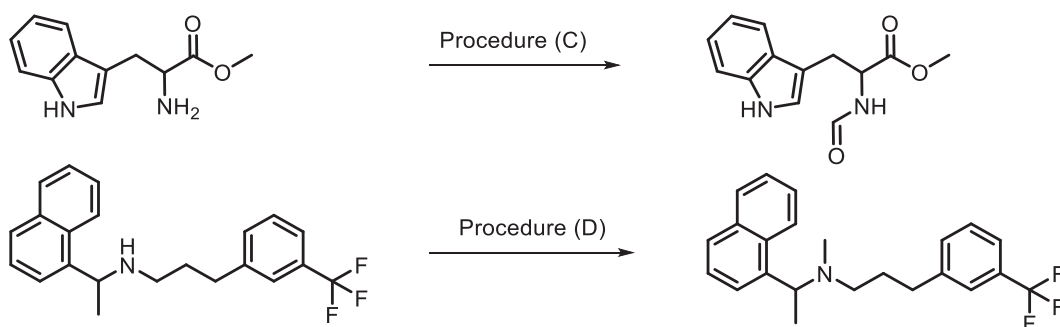
The procedure described below is suitable for the preparation of a catalytic solution working for a substrate scale ranging from 100 mg to over 1 g. Several parallel reactions can be conducted at the same time. The concentration of the catalytic solution can be easily varied and all the catalytic solutions exhibit the same activity towards N-formylation and N-methylation.

This protocol describes the N-formylation and N-methylation of four different amines (See Scheme 3.1.1 for chemical structures). The ideal scale lies between 0.5 mmol and 5 mmol of amine substrate. Certain parameters may need to be optimized for other substrates, in order to obtain maximum possible yields (for example, reaction time, temperature and the type and amount of silane employed). In particular, please note that amines with electron-withdrawing groups react more slowly than other amines, so their conversion might require longer reaction times and/or the use of higher reaction temperatures. We propose in this protocol to employ the NHC catalyst for two substrates, and the NSC catalyst for two other substrates. The procedure in both cases is essentially the same. These substrates were selected to show that the NSC catalyst can either formylate or methylate an amine, whereas the simple aniline and drug molecule are examples of methylation using NHC catalyst. For chemists that require to use a N-methylation or N-formylation step, we suggest to get familiar with the reaction using a cheap model substrate (for example N-methylaniline or Tryptophan methyl ester hydrochloride) and perform the reaction several times until good isolated yields are obtained. It is not crucial to repeat the reactions proposed hereafter, however the steps should in our opinion be followed carefully when applying the methodology to other substrates. Noteworthy, the reaction parameters such as time and temperature must be adapted if the substrates are less reactive. Importantly, isolating the compounds requires column chromatography, and the conditions vary with given substrates. If the methodology is required for a single reaction, we advise the use of the "single reaction glassware" (see below). If the reader would like to adapt this methodology in screening of conditions on his own catalytic system, the 4-parallel reaction setup would be suitable (see below for discussion and photographs).

Under NHC catalysis: Synthesis described in (A) and (B)



Under NSC catalysis: Synthesis described in (A) and (B)



Scheme 3.1.1 The four chemical reactions proposed in the Procedure hereafter.

After aqueous work-up (see step 9 of the Procedure) and concentration of the organic phase, we suggest that products are purified further using column chromatography. It should be noted that many of the tertiary amines covered as substrates in the Procedure contain no other functional groups and are non-polar. Consequently, the compounds elute very quickly through silica, even in the absence of trimethylamine (used for column deactivation). The reaction products should be dissolved in a 1:99 mixture of ethyl acetate (EtOAc):pentane prior to separation on a column. Many compounds are not soluble in pentane but the suspension can easily be added to the column *via* a syringe or a pipette. After flushing a dead volume of solvent, the compounds usually elute after 100-200 mL of solvent. To implement this protocol, we use a column with a diameter of 7.5 cm filled with 20–30 cm of silica, and we collect the fractions in 10-mL vials. We advise using GC-MS and TLC to identify the vials containing the product. In general, the R_f values for the products are low in pure hexane (0.05 to 0.5 approximately) and increase rapidly upon addition of EtOAc. The R_f value of the most important side product is very high in pure hexane (>0.8), which is why flushing with pure hexane is recommended during chromatography.

3.1.4. Materials

3.1.4.1. Reagents

Many anilines are extremely toxic, and all chemicals should be handled with care, either in a glovebox or in a ventilated fume hood. Care must be taken not to overfill the balloon with CO₂ as it results in the balloon bursting.

Solvents used in reactions (DMF or DMAc) should be obtained from commercial suppliers in absolute quality (lower grade solvent are not sufficiently dry and will lead to significantly lower yields or even no reaction whatsoever) and packed over molecular sieves (AcroSeal® for example, these solvents can be obtained from commercial sources). They should be stored under nitrogen with added molecular sieves. Solvents employed in product purification and/or isolation can be of technical grade and used as received from commercial suppliers. Reagents can be used as received from commercial suppliers without purification or drying.

- 1,3-dimesitylimidazolium chloride (TCI, cat. No. D3446)
- 3-benzyl-5-(2-hydroxyethyl)-4-methylthiazolium chloride (Acros, cat. No. 44052-0250, or Aldrich, cat. No. 256234)

CRITICAL: The catalyst precursor salts, 1,3-dimesitylimidazolium chloride and 3-benzyl-5-(2-hydroxyethyl)-4-methylthiazolium chloride, are bench-stable, but they were kept in glovebox in the original work. Notably, the thiazolium salts are about 25 times less expensive than their imidazolium counterparts.

- Sodium hydride (Aldrich, cat. No. 223441)
- CO₂ (Technical grade and medical grade were used, 50 bars cylinder)
- N,N-dimethylformamide (DMF, Acros, cat. No. 44838-1000)
- N,N-dimethylacetamide (DMAc, Acros, cat. No. 37523-1000)
- Diphenylsilane (Fluorochem, cat. No. S08050)
- Poly(methylhydrosiloxane) (PMHS) (Aldrich, cat. No. 176206)
- Ethyl acetate (EtOAc)
- n-pentane
- n-hexane
- trimethylamine
- dichloromethane
- aq. NaHCO₃ solution (saturated)

- Sodium sulfate
- Brine solution (de-ionized water saturated with NaCl)
- Silica gel (SiliaFlash® P60, Size 40-63 µm, 230-400 mesh)
- Chloroform-d
- 4-(Methylamino)benzotrile (Fluorochem, cat. No. 224548)
- Nortriptyline hydrochloride (Sigma, cat. No. N7261)
- L-Tryptophan methyl ester hydrochloride (Aldrich, cat. No. 364517)
- Cinacalcet hydrochloride (TCI, cat. No. S0507)
- Deionized water

3.1.4.2. Equipment

- Glovebox
- GC-MS/FID 7890B equipped with a 7000C MS triple quad detector, an FID and a HP-5-MS UI capillary column from Agilent (l x d x f: 30m x 0.25 mm x 0.25 µm)
- CombiFlash Rf + UV-VIS apparatus using 12 g or 25 g Luknova SuperSep columns
- Schlenk line
- Schlenk tubes (10 mL)
- Two-neck flasks (10 mL) or three-neck flasks (10 or 25 mL)
- Distillation distributor
- Distillation adaptor
- Medical balloons (Dräger, 2.0L 2165694)
- Schlenk adaptors
- Magnetic stirrer
- Oil bath (Oil: Bluesil Fluid 47 V 350, 40-131.KN)
- Magnetic stirrer hotplate
- rotary evaporator
- weighing balance
- vacuum pump

3.1.5. Equipment setup

Gas chromatography-mass spectrometry/flame ionization detector (GC-MS/FID). To monitor the progress of the reaction, a drop of the reaction mixture can be removed from the reaction flask with a nitrogen-purged syringe and added to a GC vial, to which is added EtOAc to fill the vial. This protocol involves the use of a GC-MS/FID 7890B equipped with a 7000C MS triple quad detector, an FID and a HP-5-MS UI capillary column from Agilent (l x d x f: 30m x 0.25 mm x 0.25 μ m), using N₂ as carrier gas with the following parameters: 50 °C for 3 min, then heating to 230 °C at a rate of 10 °C/min, and holding 3 minutes at 230 °C. If the substrate has a high boiling point, the hold time at 230 °C must be increased to 15 min. The order of elution is: starting material (if any is left), N-methylated product, N-formylated product.

3.1.6. Procedure

Preparation of catalytic solutions Timing 0.5 - 1 h

The scale of the preparation of the catalytic solution can be tuned depending on the intended use. For this protocol, prepare either a 5 mL catalytic solution, if you intend to conduct four reactions, or a 2 mL catalytic solution for a single reaction (see relevant discussion in the Experimental design).

For N-methylation reactions, the catalyst loading may be increased to at least 10 mol% without any loss of selectivity, in order to accelerate the reaction. For N-formylation, the catalyst loading is more important, and we recommend to use 7.5 mol%, as was used in the original publication, as the methylated product can be a side-product of the reaction.

- 1)** Calculate the appropriate weights of precursor salt (NHC1 should be used for N-methylation at 50 °C, while NSC1 should be used for N-formylation at 50 °C or for methylation at 100 °C) and sodium hydride, so that their mole ration is 1:1. Please note, however, that NaH may be added in excess with respect to the catalyst precursor salt of up to 5:1, with no adverse impact on the reaction
- 2)** In a glovebox, add the precursor salt and the sodium hydride to a 10-ml Schlenk tube equipped with a magnetic stir bar; In particular, if planning to perform the N-methylation of 4-(Methylamino)benzotrile, see step 9 option A, or the synthesis of N-methylated nortriptyline (amitriptyline), see step 9 option B, add 17.1 mg of 1,3-dimesitylimidazolium chloride and 3 mg of dry NaH (commercially available, see reagents). If planning to perform the synthesis of methyl formyl-L-tryptophanate, see step 9 option C, or that of (R)-N-methyl-N-(1-(naphthalen-1-yl)ethyl)-

3-(3-(trifluoromethyl)phenyl)propan-1-amine, see step 9 option D, add 20.2 mg of 3-benzyl-5-(2-hydroxyethyl)-4-methylthiazolium chloride and 3 mg of dry NaH.

- 3) Seal the tube with a septum, remove the Schlenk tube from the glovebox, and attach the tube to a Schlenk line.
- 4) Perform three vacuum-nitrogen cycles to purge the tube, then add the appropriate amount of reaction solvent, *i.e.*, 2 ml of dry, degassed DMF, if planning to implement step 9 options A or B, and 2 ml of dry, degassed DMAc, if planning to implement step 9 options C or D. (The dry, N₂-packed solvents can be purchased from commercial sources, see reagents) The ideal amount of catalytic solution is 1 mL, and it is useful to prepare an excess of solution. To prepare 4 parallel reactions (Figure 3.1.5), prepare 5 mL of catalytic solution (the calculations should be made accordingly), use 1 mL of solution per reaction, and discard the final 1 mL of solution.
- 5) Stir the catalytic solution for 30 min at room temperature (The temperature in the lab varies slightly (20-25 °C), and an oil bath set at 25 °C was used on occasion) at 400 rpm, during which time the NaH deprotonates the precursor salt to generate the corresponding carbene.
- 6) During deprotonation of the carbene (see step 5), prepare the materials and glassware for the catalytic transformation. Depending on how many reactions one plans to conduct, there are two possibilities: connect a 10 mL three-neck-flask equipped with a magnetic stir bar, a schlenk adaptor and a septum to a Schlenk line, or prepare a 4-parallel reactions set-up as shown in Figure 3.1.5 and step 8.
- 7) Leave the salts to precipitate for 10–30 min.

Critical step: At this point, the catalytic solution is green, when the NSC is used, or yellow, when the NHC is used. (Figure 3.1.6, Figure 3.1.7) Occasionally, the NSC solution is light orange in color, but it can still be used.



Figure 3.1.5 Photograph of the four parallel reaction apparatus with the distillation distributor and distillation head. No cross-contamination was observed under these conditions.

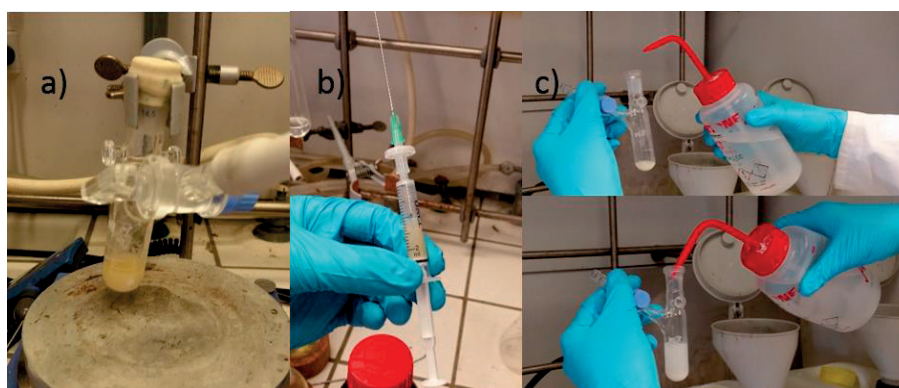


Figure 3.1.6 Photographs illustrating steps 3, 4, 5 and 7. a) Color of NHC catalyst after 30 min stirring. b) 1 mL is removed with a N_2 -purged syringe (note that extra N_2 taken in the syringe). The catalytic solution is used for the reaction. c) 3 mL of catalytic solution is prepared. The remaining 1 mL is discarded and the tube can be washed with organic solvents or water, as it contains the salt by-product. Caution: Excess NaH reacts violently with water. It reacts also with acetone and ethanol, but the reaction is much less exothermic than it is with water.



Figure 3.1.7 Change in color of the catalyst upon exposure to air. a) $t = 0$ s, b) $t = 30$ s, c) when diluted in EtOH.

3.1.7. N-formylation and N-methylation reactions

The catalytic solution prepared in step 7 of the Procedure can be used for reaction as soon as its color is yellow for the NHC and green for the NSC catalyst.

8) *Follow this step only if you want to perform 4-reactions in a parallel manner, like in Figure 3.1.5, otherwise, please refer directly to 9).*

Connect four 10 mL two-neck flasks each equipped with a magnetic stir bar, to a distillation separator, and connect the separator to a distillation adaptor. Connect the set-up to the Schlenk like and equip the set-up with a CO₂ balloon.

In the parallel reaction, all the joints must be greased. The CO₂ balloon should remain in overpressure throughout the experiment. A rapid decrease in size of the balloon is indicative of a leak.

9) Follow the directions reported hereafter for the syntheses that involve the use of both types of catalyst. In particular, options A and B make use of an NHC carbene catalyst to proceed to the *N*-methylation of 4-(Methylamino)benzotrile and nortriptyline, whereas options C and D make use of an NSC catalyst to proceed to the *N*-formylation of tryptophan methyl ester and *N*-methylate cinacalcet, see relevant discussion in the Experimental design to decide which reaction or reactions to implement.

3.1.7.1. (A) Synthesis of 4-(dimethylamino)benzotrile Timing: 50 h

(i) In a 10 mL three-neck flask equipped with a stir bar and a septum prepared in step 6 of the Procedure, weigh 66.1 mg of 4-(methylamino)benzotrile.

(ii) Attach a CO₂ balloon to the flask and connect the flask to a Schlenk line.

(iii) After three vacuum-CO₂ cycles, collect 1 mL of catalytic solution from the relevant 10-ml Schlenk tube (see step 7) with a N₂-purged syringe equipped with a syringe filter and a needle and add it to the three-neck flask just prepared, making sure to filter the catalytic solution through the syringe filter to discard any salt residues.

(iv) Add to the flask 278 µL of diphenylsilane *via* the septum with an N₂-purged syringe.

(v) Add to the flask 3 mL of dry, degassed DMF *via* the septum with a N₂-purged syringe. Rinse the flask with the solvent, if some of the substrate adheres to the walls of the vessel.

(vi) Heat the flask in an oil bath at 50 °C for 48 h.

The reaction time and amount of silane used depends on the reactivity of the substrate and if the substrate is a primary or secondary amine. The temperature can be increased if no sensitive (reducible) groups are present in the substrate.

(vii) After completion of the reaction (reaction progress can be monitored by GC-MS or TLC), cool the flask to room temperature and add to it 5 mL of EtOAc. Transfer the resulting reaction mixture to a separatory funnel, and wash the reaction flask several times with 7-ml aliquots of EtOAc and 7-mL aliquots of water (after each rinsing, the liquids are added to the extraction funnel). The total volume of solvent can be up to 70 mL. Shake the funnel vigorously to make sure the extraction is complete. After completion of this 'aqueous workup', collect, dry over sodium sulfate, and concentrate the organic phase. Please note that in the original publication, it was suggested that unreacted silane is quenched with aqueous NH₄F. However, this is not crucial for product purification, as the side-products and/or remaining silanes are quenched by the water. Please note that, after concentration of the crude reaction mixture, it is not uncommon that a white precipitate forms. This side-product is probably a polymeric siloxane generated during reaction.

CAUTION: Care should be taken when adding water to the mixture, as the reaction of silanes with water is exothermic.

The aqueous work-up often results in an emulsion. If this happens, degrade the emulsion by adding 5-10 mL of brine solution to the separatory funnel, which will result in a better separation of water-organic phase. The organic phase can then be collected, dried of sodium sulfate and concentrated under rotary evaporator

(ix) Purify the crude extract by column chromatography using pentane and EtOAc containing 1% of triethylamine (0:10 EtOAc:pentane with a gradient to pure EtOAc). Please note that both conventional column chromatography and flash chromatography (CombiFlash Rf + UV-VIS apparatus using 12 g or 25 g Luknova SuperSep columns) may be used for this step. For non-polar tertiary amines, separation from the siloxanes side-products can be problematic, because they elute very quickly (at almost the same rate as the siloxane). In the case of a non-polar tertiary amine, it is advisable to start with 100% hexane (or pentane) with 1% triethylamine, and very slowly increase the polarity to maximum of 5% EtOAc if necessary. With most compounds, the product may rapidly pass through the column even when 100% pentane or hexane is applied. This happens when the compound is added on the column in pure EtOAc. It is advisable to add some hexane to the concentrated crude reaction mixture prior to adding the solution to the column.

(x) Collect the fractions containing the pure product (this collection can be monitored by GC-MS or by TLC), combine the fractions and dry the product using by rotary evaporation at 40 °C and subsequently under high vacuum.

(xi) Assess the purity of the product by NMR spectroscopy and ESI-MS.

3.1.7.2. Synthesis of N-methylated nortriptyline (amitriptyline) Timing: 30 h

(i) The starting material, nortriptyline hydrochloride, must be converted to the free base. For this purpose, weigh 171.3 mg of nortriptyline hydrochloride and dissolve it in a 50:50 mixture of CH_2Cl_2 :aq. NaHCO_3 in a separatory funnel. The free-base product remains in the organic phase with the NaCl in the aqueous phase. Extraction should yield 100% of the product. However, the free base is often a viscous liquid and weighing the exact amount can be difficult. Consequently, it is advisable to extract a slight excess of the hydrochloride starting material.

(ii) Weigh 131.7 mg of nortriptyline in a 10 mL three-neck flask equipped with a septum, a schlenk adaptor and a stir bar.

(iii) Perform the reaction according to Steps 9A (ii)–(vii). Please note that this substrate has a high molecular weight and the reaction must be monitored by TLC, because the substrate could not be detected in our GC-MS with our method.

(iv) Purify the crude extract by column chromatography using pentane and EtOAc with added 1% trimethylamine as eluent. Start with pure pentane, then implement a gradient to pure EtOAc. Please note that both conventional column chromatography and flash chromatography (CombiFlash Rf + UV-VIS apparatus using 12 g or 25 g Luknova SuperSep columns) may be used. For non-polar tertiary amines, separation from the siloxanes side-products can be problematic, and therefore it is advisable to start with 99% hexane (or pentane) with 1% triethylamine, and slowly increase the polarity to maximum of 5% EtOAc if necessary. For several compounds, it is not necessary to include triethylamine in the solvent system.

(v) Assess the purity of the product by NMR and HR-MS. In HR-MS; please note that both the H⁺ and Na⁺ ion adduct are observed.

3.1.7.3. Synthesis of methyl formyl-L-tryptophanate Timing: 30 h

(i) The starting material, L-tryptophan methyl ester hydrochloride, must be converted to the free base. For this purpose, dissolve 133.4 mg of the starting material in a 50:50 mixture of CH₂Cl₂:aq. NaHCO₃ in a separatory funnel. Following extraction, the free-base product remains in the organic phase. Please note that extraction should yield 100% of the product. However, the free base is often a viscous liquid and weighing out the exact amount can be problematic. Therefore, it is better to extract a slight excess of the hydrochloride starting material.

(ii) Weigh 109.1 mg of L-tryptophan methyl ester in a 10 mL three-neck flask equipped with a septum, a schlenk adaptor and a magnetic stir bar.

(iii) Attach a CO₂ balloon to the flask and connect the flask to a Schlenk line.

(iv) After three vacuum-CO₂ cycles, collect 1 mL of catalytic solution from the relevant 10-ml Schlenk tube (see step 7) with a N₂-purged syringe equipped with a syringe filter and a needle, and add it to the three-neck flask just prepared, making sure to filter the catalytic solution through the syringe filter to discard any salt residues.

(v) Add to the flask 200 µL of PMHS *via* the septum *via* the syringe. Pay attention to the fact that PMHS is a viscous liquid and obtaining a precise amount can be tedious.

(vi) Add 2.5 mL of dry, degassed DMAc *via* the septum with a N₂-purged syringe. Rinse the flask with the solvent, if some substrate adheres to the walls of the flask.

(vii) Heat the flask in an oil bath at 50 °C for 15 h.

(viii) After completion of the reaction, cool the flask to room temperature, and add 5 mL of EtOAc to it. Perform an aqueous work-up and wash the flask with portions of 7 mL EtOAc and water to reach a final max. volume of 70 mL (see also step 9A (vii)). After extraction, collect and concentrate the organic phase. Please note that, in the original publication, it was suggested that the crude reaction mixture was filtered through a celite plug to remove any solid/gel-like residues. Subsequent tests on the formylation reaction using PMHS reveal that a simple paper filter is sufficient to discard the gel-residue (the residue must be washed with EtOAc).

It is advisable to extract the product as soon as the reaction is complete. PMHS and the side products tend to act as gelators. Aqueous work-up is possible even when the mixture is in gel-like form, but the gel should be broken up with a spatula, in this case.

(ix) Purify the product by column chromatography using hexane and EtOAc with added 1 vol% trimethylamine as a mobile phase. Please note that the polarity of N-formylated compounds is higher than that of their N-methylated counterparts and of the starting materials. The N-formylated product will therefore be the last product to be eluted. Therefore, we advise starting the purification with 100% pentane + 1% triethylamine and slowly increasing the polarity of the eluent to ensure the siloxanes and starting materials are discarded before collecting the desired product. Usually, N-formylated products elute with 1-20 % EtOAc depending on the substrate. By contrast, N-methylated products start to elute in the absence of EtOAc.

(x) Assess the purity of the product by NMR spectroscopy and HR-MS. Please note that N-formylated compounds form rotamers, often resulting in split peaks in the NMR spectra.

3.1.7.4. Synthesis of (R)-N-methyl-N-(1-(naphthalen-1-yl)ethyl)-3-(3-(trifluoromethyl)phenyl)propan-1-amine Timing: 30 h.

(i) The starting material, cinacalcet hydrochloride, must be converted to the free base. For this purpose, purify 171.3 mg of sertraline hydrochloride by dissolving it in a 50:50 mixture of CH₂Cl₂:aq. NaHCO₃ in a separatory funnel. After extraction, the free-base product remains in the organic phase. Please note that extraction should yield 100% of the product. However, the free base is often a viscous liquid and weighing

out the exact amount can be tedious. Therefore, it is better to extract a slight excess of the hydrochloride starting material.

(ii) Perform the reaction according to steps 9C (iii)-(viii). Note that for methylation, add 300 μL of PMHS instead of 200 μL (step 9B (v)).

(iv) Purify the desired product by column chromatography using hexane and EtOAc with added 1 vol% trimethylamine as a mobile phase. Please note that both conventional column chromatography and flash chromatography (CombiFlash Rf + UV-VIS apparatus using 12 g or 25 g Luknova SuperSep columns) may be used. For non-polar tertiary amines, separation from the siloxanes side products can be problematic; therefore, it is advisable to start with 99% hexane (or pentane) with 1% triethylamine, and very slowly increase the polarity to maximum of 5% EtOAc, if necessary.

(v) Assess the purity of the product by NMR spectroscopy and HR-MS.

- TIMING

Steps 1–8, preparation of catalytic solution: 1 h.

Step 9, *N*-methylation or *N*-formylation of amine: 15 – 48 h, depending on the substrate.

3.1.8. Troubleshooting

Step	Problem	Possible Causes	Solution
2	We do not have a glovebox.		NaH can be purchased in oil, and can be used directly after rendering it dry (not done in this work). Occasionally, bench-stored dry NaH was used in the lab for convenience, which resulted in good yields. The protocol can be followed by charging the materials in a Schlenk tube directly, and applying vacuum-N ₂ cycles. Caution: Large quantities of dry NaH should not be stored on the bench as NaH reacts violently with water and this poses serious safety issues.
2	The amount of NaH required is very small and it is difficult to weighing it out accurately.	No accurate balance, the NaH is electrostatic.	In our experience, an excess of NaH may be used. We have not experienced any problems due to the quantity of NaH.
7	The catalytic solution did not turn light yellow (NHC) or green (NSC).	There might be oxygen in the system, or not enough base was used.	Make sure to perform vacuum-N ₂ cycles and use dry and N ₂ -packed solvents. If too much air is present in the system, the yields will decrease. If the problem is due to the base the catalyst can still be used. In our work, we have used the catalyst with colors different to those

			mentioned, and, in general, the yields are good.
9A-ii, 9B-iii, 9C-iii, 9D-ii	The CO ₂ balloon becomes flat after only several minutes/hours.	There is a leak in the system (glassware joints) or the balloon is pierced.	Make sure to grease every joint. Make sure the balloon is not pierced (older balloons tend to be more fragile).
9B-i, with the reader's suitable substrate	My product is a hydrochloride salt, but after extraction the organic phase does not contain the product.	The product is highly water-soluble.	In our scope highly water-soluble hydrochloride salts were not used. The drug molecules that we extracted were soluble in DCM. While we have not tried this, we expect that the reaction can be run in presence of 1 eq. of NaHCO ₃ .
9A-vii, with the reader's suitable substrate	I cannot observe the product by GC-MS during monitoring of the reaction.	The product is not volatile enough or the reaction time is too short. The sample is not sufficiently concentrated.	Try to optimize the oven conditions for the GC-MS (longer times, prolonged heating). If this is not successful, monitor the reaction by TLC. Spot the starting material and the reaction mixture. The starting material and the siloxane materials are easily recognized. Inject a new sample with higher concentration.
9A-vii, With the reader's suitable substrate	After several hours of reaction I only see starting material on the GC-MS.	The product is less volatile than the starting material. The reaction does not proceed.	If the starting material appears at the very end of the reaction, there is a chance that the product does not elute from the GC-MS. Try a longer reaction. For some substrates, the reaction requires higher temperatures or prolonged times. In particular, the electron-deficient amines are more difficult to react. Try using higher temperatures, up to 100 °C if the substrate does not contain sensitive functional groups.
9A-vii, With the reader's suitable substrate	My product does not appear in the TLC.	The compound is not UV-active or not concentrated enough.	If the molecule is not UV-active, the TLC spot will not be visualised under UV light. Use a KMnO ₄ staining to reveal non-UV-active spots.
9A-vii	After reaction I performed an aqueous work-up, but GC-MS analysis of the organic phase shows no more product.	The compound is water-soluble.	In our experiments we have used anilines and other derivatives that had higher affinity for organic solvents than for water. Water-soluble amino acids may pose a problem for aqueous work-up. Performing chromatography by injecting the crude extract directly is possible, but in general, the separation is problematic because of the high concentration of DMF (or DMAc).
9A-ix, with the reader's	I ran a column, but the whole crude mixture eluted at once, with no separation.	The mixture was dissolved in pure EtOAc.	It is important for some compounds that the crude extract is added to the column in a highly non-polar solvent (<i>i.e.</i> , pentane:EtOAc 99:1). Add excess of

suitable substrate			pentane in the crude reaction mixture prior to addition to the column.
9A-ix	I added pentane to my crude reaction flask and now I see two phases	The two phases are DMF-pentane.	After work-up and concentration of the organic phase, some DMF almost always remains in the flask. Adding pentane will result in two phases. Add a few drops of EtOAc to make a "DMF:EtOAc:pentane" mixture that leads to homogeneous solution. This mixture can then be added directly to the column.
9a-ix	I lost my product in the column.	The elution was too fast. The product is stuck on the column.	As stated above, several anilines used in the original protocol are very non-polar and elute very fast even with 100% pentane with no added Et ₃ N. Analyze the dead volume to determine if you have missed the product. It may occur (it has not happened to us) that the product is too polar and elutes very slowly. Elute with 1:99 MeOH:EtOAc to ensure the rest of the products elute.
9a-ix	There are impurities in the product even after chromatography.	There are broad, unknown NMR peaks in the aromatic region after purification. DMF elutes through the column when EtOAc: Pentane is used. Technical pentane/hexane was used for column.	These peaks are attributed to the siloxane side-products and it occurs when the product elutes in pure hexane or, if for some reason, excess silane was used for reaction. We recommend performing a second chromatography column, even though this results in lower yields. DMF can be removed under high-vacuum at 60 °C after column chromatography or, during the extraction process, DMF can be removed by washing several times with water. We advise to remove the DMF under vacuum if some is present after purification. The solvents can be distilled by rotary evaporation prior to column chromatography. These impurities are especially important if the product elutes in many fractions.
9C-x	The ESI-MS (HRMS) does not show the "M+1" peak but the NMR indicates a pure product.	The Na ⁺ or K ⁺ adduct formed.	For the N-formyl product, we often observe two peaks, the M+1 and the M+23 peak. This depends on the ionization conditions in the ESI-MS. We recommend searching for the peaks "M+1", "M+23" where M is the molecular weight of the compound.

3.1.9. Anticipated results

4-(Dimethylamino)benzonitrile

Column chromatography yields the title compound as a white solid in 75% yield. Method: Pentane and EtOAc from 0 to 100% EtOAc using standard column chromatography. ^1H NMR (400 MHz, Chloroform-*d*) δ 7.51 – 7.46 (m, 2H), 6.75 – 6.55 (m, 2H), 3.06 (s, 6H). ^{13}C NMR (101 MHz, Chloroform-*d*) δ 152.4, 134.3, 133.4, 129.9, 127.6, 120.6, 111.5, 97.5, 39.9.

3-(10,11-dihydro-5H-dibenzo[*a,d*][7]annulen-5-ylidene)-N,N-dimethylpropan-1-amine

Column chromatography yields the title compound in liquid form in 64% yield. Method: 0 to 100% EtOAc on flash chromatography CombiFlash Rf + UV-Vis. ^1H NMR (400 MHz, Chloroform-*d*) δ 7.35 – 7.30 (m, 1H), 7.25 – 7.14 (m, 6H), 7.09 – 7.05 (m, 1H), 5.91 (t, $J = 7.1$ Hz, 1H), 3.54 – 3.28 (br, 2H), 3.07 – 2.71 (br, 2H), 2.46 – 2.28 (m, 4H), 2.20 (s, 6H). ^{13}C NMR (101 MHz, CDCl_3) δ 143.5, 141.4, 140.1, 139.3, 137.1, 129.9, 129.3, 128.6, 128.2, 128.0, 127.4, 127.0, 126.0, 125.7, 59.5, 45.3, 33.8, 32.1, 27.9.

Methyl formyl-L-tryptophanate

Column chromatography yields the title compound in liquid form with 81% yield. Method: 0 to 100% EtOAc on flash chromatography CombiFlash Rf + UV-Vis.

^1H NMR (400 MHz, Chloroform-*d*) δ 8.59 (s, 1H), 8.06 (s, 1H), 7.60 – 7.48 (m, 1H), 7.34 (m, 1H), 7.20 (m, 1H), 7.13 (m, 1H), 6.95 (s, 1H), 6.38 (d, $J = 8.0$ Hz, 1H), 5.06 – 4.91 (m, 1H), 3.70 (s, 3H), 3.40 – 3.29 (m, 2H). ^{13}C NMR (101 MHz, CDCl_3) δ 172.0, 161.0, 136.2, 127.6, 123.1, 122.2, 119.6, 118.5, 111.4, 109.4, 52.5, 51.7, 27.5.

(R)-N-methyl-N-(1-(naphthalen-1-yl)ethyl)-3-(3-(trifluoromethyl)phenyl)propan-1-amine

Column chromatography yields the title compound in liquid form with 83% yield. Method: 0 to 100% EtOAc on flash chromatography CombiFlash Rf + UV-Vis. ^1H NMR (400 MHz, Chloroform-*d*) δ 8.49 – 8.35 (m, 1H), 7.92 – 7.74 (m, 2H), 7.62 – 7.39 (m, 5H), 7.37 – 7.29 (m, 2H), 7.18 (d, $J = 7.7$ Hz, 1H), 4.33 (d, $J = 6.9$ Hz, 1H), 2.60 – 2.42 (m, 4H), 2.33 (s, 3H), 1.79 (m, 2H), 1.49 (d, $J = 6.7$ Hz, 3H). ^{13}C NMR (101 MHz, CDCl_3) δ 148.9, 143.4, 134.1, 131.9, 131.7, 128.7, 128.5, 127.4, 125.6, 125.4, 125.3, 125.2, 124.9, 124.9, 124.5, 122.9, 122.4, 60.6, 53.5, 38.6, 33.2, 28.9, 16.8. ^{19}F NMR (376 MHz, CDCl_3) δ -62.52.

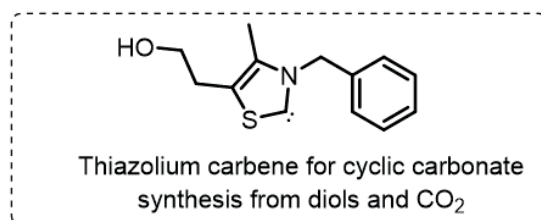
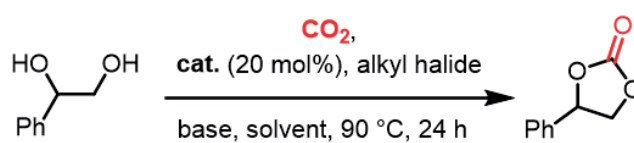
3.2. Metal-free catalyst for the synthesis of carbonates from diols and CO₂

This section is published as an article in *Chem. Commun.*, 2016, **52**, 10787–10790.

List of authors: **Felix D. Bobbink***, Weronika Gruszka*, Martin Hulla, Shoubhik Das, Paul J. Dyson,

*= equal contribution

Graphical abstract:



3.2.1. Introduction

From a thermodynamic perspective, oxygenated cyclic carbonates are particularly suitable synthetic targets from CO₂. These compounds have been exploited as electrolytes for lithium ion batteries,²⁴⁶ building blocks for polymeric materials,^{247,248} solvents^{249,250} and intermediates in the synthesis of compounds such as dimethyl carbonate (DMC)²⁵¹ and ethylene glycol.²⁵² Industrial production of cyclic carbonates involves either the transesterification of diols with phosgene in an energy-intensive process²⁵³ or the cycloaddition of CO₂ to epoxides.^{87,91,254} Despite the latter route exhibiting 100 % atom economy and industrial scalability, the synthesis of epoxides combined with their high reactivity and volatility are problematic. Recently, more stable, biodegradable 1,2-diols have been proposed as promising alternatives for the synthesis of cyclic carbonates with CO₂.⁵⁴ Their reaction with CO₂ is, however, neither kinetically nor thermodynamically-favored due to the formation of water as the sole by-product.²⁵⁵ Attempts have been made to by-pass this problem by the implementation of a suitable catalyst system and a dehydrating agent. Both heterogeneous and homogeneous catalysts have been proposed for this reaction. For example, a heterogeneous cascade catalysis comprising CeO₂ and 2-cyanopyridine is arguably the most efficient system.⁵³ However, this process requires harsh reaction conditions (150 °C and 50 bars of CO₂), an expensive reagent (2-cyanopyridine) and the activity is highly sensitive to the size of ceria particles. A number of homogeneous metal-free catalysts run under milder conditions and, interestingly, all are based on the 1,8-diazabicyclo[5.4.0]undec-7-ene (DBU) aided insertion of CO₂. Different reagents are used to facilitate the subsequent alkylation step to afford cyclic carbonates in good yield under only 10 bars of CO₂.²⁵⁶ The reaction may even proceed at an atmospheric pressure of CO₂ if DBU and the alkyl halide are used in large excess.⁵⁵ The same mild conditions are employed in a system in which tosyl chloride and triethylamine are used to afford cyclic carbonates with 6-membered rings in good yields.⁵⁶ Ultimately, only a few efficient processes exist and finding an increasingly sustainable process for this reaction remains important.

Recently, *N*-heterocyclic carbenes (NHCs) have gained interest as catalysts for reactions which employ CO₂ as a substrate.^{16,50,232,257,258} This stems from their ability to act as nucleophiles which activate CO₂ *via* the formation of imidazolium carboxylates.^{259,260} Interestingly, these intermediates have been previously reported to catalyze the synthesis of cyclic carbonates from diols employing DMC as the carbonyl source rather than CO₂.²⁶¹ Herein, we show the utility of carbene catalysts for the synthesis of cyclic carbonates from diols and CO₂ and, based on key experiments, propose plausible mechanisms for this transformation.

3.2.2. Results and discussion

Initially, reaction conditions were optimized using 1-phenyl-1,2-ethanediol (**1a**) as the substrate, Table 3.2.1. Several imidazolium and thiazolium carbene catalysts (**1c-4c**) were evaluated. NHCs **1c** and **3c**²³² and the thiazolium carbene catalysts **1b** and **1d**²³³ have been previously shown to catalyze the *N*-methylation of amines using CO₂ as the carbon source. The efficiency of a variety of bases and alkyl halides was also studied as they are essential for the reaction to proceed (see below).^{56,256}

The ability of cesium carbonate (Cs₂CO₃) to activate CO₂ and other small molecules^{61,262-265} encouraged us to employ it as a base in the reaction. Dibromomethane (CH₂Br₂) was also used due its efficiency in forming an effective leaving group.²⁵⁶ The activity of **1c-4c** was investigated in the presence of 2 eq. of CH₂Br₂ and 2 eq. of Cs₂CO₃. The highest yields of styrene carbonate (**1b**) were obtained with catalysts **1c** and **2c** (Table 3.2.1, entries 1 and 2). In contrast, **3c** and **4c** resulted in lower product yields (Table 3.2.1, entries 3 and 4). The effect of quantities of CH₂Br₂ and Cs₂CO₃ on the reaction was studied. Increasing CH₂Br₂ to 5 eq. resulted in 61% yield of styrene carbonate **1b** (Table 3.2.1, entry 6). Interestingly, a larger excess of the base (3 eq. instead of 2 eq.) led to a slight decrease in the yield of **1b** (Table 3.2.1, entry 7). It should be noted that the reaction proceeds in low yield using Cs₂CO₃ as the base in the absence of CO₂. However, ¹³C labeled CO₂ was used to confirm that the main source of the carbonyl group incorporated in the cyclic carbonate product originates from CO₂ (See Fig. A.3.2.1).

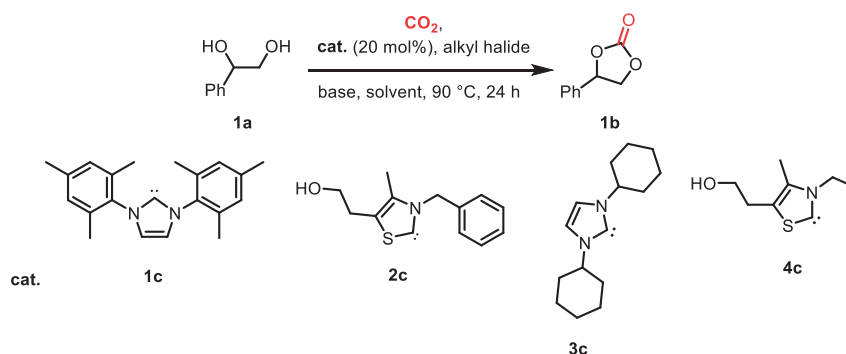
The enhanced activity of catalyst **2c** might be due to a greater stability to moisture; note that **1b** was not observed in a control experiment in which water was introduced into the system (See Table A.3.2.1). In the initial catalytic runs the active carbene catalyst was generated prior to reaction by the deprotonation of the corresponding salt with NaH. Subsequently, we found that the *in situ* generation of the carbene catalyst yielded **1b** in 71% in presence of 3 eq. of Cs₂CO₃ (Table 3.2.1, entry 8). Interestingly, in a previous study using the ionic liquid 1-butyl-3-methylimidazolium hexafluorophosphate ([BMIm][PF₆]) as solvent, the increased carbonate yield was attributed to the increased solubility of CO₂.²⁵⁶ Presumably, an active carbene was also generated by the deprotonation of the imidazolium salt by DBU – the ability of DBU and Cs₂CO₃ to deprotonate [BMIm][BF₄] to form a NHC has been reported.²⁶⁶ DBU was evaluated under our conditions, but yielded **1b** in a significantly lower yield (Table 3.2.1, entry 11).²⁵⁶ Na₂CO₃ and K₂CO₃ were evaluated in place of Cs₂CO₃, but afford the product in 0 and 5% yield, respectively, presumably due to the lower solubility of these carbonates in DMF (Table 3.2.1, entries 9 and 10). No product was observed with Et₃N (Table 3.2.1, entry 12). We speculate that Et₃N, which is often employed in the Stetter reaction, may undergo a Menshutkin reaction with CH₂Br₂ thereby inhibiting the reaction. Notably, Cs₂CO₃ was found to

be the optimal base in this reaction owing to its ability to generate the active carbene catalyst as well as to act as a minor carbonyl donor and a dehydrating agent.

Dimethylformamide (DMF) was selected as a reaction solvent as it can activate CO_2 .²⁶⁷ As expected, other polar aprotic solvents (dimethyl sulfoxide (DMSO) or dimethylacetamide (DMA)) could also be used (Table 3.2.1, entries 21 and 22), whereas no reaction was observed in toluene (Table 3.2.1, entry 23).

The optimum reaction temperature is 90 °C, with lower temperatures leading to a decrease in product yield (Table 3.2.1, entries 13 and 14) and with more elevated temperatures, e.g. 110 °C, leading to deactivation of the catalytic system (Table 3.2.1, entry 15). The alkyl halide also affects the reaction, in particular, 2 eq. of bromobutane ($\text{C}_4\text{H}_9\text{Br}$) results in a higher yield than 5 eq. of CH_2Br_2 (Table 3.2.1, entries 8 and 20). The other alkyl halides evaluated were less effective (Table 3.2.1, entries 16, 17 and 19).

Table 3.2.1 Optimization of the reaction conditions for the transformation of 1-phenyl-1,2-ethanediol (**1a**) used as a model substrate.



Entry	Catalyst	Alkyl halide (Eq.)	Base (Eq.)	Yield (%)
1	1c ^a	CH_2Br_2 (2)	Cs_2CO_3 (2)	44
2	2c ^a	CH_2Br_2 (2)	Cs_2CO_3 (2)	45
3	3c ^a	CH_2Br_2 (2)	Cs_2CO_3 (2)	29
4	4c ^a	CH_2Br_2 (2)	Cs_2CO_3 (2)	32
5	1c ^a	CH_2Br_2 (5)	Cs_2CO_3 (2)	42
6	2c ^a	CH_2Br_2 (5)	Cs_2CO_3 (2)	61
7	2c ^a	CH_2Br_2 (5)	Cs_2CO_3 (3)	53
8	2c	CH_2Br_2 (5)	Cs_2CO_3 (3)	71
9	2c	CH_2Br_2 (5)	Na_2CO_3 (3)	0
10	2c	CH_2Br_2 (5)	K_2CO_3 (3)	5
11	2c	CH_2Br_2 (5)	DBU (3)	21
12	2c	CH_2Br_2 (5)	Et_3N (3)	0
13 (50 °C)	2c	CH_2Br_2 (5)	Cs_2CO_3 (3)	5
14 (70 °C)	2c	CH_2Br_2 (5)	Cs_2CO_3 (3)	12
15 (110 °C)	2c	CH_2Br_2 (5)	Cs_2CO_3 (3)	25
16	2c	$(\text{CH}_2\text{Br})_2$ (5)	Cs_2CO_3 (3)	37
17	2c	$(\text{C}_2\text{H}_4\text{Br})_2$ (5)	Cs_2CO_3 (3)	32
18	2c	$\text{C}_4\text{H}_9\text{Br}$ (5)	Cs_2CO_3 (3)	59

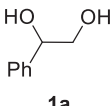
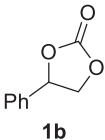
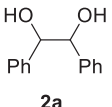
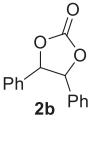
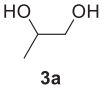
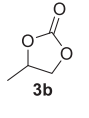
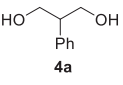
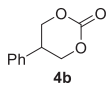
19	2c	C ₄ H ₉ Cl (5)	Cs ₂ CO ₃ (3)	20
20	<u>2c</u>	<u>C₄H₉Br (2)</u>	<u>Cs₂CO₃ (3)</u>	<u>81</u>
21 (DMSO)	2c	C ₄ H ₉ Br (2)	Cs ₂ CO ₃ (3)	33
22 (DMA)	2c	C ₄ H ₉ Br (2)	Cs ₂ CO ₃ (3)	50
23 (Toluene)	2c	C ₄ H ₉ Br (2)	Cs ₂ CO ₃ (3)	0

Reaction conditions: 1a (0.5 mmol), catalyst (20 mol%), alkyl halide (1–2.5 mmol), base (1–1.5 mmol), DMF (4 mL), CO₂ (1 atm.). Yields were determined by GC-FID using *n*-decane as internal standard. [a] The carbene catalyst was generated with NaH. Otherwise, the carbene is generated *in situ* using an extra 20 mol% base.

Based on the optimized conditions, which afford **1b** in up to 81% yield, the scope of the reaction was explored using catalyst **2c** (Table 3.2.2). The substrates varied from 1,2-diols to 1,3-diols (**2a – 4a**) bearing functional groups with varying steric influence. The diols were subjected to the optimized conditions of 2 eq. bromobutane, 3.2 eq. Cs₂CO₃ at 90 °C and 1 atm. CO₂ pressure.

The model product 4-phenyl-1,3-dioxolan-2-one was isolated in 61% yield (Table 3.2.2, entry 1). Five-membered cyclic carbonates, 4,5-diphenyl-1,3-dioxolan-2-one (**2b**) and propylene carbonate (**3b**) were obtained in yields of 63 and 54%, respectively (Table 3.2.2, entries 2 and 3). The six-membered cyclic carbonate, 5-phenyl-1,3-dioxan-2-one (**4b**) was produced in 53% (Table 3.2.2, entry 4). These yields are comparable to those obtained using alternative methods.^{55,256}

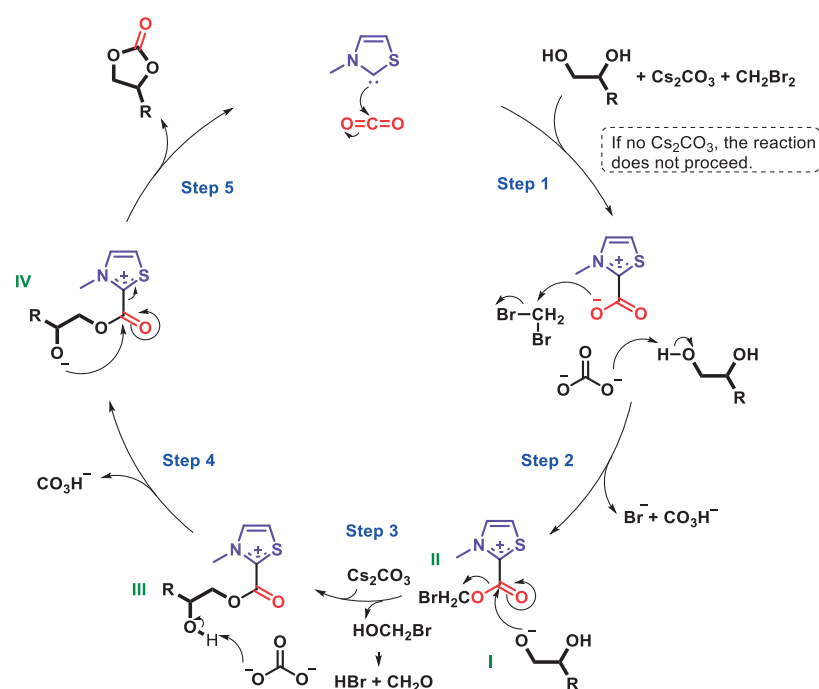
Table 3.2.2 Reaction of various diols with CO₂ under optimized conditions.

Entry	Reactant	Product	Yield (%)
1	 1a	 1b	61 ^a
2	 2a	 2b	63 ^a
3	 3a	 3b	54 ^b
4	 4a	 4b	53 ^b

Reaction conditions: substrate (0.5 mmol), cat. **2c** (20 mol%), C₄H₉Br (1.0 mmol), Cs₂CO₃ (1.6 mmol), DMF (4 mL), CO₂ (1 atm), 24 h, 90 °C. [a] Isolated yield. [b] GC yield.

On the basis of our results and previous literature, two plausible reaction mechanisms in Scheme 3.2.1

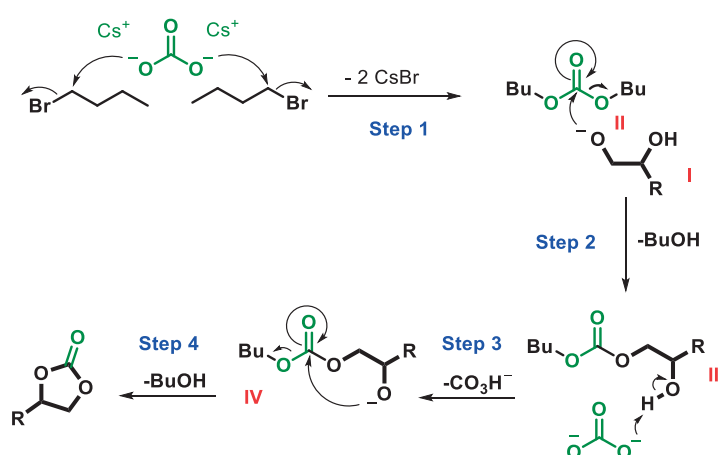
and Scheme 3.2.2 are suggested.^{108,256,261,268} Scheme 1 presents the principal mechanism for the carbene-catalyzed reaction. As mentioned above, both the base and alkyl halide are essential in the reaction, as confirmed in control experiments in which no carbonate was formed in their absence. Scheme 3.2.2 represents the mechanism for the minor non-catalytic formation of cyclic carbonate in the absence of CO₂. C₄H₉Br is included in the second mechanism due to detection of dibutyl carbonate and n-butanol in the reaction mixture using GC-MS, see SI. However, a similar mechanism is likely to take place in presence of other alkyl halides. Moreover, both of these mechanisms appear to occur concurrently to form the cyclic carbonate. This hypothesis is based on our finding that while 25% of **1b** was obtained in the absence of CO₂, addition of CO₂ increased the yield of **1b** to 81% (Table 3.2.1, entry 17 and Table A.3.2.1 in Appendix of Section 3.2).



Scheme 3.2.1 Tentative mechanism for the carbene-catalyzed reaction of diols and CO₂ to form cyclic carbonates. The substituents of the catalyst are omitted for clarity.

In the mechanism in Scheme 3.2.1, **step 2** involves the generation of an alkoxide **I** and the parallel attack of the carbene-CO₂ adduct on CH₂Br₂ after activation of CO₂ by the carbene in **step 1**. Nucleophilic attack of the alkoxide **I** on intermediate **II** in **step 3** results in the elimination of the leaving group and formation of intermediate **III**. In **step 4**, the secondary hydroxyl group of the diol is deprotonated, leading to the generation of intermediate **IV** and, in the final step (**step 5**), the intramolecular addition of the alcohol

occurs in intermediate **IV**, which affords the cyclic carbonate and regenerates the catalyst. Notably, bromomethanol is eliminated as a leaving group, however bromomethanol is unstable, and hence it is believed to decompose to a mixture of hydrogen bromide (HBr) and formaldehyde (CH₂O).²⁶⁹ Note, the formation of these side-products was not detected by spectroscopic or chromatographic studies, possibly due to neutralization of HBr by Cs₂CO₃ and the volatility of CH₂O.



Scheme 3.2.2 Proposed mechanism for the non-catalytic reaction of diols and CO₂ to form cyclic carbonates.

The secondary (non-catalytic) reaction in Scheme 3.2.2 proceeds by the attack of Cs₂CO₃ on C₄H₉Br in **step 1**, leading to the formation of intermediate **II** (dibutyl carbonate was observed by GC-MS, see Scheme A.3.2.1). Similar to the mechanism in Scheme 1, the reaction of the alkoxide **I** with intermediate **II** in **step 2** leads to the elimination of butanol (observed by GC-MS) and the formation of intermediate **III**. Again, the deprotonation of the secondary hydroxyl group in intermediate **III** in **step 3** results in the formation of intermediate **IV**. The final cyclization in **step 4** leads to the elimination of the second leaving group and the formation of the cyclic carbonate.

3.2.3. Conclusions

In summary, the work presented here offers an approach for the synthesis of cyclic carbonates from diols and CO₂. The proposed system benefits from the use of environmentally-friendly metal-free carbene catalysts. Using this methodology cyclic carbonates were obtained under mild conditions (90 °C and

atmospheric pressure of CO₂) in yields comparable or better to those obtained with other catalysts that operate under more forcing conditions. Based on labelling studies and other experiments two-mechanisms are proposed, one non-catalytic and one catalytic that account for the overall reaction.

3.2.4. Experimental details

3.2.4.1. General remarks

All reagents and solvents were purchased from commercial sources and used as received without further purification. Dry solvents from Acros were used throughout the experiments. In order to avoid water contamination all chemicals were stored in a dry glovebox. The reaction is very water sensitive and yields decrease if lower quality solvents or bench-stored Cs₂CO₃ are used. The GC-MS/FID were recorded on a Gas Chromatograph Agilent 7890B equipped with an Agilent 7000C MS triple quad detector and a capillary column from Agilent (l x d x f: 25 m x 0.25 mm x 0.25 μm) using N₂ as carrier gas. ¹H and ¹³C NMR spectra were recorded on a Bruker 400 MHz instrument.

3.2.4.2. Catalytic procedure

Typical procedure for the synthesis of cyclic carbonates: In a dry glovebox, a three-neck flask was charged with the starting material (0.5 mmol), base (1.0-1.5 mmol) and the imidazolium/thiazolium salt (0.1 mmol). The flask was then removed from the glovebox and connected to a Schlenk line and a CO₂-filled balloon. Three vacuum and CO₂-purge cycles were performed, and then alkyl halide (1.0-2.5 mmol) and solvent (4 mL) were added to the system. The reaction was heated in an oil bath at the desired temperature and the reaction mixture stirred for the appropriate time. After reaction, the mixture was diluted with EtOAc (5-10 mL) and the crude mixture was analyzed by GC-MS using decane as an internal standard. Yields were determined by GC-FID. For the isolated yields, an aqueous work-up was performed and the product was obtained by column chromatography using pentane:EtOAc as an eluent (100:0 to 70:30).

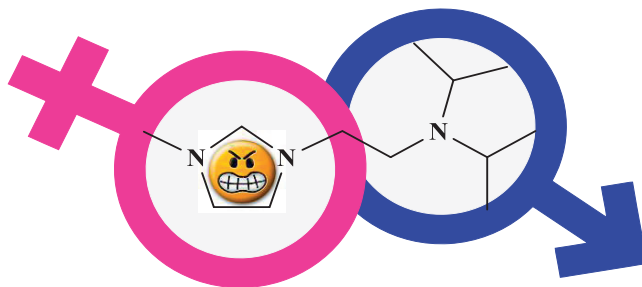
3.3. Towards a frustrated Lewis pair-ionic liquid system

This section is published as an article in *Inorganica Chim. Acta*, **2017**, 3, 4–8.

List of authors: Florian G. Perrin, **Felix D. Bobbink**, Emilia Păunescu, Zhaofu Fei, Rosario Scopelliti, Gabor Laurenczy, Sergey Katsyuba, Paul J. Dyson.

Statement of contribution: Felix D. Bobbink performed *in situ* NMR measurements and co-wrote the manuscript.

Graphical abstract:



3.3.1. Introduction

Frustrated Lewis pairs (FLPs) are composed of sterically or electronically hindered Lewis acids (LA) and Lewis bases (LB) that do not form strong LA-LB adducts.²⁷⁰⁻²⁷³ This property makes FLPs highly reactive and some are able to heterolytically split hydrogen and catalyse hydrogenation reactions,²⁷⁴ and activate carbon dioxide,^{275,276} nitric oxide²⁷⁷ and carbon monoxide.²⁷⁸ Not surprisingly, these properties have led to considerable interest in FLPs as catalysts.²⁷⁹⁻²⁸¹ Interestingly, FLPs share certain features with ionic liquids (ILs), in the sense that the Lewis acids and bases employed in FLPs are similar to IL cations and anions as they interact *via* non-covalent interactions. Despite considerable interest in hydrogen activation in both domains, to the best of our knowledge, these two areas have not been combined. Since FLPs are regarded as excellent catalysts for hydrogenation reactions and ILs are recognized as excellent solvents for hydrogenation reactions, we thought that merging these two areas could lead to an ionic solvent able to activate hydrogen.²⁸²⁻²⁸⁶

3.3.2. Results and Discussion

In preliminary studies, we found that the ability of classic FLPs, *i.e.* $B(C_6F_5)_3$ with 2,2,6,6-tetramethylpiperidine (TMP),²⁸⁷⁻²⁸⁹ to cleave hydrogen was reduced in the IL [EMIm][Tf₂N] (See Table A.3.3.1 in Appendix Section 3.3). However, an interesting feature of ILs is that they can be functionalized to afford so called “designer” ionic liquids. We foresaw that an IL bearing a part of the FLP could work in concert with the other part to potentially activate hydrogen. Consequently, we decided to evaluate an imidazolium salt encompassing a tertiary amine (see Figure 3.3.1), as tertiary amines such as diisopropylethylamine are known to form adducts with the Lewis base $B(C_6F_5)_3$ as well as FLPs.^{18,290}

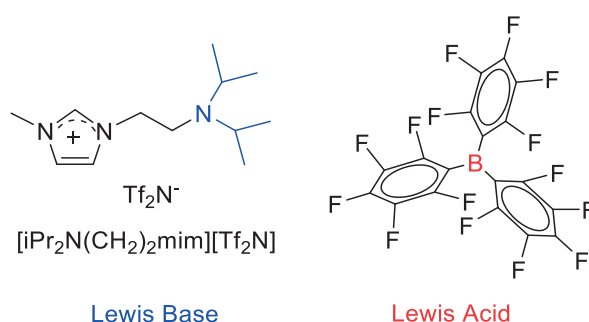


Figure 3.3.1 FLP-IL system designed for hydrogen activation.

The IL [iPr₂N(CH₂)₂mim][Tf₂N] was used previously as a base/catalyst in Heck and Knoevenagel reactions.²⁹¹ We speculated that the bulkiness of this amine would allow it to form either an FLP or an adduct, as reported for related amines.²⁹⁰ [iPr₂N(CH₂)₂mim][Tf₂N] is a liquid at room temperature but crystallizes at 0°C and the structure of [iPr₂N(CH₂)₂mim][Tf₂N] was determined by X-ray diffraction analysis. The

asymmetric unit contains two molecules and the cation of the molecule shown in Figure 3.3.2. The figure also shows that the diisopropylamine group can adopt two configurations, *anti* and *gauche*, which is in agreement with calculations.

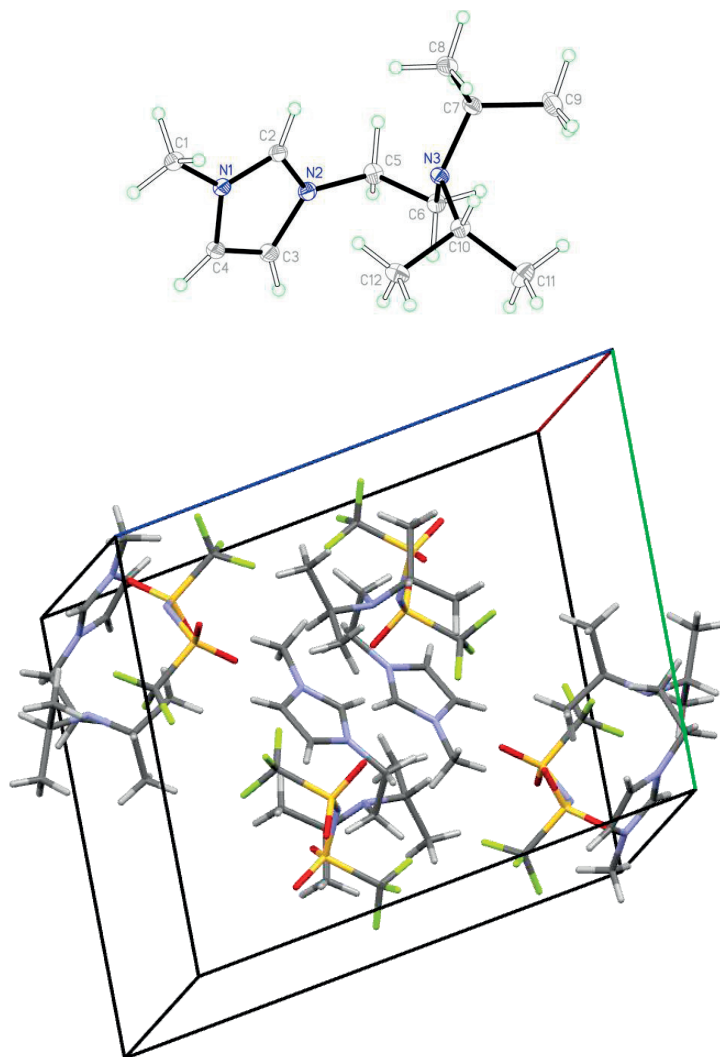


Figure 3.3.2 (top) ORTEP plot of the cation of the Lewis basic imidazolium cation in the crystal of $[\text{iPr}_2\text{N}(\text{CH}_2)_2\text{mim}][\text{Tf}_2\text{N}]$. Key bond lengths (\AA) and angles ($^\circ$): N(1)-C(2) 1.331(2), N(2)-C(2) 1.328(2), C(3)-C(4) 1.351(3), N(2)-C(2)-N(1) 108.71(13), C(10)-N(3)-C(7) 117.05(12). (bottom) Crystal packing of $[\text{iPr}_2\text{N}(\text{CH}_2)_2\text{mim}][\text{Tf}_2\text{N}]$.

To obtain information about the potential interactions between the IL and $\text{B}(\text{C}_6\text{F}_5)_3$, DFT calculations were performed on the structure of the IL. The conformation of the diisopropylamineethyl group of the $[\text{iPr}_2\text{N}(\text{CH}_2)_2\text{mim}]^+$ cation is determined by the torsion angle $\tau_1 = \text{N}(2)\text{-C}(5)\text{-C}(6)\text{-N}(3)$, which is equal to *ca.* 180° in the *anti*-conformation or *ca.* $\pm 60^\circ$ in the \pm *gauche*-conformation. The computations suggest that the *gauche*-conformation about the C(5)-C(6) bond observed in the crystal of $[\text{iPr}_2\text{N}(\text{CH}_2)_2\text{mim}][\text{Tf}_2\text{N}]$

(Figure 3.3.2) is energetically preferable relative to the *anti*-conformation shown in Figure 3.3.3 ($\Delta E \approx 6$ kcal·mol⁻¹, $\Delta G \approx 4$ kcal·mol⁻¹). To obtain possible structures of the complex formed by the [iPr₂N(CH₂)₂mim]⁺ cation and B(C₆F₅)₃, the latter molecule was placed at various positions in close proximity to the diisopropylamine moiety of the *anti*-conformer of the cation. The *gauche*-conformer was not regarded as a possible component of the [iPr₂N(CH₂)₂mim]⁺-B(C₆F₅)₃ complex because the formation of such complex would be sterically hindered. The optimized structure of the complex formed by the *anti*-conformer and B(C₆F₅)₃ is shown in Figure 3.3.3, A.

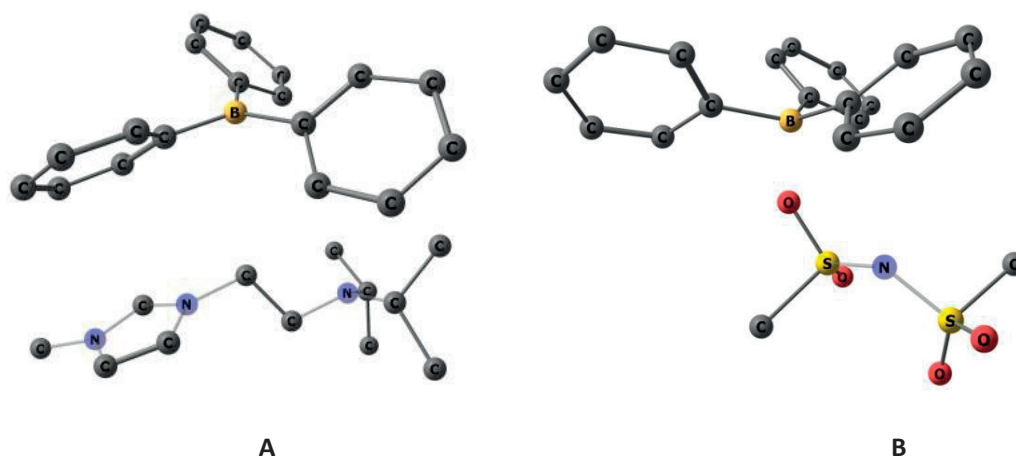


Figure 3.3.3 Optimized structures of the [iPr₂N(CH₂)₂mim]⁺-B(C₆F₅)₃ (A) and [Tf₂N]⁻-B(C₆F₅)₃ (B) complexes. Fluorine and hydrogen atoms are omitted for clarity. A: B··N(i-Pr)₂ distance = 4.35 Å. B: B··O distance = 1.66 Å.

According to the quantum-chemical computations at the PBE0-D3/def2-QZVP//TPSS/def2-TZVP level, the formation of the complex is exoenergetic with a binding energy (BE) ≈ -9 kcal·mol⁻¹. Nevertheless, the process results in a decrease of entropy of the system, which is reflected in a positive binding free energy, BG ≈ 7 kcal·mol⁻¹. The same approach applied to the [Tf₂N]⁻-B(C₆F₅)₃ complex produced rather similar values, *i.e.* BE ≈ -10 kcal·mol⁻¹ and BG ≈ 5 kcal·mol⁻¹ in spite of the quite short B··O distance (Figure 3.3.3, B). This indicates that a B-N adduct could be formed with either the anion or the cation, with comparable energies.

The LA, B(C₆F₅)₃, is insoluble in the ILs at room temperature, but the mixture can be homogenized upon heating. NMR spectra recorded at temperatures above 100 °C in neat form or in DMSO-d₆ show that stable adducts form between the IL and the LA (Scheme 3.3.1). In particular, tertiary amines are known to form iminium species with B(C₆F₅)₃, and this was confirmed by the distinctive peak at -25 ppm in the ¹¹B NMR

spectrum (see Figure 3.3.4). At least two more species are present, consistent with previous studies.^{18,292} Furthermore, the ^1H NMR spectrum confirms that ionic species are formed, with signals at 3.6 ppm for the anion and 4.3 ppm for the cation, that match those from related species.²¹ In the ^{13}C NMR spectrum a peak at 190 ppm is observed, which may be attributed to an iminium species (See Appendix Section 3.3, Figures A.3.3.1 to A.3.3.3 for overlay of NMR spectra).

The LA was mixed with the IL in a 1:4 ratio and the system was pressurized with H_2 to establish whether the system can cleave hydrogen. The ^1H NMR spectra did not distinctively change from that attributed to the boron-nitrogen adduct (see Scheme 3.3.1), whereas the ^{11}B NMR no longer exhibits the hydride peak at -25 ppm, and ^{13}C spectra indicate that the iminium species at 190 ppm is no longer present. While common FLPs based on DIPA usually split hydrogen under mild conditions, the utilization of the hydrogen in subsequent transformations usually requires high temperatures ($> 100^\circ\text{C}$). In our case, the IL-LA adduct did not cleave H_2 since both components presumably already were in ionic form (Scheme 3.3.1) however the adduct is no longer present following exposure of the reaction mixture to H_2 .

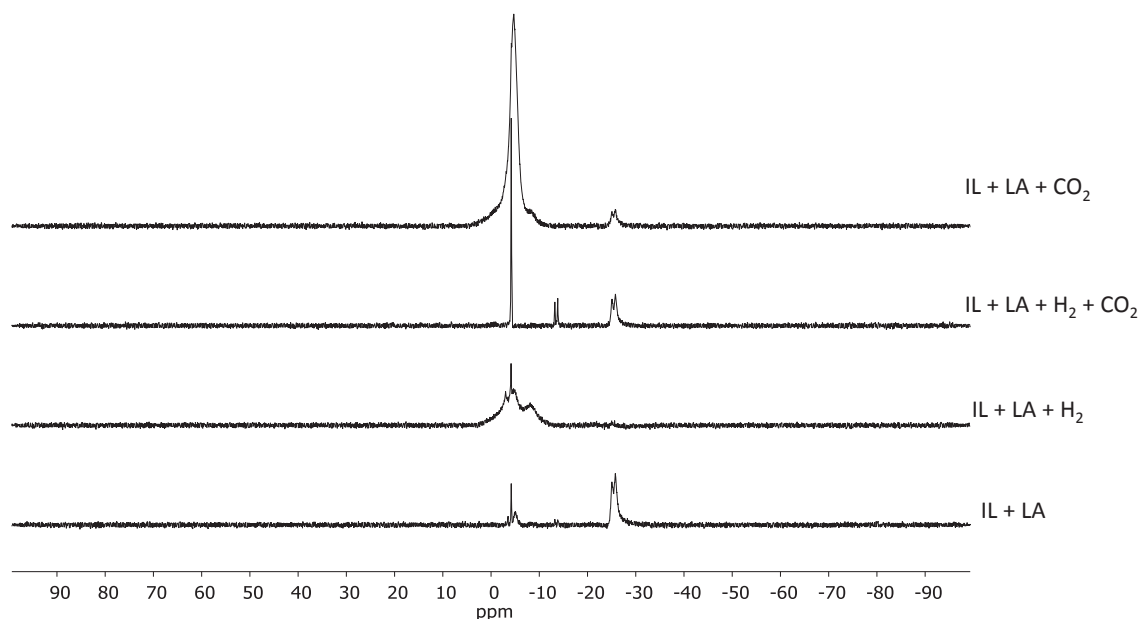
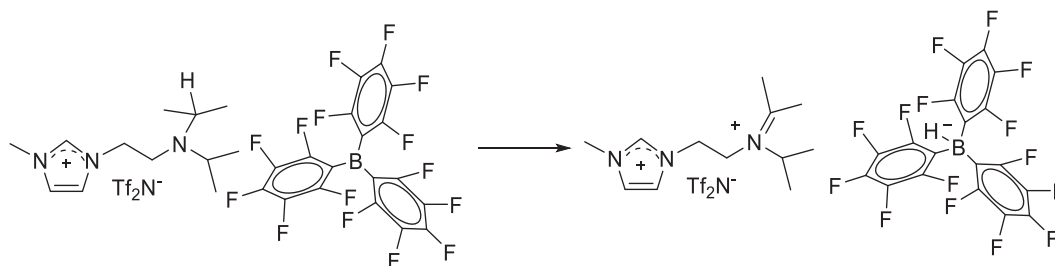


Figure 3.3.4 Overlay of ^{11}B NMR spectra of $\text{B}(\text{C}_6\text{F}_5)_3$ (25 mol%) in $[\text{Pr}_2\text{N}(\text{CH}_2)_2\text{mim}][\text{Tf}_2\text{N}]$ under N_2 , and in the presence of H_2 (30 bars), CO_2 (20 bars) and H_2/CO_2 ($P_{\text{H}_2} = 30$ bars, $P_{\text{CO}_2} = 20$ bars).



Scheme 3.3.1 Reaction of the [*i*Pr₂N(CH₂)₂mim][Tf₂N]-B(C₆F₅)₃ IL-FLP system without H₂.

Based on the ability of the [*i*Pr₂N(CH₂)₂mim][Tf₂N]-B(C₆F₅)₃ system to form an hydride, and previous studies that show FLPs can reduce CO₂,^{293,294} the potential of the IL-FLP to reduce CO₂ was evaluated under similar conditions to FLPs in toluene. The IL-B(C₆F₅)₃ mixture was heated to 135 °C under 20 bars of CO₂ and 40 bars of H₂ in a stainless-steel autoclave. After reaction, the ¹³C NMR spectrum of the solution was found to contain a signal at 167 ppm, indicative of possible formate salt or CO₂ adduct (Figure 3.3.5).^{275,276,293} Moreover, the ¹¹B NMR spectrum contains new signals, indicative of boron-CO₂/boron-formates (See Figure 3.3.4). The ¹H NMR spectrum displayed several new peaks in the formate region (7.0 - 9.2 ppm) when CO₂ was added to the system, confirming that formate-type species form under these conditions. Finally, overlaying the ¹⁹F NMR spectra of the system with H₂ only with the one containing both H₂ and CO₂ demonstrate that several new sets of peaks are formed in the latter case, consistent with the ¹H and ¹¹B NMR spectra (See Appendix Section 3.3, Figures A.3.3.1 to A.3.3.4 for overlay of NMR spectra). Earlier reports have carefully detailed the possible products that are formed during the reaction of a FLP with CO₂.^{290,295,296} CO₂ seems to react with the hydride in the IL-LA adduct, this inference being consistent with the observed signal on the ¹³C NMR spectrum and the new set of peaks on the ¹⁹F NMR spectrum.

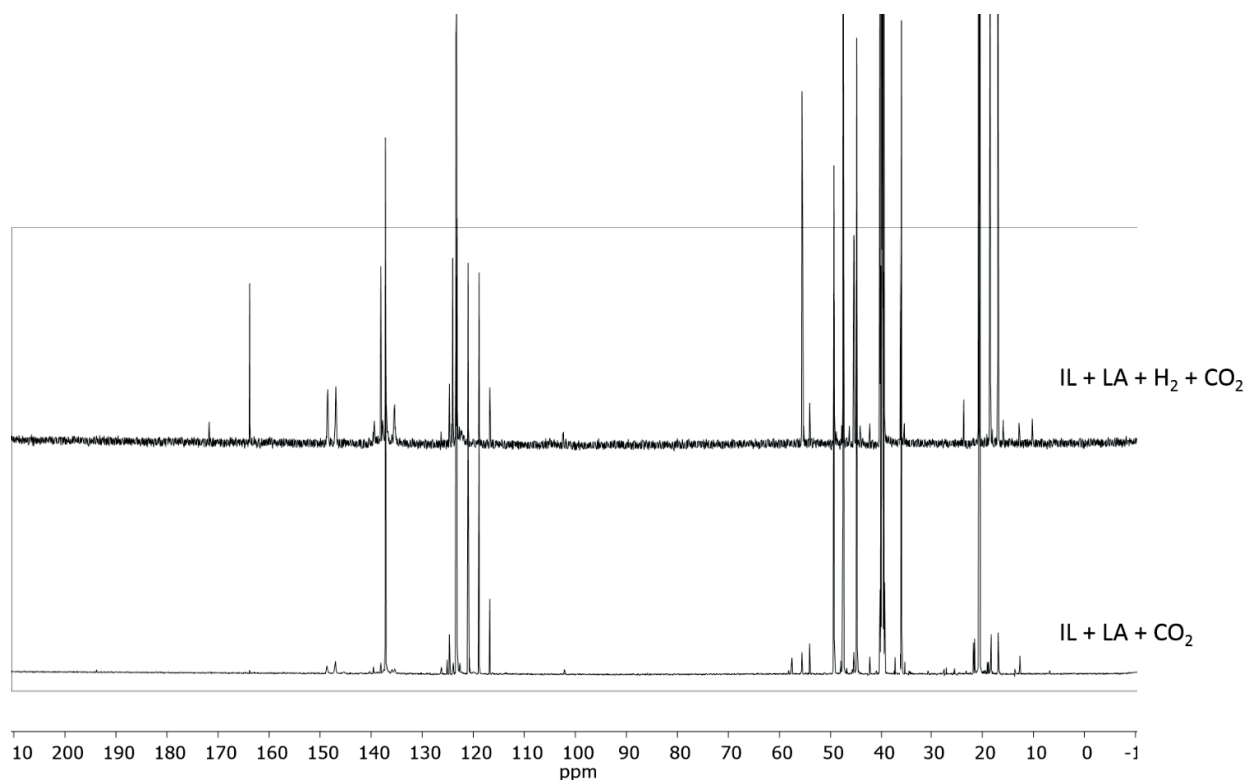


Figure 3.3.5 Overlay of ^{13}C NMR spectra of $\text{B}(\text{C}_6\text{F}_5)_3$ (25 mol%) in $[\text{Pr}_2\text{N}(\text{CH}_2)_2\text{mim}][\text{Tf}_2\text{N}]$ in the presence of H_2/CO_2 ($P_{\text{H}_2} = 30$ bars, $P_{\text{CO}_2} = 20$ bars) and CO_2 (20 bars, top).

3.3.3. Conclusions

In summary, we have attempted to develop a FLP-IL system that activates hydrogen and can be used to reduce carbon dioxide. However, an adduct of iminium and boron hydride forms between the LA and the LB as well as several other species, which is consistent with self-ionization processes. These interactions subsequently hinder H_2 cleavage. Nevertheless, CO_2 adducts could be formed, presumably with the boron-hydride species. Upon the addition of H_2 and CO_2 , the formate concentration increases, indicating that even if the adduct does not activate H_2 , it is able to mediate CO_2 hydrogenation. It should be emphasized that this kind of system can likely be improved by varying the components of the IL, *i.e.* preparing an IL encompassing a secondary amine rather than tertiary amines presented herein. As some ILs are known to act as ‘sponges’ for CO_2 or dissolve relatively high concentrations of H_2 , it may be possible to develop highly reactive FLP-IL systems. Such systems could store hydrogen or be employed as biphasic solutions for various catalytic transformations.

3.3.4. Experimental details

All starting materials were obtained from commercial sources and used as received. ILs 1-ethyl-3-methylimidazolium bis(trifluoromethylsulfonyl)imide $[\text{Emim}][\text{Tf}_2\text{N}]$, 1-ethyl-3-methylimidazolium acetate

[Emim][Ac], 1-butyl-3-methylimidazolium trifluoromethanesulfonate [Bmim][TOF] and 1-propyl-1-methylpyrrolidinium bis((trifluoromethyl)sulfonyl)imide [Pyr][Tf₂N], were purchased from Iolitec. [¹Pr₂N(CH₂)₂mim]Cl and [¹Pr₂N(CH₂)₂mim][Tf₂N] were synthesized using a literature protocol.²² ¹H (400.13 MHz), ¹⁹F (376.60 MHz), ¹¹B (128.34 MHz) and ¹³C (100.62 MHz) NMR spectra were recorded on a Bruker Avance II 400 spectrometer at 298 K. For the NMR spectra taken without a deuterated solvent the shim was realized on the FID signal.

3.3.4.1. Reactions in [Emim][Tf₂N]

High pressure experiments were performed in a Parr 25 mL autoclave. In a typical reaction, a mixture of B(C₆F₅)₃ (525.6 mg, 1.03 mmol) and 2,2,6,6-tetramethylpiperidine (0.12 mL, 0.99 mmol) in [EMIm][Tf₂N] (8 mL) was introduced into the autoclave. The autoclave was placed under a constant pressure of H₂ and then heated to the required temperature under rapid stirring. After the appropriate time, the autoclave was cooled to 0 °C and depressurized. High pressure NMR experiments were performed in 10 mm external diameter medium pressure sapphire NMR tubes.

3.3.4.2. Typical reaction between [¹Pr₂N(CH₂)₂mim][Tf₂N] and B(C₆F₅)₃

In a glovebox, [¹Pr₂N(CH₂)₂mim][Tf₂N] (0.78 mmol, 0.38 g, 4 eq.) and B(C₆F₅)₃ (0.19 mmol, 100 mg, 1 eq.) were mixed together in a GC vial. The mixture was then pressurized with the suitable gas (H₂ (30 bars) or CO₂ (20 bars) or both (p_{tot} = 50 bars)) and left to stirring at 135 °C for 16 h in an oil bath. After the reaction, the autoclave was cooled to 0 °C in an ice bath, depressurized to retrieve the crude reaction mixture which was analyzed by NMR spectroscopy, both in pure form and diluted in DMSO-d₆.

3.3.4.3. DFT computations

All geometries were fully optimized at the TPSS-D3/def2-TZVP level, using the ORCA program of version 3.0. The appended “-D3” denotes Grimme’s atom-pairwise D3 dispersion correction, combined with the Becke-Johnson damping scheme. DFT-D3 was recently benchmarked for interactions of various frustrated lone pairs and found to provide results close to those of CCSD(T) benchmark quality. The optimization of the structures was conducted with the conductor-like screening model (COSMO) with a dielectric constant $\epsilon = 24.85$ to simulate the “real” environment. Harmonic frequencies were calculated on the optimized geometries in order to verify these as minima. The frequencies were used to calculate free energies at 298.15 K and 1 atm. (termed ΔG). The ro-vibrational corrections (including zero-point vibrational energies) to the free energy were obtained from a modified rigid rotor, harmonic oscillator statistical treatment, based on the harmonic frequencies obtained at the TPSS level (see above). In the entropy calculation, frequencies with wavenumbers below 100 cm⁻¹ were treated partially as rigid rotors and harmonic oscillators (see ref. 44 for details). The computed free energies were obtained from:

$$\Delta G = \Delta E + \Delta G_{RRHO}$$

The last term refers to the abovementioned ro-vibrational contribution to the free energy. The optimized geometries were further used for the single-point calculations of the electronic energies by applying the PBE0 hybrid density functional in combination with the quadruple-zeta def2-QZVP Ahlrich's basis set and COSMO model. In all calculations the RIJCOSX algorithm for the two-electron integrals was employed for speed up calculations as implemented in the ORCA program. The algorithm treats the Coulomb term *via* a RI approximation and the exchange term *via* semi-numerical integration. The binding energy (BE) and binding Gibbs free energy (BG) of complexes formed by B(C₆F₅)₃ and the [Pr₂N(CH₂)₂mim]⁺ cation or the [Tf₂N]⁻ anion was computed in the supermolecular approach as the difference of the energy of the complex and the energies of the optimized separated counterparts:

$$BE = \Delta E \text{ (PBE0/def2-QZVP//TSPP/def2-TZVP)}$$

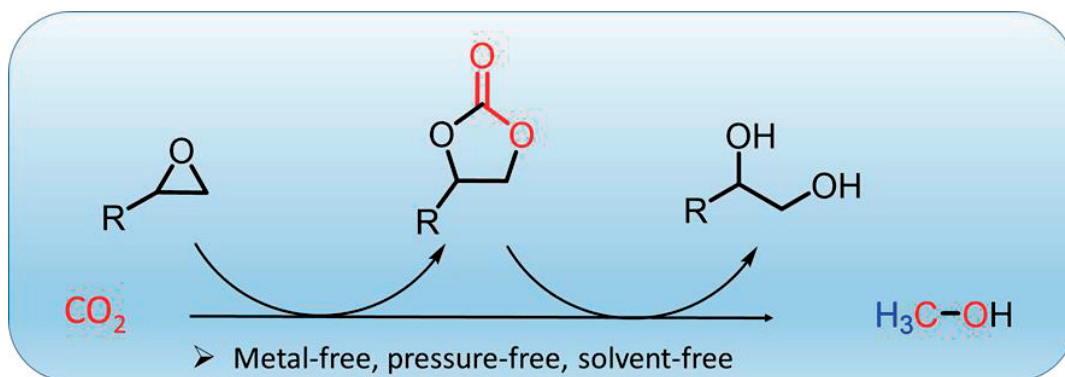
$$BG = BE + \Delta G_{RRHO}(\text{TPSS/def2-TZVP})$$

3.4. One-pot, two-step MeOH production from CO₂ via cyclic carbonates under metal-free and atmospheric conditions

Manuscript submitted.

List of authors: **Felix D. Bobbink**, Florent Menoud, Paul J. Dyson

Graphical abstract:



3.4.1. Introduction

The reaction between epoxides and CO₂ to afford cyclic carbonates represents a benchmark reaction in CO₂ chemistry.^{57,87} In this respect, numerous catalytic systems have been reported, and simple organic salts such as n-tetrabutylammonium (TBA)¹²³ or imidazolium halides⁹³ are potent catalysts for the reaction. Interestingly, the fluoride salt of TBA also catalyzes the deprotection of silylated-alcohols (silyl ethers)²⁹⁷, and possesses a remarkable cooperativity with hydrosilanes. For example, TBAF-silane mixtures are potent catalysts for amide reductions to amines or nitriles²⁹⁸ and for the formylation of amines using CO₂ as the C1 source.⁹⁸ Based on the ability of TBA salts to catalyze both epoxide-CO₂ coupling¹²³ and hydrosilylation/reduction reactions,^{299–301} we set-out to develop a simple, metal-free route to simultaneously produce MeOH and PG from PC, which itself can be derived from propylene oxide and CO₂ while employing a compatible catalytic system that is efficient for both steps of the process (See Figure 3.4.1).

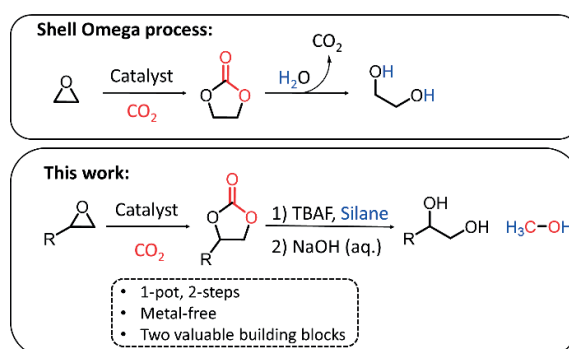


Figure 3.4.1 Shell Omega process for PG production, and the method reported here for the simultaneous synthesis of MeOH and diols.

3.4.2. Results and discussion

The hydrosilylation/hydrolysis reaction of propylene carbonate was optimized under solvent-free conditions (Table 3.4.1, see Experimental for full details). The initial reaction conditions were chosen according to results obtained for analogous TBAF-hydrosilane mixtures, *i.e.* 10 mol% TBAF catalyst and PhSiH₃ as a hydride source,⁹⁸ followed by addition of water to release the alcohol product. These conditions resulted in the full conversion of propylene carbonate (PC) to PG and MeOH (Table 3.4.1, entry 1, 100% conversion and 70% MeOH). In the absence of PhSiH₃, hydrolysis of PC affords PG in 23% yield (Table 3.4.1, entry 2), indicating why the selectivity of the process towards MeOH is lower than that of PG in most cases. Increasing the hydrosilane concentration led to an increase in conversion, but to a decrease in the yield of MeOH (Table 3.4.1, entries 3 and 4), with the optimized quantity of silane being two equivalents to achieve full conversion and one equivalent to maximize the production of MeOH. One

equivalent of PhSiH_3 was sufficient to produce a near-quantitative yield of MeOH, suggesting that all three hydrogens of the hydrosilane are transferred in the reaction.

The N-formylation of amines using CO_2 as the C1 source and hydrosilanes as the reductant is efficiently catalyzed by simple potassium salts or basic salts.^{98,302} Consequently, a series of related salts were evaluated as catalysts in the conversion of PC to PG and MeOH, but the reaction proceeded in low yields (KF - 4% MeOH, Cs_2CO_3 - 16% MeOH and TBACl - 9% MeOH). In addition, other silanes were screened, but all of them resulted in a lower yields and selectivities (Table 3.4.1, entries 8-10), although the reaction proceeds to some extent (63% MeOH with Ph_2SiH_2 , 11% MeOH with Et_3SiH – commonly employed in hydrosilylation reactions including the hydrosilylation of CO_2 ³⁰³ and 21% MeOH with poly-methylhydrosiloxane, PMHS). PMHS is particularly interesting because it is a waste-product from the silicon industry.^{50,233} Under the solvent-free reaction conditions the polymer rapidly solidifies, presumably due to cross-linking, and the product becomes trapped in the pores hindering efficient extraction. For all the hydrosilanes used herein, the addition of water results in the formation of a white solid precipitate (mixture of siloxanes and silyl ethers). Polar aprotic solvents can be applied in the reaction mixture, but they lower the yield of MeOH (Table 3.4.1, entries 11-13). However, as the reaction is exothermic, for larger scale a solvent such as DMSO or DMF helps to dissipate the heat.

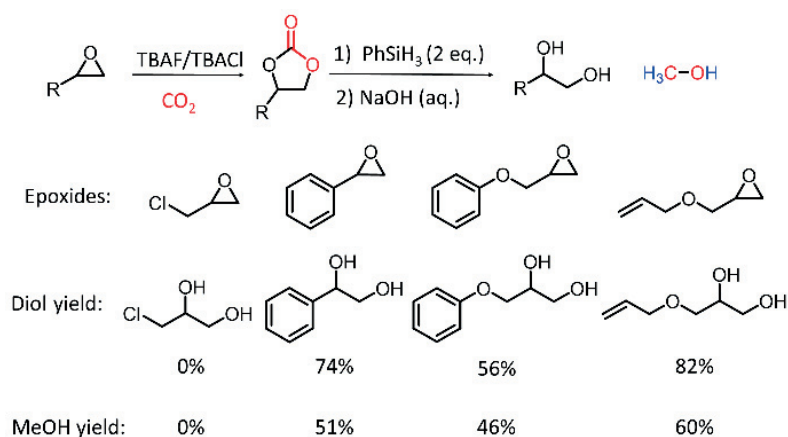
Table 3.4.1 Optimization of the reaction conditions for the transformation of PC to PG and MeOH.

Entry	Catalyst	Silane (eqs.)	Solvent	Conversion [%]	Yield PG [%]	Yield MeOH [%]
1	TBAF.3H ₂ O	PhSiH ₃ (3)	none	100	98	70
2	TBAF.3H ₂ O	PhSiH ₃ (0)	none	24	23	0
3	TBAF.3H ₂ O	PhSiH ₃ (1)	none	93	93	93
4	TBAF.3H ₂ O	PhSiH ₃ (2)	none	100	99	78
5	TBACl	PhSiH ₃ (2)	none	44	11	9
6	KF	PhSiH ₃ (2)	none	54	8	4
7	Cs ₂ CO ₃	PhSiH ₃ (2)	none	76	23	16
8	TBAF.3H ₂ O	Ph ₂ SiH ₂ (2)	none	100	67	63
9	TBAF.3H ₂ O	PMHS (2)	none	53	25	21
10	TBAF.3H ₂ O	Et ₃ SiH (2)	none	70	22	11
11	TBAF.3H ₂ O	PhSiH ₃ (2)	DMF-d ₇ (1 mL)	87	87	73
12	TBAF.3H ₂ O	PhSiH ₃ (2)	DMSO-d ₆ (1 mL)	72	72	67
13	TBAF.3H ₂ O	PhSiH ₃ (2)	CH ₃ CN-d ₃ (1 mL)	76	76	54

Conditions: Cat (10 mol%), PC (1 mmol), silane (1-3 eq.), 60 °C, 3 h. Then NaOH_{aq} (5%, 0.1 mL), r.t., 2 h. Yields determined by ¹H NMR spectroscopy using CH₂Br₂ as a standard.

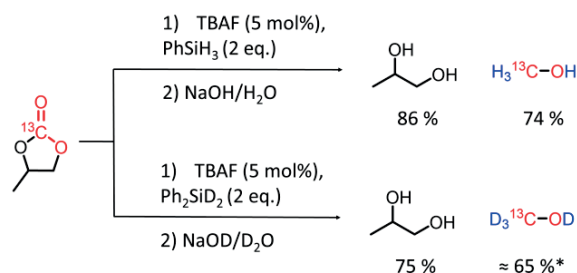
To demonstrate the versatility of the system for glycol production, *i.e.* as an alternative to the Shell Omega Process, several epoxides (epichlorohydrin, allyl glycidyl ether, phenyl glycidyl ether and styrene oxide) were converted to their corresponding carbonates *via* insertion of CO₂, catalyzed by a TBAF-TBACl mixture. After reaction the mixture was allowed to cool to room temperature and the atmosphere was purged with N₂. PhSiH₃ (2 equivalents) was introduced and the reaction was performed according to the optimized procedure (60 °C, 3 h, then hydrolysis at r.t. for 2 h). The first step (*i.e.* cycloaddition of CO₂ into the epoxide) proceeds in a near-quantitative yield for all the epoxides (determined by ¹H NMR spectroscopy). The yields of the diols and MeOH are summarized in Scheme 3.4.1. Styrene oxide resulted in a yield of 51% of MeOH and 74% of glycol while phenyl glycidyl ether gave 46% of MeOH and 56% of corresponding diol. The use of allyl glycidyl ether resulted in a yield of 60% of MeOH and 82% of the corresponding diol. Notably, the double bond of allyl glycidyl ether remained intact under the hydrosilylation conditions. Epichlorohydrin did not react to form MeOH under the conditions employed despite the carbonate being formed quantitatively after the first step, presumably due to the electron withdrawing chlorine atom in the

substrate. In all the cases, the sequential reaction of epoxide to carbonate to MeOH (3-steps including hydrolysis, performed in a single pot) was less efficient than the reaction starting with the pure carbonate (results in Table 3.4.1), as the TBAF salt slowly decomposes at 80 °C under the reaction conditions (the mixtures turn yellow to brown).³⁰⁴



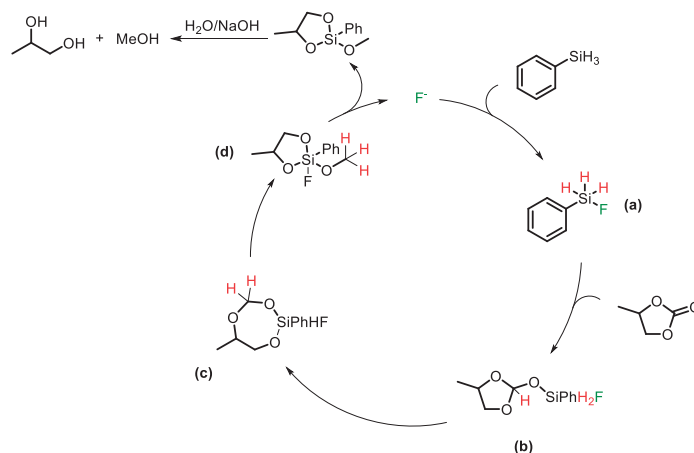
Scheme 3.4.1 Epoxides used in the synthesis of glycols and MeOH from epoxides in a single pot reaction.

Labelling experiments showed that $^{13}\text{CH}_3\text{OH}$ and $^{13}\text{CD}_3\text{OD}$ were accessible using this method (Scheme 3.4.2). Labelled propylene carbonate was prepared from propylene oxide and $^{13}\text{CO}_2$ using a heterogeneous polymeric salt catalyst³⁰⁵ affording ^{13}C -PC in high yield. Employing ^{13}C -PC as the starting material in combination with PhSiH_3 or Ph_2SiD_2 , ^{13}C NMR spectra of the crude reaction mixture demonstrate that the carbon atom of the propylene carbonate is transformed into $^{13}\text{CH}_3\text{OH}$ or $^{13}\text{CD}_3\text{OD}$, respectively (See Appendix Section 3.4, Figures A.3.4.1 and A.3.4.2). Further spectroscopic studies show that the protons of the methanol are derived from the hydrosilane, whereas the methanol OH and diol protons of PG are derived from water. Note, prior to the hydrolysis step, MeOH is detected by ^1H and ^{13}C NMR spectroscopy due to the presence of water in the hygroscopic catalyst. Currently, $^{13}\text{CH}_3\text{OH}$ and $^{13}\text{CD}_3\text{OD}$ are produced from appropriately labelled syngas mixtures under pressure in the presence of metal catalysts, and our procedure is advantageous as it avoids toxic ^{13}CO (and D_2).



Scheme 3.4.2 Labelling experiments for the hydrosilylation/hydrolysis of propylene carbonate to produce labelled MeOH. * Yield estimated based on PG.

The hydrosilylation/hydrolysis of carbonates presumably occurs *via* a mechanism similar to that for ketones, which has been proposed for different types of catalysts, usually proceeding by the same pathway. In the first step, the hydrosilane is activated by the catalyst, enabling a hydride to react with the electropositive C-atom of the carbonate with simultaneous binding of the oxygen atom to the silicon centre,^{306,307} as depicted in Scheme 3.4.3 (intermediate **b**). All the hydrogen atoms from the silane can be donated to the C-atom, since only 1 eq. of PhSiH₃ is sufficient (see Table 3.4.1 1, entry 3). Moreover, labelling experiments with Ph₂SiD₂ demonstrate that the deuterium atoms are incorporated into the methanol, rather than the diol. Since silicon is oxophilic, a 7-membered ring (**c**) can be formed upon hydride transfer. An example of a similar scaffold has been isolated from the silylation of ribose with a source of bis(*tert*butyl)silyl.³⁰⁸ Moreover, pentacoordinated species analogous to that of (**d**) have been proposed in the past, albeit with a N-donor group to stabilize the silicon centre.^{309,310} In the final step, the hydrolysis of intermediate (**d**) generates MeOH and PG and various siloxanes, explaining the broad peaks observed in the aromatic region in the ¹H NMR spectrum of the crude reaction mixture prior to product purification.



Scheme 3.4.3 Proposed mechanism for the transformation of propylene carbonate into MeOH and PG.

^{29}Si NMR and ^{19}F NMR spectra were recorded in DMSO- d_6 for the typical reaction prior to the hydrolysis step in an attempt to identify possible intermediates in the catalytic cycle. The ^{29}Si NMR spectrum (see Figure A.3.4.3 in Appendix Section 3.4 for a representative ^{29}Si NMR spectrum) contains three singlets at -56, -57 and -58 ppm, which are in the same region as PhSiH_3 (singlet at -59 ppm). These peaks may be tentatively attributed to $\text{PhSi}(\text{OMe})_2\text{F}$ -type species related to intermediate (d) in Scheme 3.^{311,312} A triplet was also observed at -109 ppm, with a J-coupling of 206 Hz – this value is typical of a SiF_2 species,³¹³ indicating that a catalytic intermediate with two F-atoms is also present. The corresponding ^{19}F NMR spectrum (see Figure S8) possesses a peak at c.a. -140 ppm, which has previously been attributed to a SiF_2 -type compound.³¹³ Finally, a singlet peak is observed at -35 ppm in the ^{29}Si NMR spectrum which is close in value to $\text{PhSiH}(\text{OEt})_2$ ³¹⁴ and a related species could possibly form following elimination of the F-atom in structure (c).

As a control, TBAF and PhSiH_3 were reacted in the absence of PC, and the resulting NMR spectra are completely different to those described above (see Appendix Section 3.4, Fig. A.3.4.4 for a comparison). Moreover, the TBAF- PhSiH_3 mixture was markedly less stable in DMSO- d_6 in comparison with the TBAF- PhSiH_3 -PC mixture, and a white suspension is observed in the TBAF- PhSiH_3 system, whereas the reaction of PC-TBAF- PhSiH_3 remains clear, suggesting that the substrate helps to stabilize the catalytic system.

3.4.3. Conclusions

We have developed a simple, cheap and user-friendly approach to produce methanol and diols, in high yields from CO_2 and epoxides that is related to the Shell-Omega process, but advantageously consumes

CO₂ to afford MeOH and not only the glycol. The remarkable cooperativity between a simple fluoride salt (TBAF) and a hydrosilane (PhSiH₃), allows the reaction to take place under mild conditions. Fully labelled ¹³CD₃OD can be obtained from the reaction of ¹³CO₂ and Ph₂SiD₂, which avoids toxic ¹³CO/D₂ mixtures and high pressures. Based on the available experimental/spectroscopic evidence a tentative catalytic cycle for the reaction has been proposed.

3.4.4. Experimental details

3.4.4.1. Typical procedure for catalytic reaction:

Four-parallel reactions were conducted in parallel in a set-up that was described earlier.¹⁹⁰ Briefly, in a two-neck flask equipped with a stirrer bar, the catalyst (5 mol%) and the appropriate carbonate (1 mmol) were loaded and dissolved in the solvent (under solvent-free conditions, the salt and the carbonate were weighed in the flask). After three vacuum-N₂ cycles, the hydrosilane (1-3 mmol) was added dropwise, which results in a highly exothermic reaction. After addition, the reaction mixture was heated to 60 °C for 4 h. After this time, the reaction mixture was allowed to cool to RT, and 2 eq. of 5 % aqueous NaOH was added to hydrolyze the formed silyl ether, upon which a white solid instantly formed. After 2 h, the reaction mixture was diluted in 1 mL DMSO-d₆ and the internal standard was added to the reaction mixture. The yield was determined by ¹H NMR spectroscopy by integral comparison with the internal standard.

3.4.4.2. Typical procedure for 1-pot synthesis of MeOH from epoxides and CO₂:

In a 10 mL two-neck flask, the catalysts (5 mol% TBAF and 5 mol% TBACl) and the epoxide (100 mg) were added. The atmosphere was replaced by CO₂ (1 atm.). The reaction mixture was heated to 80 °C for 15 h, which resulted in a complete conversion of the epoxide to the carbonate, as reported previously.¹¹⁷ Then, the reaction mixture was cooled to RT and PhSiH₃ (2 eq.) was added dropwise (caution: exothermic reaction), and the reaction was continued according to the typical procedure.

3.4.4.3. Preparation of ¹³C-labelled propylene carbonate:

Due to the low boiling point of propylene oxide, it is preferable to use a stainless-steel autoclave for the reaction between propylene oxide and CO₂ to avoid evaporation of the starting material. In a 25 mL autoclave, 2 grams of PO and 5 mol% of catalyst were added.³⁰⁵ The autoclave was pressurized with 8 bars of ¹³CO₂ and heated to 130 °C for 15 h. After cooling and releasing the pressure, the resulting mixture was diluted in EtOAc, filtered, and dried, leading to pure ¹³C-labeled PC. The PC was then reacted with PhSiH₃ under TBAF catalysis to form ¹³CH₃OH and propylene glycol according to the procedure described above.

3.5. General conclusions

3.5.1. Summary

Methodologies that employ CO₂ as a reactive synthon were discussed. Section 3.1 was presented in the form of a protocol that detailed every step of a N-methylation of N-formylation reaction employing an N-heterocyclic carbene catalyst. The protocol also reviewed recent advances on the topic, and was based on two publications from our laboratory where we described the utilization of NHC and thiazolium carbenes for the N-methylation and N-formylation of amines, respectively (*Angew. Chem, Int. Ed.*, **2014**, *53*, 12876–12879 and *Chem. Commun.*, **2016**, *52*, 2497–2500). In both case, the reaction proceeds following a similar mechanism and relies on the capability of the NHC to activate the hydrosilane as well as the amine. Section 3.2 described the preparation of cyclic carbonates from diols rather than epoxides. This expands on the reaction detailed in Chapter 1 with an alternative substrate. Diols are usually less toxic than their corresponding epoxide and are easy to handle. Moreover, they can be derived from biomass, thus adding to the sustainability of the process. However, transforming the diol into a carbonate by using CO₂ requires the release of a water molecule, which makes the overall transformation difficult. In fact, the reverse reaction (the hydrolysis of the carbonate to afford diols and CO₂) is the industrial process to prepare ethylene glycol (Shell Omega Process). Our methodology relied on the utilization of dibromomethane and Cs₂CO₃ that both aided in the capture of the released water. Sections 3.3 and 3.4 dealt with the reduction of CO₂. Based on FLP catalysis, an ionic version of a common amine based used in FLP chemistry was synthesized and reacted with B(C₆F₅)₃. Upon heating, a stable adduct was formed, which was capable of reacting with CO₂ and H₂. In Section 3.4, we took advantage of our knowledge gained in Chapter 1 and on our work on TBAF/hydrosilanes for N-formylation to develop a simple, user-friendly methodology to indirectly reduce CO₂ to MeOH *via* the formation of a cyclic carbonate, in one-pot using a single catalytic system.

3.5.2. Future perspectives

The utilization of CO₂ allows for the formation of C-N, C-C and C-O bonds under very mild conditions (no pressure, r.t. to 100 °C), as was presented in the different sections of the thesis (Section 1.3 for review and Sections 3.1 to 3.4). CO₂ is thermodynamically stable and kinetically inert, but recent progress made on the utilization of CO₂ as a building block has demonstrated that reactions involving CO₂ do not necessarily require harsh conditions. We expect that further catalyst development could yield a valuable ionic FLP for CO₂ reduction (Section 3.3), since solubility of CO₂ in ILs is high and that functionalization on ILs is feasible. Moreover, the activation *via* FLP represents an attractive metal-free strategy to activate molecular

hydrogen. Further, the cooperativity between the fluoride salt TBAF and hydrosilanes that was employed in Section 3.4 has previously been employed in different types of reductions such as amide or nitrile reduction to amines. The new insights gained on the system by our study could potentially lead to novel utilizations of the remarkable cooperation between TBAF and simple, cheap hydrosilanes including the waste silane PMHS.

4. Thesis conclusions

4.1. Summary

Throughout this thesis, we have demonstrated how catalysis can enable the utilization of CO₂ as a reactive synthon. We have shown that the use of CO₂ in combination with a suitable reactive substrate and a catalyst can lead to a variety of new C-N, C-C or C-O bonds. We have studied in detail the mechanism of the cycloaddition of CO₂ into epoxides to generate cyclic carbonates and prepared active polymer catalysts for the reaction. These studies (Chapter 2) led to the development of a catalytic CO₂ extractor from waste gas streams under continuous conditions. We also studied the utilization of diols as starting material for the reaction (instead of epoxides), which led to the development of an entirely different strategy because of release of water during the reaction. We have contributed to the development of catalysis for the N-methylation and N-formylation of amines using CO₂ as the C1 source and hydrosilanes as the reducing agent by demonstrating that NHC and thiazolium carbenes are potent catalysts for the reaction. Our knowledge of ILs and the existing literature has led us to develop an IL able to form adducts with the Lewis acid B(C₆F₅)₃ and that could react with H₂ and CO₂. Finally, due to the importance of CO₂ reduction to fuels, we have developed a methodology relying on the cooperativity of a fluoride salt and hydrosilanes to catalytically reduce cyclic carbonates to methanol and diols, which are two valuable building blocks. The reduction of cyclic carbonates represents an indirect reduction of CO₂ *via* cyclic carbonates that act as a relay molecule.

For the CCE reaction, three generations of imidazolium polymers were synthesized and used as catalysts for the cycloaddition of CO₂ into epoxides. The inspiration for the linear ionic (polystyrenes) presented in section 2.3 combined our previous work on the subject⁹¹ and the importance of functional groups, as described by other groups and summarized in the introduction on the topic (Section 2.1).⁸⁷ During the course of the investigation, the slight solubility in EtOH and DMSO led us to develop ionic polymers that were the result of the polymerization of bis(imidazolium) monomers, ultimately leading to cross-linked, functionalized polymers that were completely insoluble. This second generation of catalysts efficiently catalyzed the CCE reaction even under atmospheric pressure and was easily extracted and recycled. Both these generations of polymers were based on a styrene functional group, and would be acceptable candidates for membrane preparation for gas separation processes.³¹⁵ It is envisioned that these materials will find widespread applications in these areas, both in pure form, or co-polymerized with other monomers such as divinylbenzene. Finally, inspired by polymers prepared by simple condensation reactions (for example Nylon), we developed highly cross-linked networks of imidazolium salts, that were

robust catalysts for the CCE reaction. These polymers have the advantage of being prepared in one-step from commercial reagents, but did not encompass a polar functional group. Nonetheless, these materials were active at 1 bar reaction pressure and exhibited excellent stability, since they were reused 10 times without a noticeable loss in activity.³⁰⁵

The ability of NHC carbenes to activate both hydrosilanes (reducing agents) and CO₂ resulted in the development of two methodologies, one that was based on an imidazolium-based carbene that led to methylation of primary and secondary amines chemoselectively,²³² and one that was used for the formylation of primary and secondary amines using a bio-inspired thiazolium carbene.²³³ Interestingly, methylating amines using standard routes, for example through the use of methyl iodide, often results in selectivity issues as well as safety concerns. Therefore, it is hoped that these simple methodologies can be adopted in synthetic labs requiring to methylate or formylate amines, without requiring the utilization of methyl iodide. Based upon these results, a protocol was published providing detailed explanations on the methodology. Finally, the affinity of TBAF as activating agent for hydrosilanes has been taken advantage of to formylate amines using CO₂ as the C1 source, and more details will be provided in a future thesis by **Martin Hulla**.⁹⁸ The cooperativity of the TBAF-hydrosilane mixture has led us to discover that cyclic carbonates can be reduced to methanol and diols under solvent-free conditions, thus allowing to formally reduce CO₂ into MeOH while simultaneously forming a diol product, which is itself of added value.

Diols are in general less toxic than epoxides and can be derived from biomass wastes. These compounds would serve as good substrates in combination with CO₂ to form an alternative production possibility for cyclic carbonates. Unfortunately, the reaction is hindered by the release of water, which must be captured by additives (here CH₂Br₂) in order to achieve high yields.³¹⁶ Hopefully, the insights gained during our studies will lead to the development of more efficient catalytic systems in the future.

4.2. Outlook

The properties of CO₂ and its availability make it an ideal C1 candidate for lab scale and industrial scale applications, in pure or diluted form.

We have shown throughout the thesis that CO₂ can conveniently be used in an array of reactions including N-Methylation and N-formylation of amines, which simultaneously eliminates the need to employ harmful and toxic chemicals in comparison to the established methods. Further catalyst research will likely result in the development of CO₂-based chemical reactions that will lead to more sustainable synthetic methodologies. Recent examples in literature have shown that it is possible to functionalize inert alkyl C-H bonds under specific catalytic conditions, and this highlights that the synthetic possibilities of CO₂ are vast.

The ionic polymers that we have prepared can find applications that are not limited to catalysis. For example, we expect the polymers that were presented in Chapter 2 of the thesis to be ideal candidates for membranes that can serve for purification of gas streams (for example biogas). Our results have demonstrated that a simple catalyst-epoxide mixture can be used as a CO₂-scavenger, meaning that the reaction can be implemented at industrial plants producing CO₂ (power plants, biogas upgrading plants, etc). Therefore, the production of cyclic carbonates (precursors of bio-based polyurethanes, produced on MTons scale annually) can presumably become a valuable post-combustion technology, *i.e.* it can be a profitable way to purify CO₂-containing gas streams. Our results showed that a shift in paradigm is possible, where chemical processes are directly performed at the exhaust pipe of a CO₂-releasing industry, rather than being performed in an independent chemical plant.

4.3. References

- 1 X. B. Lu, *Carbon Dioxide and Organometallics*, Springer, 2015.
- 2 S. A. Zimov, E. A. G. Schuur and F. S. Chapin III, *Science*, 2006, **312**, 1612–1613.
- 3 P. Falkowski, R. J. Scholes, E. Boyle, J. Canadell, D. Canfield, J. Elser, N. Gruber, K. Hibbard, P. Högberg, S. Linder, F. T. Mackenzie, B. Moore III, T. Pedersen, Y. Rosenthal, S. Seitzinger, V. Smetacek, W. Steffen, *Science*, 2000, **290**, 291-296.
- 4 R. Monastersky, *Nature*, 2013, **497**, 13–14.
- 5 K. M. K. Yu, I. Curcic, J. Gabriel and S. C. E. Tsang, *ChemSusChem*, 2008, **1**, 893–899.
- 6 C. P. Kelley, S. Mohtadi, M. A. Cane, R. Seager and Y. Kushnir, *Proc. Natl. Acad. Sci.*, 2015, **112**, 3241–3246.
- 7 IPCC, in *Climate Change 2013 - The Physical Science Basis*, ed. Intergovernmental Panel on Climate Change, Cambridge University Press, Cambridge, 2014, pp. 1–30.
- 8 C. F. Schleussner, T. K. Lissner, E. M. Fischer, J. Wohland, M. Perrette, A. Golly, J. Rogelj, K. Childers, J. Schewe, K. Frieler, M. Mengel, W. Hare and M. Schaeffer, *Earth Syst. Dyn.*, 2016, **7**, 327–351.
- 9 C. McGlade and P. Ekins, *Nature*, 2015, **517**, 187–190.
- 10 H. Lv, Q. Xing, C. Yue, Z. Lei and F. Li, *Chem. Commun.*, 2016, **52**, 6545–6548.
- 11 Q. Liu, L. Wu, R. Jackstell and M. Beller, *Nat. Commun.*, 2015, **6**, 5933.
- 12 N. R. Stuckert and R. T. Yang, *Environ. Sci. Technol.*, 2011, **45**, 10257–10264.
- 13 B. Smit, A.-H. A. Park and G. Gadikota, *Front. Energy Res.*, 2014, **2**, 2013–2015.
- 14 J. Qiao, Y. Liu, F. Hong and J. Zhang, *Chem. Soc. Rev.*, 2014, **43**, 631–675.
- 15 E. Balaraman, C. Gunanathan, J. Zhang, L. J. W. Shimon and D. Milstein, *Nat. Chem.*, 2011, **3**, 609–614.
- 16 S. Das, F. D. Bobbink, A. Gopakumar and P. J. Dyson, *Chimia.*, 2015, **69**, 765–768.
- 17 P. G. Jessop, T. Ikariya and R. Noyori, *Chem. Rev.*, 1995, **95**, 259–272.
- 18 S. G. Jadhav, P. D. Vaidya, B. M. Bhanage and J. B. Joshi, *Chem. Eng. Res. Des.*, 2014, **92**, 2557–2567.
- 19 S. Saeidi, N. A. S. Amin and M. R. Rahimpour, *J. CO2 Util.*, 2014, **5**, 66–81.
- 20 X. Su, J. Xu, B. Liang, H. Duan, B. Hou and Y. Huang, *J. Energy Chem.*, 2016, **25**, 553–565.
- 21 T. Abe, M. Tanizawa, K. Watanabe and A. Taguchi, *Energy Environ. Sci.*, 2009, **2**, 315-321.
- 22 C. Swalus, M. Jacquemin, C. Poleunis, P. Bertrand and P. Ruiz, *Appl. Catal. B Environ.*, 2012, **125**, 41–50.

- 23 W. Wang and J. Gong, *Front. Chem. Eng. China*, 2011, **5**, 2–10.
- 24 W. Wang, S. Wang, X. Ma and J. Gong, *Chem. Soc. Rev.*, 2011, **40**, 3703–3727.
- 25 P. Frontera, A. Macario, M. Ferraro and P. Antonucci, *Catalysts*, 2017, **7**, 59.
- 26 S. T. Omaye, *Toxicology*, 2002, **180**, 139–150.
- 27 J. H. Jones, *Platin. Met. Rev.*, 2000, **44**, 94–105.
- 28 M. E. Dry, *Catal. Today*, 2002, **71**, 227–241.
- 29 O. Sørheim, H. Nissen and T. Nesbakken, *Meat Sci.*, 1999, **52**, 157–164.
- 30 W. J. Evans, M. J. Lipp, C. S. Yoo, H. Cynn, J. L. Herberg, R. S. Maxwell and M. F. Nicol, *Chem. Mater.*, 2006, **18**, 2520–2531.
- 31 Y. Liu and D. Liu, *Int. J. Hydrogen Energy*, 1999, **24**, 351–354.
- 32 G. P. S. Lau, M. Schreier, D. Vasilyev, R. Scopelliti, M. Grätzel and P. J. Dyson, *J. Am. Chem. Soc.*, 2016, **138**, 7820–7823.
- 33 B. A. Rosen, A. Salehi-khojin, M. R. Thorson, W. Zhu, D. T. Whipple, P. J. A. Kenis and R. I. Masel, *Science*, 2011, **334**, 643–645.
- 34 J. Medina-Ramos, R. C. Pupillo, T. P. Keane, J. L. Dimeglio and J. Rosenthal, *J. Am. Chem. Soc.*, 2015, **137**, 5021–5027.
- 35 J. L. Dimeglio and J. Rosenthal, *J. Am. Chem. Soc.*, 2013, **135**, 8798–8801.
- 36 H. A. Hansen, J. B. Varley, A. A. Peterson and J. K. Nørskov, *J. Phys. Chem. Lett.*, 2013, **4**, 388–392.
- 37 L. C. Grabow and M. Mavrikakis, *ACS Catal.*, 2011, **1**, 365–384.
- 38 F. Studt, I. Sharafutdinov, F. Abild-Pedersen, C. F. Elkjær, J. S. Hummelshøj, S. Dahl, I. Chorkendorff and J. K. Nørskov, *Nat. Chem.*, 2014, **6**, 320–324.
- 39 W. Cai, P. R. de la Piscina, J. Toyir and N. Homs, *Catal. Today*, 2015, **242**, 193–199.
- 40 C. A. Huff and M. S. Sanford, *J. Am. Chem. Soc.*, 2011, **133**, 18122–18125.
- 41 K. Sordakis, C. Tang, L. K. Vogt, H. Junge, P. J. Dyson, M. Beller and G. Laurency, *Chem. Rev.*, 2018, **118**, 372–433.
- 42 M. Grasemann and G. Laurency, *Energy Environ. Sci.*, 2012, **5**, 8171.
- 43 M. Montandon-Clerc, A. F. Dalebrook and G. Laurency, *J. Catal.*, 2016, **343**, 62–67.
- 44 S. Moret, P. J. Dyson and G. Laurency, *Nat. Commun.*, 2014, **5**, 4017.
- 45 R. Tanaka, M. Yamashita and K. Nozaki, *J. Am. Chem. Soc.*, 2009, **131**, 14168–14169.
- 46 Y. Song, R. Peng, D. K. Hensley, P. V. Bonnesen, L. Liang, Z. Wu, H. M. Meyer, M. Chi, C. Ma, B. G. Sumpter and A. J. Rondinone, *ChemistrySelect*, 2016, **1**, 6055–6061.
- 47 L. González-Sebastián, M. Flores-Alamo and J. J. García, *Organometallics*, 2015, **34**, 763–769.

- 48 Y. Li, I. Sorribes, T. Yan, K. Junge and M. Beller, *Angew. Chemie - Int. Ed.*, 2013, **52**, 12156–12160.
- 49 A. Tlili, E. Blondiaux, X. Frogneux and T. Cantat, *Green Chem.*, 2015, **17**, 157–168.
- 50 O. Jacquet, C. Das Neves Gomes, M. Ephritikhine and T. Cantat, *J. Am. Chem. Soc.*, 2012, **134**, 2934–2937.
- 51 E. Blondiaux, J. Pouessel and T. Cantat, *Angew. Chemie - Int. Ed.*, 2014, **53**, 12186–12190.
- 52 Y. Li, X. Cui, K. Dong, K. Junge and M. Beller, *ACS Catal.*, 2017, **7**, 1077–1086.
- 53 M. Honda, M. Tamura, K. Nakao, K. Suzuki, Y. Nakagawa and K. Tomishige, *ACS Catal.*, 2014, **4**, 1893–1896.
- 54 M. Tamura, M. Honda, Y. Nakagawa and K. Tomishige, *J. Chem. Technol. Biotechnol.*, 2014, **89**, 19–33.
- 55 T. Kitamura, Y. Inoue, T. Maeda and J. Oyamada, *Synth. Commun.*, 2016, **46**, 39–45.
- 56 G. L. Gregory, M. Ulmann and A. Buchard, *RSC Adv.*, 2015, **5**, 39404–39408.
- 57 J. Rintjema and A. W. Kleij, *ChemSusChem*, 2017, **10**, 1274–1282.
- 58 J. Y. Jeon, J. J. Lee, J. K. Varghese, S. J. Na, S. Sujith, M. J. Go, J. Lee, M.-A. Ok and B. Y. Lee, *Dalton Trans.*, 2013, **42**, 9245–9254.
- 59 D. Yu, M. X. Tan and Y. Zhang, *Adv. Synth. Catal.*, 2012, **354**, 969–974.
- 60 Y. Dingyi and Z. Yugen, *Green Chem.*, 2011, **13**, 1275–1279.
- 61 Y. P. Patil, P. J. Tambade, S. R. Jagtap and B. M. Bhanage, *Green Chem. Lett. Rev.*, 2008, **1**, 127–132.
- 62 Y. Zhao, B. Yu, Z. Yang, H. Zhang, L. Hao, X. Gao and Z. Liu, *Angew. Chemie*, 2014, **126**, 6032–6035.
- 63 C. Wu, H. Cheng, R. Liu, Q. Wang, Y. Hao, Y. Yu and F. Zhao, *Green Chem.*, 2010, **12**, 1811–1816.
- 64 J. S. Wilkes, *Green Chem.*, 2002, **4**, 73–80.
- 65 N. V. Plechkova and K. R. Seddon, *Chem. Soc. Rev.*, 2008, **37**, 123–150.
- 66 T. Welton, *Coord. Chem. Rev.*, 2004, **248**, 2459–2477.
- 67 K. N. Marsh, A. Deev, A. C.-T. Wu, E. Tran and A. Klamt, *Korean J. Chem. Eng.*, 2002, **19**, 357–362.
- 68 Z. Fei and P. J. Dyson, *Chem. Commun.*, 2013, **49**, 2594–2596.
- 69 H. Olivier-Bourbigou, L. Magna and D. Morvan, *Appl. Catal. A Gen.*, 2010, **373**, 1–56.
- 70 R. D. Rogers, *Science*, 2003, **302**, 792–793.
- 71 J. P. Hallett and T. Welton, *Chem. Rev.*, 2011, **111**, 3508–3576.
- 72 Z. Fei, D. Kuang, D. Zhao, C. Klein and H. Ang, *Inorg. Chem.*, 2006, **45**, 10407–10409.
- 73 Z. S. Qureshi, K. M. Deshmukh and B. M. Bhanage, *Clean Technol. Environ. Policy*, 2014, **16**, 1487–1513.

- 74 P. Nancarrow and H. Mohammed, *ChemBioEng Rev.*, 2017, **4**, 106–119.
- 75 C. Ye, W. Liu, Y. Chen and L. Yu, *Chem. Commun.*, 2001, 2244–2245.
- 76 A. Taheri, B. Lai, C. Cheng and Y. Gu, *Green Chem.*, 2015, **17**, 812–816.
- 77 A. Taheri, X. Pan, C. Liu and Y. Gu, *ChemSusChem*, 2014, **7**, 2094–2098.
- 78 S. Bulut, Z. Fei, S. Siankevich, J. Zhang, N. Yan and P. J. Dyson, *Catal. Today*, 2015, **247**, 96–103.
- 79 J. Yuan, D. Mecerreyes and M. Antonietti, *Prog. Polym. Sci.*, 2013, **38**, 1009–1036.
- 80 J. Yuan and M. Antonietti, *Polymer.*, 2011, **52**, 1469–1482.
- 81 T. Sakai, Y. Tsutsumi and T. Ema, *Green Chem.*, 2008, **10**, 337–341.
- 82 W.-L. Dai, L. Chen, S.-F. Yin, W.-H. Li, Y.-Y. Zhang, S.-L. Luo and C.-T. Au, *Catal. Letters*, 2010, **137**, 74–80.
- 83 R. A. Watile, K. M. Deshmukh, K. P. Dhake and B. M. Bhanage, *Catal. Sci. Technol.*, 2012, **2**, 1051–1055.
- 84 H. Hagiwara, Y. Sugawara, K. Isobe, T. Hoshi and T. Suzuki, *Org. Lett.*, 2004, **6**, 2325–2328.
- 85 Y. Du, J. Q. Wang, J. Y. Chen, F. Cai, J. S. Tian, D. L. Kong and L. N. He, *Tetrahedron Lett.*, 2006, **47**, 1271–1275.
- 86 X. Zheng, S. Luo, L. Zhang and J.-P. Cheng, *Green Chem.*, 2009, **11**, 455–458.
- 87 F. D. Bobbink and P. J. Dyson, *J. Catal.*, 2016, **343**, 52–61.
- 88 Q. Ye, T. Gao, F. Wan, B. Yu, X. Pei, F. Zhou and Q. Xue, *J. Mater. Chem.*, 2012, **22**, 13123–13131.
- 89 B. Xin and J. Hao, *Chem. Soc. Rev.*, 2014, **43**, 7171–7187.
- 90 S. Siankevich, Z. Fei, R. Scopelliti, G. Laurenczy, S. Katsyuba, N. Yan and P. J. Dyson, *ChemSusChem*, 2014, **7**, 1647–1654.
- 91 S. Ghazali-Esfahani, H. Song, E. Păunescu, F. D. Bobbink, H. Liu, Z. Fei, G. Laurenczy, M. Bagherzadeh, N. Yan and P. J. Dyson, *Green Chem.*, 2013, **15**, 1584–1589.
- 92 L. Hao, Y. Zhao, B. Yu, Z. Yang, H. Zhang, B. Han, X. Gao and Z. Liu, *ACS Catal.*, 2015, **5** (9), 4989–4993.
- 93 J. Peng and Y. Deng, *New J. Chem.*, 2001, **25**, 639–641.
- 94 F. D. Bobbink, A. P. Van Muyden, A. Gopakumar, Z. Fei and P. J. Dyson, *ChemPlusChem.*, 2017, **82**, 144–151.
- 95 Z. Guo, X. Cai, J. Xie, X. Wang, Y. Zhou and J. Wang, *ACS Appl. Mater. Interfaces*, 2016, **8**, 12812–12821.
- 96 A. Tlili, X. Frogneux, E. Blondiaux and T. Cantat, *Angew. Chemie - Int. Ed.*, 2014, **53**, 2543–2545.
- 97 J. Klankermayer, S. Wesselbaum, K. Beydoun and W. Leitner, *Angew. Chemie - Int. Ed.*, 2016, **55**,

- 2–50.
- 98 M. Hulla, F. D. Bobbink, S. Das and P. J. Dyson, *ChemCatChem*, 2016, **8**, 3338–3342.
- 99 M. a. Pacheco and C. L. Marshall, *Energy & Fuels*, 1997, **11**, 2–29.
- 100 B. Schöffner, S. P. Verevkin and A. Börner, *Chemie Unserer Zeit*, 2009, **43**, 12–21.
- 101 N. Ribeiro, A. C. Pinto, C. M. Quintella, G. O. da Rocha, L. S. G. Teixeira, L. L. N. Guarieiro, M. D. C. Rangel, M. C. C. Veloso, M. J. C. Rezende, R. S. da Cruz, A. M. de Oliveira, E. A. Torres and J. B. de Andrade, *Energy and Fuels*, 2007, **21**, 2433–2445.
- 102 H. E. T. Ulhoff and H. C. S. Berlin, *Ullmann's Encycl. Ind. Chem. Vol.6*, 2012, 565–582.
- 103 B. Schöffner, F. Schöffner, S. P. Verevkin and A. Börner, *Chem. Rev.*, 2010, **110**, 4554–81.
- 104 T. Yamada and H. Ono, *Bioresour. Technol.*, 1999, **70**, 61–67.
- 105 J. H. Clements, *Ind. Eng. Chem. Res.*, 2003, **42**, 663–674.
- 106 K. Xu, *Chem. Rev.*, 2004, **104**, 4303–4418.
- 107 M. North, P. Villuendas and C. Young, *Chem. Eur. J.*, 2009, **15**, 11454–11457.
- 108 M. O. Sonnati, S. Amigoni, E. P. Taffin de Givenchy, T. Darmanin, O. Choulet and F. Guittard, *Green Chem.*, 2013, **15**, 283–306.
- 109 A. E. Díaz-Álvarez, J. Francos, B. Lastra-Barreira, P. Crochet and V. Cadierno, *Chem. Commun.*, 2011, **47**, 6208–6227.
- 110 F. Manjolinho, M. Arndt, K. Gooßen and L. J. Gooßen, *ACS Catal.*, 2012, **2**, 2014–2021.
- 111 J. Britz, W. H. Meyer and G. Wegner, *Macromolecules*, 2007, **40**, 7558–7565.
- 112 M. R. Kember and C. K. Williams, *J. Am. Chem. Soc.*, 2012, **134**, 15676–15679.
- 113 M. Tóth, J. Kiss, a. Oszkó, G. Pótári, B. László and a. Erdőhelyi, *Top. Catal.*, 2012, **55**, 747–756.
- 114 F. Suriano, O. Coulembier, J. L. Hedrick and P. Dubois, *Polym. Chem.*, 2011, **2**, 528–533.
- 115 J. Sun, J. Ren, S. Zhang and W. Cheng, *Tetrahedron Lett.*, 2009, **50**, 423–426.
- 116 J. Sun, S. Zhang, W. Cheng and J. Ren, *Tetrahedron Lett.*, 2008, **49**, 3588–3591.
- 117 N. Kihara, N. Hara and T. Endo, *J. Org. Chem.*, 1993, **58**, 6198–6202.
- 118 M. H. Anthofer, M. E. Wilhelm, M. Cokoja, I. I. E. Markovits, A. Pöthig, J. Mink, W. A. Herrmann and F. E. Kühn, *Catal. Sci. Technol.*, 2014, **4**, 1749–1758.
- 119 A. Girard, N. Simon, M. Zanatta, S. Marmitt, P. Gonçalves and J. Dupont, *Green Chem.*, 2014, **16**, 2815–2825.
- 120 H. Sun and D. Zhang, *J. Phys. Chem. A*, 2007, **111**, 8036–8043.
- 121 J.-Q. Wang, K. Dong, W.-G. Cheng, J. Sun and S.-J. Zhang, *Catal. Sci. Technol.*, 2012, **2**, 1480–1484.
- 122 H. Kawanami, A. Sasaki, K. Matsui and Y. Ikushima, *Chem. Commun.*, 2003, 896–897.

- 123 V. Caló, A. Nacci, A. Monopoli and A. Fanizzi, *Org. Lett.*, 2002, **4**, 2561–2563.
- 124 W. L. Wong, P. H. Chan, Z. Y. Zhou, K. H. Lee, K. C. Cheung and K. Y. Wong, *ChemSusChem*, 2008, **1**, 67–70.
- 125 J. Hu, J. Ma, Q. Zhu, Z. Zhang, C. Wu and B. Han, *Angew. Chemie - Int. Ed.*, 2015, **54**, 5399–5403.
- 126 K. R. Seddon, *J. Chem. Technol. Biotechnol.*, 1997, **68**, 351–356.
- 127 H. L. Ngo, K. LeCompte, L. Hargens and A. B. McEwen, *Thermochim. Acta*, 2000, **357–358**, 97–102.
- 128 S. Wellens, B. Thijs and K. Binnemans, *Green Chem.*, 2013, **15**, 3484–3485.
- 129 E. Liwarska-Bizukojc, C. Maton, C. V. Stevens and D. Gendaszewska, *J. Chem. Technol. Biotechnol.*, 2014, **89**, 763–768.
- 130 A. Romero, A. Santos, J. Tojo and A. Rodríguez, *J. Hazard. Mater.*, 2008, **151**, 268–273.
- 131 A. Stark, P. Behrend, O. Braun, A. Müller, J. Ranke, B. Ondruschka and B. Jastorff, *Green Chem.*, 2008, **10**, 1152–1161.
- 132 K. McCamley, N. A. Warner, M. M. Lamoureux, P. J. Scammells and R. D. Singer, *Green Chem.*, 2004, **6**, 341–344.
- 133 Cooper, J F Myri, L, US2773070A, US patent, 1956.
- 134 J.-Q. Wang, D.-L. Kong, J.-Y. Chen, F. Cai and L.-N. He, *J. Mol. Catal. A Chem.*, 2006, **249**, 143–148.
- 135 W. Cheng, B. Xiao, J. Sun, K. Dong, P. Zhang, S. Zhang and F. T. T. Ng, *Tetrahedron Lett.*, 2015, **56**, 1416–1419.
- 136 Y. Zhao, C. Yao, G. Chen and Q. Yuan, *Green Chem.*, 2013, **15**, 446–452.
- 137 Y. Y. Zhang, L. Chen, S. F. Yin, S. L. Luo and C. T. Au, *Catal. Letters*, 2012, **142**, 1376–1381.
- 138 S. Baj, T. Krawczyk, K. Jasiak, A. Siewniak and M. Pawlyta, *Appl. Catal. A Gen.*, 2014, **488**, 96–102.
- 139 S. A. Katsyuba, M. V. Vener, E. E. Zvereva, Z. Fei, R. Scopelliti, G. Laurenczy, N. Yan, E. Paunescu and P. J. Dyson, *J. Phys. Chem. B*, 2013, **117**, 9094–9105.
- 140 L. Benhamou, E. Chardon, G. Lavigne, S. Bellemin-Laponnaz and V. César, *Chem. Rev.*, 2011, **111**, 2705–2733.
- 141 D. Mecerreyes, *Prog. Polym. Sci.*, 2011, **36**, 1629–1648.
- 142 J. E. Bara, *Ind. Eng. Chem. Res.*, 2011, **50**, 13614–13619.
- 143 J. C. Schleicher and A. M. Scurto, *Green Chem.*, 2009, **11**, 694–703.
- 144 K. R. Harris, L. A. Woolf and M. Kanakubo, *J. Chem. Eng. Data*, 2005, **50**, 1777–1782.
- 145 C. C. Cassol, G. Ebeling, B. Ferrera and J. Dupont, *Adv. Synth. Catal.*, 2006, **348**, 243–248.
- 146 J.-Q. Wang, W.-G. Cheng, J. Sun, T.-Y. Shi, X.-P. Zhang and S.-J. Zhang, *RSC Adv.*, 2014, **4**, 2360–2367.

- 147 J. Sun, L. Han, W. Cheng, J. Wang, X. Zhang and S. Zhang, *ChemSusChem*, 2011, **4**, 502–507.
- 148 L.-F. Xiao, D.-W. Lv, D. Su, W. Wu and H.-F. Li, *J. Clean. Prod.*, 2014, **67**, 285–290.
- 149 M. Liu, K. Gao, L. Liang, F. Wang, L. Shi, L. Sheng and J. Sun, *Phys. Chem. Chem. Phys.*, 2015, **17**, 5959–5965.
- 150 T. Chang, X. Gao, L. Bian, X. Fu, M. Yuan and H. Jing, *Chinese J. Catal.*, 2015, **36**, 408–413.
- 151 M. H. Anthofer, M. E. Wilhelm, M. Cokoja, M. Drees, W. A. Herrmann and F. E. Kühn, *ChemCatChem*, 2015, **7**, 94–98.
- 152 E. H. Lee, J. Y. Ahn, M. M. Dharman, D. W. Park, S. W. Park and I. Kim, *Catal. Today*, 2008, **131**, 130–134.
- 153 C. Yue, D. Su, X. Zhang, W. Wu and L. Xiao, *Catal. Letters*, 2014, **144**, 1313–1321.
- 154 L. Xiao, D. Su, C. Yue and W. Wu, *J. CO₂ Util.*, 2014, **6**, 1–6.
- 155 T.-Y. Shi, J.-Q. Wang, J. Sun, M.-H. Wang, W.-G. Cheng and S.-J. Zhang, *RSC Adv.*, 2013, **3**, 3726–3732.
- 156 Y. Xie, Z. Zhang, T. Jiang, J. He, B. Han, T. Wu and K. Ding, *Angew. Chemie - Int. Ed.*, 2007, **46**, 7255–7258.
- 157 J. Sun, J. Wang, W. Cheng, J. Zhang, X. Li, S. Zhang and Y. She, *Green Chem.*, 2012, **14**, 654–660.
- 158 K. R. Roshan, G. Mathai, J. Kim, J. Tharun, G.-A. Park and D.-W. Park, *Green Chem.*, 2012, **14**, 2933–2940.
- 159 M. N. Ravi Kumar, *React. Funct. Polym.*, 2000, **46**, 1–27.
- 160 L. Han, H. J. Choi, D. K. Kim, S. W. Park, B. Liu and D. W. Park, *J. Mol. Catal. A Chem.*, 2011, **338**, 58–64.
- 161 B. Zhang, L. Zhang, Q. Wu, Q. Wang, B. Song, W. Wu, B. Lu and T. Ren, *RSC Adv.*, 2014, **4**, 20506–20515.
- 162 L. Han, S.-W. Park and D.-W. Park, *Energy Environ. Sci.*, 2009, **2**, 1286–1292.
- 163 S. Udayakumar, V. Raman, H. L. Shim and D. W. Park, *Appl. Catal. A Gen.*, 2009, **368**, 97–104.
- 164 W. L. Dai, L. Chen, S. F. Yin, S. L. Luo and C. T. Au, *Catal. Letters*, 2010, **135**, 295–304.
- 165 D. Wei-Li, J. Bi, L. Sheng-Lian, L. Xu-Biao, T. Xin-Man and A. Chak-Tong, *Catal. Sci. Technol.*, 2014, **4**, 556–562.
- 166 Z.-Z. Yang, L.-N. He, C.-X. Miao and S. Chanfreau, *Adv. Synth. Catal.*, 2010, **352**, 2233–2240.
- 167 Y. Li, L. Wang, T. Huang, J. Zhang and H. He, *Ind. Eng. Chem. Res.*, 2015, **54**, 8093–8099.
- 168 W. Cheng, X. Chen, J. Sun, J. Wang and S. Zhang, *Catal. Today*, 2013, **200**, 117–124.
- 169 A. Zhu, T. Jiang, B. Han, J. Zhang, Y. Xie and X. Ma, *Green Chem.*, 2007, **9**, 169–172.

- 170 A. P. Abbott, D. Boothby, G. Capper, D. L. Davies and R. K. Rasheed, *J. Am. Chem. Soc.*, 2004, **126**, 9142–9147.
- 171 K. R. Roshan, T. Jose, D. Kim, K. A. Cherian and D. W. Park, *Catal. Sci. Technol.*, 2014, **4**, 963–970.
- 172 D. Wei-Li, J. Bi, L. Sheng-Lian, L. Xu-Biao, T. Xin-Man and A. Chak-Tong, *J. Mol. Catal. A Chem.*, 2013, **378**, 326–332.
- 173 D. Wei-Li, J. Bi, L. Sheng-Lian, L. Xu-Biao, T. Xin-Man and A. Chak-Tong, *Appl. Catal. A Gen.*, 2014, **470**, 183–188.
- 174 T. Werner and H. Büttner, *ChemSusChem*, 2014, **7**, 3268–3271.
- 175 H. Büttner, J. Steinbauer and T. Werner, *ChemSusChem*, 2015, **8**, 2655–2669.
- 176 M. Galvan, M. Selva, A. Perosa and M. Noè, *Asian J. Org. Chem.*, 2014, **3**, 504–513.
- 177 Y. Xiong, F. Bai, Z. Cui, N. Guo and R. Wang, *J. Chem.*, 2013, **2013**, 1–9.
- 178 D. Wei-Li, J. Bi, L. Sheng-Lian, L. Xu-Biao, T. Xin-Man and A. Chak-Tong, *Catal. Today*, 2014, **233**, 92–99.
- 179 S. Marmitt and P. F. B. Gonçalves, *J. Comput. Chem.*, 2015, **36**, 1322–1333.
- 180 S. A. Katsyuba, M. V. Vener, E. E. Zvereva, Z. Fei, R. Scopelliti, J. G. Brandenburg, S. Siankevich and P. J. Dyson, *J. Phys. Chem. Lett.*, 2015, **6**, 4431–4436.
- 181 Y. V. Nelyubina, A. A. Korlyukov and K. A. Lyssenko, *RSC Adv.*, 2015, **5**, 75360–75373.
- 182 Q. He, J. W. O'Brien, K. a. Kitselman, L. E. Tompkins, G. C. T. Curtis and F. M. Kerton, *Catal. Sci. Technol.*, 2014, **4**, 1513–1528.
- 183 M. E. Wilhelm, M. H. Anthofer, R. M. Reich, V. D'Elia, J.-M. Basset, W. A. Herrmann, M. Cokoja and F. E. Kühn, *Catal. Sci. Technol.*, 2014, **4**, 1638–1643.
- 184 P. L. Arnold and S. Pearson, *Coord. Chem. Rev.*, 2007, **251**, 596–609.
- 185 J.-Q. Wang, J. Sun, W.-G. Cheng, K. Dong, X.-P. Zhang and S.-J. Zhang, *Phys. Chem. Chem. Phys.*, 2012, **14**, 11021–11026.
- 186 S. Gennen, M. Alves, R. Méreau, T. Tassaing, B. Gilbert, C. Detrembleur, C. Jerome and B. Grignard, *ChemSusChem*, 2015, **8**, 1845–1849.
- 187 Z. Luo, B. Wang, Y. Liu, G. Gao and F. Xia, *Phys. Chem. Chem. Phys.*, 2016, **18**, 27951–27957.
- 188 C. Daguenet and P. J. Dyson, *Organometallics*, 2004, **23**, 6080–6083.
- 189 Y. A. Rulev, Z. T. Gugkaeva, A. V. Lokutova, V. I. Maleev, A. S. Peregudov, X. Wu, M. North and Y. N. Belokon, *ChemSusChem*, 2017, **10**, 1152–1159.
- 190 F. D. Bobbink, S. Das and P. J. Dyson, *Nat. Protoc.*, 2017, **12**, 417–428.
- 191 F. Neese, *Wiley Interdiscip. Rev. Comput. Mol. Sci.*, 2012, **2**, 73–78.

- 192 A. D. Becke, *J. Chem. Phys.*, 1993, **98**, 5648-5652.
- 193 J. P. Perdew and Y. Wang, 1992, **45**, 244-249.
- 194 K. Fukui, *J. Phys. Chem.*, 1970, **74**, 4161-4163.
- 195 S. Grimme, *Wiley Interdiscip. Rev. Comput. Mol. Sci.*, 2011, **1**, 211-228.
- 196 S. Grimme, A. Hansen, J. G. Brandenburg and C. Bannwarth, *Chem. Rev.*, 2016, **116**, 5105-5154.
- 197 A. Schäfer, C. Huber and R. Ahlrichs, *J. Chem. Phys.*, 1994, **100**, 5829-5835.
- 198 F. Weigend and R. Ahlrichs, *Phys. Chem. Chem. Phys.*, 2005, **7**, 3297-3305.
- 199 M. D. Green, J.-H. Choi, K. I. Winey and T. E. Long, *Macromolecules*, 2012, **45**, 4749-4757.
- 200 L. Leclercq, M. Simard and A. R. Schmitzer, *J. Mol. Struct.*, 2009, **918**, 101-107.
- 201 J. Sun, W. Cheng, W. Fan, Y. Wang, Z. Meng and S. Zhang, *Catal. Today*, 2009, **148**, 361-367.
- 202 Z.-Z. Yang, Y. Zhao, G. Ji, H. Zhang, B. Yu, X. Gao and Z. Liu, *Green Chem.*, 2014, **16**, 3724-3728.
- 203 Z.-Z. Yang, Y.-N. Zhao and L.-N. He, *RSC Adv.*, 2011, **1**, 545-567.
- 204 A. J. M. Duisenberg, L. M. J. Kroon-Batenburg and A. M. M. Schreurs, *J. Appl. Crystallogr.*, 2003, **36**, 220-229.
- 205 R. H. Blessing, *Acta Crystallogr. Sect. A*, 1995, **51**, 33-38.
- 206 G. M. Sheldrick, *Acta Crystallogr. Sect. C*, 2015, **71**, 3-8.
- 207 H. Nakajima and H. Ohno, *Polymer.*, 2005, **46**, 11499-11504.
- 208 J. E. Bara, E. S. Hatakeyama, C. J. Gabriel, X. Zeng, S. Lessmann, D. L. Gin and R. D. Noble, *J. Memb. Sci.*, 2008, **316**, 186-191.
- 209 F. D. Bobbink, Z. Fei, R. Scopelliti, S. Das, P. J. Dyson and J. Paul, *Helv. Chim. Acta*, 2016, **99**, 821-829.
- 210 L. Han, S.-J. Choi, M.-S. Park, S.-M. Lee, Y.-J. Kim, M.-I. Kim, B. Liu and D.-W. Park, *React. Kinet. Mech. Catal.*, 2011, **106**, 25-35.
- 211 L. Han, H.-J. Choi, S.-J. Choi, B. Liu and D.-W. Park, *Green Chem.*, 2011, **13**, 1023-1028.
- 212 J. Wang, J. G. Wei Yang, G. Yi and Y. Zhang, *Chem. Commun.*, 2015, **51**, 15708-15711.
- 213 C. J. Whiteoak, A. H. Henseler, C. Ayats, A. W. Kleij and M. A. Pericàs, *Green Chem.*, 2014, **16**, 1552-1559.
- 214 C. J. Whiteoak, A. Nova, F. Maseras and A. W. Kleij, *ChemSusChem*, 2012, **5**, 2032-2038.
- 215 J. A. Castro-Osma, M. North, W. K. Offermans, W. Leitner and T. E. Müller, *ChemSusChem*, 2016, **9**, 791-794.
- 216 P. J. Dyson, J. S. McIndoe and D. Zhao, *Chem. Commun.*, 2003, **41**, 508-509.
- 217 Y. Jeon, J. Sung, C. Seo, H. Lim, H. Cheong, M. Kang, B. Moon, Y. Ouchi and D. Kim, *J. Phys. Chem.*

- B, 2008, **112**, 4735–4740.
- 218 A. S. Amarasekara, B. Callis and B. Wiredu, *Polym. Bull.*, 2012, **68**, 901–908.
- 219 S. Yuan, Q. Deng, G. Fang, M. Pan, X. Zhai and S. Wang, *J. Mater. Chem.*, 2012, **22**, 3965–3972.
- 220 X. Wang, Y. Zhou, Z. Guo, G. Chen, J. Li, Y. Shi, Y. Liu and J. Wang, *Chem. Sci.*, 2015, **6**, 6916–6924.
- 221 Y. Toda, Y. Komiyama, A. Kikuchi and H. Suga, *ACS Catal.*, 2016, **6**, 6906–6910.
- 222 P. Z. Li, X. J. Wang, J. Liu, J. S. Lim, R. Zou and Y. Zhao, *J. Am. Chem. Soc.*, 2016, **138**, 2142–2145.
- 223 J. Sun, S. I. Fujita, F. Zhao and M. Arai, *Appl. Catal. A Gen.*, 2005, **287**, 221–226.
- 224 D. J. Darensbourg and S. J. Wilson, *Green Chem.*, 2012, **14**, 2665–2671.
- 225 M. Yoshida, T. Mizuguchi and K. Shishido, *Chem. A Eur. J.*, 2012, **18**, 15578–15581.
- 226 P. Izák, F. D. Bobbink, M. Hulla, M. Klepic, K. Friess, Š. Hovorka and P. J. Dyson, *ChemPlusChem.*, 2018, **83**, 7–18.
- 227 J. E. Bara, S. Lessmann, C. J. Gabriel, E. S. Hatakeyama, R. D. Noble and D. L. Gin, *Ind. Eng. Chem. Res.*, 2007, **46**, 5397–5404.
- 228 Y. Zhang, Z. Fei, P. Gao, Y. Lee, F. F. Tirani, R. Scopelliti, Y. Feng, P. J. Dyson and M. K. Nazeeruddin, *Adv. Mater.*, 2017, **29**, 1702157.
- 229 L.-Y. Chang, C.-P. Lee, C.-T. Li, M.-H. Yeh, K.-C. Ho and J.-J. Lin, *J. Mater. Chem. A*, 2014, **2**, 20814–20822.
- 230 Z. Geng and M. G. Finn, *J. Am. Chem. Soc.*, 2017, **139**, 15401–15406.
- 231 M. K. Oulé, R. Azinwi, A. M. Bernier, T. Kablan, A. M. Maupertuis, S. Mauler, R. K. Nevry, K. Dembélé, L. Forbes and L. Diop, *J. Med. Microbiol.*, 2008, **57**, 1523–1528.
- 232 S. Das, F. D. Bobbink, G. Laurenczy and P. J. Dyson, *Angew. Chemie - Int. Ed.*, 2014, **53**, 12876–12879.
- 233 S. Das, F. D. Bobbink, S. Bulut, M. Soudani and P. J. Dyson, *Chem. Commun.*, 2016, **52**, 2497–2500.
- 234 Y. Li, X. Fang, K. Junge and M. Beller, *Angew. Chemie*, 2013, **125**, 9747–9750.
- 235 K. Beydoun, T. Vom Stein, J. Klankermayer and W. Leitner, *Angew. Chemie - Int. Ed.*, 2013, **52**, 9554–9557.
- 236 O. Jacquet, X. Frogneux, C. Das Neves Gomes and T. Cantat, *Chem. Sci.*, 2013, **4**, 2127–2131.
- 237 Q. Zhou and Y. Li, *J. Am. Chem. Soc.*, 2015, **137**, 10182–10189.
- 238 S. N. Riduan, J. Y. Ying and Y. Zhang, *ChemCatChem*, 2013, **5**, 1490–1496.
- 239 C. C. Chong and R. Kinjo, *Angew. Chemie Int. Ed.*, 2015, **54**, 12116–12120.
- 240 S. N. Riduan, J. Y. Ying and Y. Zhang, *J. Catal.*, 2016, **343**, 46–51.
- 241 X. Frogneux, E. Blondiaux, P. Thuéry and T. Cantat, *ACS Catal.*, 2015, **5**, 3983–3987.

- 242 S. Zhang, Q. Mei, H. Liu, H. Liu, Z. Zhang and B. Han, *RSC Adv.*, 2016, **6**, 32370–32373.
- 243 D. Nale and B. Bhanage, *Synlett*, 2016, **27**, 1413–1417.
- 244 I. Sorribes, K. Junge and M. Beller, *J. Am. Chem. Soc.*, 2014, **136**, 14314–14319.
- 245 M. C. Fu, R. Shang, W. M. Cheng and Y. Fu, *Angew. Chemie - Int. Ed.*, 2015, **54**, 9042–9046.
- 246 B. Scrosati, J. Hassoun and Y.-K. Sun, *Energy Environ. Sci.*, 2011, **4**, 3287–3295.
- 247 B. Nohra, L. Candy, J.-F. Blanco, C. Guerin, Y. Raoul and Z. Mouloungui, *Macromolecules*, 2013, **46**, 3771–3792.
- 248 W. Guerin, A. K. Diallo, E. Kirilov, M. Helou, M. Slawinski, J. M. Brusson, J. F. Carpentier and S. M. Guillaume, *Macromolecules*, 2014, **47**, 4230–4235.
- 249 C. Beattie, M. North and P. Villuendas, *Molecules*, 2011, **16**, 3420–3432.
- 250 H. L. Parker, J. Sherwood, A. J. Hunt and J. H. Clark, *ACS Sustain. Chem. Eng.*, 2014, **2**, 1739–1742.
- 251 P. Wang, S. Liu, F. Zhou, B. Yang, A. S. Alshammari, L. Lu and Y. Deng, *Fuel Process. Technol.*, 2014, **126**, 359–365.
- 252 C. Lian, F. Ren, Y. Liu, G. Zhao, Y. Ji, H. Rong, W. Jia, L. Ma, H. Lu, D. Wang and Y. Li, *Chem. Commun.*, 2015, **51**, 1252–1254.
- 253 A.-A. G. Shaikh and S. Sivaram, *Chem. Rev.*, 1996, **96**, 951–976.
- 254 J. W. Comerford, I. D. V. Ingram, M. North and X. Wu, *Green Chem.*, 2015, **17**, 1966–1987.
- 255 K. Müller, L. Mokrushina and W. Arlt, *Chemie-Ingenieur-Technik*, 2014, **86**, 497–503.
- 256 Y. N. Lim, C. Lee and H. Y. Jang, *Eur. J. Org. Chem.*, 2014, **2014**, 1823–1826.
- 257 D. Bourissou, O. Guerret, F. P. Gabbaï and G. Bertrand, *Chem. Rev.*, 2000, **100**, 39–92.
- 258 P. de Frémont, N. Marion and S. P. Nolan, *Coord. Chem. Rev.*, 2009, **253**, 862–892.
- 259 A. M. Voutchkova, M. Feliz, E. Clot, O. Eisenstein and R. H. Crabtree, *J. Am. Chem. Soc.*, 2007, **129**, 12834–12846.
- 260 S. N. Riduan, Y. Zhang and J. Y. Ying, *Angew. Chemie*, 2009, **121**, 3372–3375.
- 261 J. a. Stewart, R. Drexel, B. Arstad, E. Reubsaet, B. M. Weckhuysen and P. C. a. Bruijninx, *Green Chem.*, 2016, **18**, 1605–1618.
- 262 A. Ion, V. Parvulescu, P. Jacobs and D. De Vos, *Green Chem.*, 2007, **9**, 158–161.
- 263 R. N. Salvatore, Seung Il Shin, a. S. Nagle and Kyung Woon Jung, *J. Org. Chem.*, 2001, **66**, 1035–1037.
- 264 T. Niemi, J. E. Perea-Buceta, I. Fernández, O.-M. Hiltunen, V. Salo, S. Rautiainen, M. T. Räisänen and T. Repo, *Chem. Eur. J.*, 2016, **22**, 10355–10359.
- 265 D. Riemer, P. Hirapara and S. Das, *ChemSusChem*, 2016, **9**, 1916–1920.

- 266 I. Chiarotto, M. Feroci, G. Forte, M. Orsini and A. Inesi, *ChemElectroChem*, 2014, **1**, 1525–1530.
- 267 B. Liu, A. G. Wong-Foy and A. J. Matzger, *Chem. Commun.*, 2013, **49**, 1419–1421.
- 268 A. Schmidt, A. Beutler, M. Albrecht, B. Snovydyovych and F. J. Ramírez, *Org. Biomol. Chem.*, 2008, **6**, 287–295.
- 269 A. R. Katritzky, O. Meth-Cohn and C. W. Rees, *Comprehensive Organic Functional Group Transformations: Synthesis: carbon with one heteroatom attached by a single bond.*, Elsevier, Vol. 2., 1995.
- 270 D. W. Stephan, *Org. Biomol. Chem.*, 2008, **6**, 1535–1539.
- 271 D. W. Stephan, *Dalton Trans.*, 2009, **9226**, 3129–3136.
- 272 D. W. Stephan and G. Erker, *Angew. Chemie - Int. Ed.*, 2010, **49**, 46–76.
- 273 D. W. Stephan and G. Erker, *Angew. Chemie - Int. Ed.*, 2015, **54**, 6400–6441.
- 274 P. A. Chase and D. W. Stephan, *Angew. Chemie - Int. Ed.*, 2008, **47**, 7433–7437.
- 275 C. M. Mömming, E. Otten, G. Kehr, R. Fröhlich, S. Grimme, D. W. Stephan and G. Erker, *Angew. Chemie - Int. Ed.*, 2009, **48**, 6643–6646.
- 276 C. Appelt, H. Westenberg, F. Bertini, A. W. Ehlers, J. C. Slootweg, K. Lammertsma and W. Uhl, *Angew. Chemie*, 2011, **123**, 4011–4014.
- 277 M. Sajid, A. Stute, A. J. P. Cardenas, B. J. Culotta, J. A. M. Hepperle, T. H. Warren, B. Schirmer, S. Grimme, A. Studer, C. G. Daniliuc, R. Fröhlich, J. L. Petersen, G. Kehr and G. Erker, *J. Am. Chem. Soc.*, 2012, **134**, 10156–10168.
- 278 A. Berkefeld, W. E. Piers, M. Parvez, L. Castro, L. Maron and O. Eisenstein, *J. Am. Chem. Soc.*, 2012, **134**, 10843–10851.
- 279 P. I. Dalko and L. Moisan, *Angew. Chemie - Int. Ed.*, 2004, **43**, 5138–5175.
- 280 J. G. Hernández and E. Juaristi, *Chem. Commun.*, 2012, **48**, 5396–5409.
- 281 L. J. Hounjet and D. W. Stephan, *Org. Process Res. Dev.*, 2014, **18**, 385–391.
- 282 N. Yan, Y. Yuan, R. Dykeman, Y. Kou and P. J. Dyson, *Angew. Chemie - Int. Ed.*, 2010, **49**, 5549–5553.
- 283 Z. Fei, T. J. Geldbach, D. Zhao and P. J. Dyson, *Chem. Eur. J.*, 2006, **12**, 2122–2130.
- 284 P. Domínguez de María, *Angew. Chemie - Int. Ed.*, 2008, **47**, 6960–6968.
- 285 A. Sarkar, S. R. Roy, N. Parikh and A. K. Chakraborti, *J. Org. Chem.*, 2011, **76**, 7132–7140.
- 286 V. Lucchini, M. Noè, M. Selva, M. Fabris and A. Perosa, *Chem. Commun.*, 2012, **48**, 5178–5180.
- 287 V. Sumerin, F. Schulz, M. Nieger, M. Leskelä, T. Repo and B. Rieger, *Angew. Chemie - Int. Ed.*, 2008, **47**, 6001–6003.

- 288 C. Jiang, O. Blacque, T. Fox and H. Berke, *Dalt. Trans.*, 2011, **40**, 1091–1097.
- 289 H. Zaher, A. E. Ashley, M. Irwin, A. L. Thompson, M. J. Gutmann, T. Krämer and D. O'Hare, *Chem. Commun.*, 2013, **49**, 9755–9757.
- 290 N. Millot, C. C. Santini, B. Fenet and J. M. Basset, *Eur. J. Inorg. Chem.*, 2002, **2002**, 3328–3335.
- 291 S. A. Forsyth, U. Fröhlich, P. Goodrich, H. Q. N. Gunaratne, C. Hardacre, A. McKeown and K. R. Seddon, *New J. Chem.*, 2010, **34**, 723–731.
- 292 M. Erdmann, T. Wiegand, J. Blumenberg, H. Eckert, J. Ren, C. G. Daniliuc, G. Kehr and G. Erker, *Dalt. Trans.*, 2014, **43**, 15159–15169.
- 293 A. E. Ashley, A. L. Thompson and D. O'Hare, *Angew. Chemie - Int. Ed.*, 2009, **48**, 9839–9843.
- 294 M. A. Courtemanche, M. A. Légaré, L. Maron and F. G. Fontaine, *J. Am. Chem. Soc.*, 2014, **136**, 10708–10717.
- 295 G. Ménard and D. W. Stephan, *Dalt. Trans.*, 2013, **42**, 5447–5453.
- 296 A. P. Pulis and D. W. Stephan, 2015, 9797–9800.
- 297 T. D. Nelson and R. D. Crouch, *Synthesis.*, 1996, **1996**, 1031–1069.
- 298 S. Zhou, K. Junge, D. Addis, S. Das and M. Beller, *Org. Lett.*, 2009, **11**, 2461–2464.
- 299 Y. Q. Zhang, N. Funken, P. Winterscheid and A. Gansäuer, *Angew. Chemie - Int. Ed.*, 2015, **54**, 6931–6934.
- 300 C. Bornschein, S. Werkmeister, K. Junge and M. Beller, *New J. Chem.*, 2013, **37**, 2061–2065.
- 301 S. Das, D. Addis, L. R. Knöpke, U. Bentrup, K. Junge, A. Brückner and M. Beller, *Angew. Chemie - Int. Ed.*, 2011, **50**, 9180–9184.
- 302 C. Fang, C. Lu, M. Liu, Y. Zhu, Y. Fu and B.-L. Lin, *ACS Catal.*, 2016, **6**, 7876–7881.
- 303 A. Berkefeld, W. E. Piers and M. Parvez, *J. Am. Chem. Soc.*, 2010, **132**, 10660–10661.
- 304 H. Sun and S. G. DiMagno, *J. Am. Chem. Soc.*, 2005, **127**, 2050–2051.
- 305 W. Zhong, F. D. Bobbink, Z. Fei and P. J. Dyson, *ChemSusChem*, 2017, **10**, 2728–2735.
- 306 K. Revunova and G. I. Nikonov, *Chem. Eur. J.*, 2014, **20**, 839–845.
- 307 D. J. Parks, J. M. Blackwell and W. E. Piers, *J. Org. Chem.*, 2000, **65**, 3090–3098.
- 308 J. Schulten and P. Klüfers, *Carbohydr. Res.*, 2011, **346**, 1767–1775.
- 309 P. Arya, R. J. P. Corriu, K. Gupta, G. F. Lanneau and Z. Yu, *J. Organomet. Chem.*, 1990, **399**, 11–33.
- 310 F. H. Carré, R. J. P. Corriu, G. F. Lanneau and Z. Yu, *Organometallics*, 1991, **10**, 1236–1243.
- 311 A. S. Lee, S.-S. Choi, H. S. Lee, K.-Y. Baek and S. S. Hwang, *Dalt. Trans.*, 2012, **41**, 10585–10588.
- 312 R. Wakabayashi, Y. Sugiura, T. Shibue and K. Kuroda, *Angew. Chemie - Int. Ed.*, 2011, **50**, 10708–10711.

- 313 M. G. Voronkov, E. V. Boyarkina, I. A. Gebel, A. I. Albanov and S. V. Basenko, *Russ. J. Gen. Chem.*, 2005, **75**, 1927–1929.
- 314 A. Y. Khalimon, R. Simionescu and G. I. Nikonov, *J. Am. Chem. Soc.*, 2011, **133**, 7033–7053.
- 315 Z. Dai, R. D. Noble, D. L. Gin, X. Zhang and L. Deng, *J. Memb. Sci.*, 2016, **497**, 1–20.
- 316 F. D. Bobbink, W. Gruszka, M. Hulla, S. Das and P. J. Dyson, *Chem. Commun.*, 2016, **52**, 10787–10790.

Appendices

Appendix Section 2.3

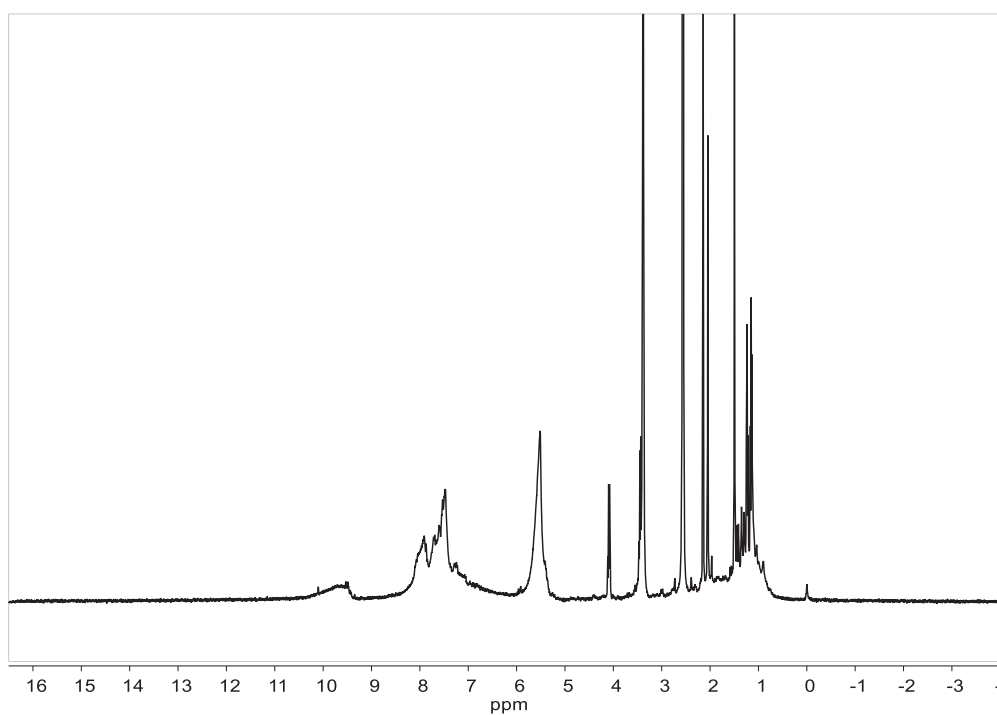


Fig A2.3.1. Example of soluble fraction of polymer 1b.

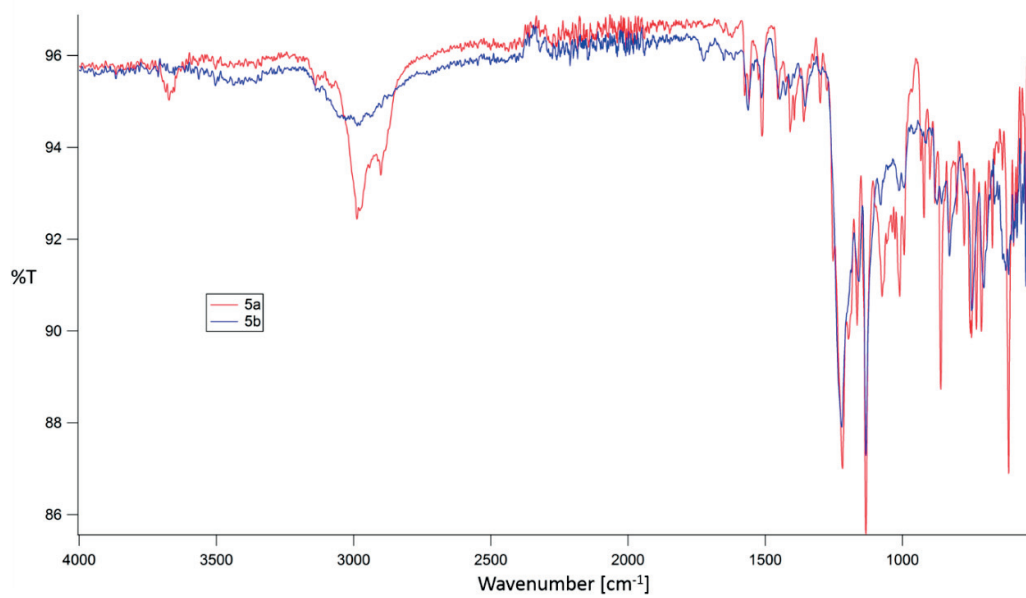


Fig A2.3.2. Overlapped IR spectra of monomeric 5a and polymeric 5b.

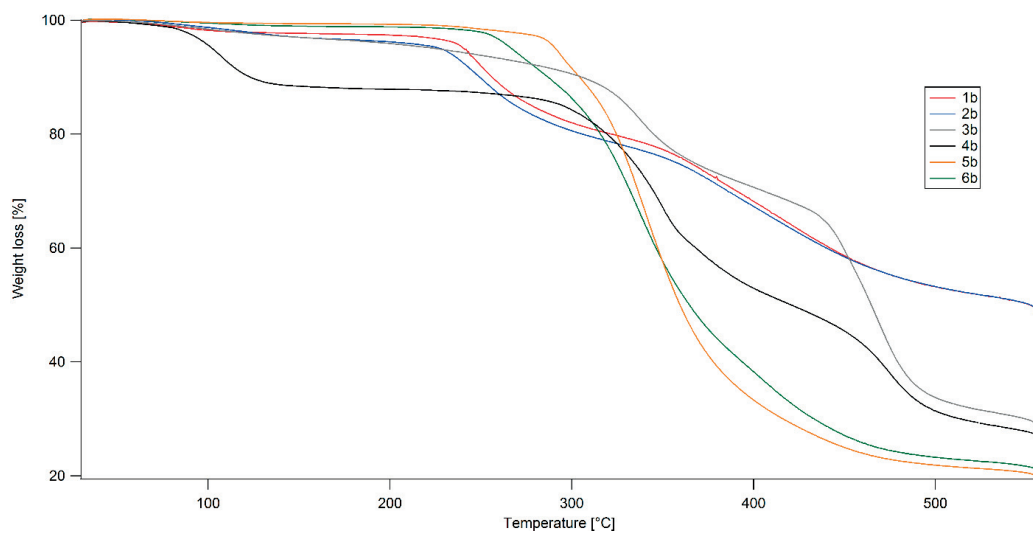
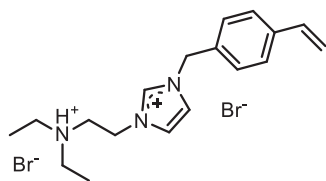
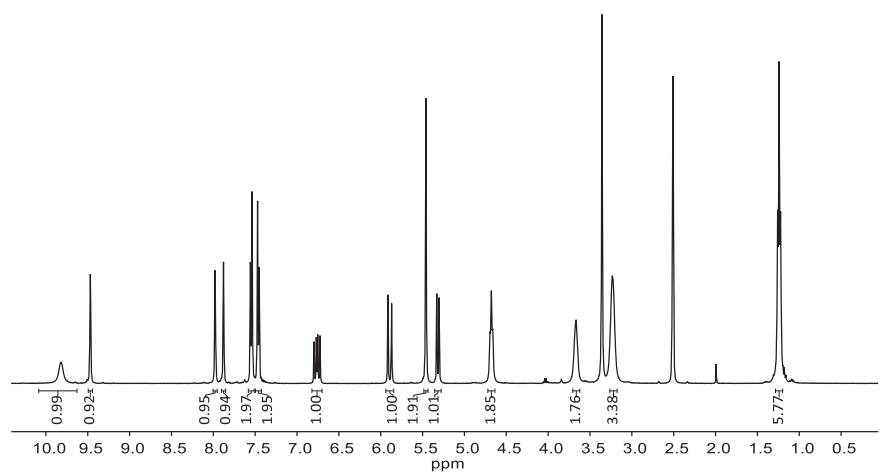


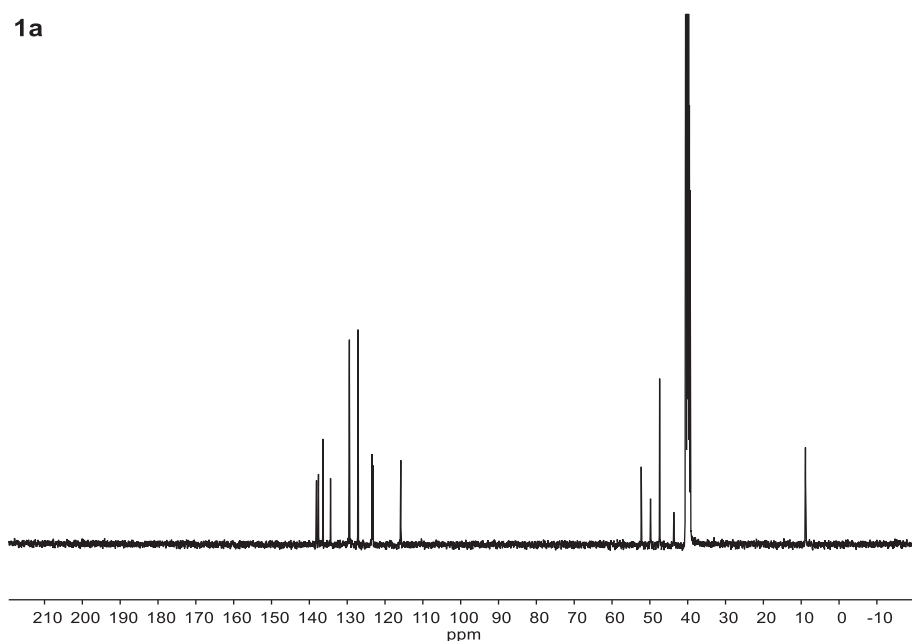
Fig A2.3.3. TGA data for polymers 1b – 6b.

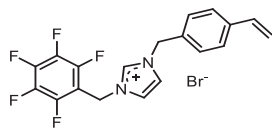


1a

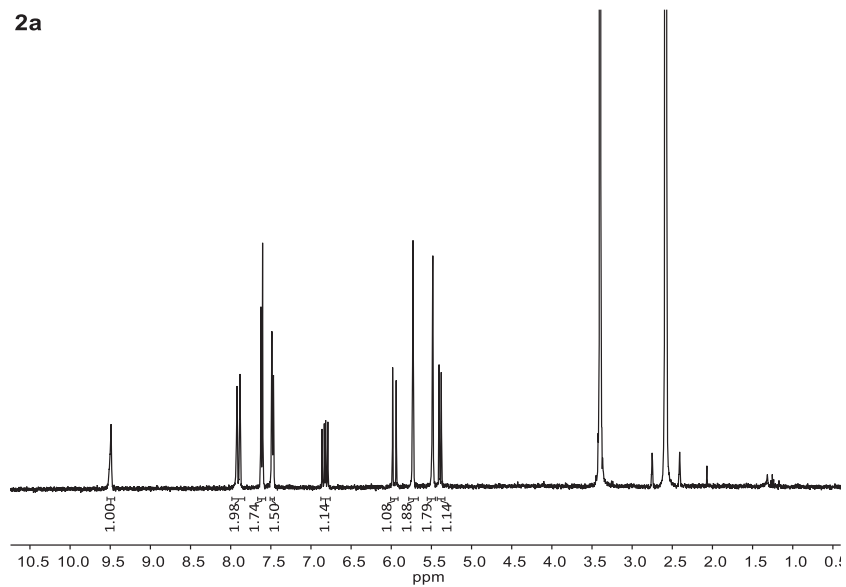


1a

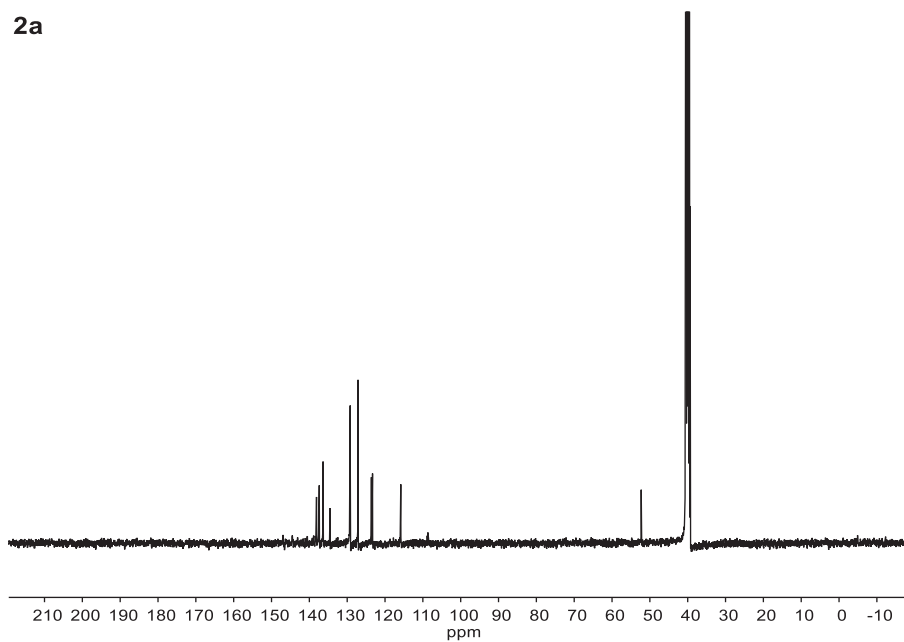


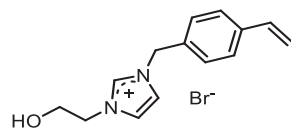


2a

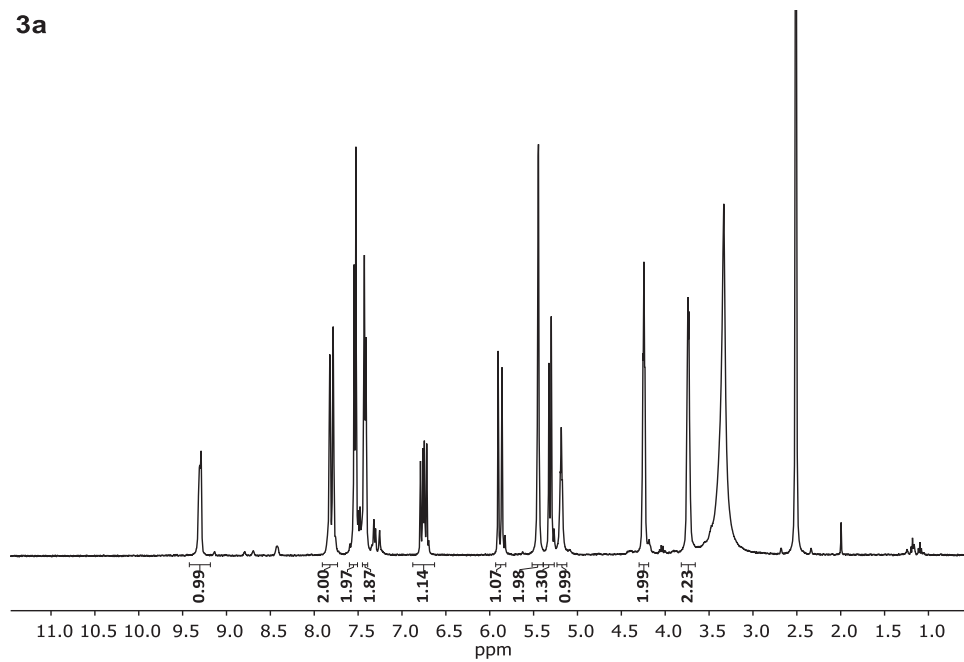


2a

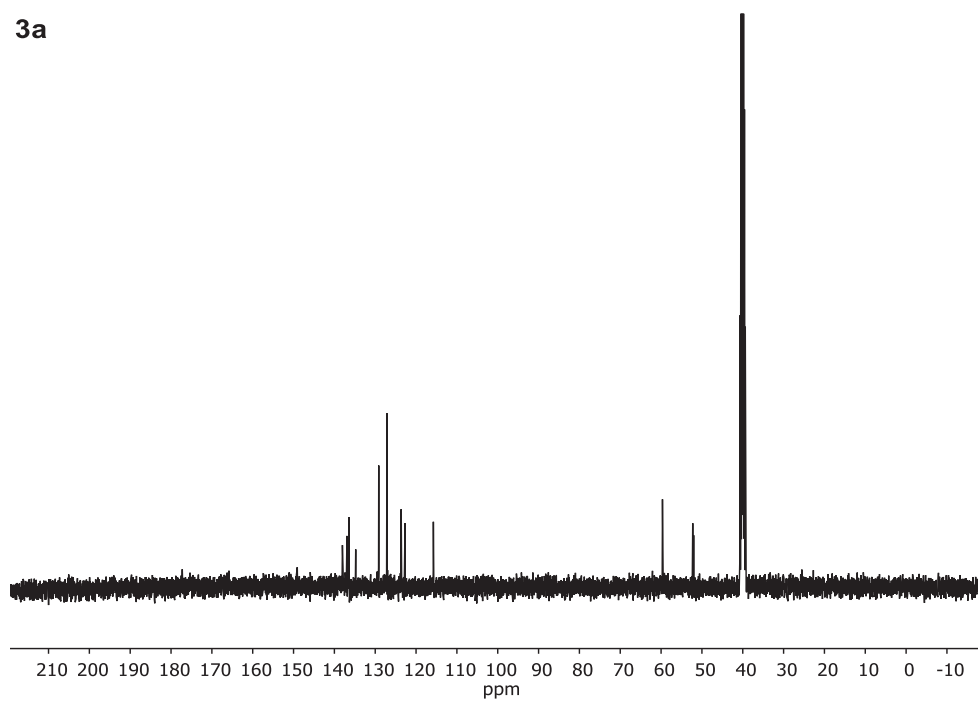


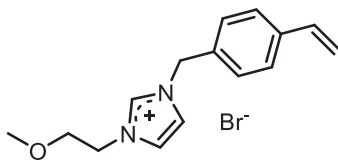


3a

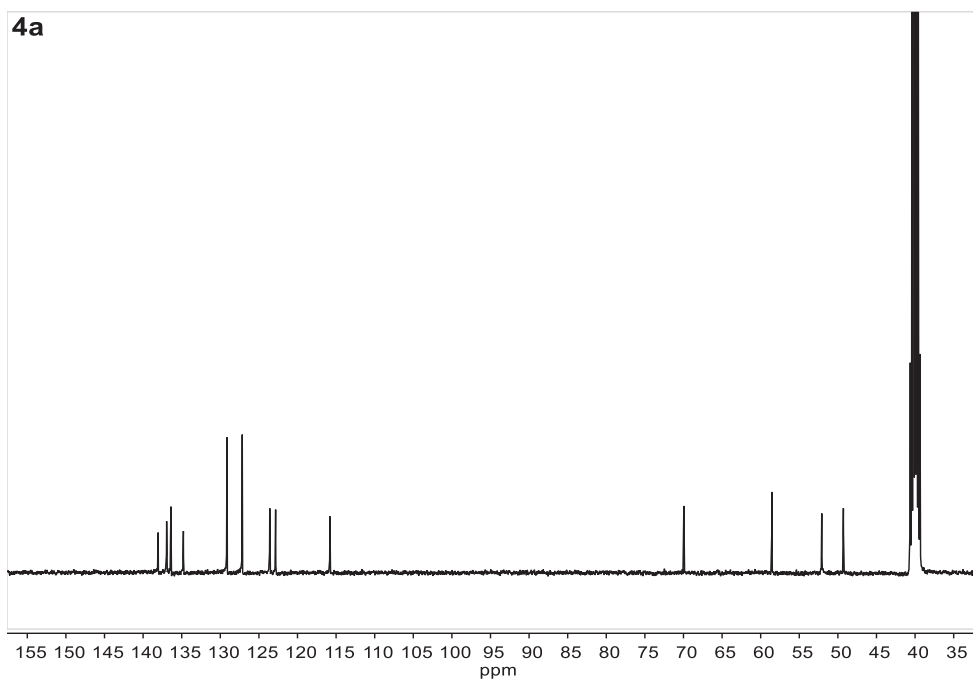
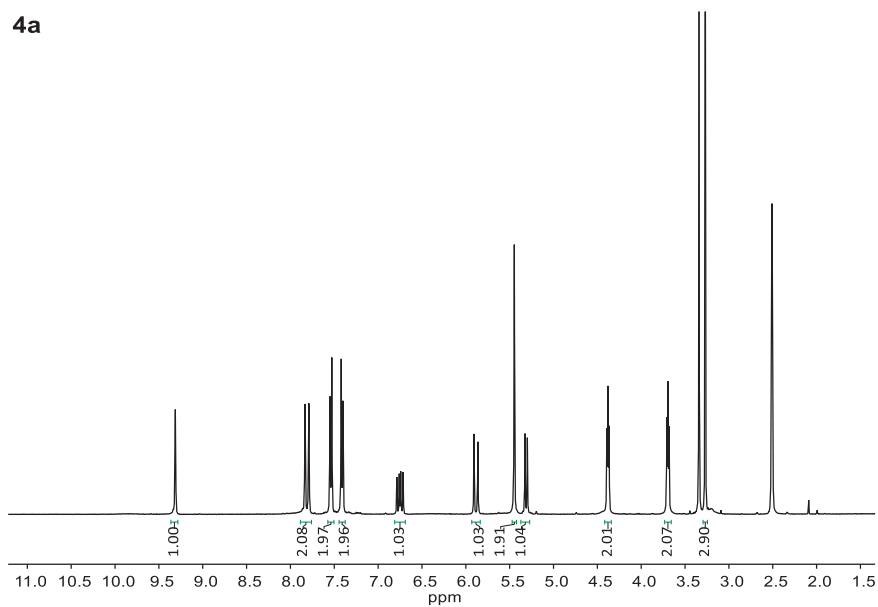


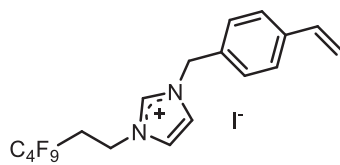
3a



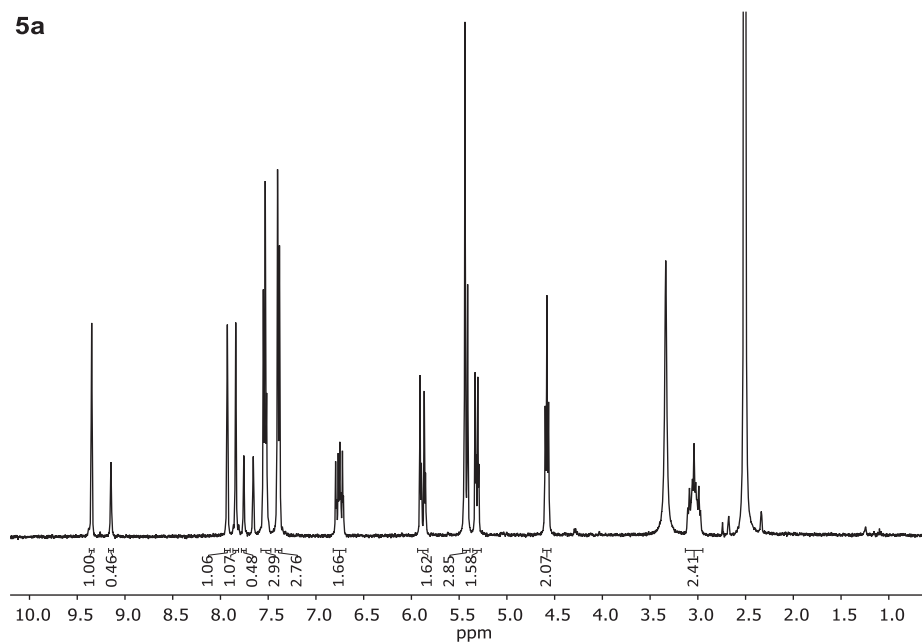


4a

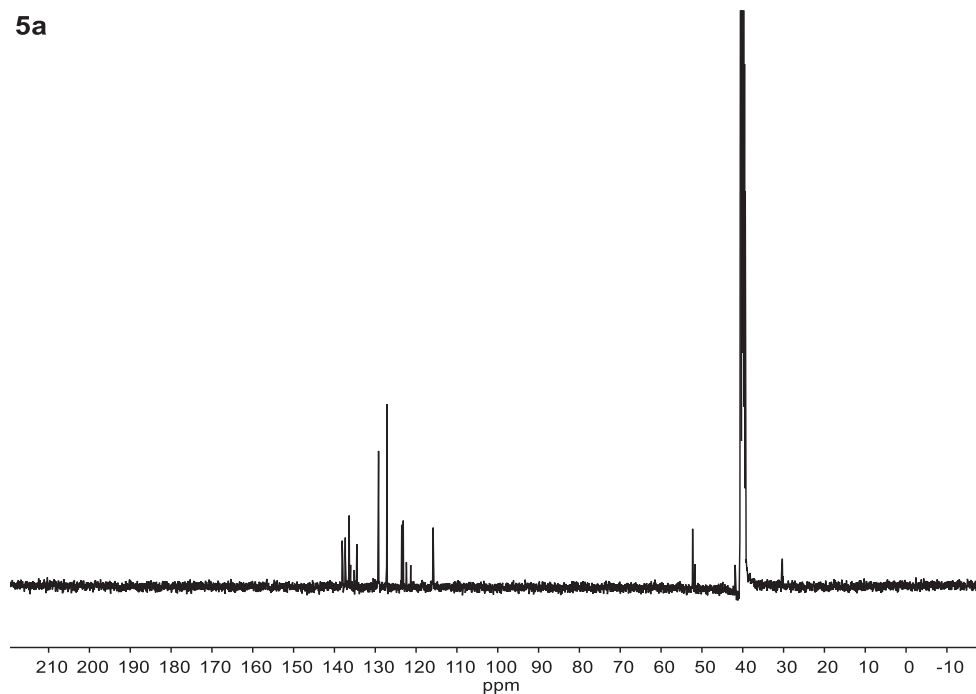


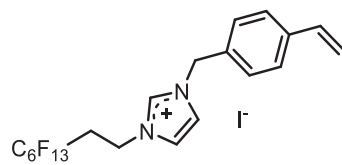


5a

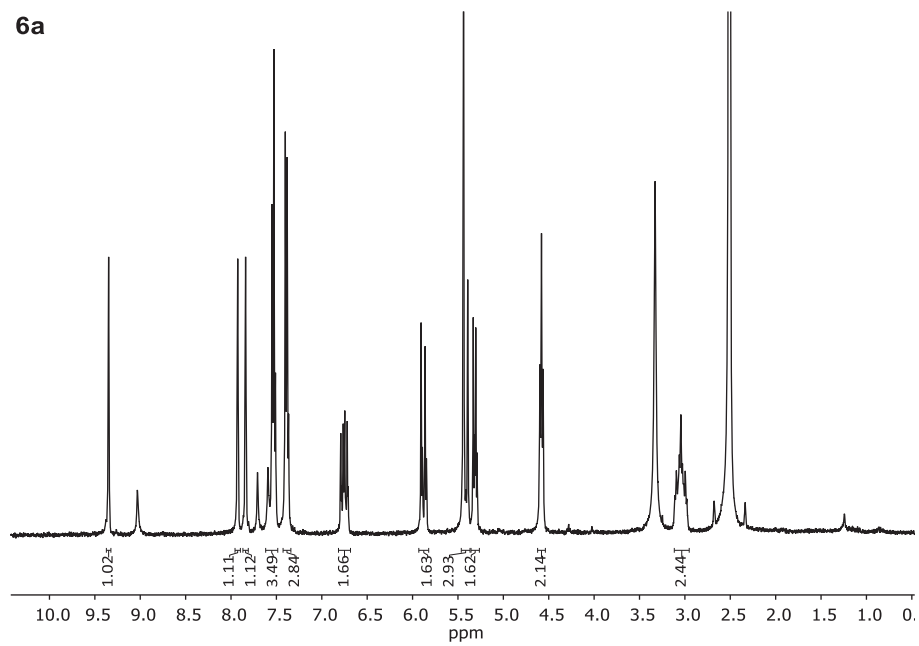


5a

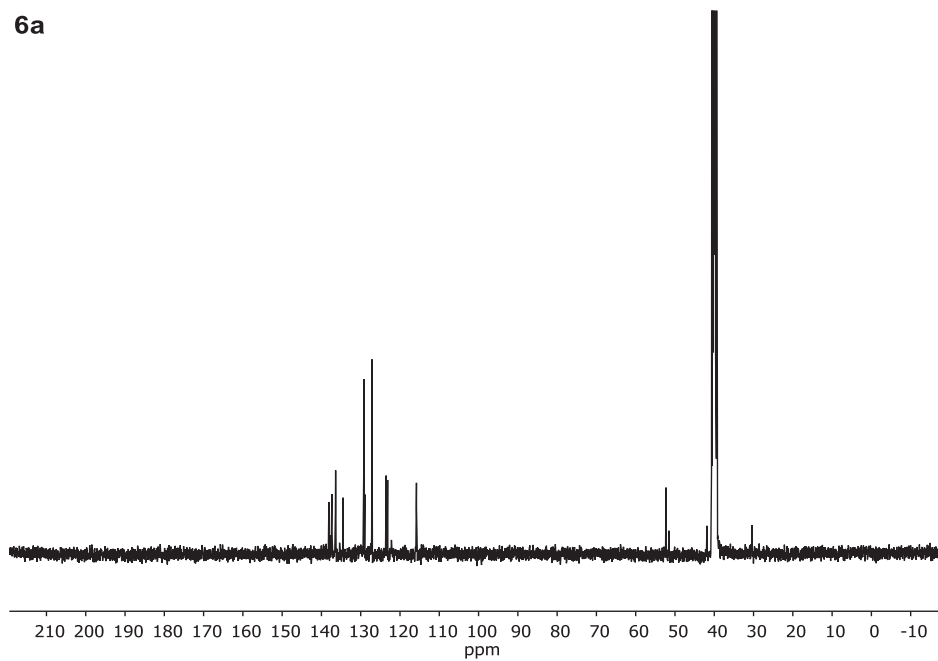




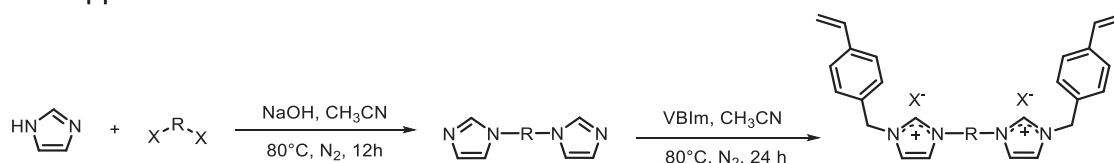
6a



6a



Appendix Section 2.4



Scheme A2.4.1: Synthesis of the monomeric imidazolium salts.

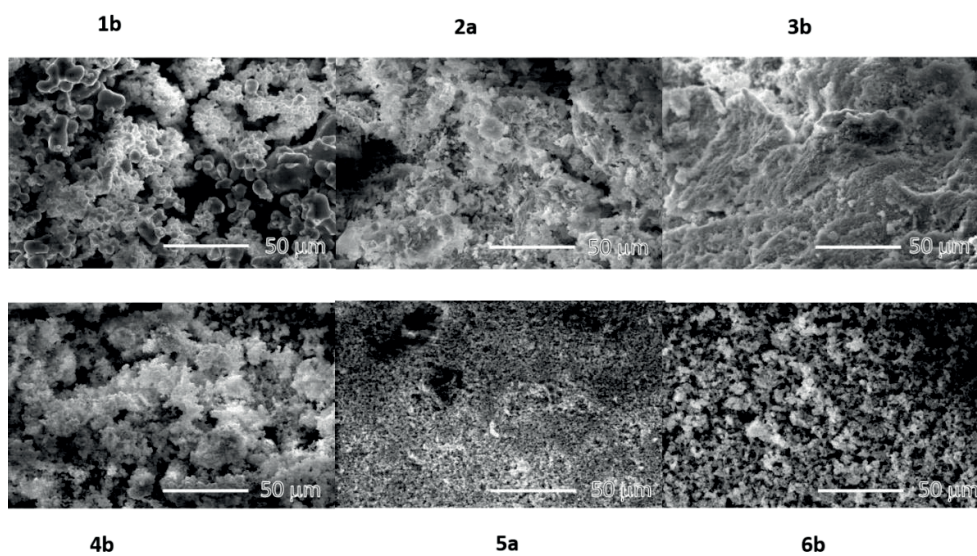


Fig A.2.4.1: SEM pictures for selected catalysts.

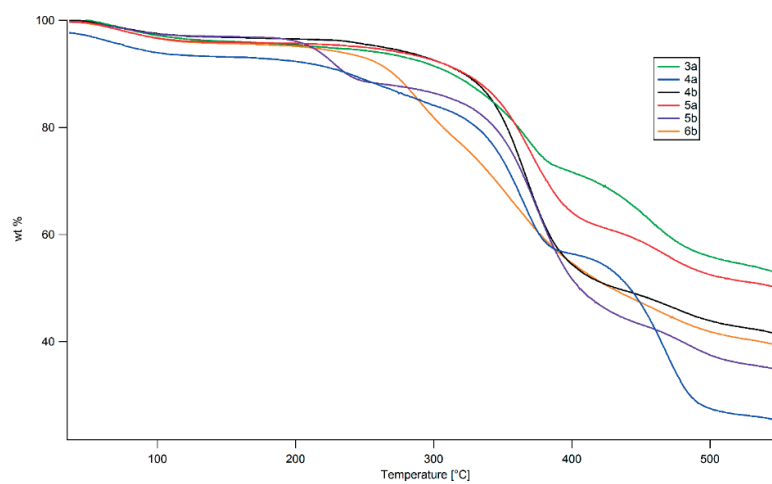
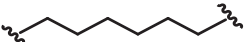
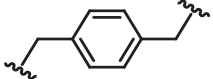
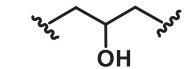
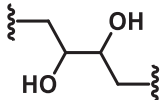
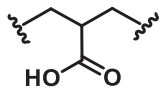


Fig A.2.4.2: Typical TGA curves for selected polymers.

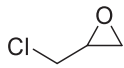
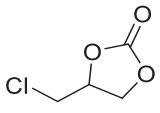
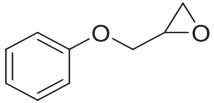
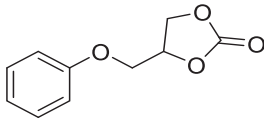
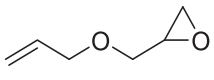
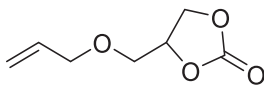
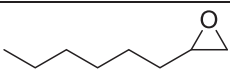
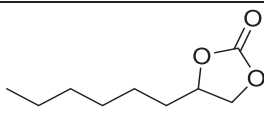
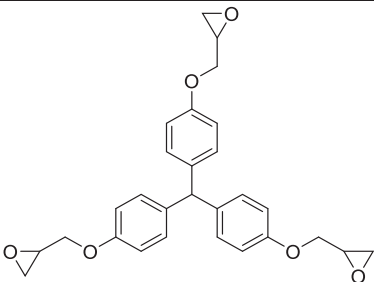
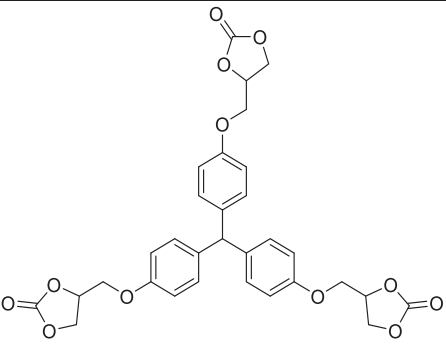
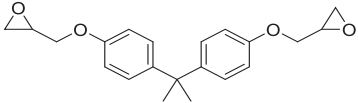
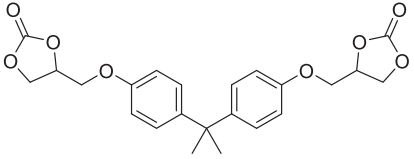
Table A.2.4.1: BET results for selected catalysts.

Catalyst	Spacer	Surface area [m ² /g]
1A/B		9.1/1.5
2A		19.1
4B		18.8
5B		34.7
6B		16.7

Conditions: Heating under vacuum from 30 °C to 180 °C at 5 °C/min, soak time (5 h), 10 point BET.

Appendix Section 2.6

Table A.2.6.1. Scope of the reaction. Conditions: epoxide (0.83 mmol), [BMIm]Cl (25 mol%), CO₂ (balloon) 100 °C, 24 h. Yield determined by ¹H-NMR.

Entry	Epoxide	Carbonate	Yield [%, by NMR]
1			>99%
2			>99%
3			>98%
4			<15%
5			20%, decomposition/ polymerization occurs
6			91%

I) Additional experiments

Table A.2.6.2. Effect of temperature and alternative CO₂ sources on the cyclic carbonate yield.

Entry	Epoxide	CO ₂ source	Catalyst (mol%)	Time [h]	T [°C]	Yield (%)
1	PO	1 atm., pure	[BMIm]Cl (100)	24	rt	5
2	SO	1 atm., pure	[BMIm]Cl (100)	24	rt	5
3	SO	Dry ice (100 mg)	[BMIm]Cl (25)	1	80	16
4	SO	Dry ice (200 mg)	[BMIm]Cl (25)	1	80	21
5	SO	Dry ice (1 g)	[BMIm]Cl (25)	1	80	46
6	SO	Breath	[BMIm]Cl (25)	1	80	4

Reaction conditions: Catalyst, Epoxide (0.83 mmol), CO₂ source. The yields were determined by ¹H NMR.

Table A.2.6.3. Control experiments.

Entry	T °C	Catalyst	Atmosphere	Products:
1	80	[BMIm]Cl	N ₂	Recovered SO
2	80	[BMIm]Cl	Wet air	Recovered SO , AD (approx. 4%), SC (< 1 %)
3	100	[BMIm]Cl	N ₂	Recovered SO
4	100	[BMIm]Cl	Wet air	Recovered SO , AD (approx. 6%), SC (< 1 %)
7	100	TBAB/TBAI	N ₂	Recovered SO
8	100	TBAB/TBAI	Wet air	Mixture of products including SD and the corresponding bromohydrin. AD isomerization (approx. 30 %)
9	100	[BMIm]Cl	N ₂ , 1 eq. H ₂ O added	Mixture of SO and CPO
10	100	None	N ₂ , 1 eq. H ₂ O added.	Mixture of SO and PD

Conditions: catalyst (25 mol%), epoxide (8.3 mmol). The reaction was stopped after 24 h. After this time the products were extracted with Et₂O and characterized by GC-MS/FID. TBAB = N-tetrabutylammonium bromide, TBAI = N-tetrabutylammonium iodide.

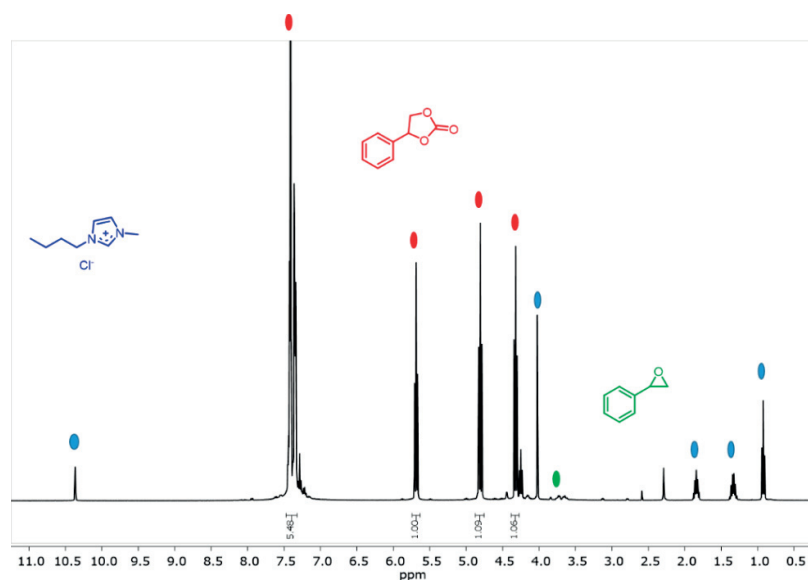


Fig A.2.6.1. ¹H-NMR spectra after reaction. Conditions: [BMIm]Cl (5 mol%), SO (100 mg), CO₂ (balloon), 20 h, 100 °C. Impurity is [BMIm]Cl (soluble in CDCl₃).

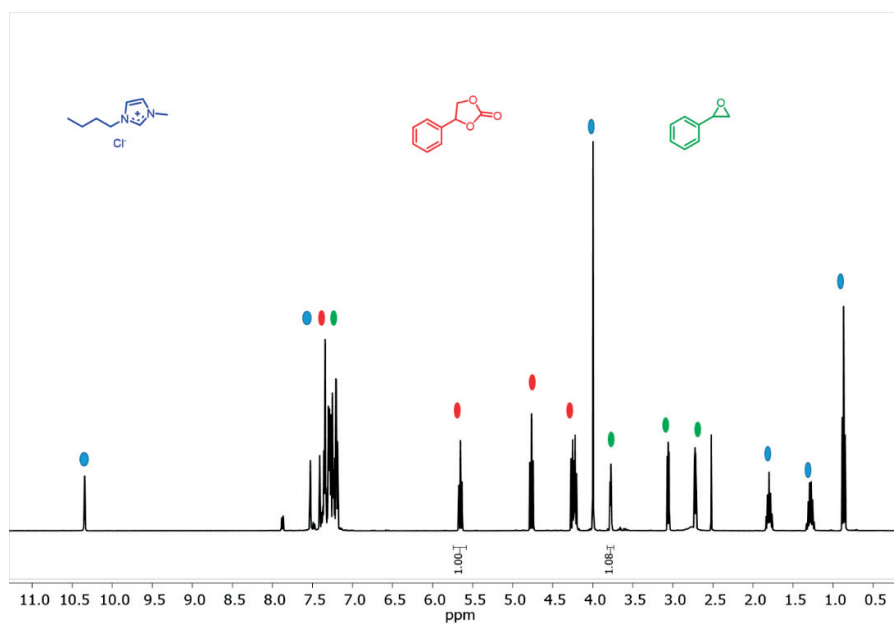


Fig A.2.6.2. $^1\text{H-NMR}$ spectra after reaction when dry ice was used as CO_2 source. Reaction conditions: [BMIm]Cl (25 mol%), Epoxide (0.83 mmol), dry ice (1 g), 100°C , 2 h.

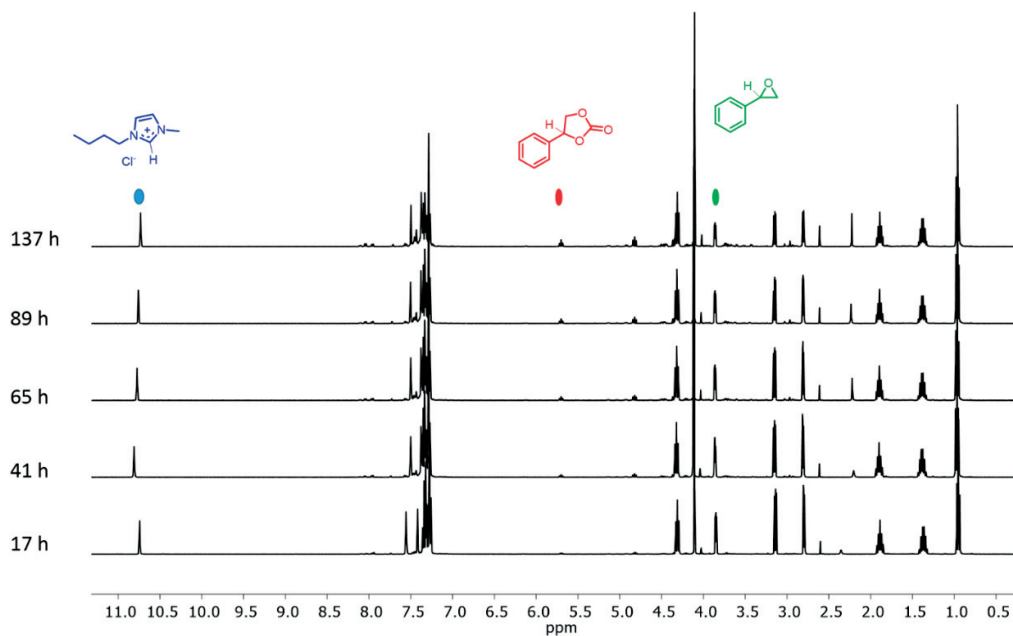


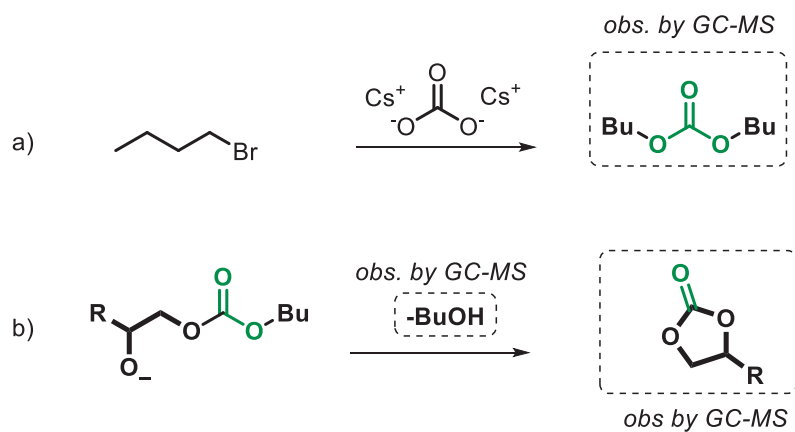
Fig A.2.6.3. Overlay of $^1\text{H-NMR}$ spectra over time at different reaction times. Conditions: [BMIm]Cl (18 g, 50 mol%), SO (25 g, 0.208 mol), 80°C , dried air-flow.

Appendix Section 3.2

Table A.3.2.1 Control experiments.

Entry	Cat.	Bu-Br (2 eq or 5 eq)	Cs ₂ CO ₃ (3.2 eq)	CO ₂ (1 bar)	Yield (%) ^[b]
1	Yes	Yes	Yes	Yes	81
2	Yes	Yes	Yes	No	25
3	No	Yes	Yes	Yes	53
4	Yes	No	Yes	Yes	0
5	Yes	Yes	No	Yes	0
6 ^a	Yes	Yes	Yes	Yes	0

Conditions: diol (0.5 mmol), cat (20 mol%), ⁿBu-Br (1-2.5 mmol), Cs₂CO₃ (3.2 eq), DMF (4 mL), CO₂ (1 bar). 90 °C, 24 h. ^a: 5 mmol H₂O is added to the reaction.



Scheme A.3.2.1. Observed intermediates from the non-catalytic pathway. The first step (a) can be promoted by the solvent (see Y. R. Jorapur, D. Y. Chi, *J. Org. Chem.* **2005**, *70*, 10774–10777). The second step (b) represents step 4 in Scheme 2.

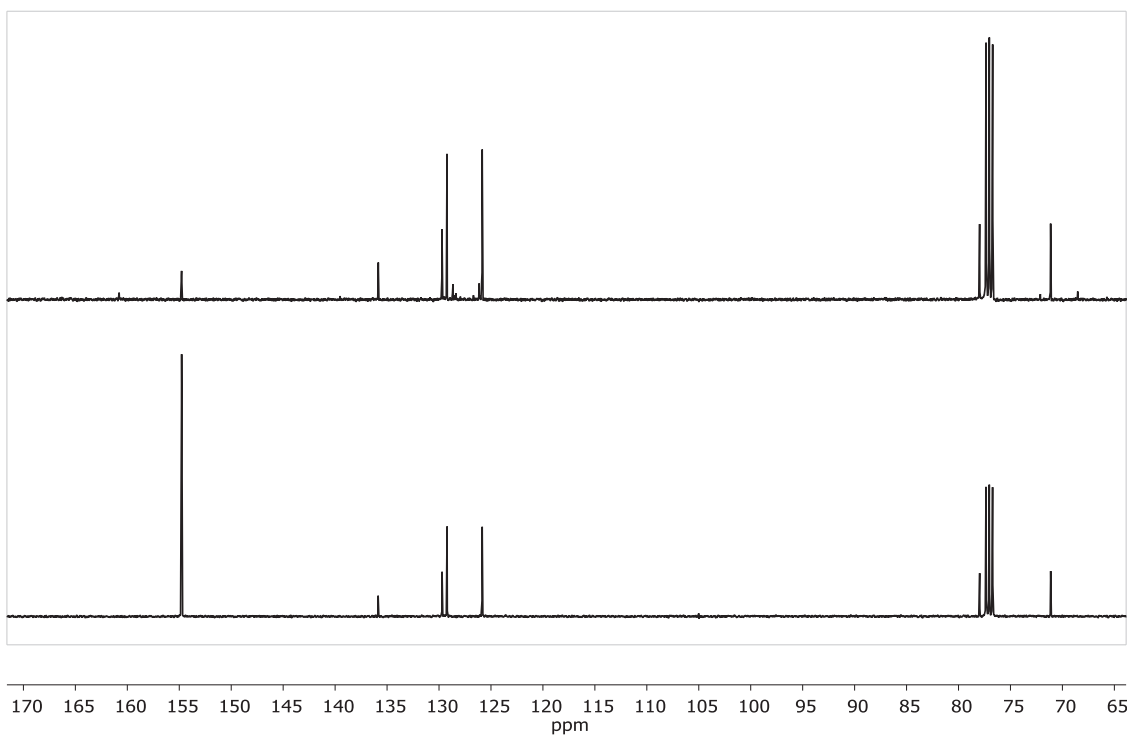
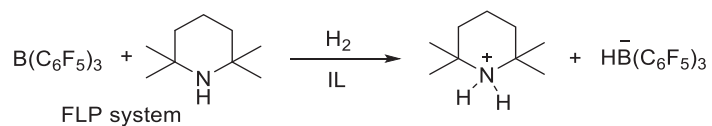


Fig A.3.2.1. Comparison between ^{13}C NMR of unlabeled (top) and ^{13}C -labelled (bottom) styrene carbonate.

Appendix Section 3.3

Table A.3.3.1. Attempted activation of hydrogen by FLPs dissolved in ILs.



Entry	FLP ratio B(C ₆ F ₅) ₃ /TMP (mmol/mmol)	Solvent (amount) (mL)	Conditions	Hydrogen Splitting (¹ NMR)
1	0.07/0.07	[Pyr][Tf ₂ N] 0.3	H ₂ (1.0 atm),* r.t., 1 h	none
2	1.03/0.99	[Emim][Tf ₂ N] 8	H ₂ (1.0 atm),* r.t., 1 h	none
3	0.59/0.62	[Pyr][Tf ₂ N] 3	H ₂ (1.0 atm),* r.t., 4 h	none
4	0.4/0.4	[Pyr][Tf ₂ N] 2	H ₂ (35 bar),** 40°C, 1 h	none
5	1.03/0.99	[Emim][Tf ₂ N] 8	H ₂ (1.0 atm),* r.t., 12 h	none
6	1.03/0.99	[Emim][Tf ₂ N] 8	H ₂ (30 bar),** r.t., 1 h	none
7	0.51/0.53	[Emim][Tf ₂ N] 4	H ₂ (40 bar),** 40°C, 1.5 h	none
8	0.39/0.42	[Bmim][TOF] 2.75	H ₂ (40 bar),** 40°C, 1 h	none
9	0.41/0.44	[Emim][Ac] 1.9	H ₂ (35 bar),** 40°C, 5.3 h	none
10	B(C ₆ F ₅) ₃ /DMPy 0.046/0.093	[Pyr][Tf ₂ N] 0.4	H ₂ (1.0 atm),* r.t., 8 h	none
11	B(C ₆ F ₅) ₃ /DMPy 0.046/0.093	[Emim][Tf ₂ N] 0.4	H ₂ (1.0 atm),* r.t., 8 h	none

* bubbling 1 atm H₂

** pressurized in autoclaves

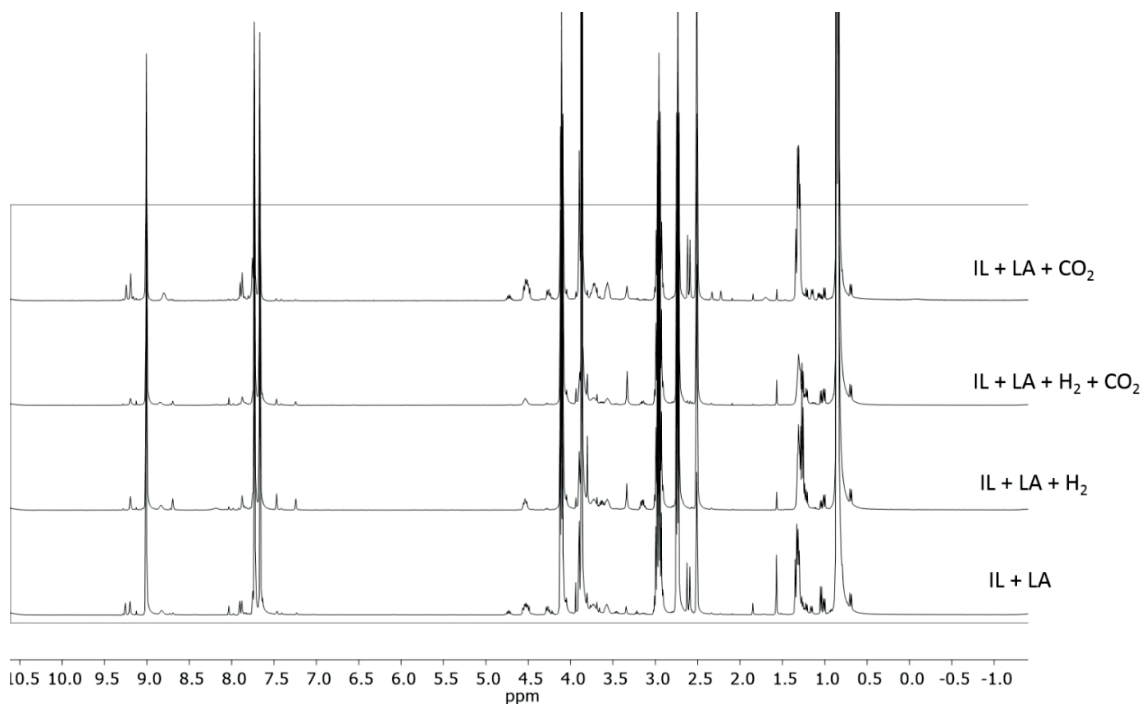


Figure A.3.3.1. Overlay of ^1H NMR spectra of the reaction mixture of $\text{B}(\text{C}_6\text{F}_5)_3$ in $[\text{Pr}_2\text{N}(\text{CH}_2)_2\text{mim}][\text{Tf}_2\text{N}]$. (conditions: H_2 (40 bars), CO_2 (20 bars), 135°C , 16 h).

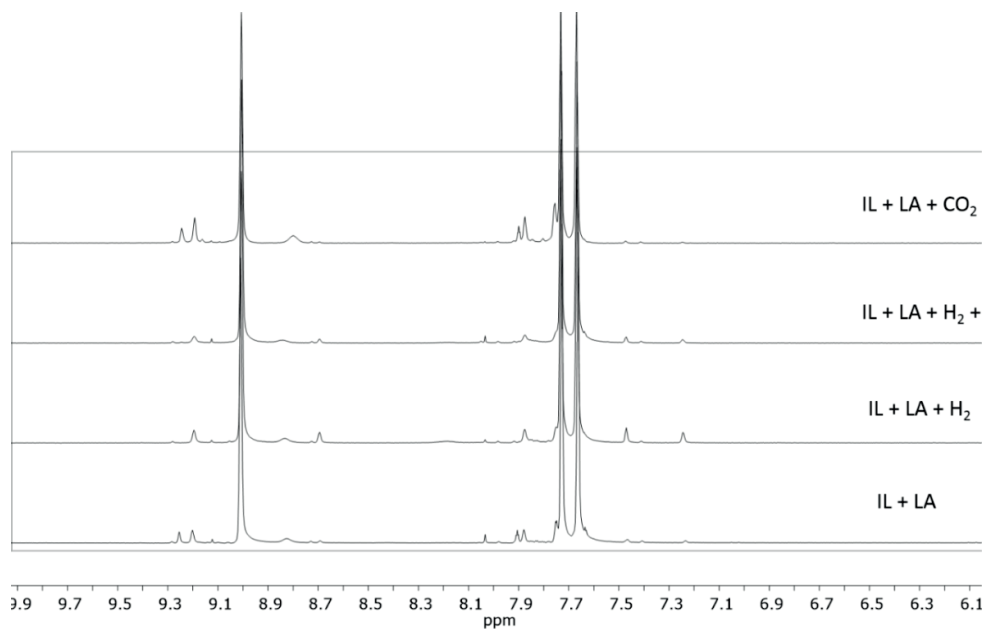


Figure A.3.3.2. Overlay of ^1H NMR spectra of the reaction mixture of $\text{B}(\text{C}_6\text{F}_5)_3$ in $[\text{Pr}_2\text{N}(\text{CH}_2)_2\text{mim}][\text{Tf}_2\text{N}]$. (conditions: H_2 (40 bars), CO_2 (20 bars), 135°C , 16 h). Zoom on the formate region

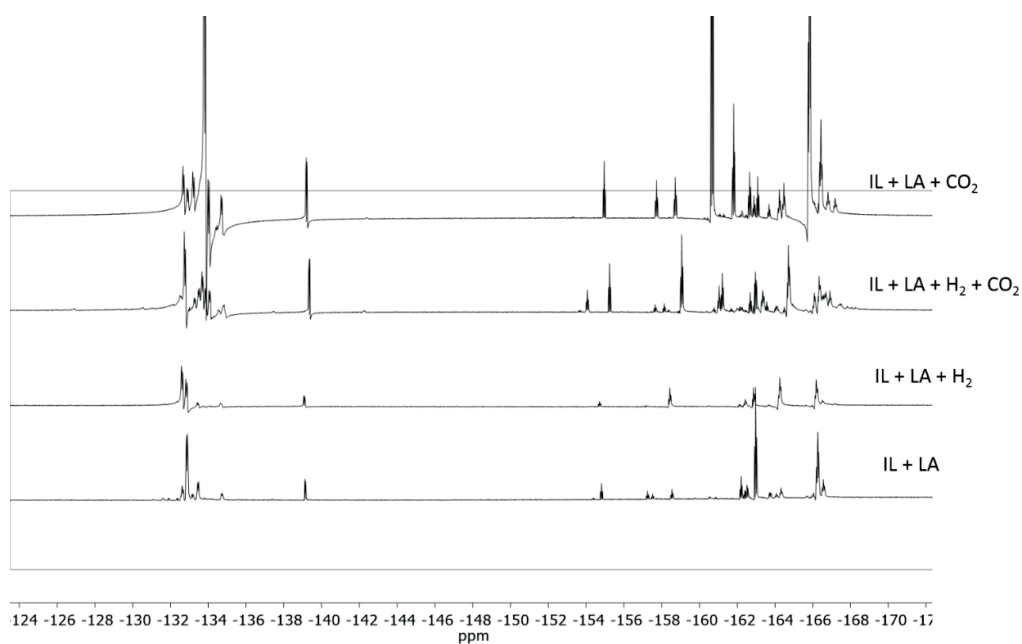


Figure A.3.3.3. Overlay of ^{19}F -NMR spectra of the reaction mixture of $\text{B}(\text{C}_6\text{F}_5)_3$ in $[\text{iPr}_2\text{N}(\text{CH}_2)_2\text{mim}][\text{Tf}_2\text{N}]$. (conditions: H_2 (40 bars), CO_2 (20 bars), 135°C , 16 h)

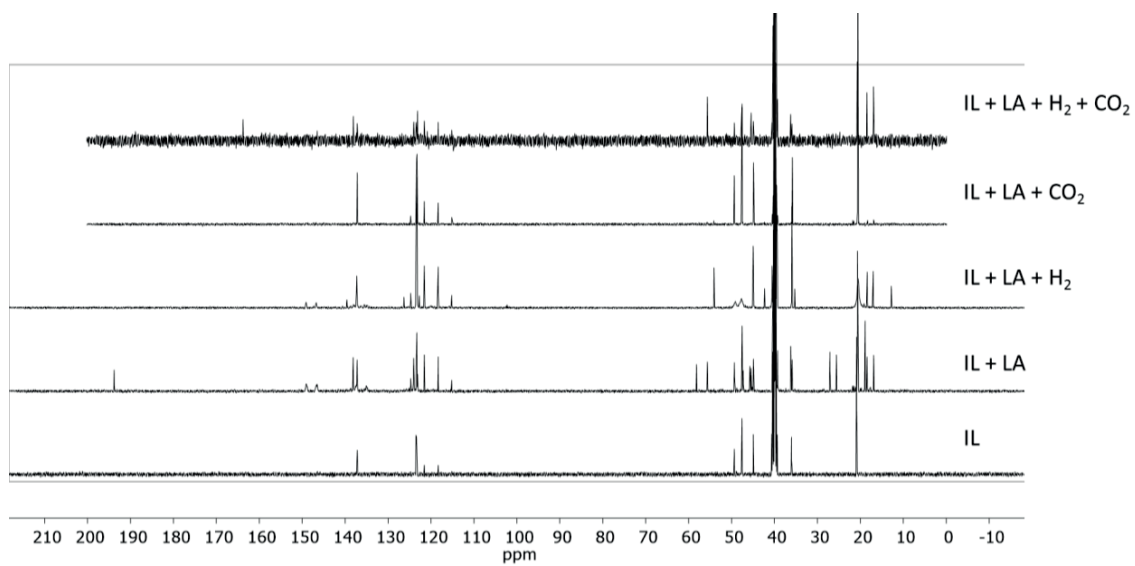


Figure A.3.3.4. Overlay of ^{13}C -NMR spectra of the reaction mixture of $\text{B}(\text{C}_6\text{F}_5)_3$ in $[\text{iPr}_2\text{N}(\text{CH}_2)_2\text{mim}][\text{Tf}_2\text{N}]$. (conditions: H_2 (40 bars), CO_2 (20 bars), 135°C , 16 h)

Appendix Section 3.4

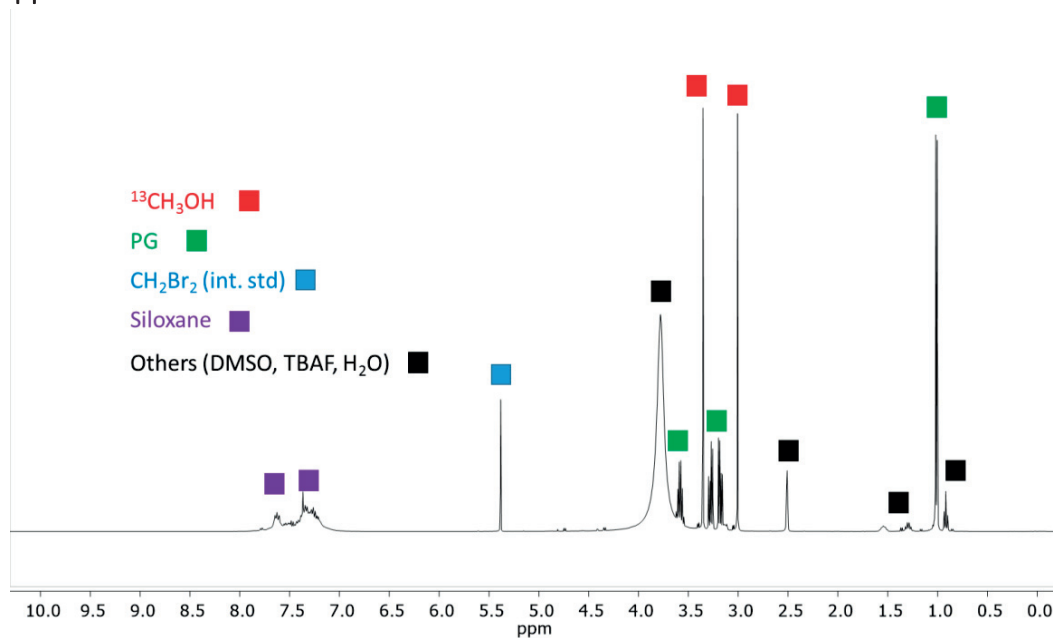


Fig. A.3.4.1. ^1H NMR spectrum of the crude reaction mixture after hydrolysis. Conditions: (1) ^{13}C -PC (100 mg), TBAF (10 mg), PhSiH_3 (2 eq.), 60°C , 3 h. (2) aq. NaOH (0.1 mL, 5%), r.t., 2 h. Yield determined by comparison with CH_2Br_2 .

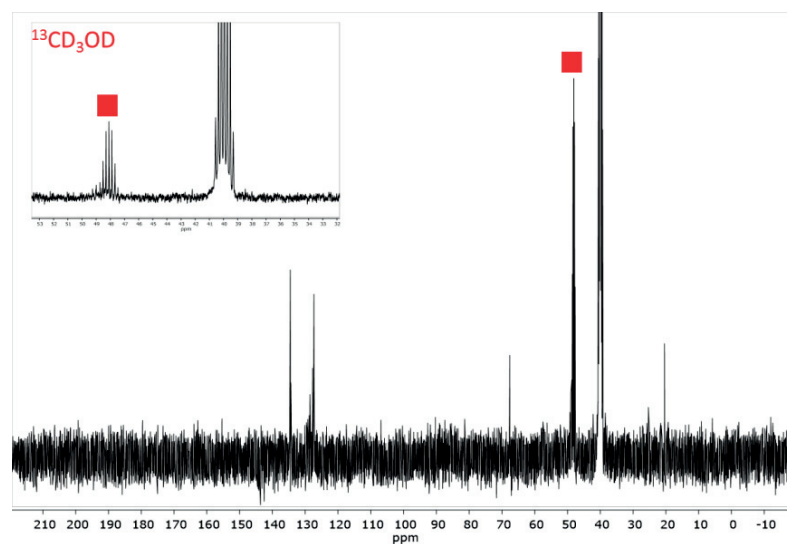


Fig. A.3.4.2. ^{13}C NMR spectrum of the crude reaction mixture after hydrolysis. Conditions: (1) ^{13}C -PC (100 mg), TBAF (10 mg), Ph_2SiD_2 (2 eq.), 60°C , 3 h. (2) aq. NaOD (0.1 mL, 5%), r.t., 2 h.

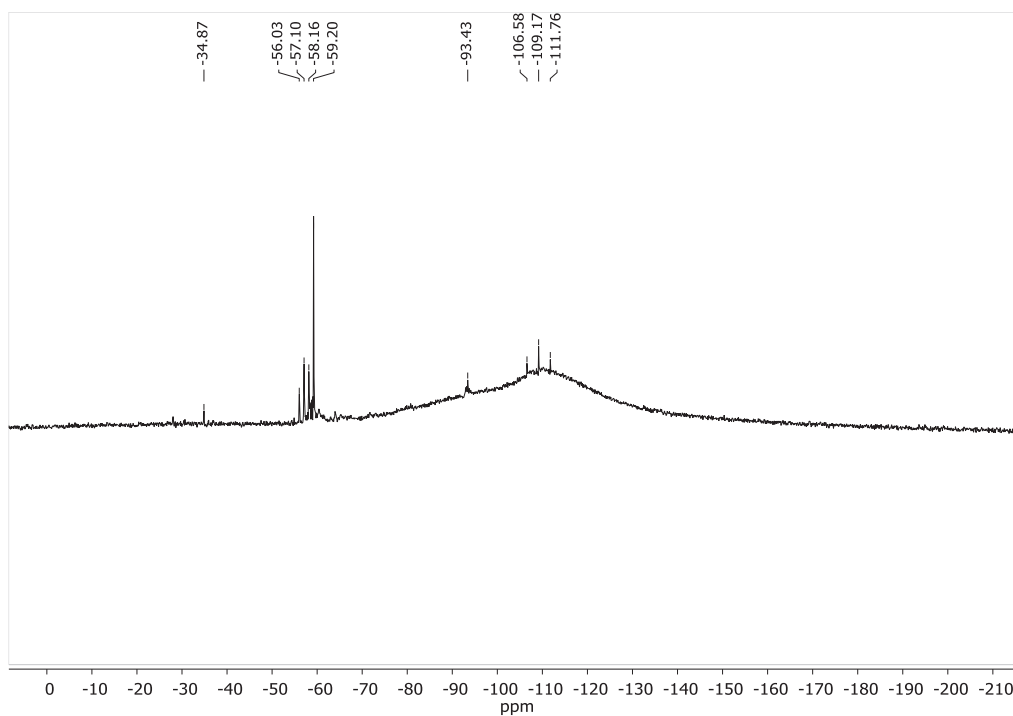


Fig. A.3.4.3. ^{29}Si NMR spectrum of the crude reaction mixture in DMSO-d₆ prior to hydrolysis. Conditions: PC (100 mg), TBAF (16 mg), Ph₂SiH₃ (1 eq.), 60 °C, 3 h.

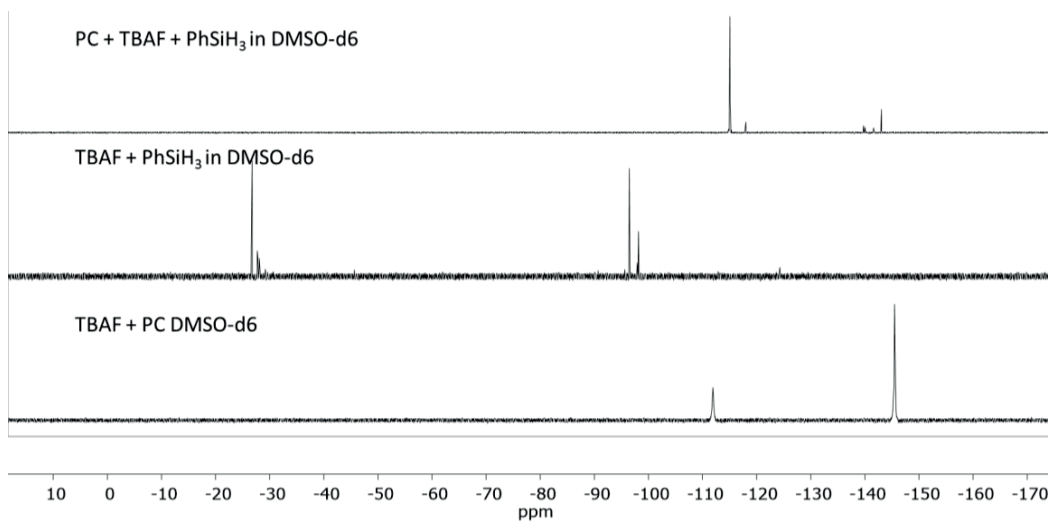


Fig. A.3.4.4. ^{19}F NMR spectra of different TBAF mixtures in DMSO-d₆. Conditions: top, PC (100 mg), TBAF (16 mg), Ph₂SiH₃ (1 eq.), 60 °C, 3 h), middle, TBAF (16 mg), PhSiH₃ (1 mmol), DMSO-d₆ (0.5 mL), 60 °C, 3 h, bottom: TBAF (16 mg) in DMSO-d₆ (0.5 mL).

Curriculum Vitae

Bobbink Felix Daniel

+41789204771 (mobile phone)

Felix.bobbink@gmail.com

Route du Boiron 55, 1260

Nyon

Born on August 30th, 1991, Switzerland

Nationality: Dutch

Marital status: Single

Education

- 2014 – 2018 PhD in the laboratory of Prof. Dyson,
Swiss Federal Institute of Technology (EPFL), Lausanne, Switzerland
Catalyst design for the transformation of CO₂ into value-added products.
- 2013 – 2014 Master project in the laboratory of Prof. Ning Yan,
National University of Singapore, Singapore
Conversion of chitin derived N-acetyl-D-glucosamine (NAG) into polyols over transition metal catalysts and hydrogen in water
- 2012 – 2014 Master of Science in Molecular and Biological Chemistry
Swiss Federal Institute of Technology (EPFL), Lausanne, Switzerland
- 2009 – 2012 Bachelor of Science in Chemistry and Chemical Engineering
Swiss Federal Institute of Technology (EPFL), Lausanne, Switzerland
- 2005 – 2008 Baccalauréat à option international (Néerlandais), mention bien
Lycée International de Ferney-Voltaire, Ferney-Voltaire, France

Professional experiences

Autumn 2016 Joined the “Comission d’Enseignement” at EPFL
Responsibility

Autumn 2016 Teaching assistant for “General Chemistry” (Prof. Lothar Helm)
Supervision, responsibility

Autumn 2016 Teaching assistant for the master project of Alexandre Redondo

Autumn 2015 Teaching assistant for “General Chemistry” (Prof. Lothar Helm)
Supervision, responsibility

Autumn 2015 – June 2016 Supervision of the 4th year project of Weronika Gruszka (University of Edinburgh)
Supervision, responsibility, resulted in Weronika’s first research paper

Autumn 2015 Teaching assistant for the master project of Antoine Van Muyden
Supervision, responsibility, resulted in Antoine’s first research paper

Spring 2014 Teaching assistant for the semester project (master level) of Johanna Burri
Supervision, responsibility

Autumn 2014 Teaching assistant for a chemistry practical course for third year chemistry students
Supervision, responsibility

Autumn 2012 Teaching assistant for “General chemistry” and “Organic chemistry” (Prof. Luc Patiny) courses
Supervision, involvement

Spring 2012 Project in the Laboratory for Computational Molecular Design (LCMD)
“Absorption spectrum of Azulene using ab-initio on-the-fly methods”

Autumn 2013 Teaching assistant for “General Chemistry” course (Prof. Luc Patiny)
Supervision, involvement

Summer 2010 Internship at “car-pool” service at CERN (Centre Européen de Recherches Nucléaires)

May 2009 Staff member for Balelec (student music festival)
Sociability

2010 - 2014 Private tuition in sciences for high school and Bachelor students
Supervision, involvement

Publication, Posters, Presentations & Prizes

Publications:

2013:

1) Ghazali-Esfahani, S.; Song, H.; Păunescu, E.; **Bobbink, F. D.**; Liu, H.; Fei, Z.; Laurenczy, G.; Bagherzadeh, M.; Yan, N.; Dyson, P. J., “Cycloaddition of CO₂ to epoxides catalyzed by imidazolium-based polymeric ionic liquids”, *Green Chem.* **2013**, *15*, 1584-1589.

2014:

2) Pierson, Y.; Chen, X.; **Bobbink, F. D.**; Zhang, J.; Yan, N., “Acid-Catalyzed Chitin Liquefaction in Ethylene Glycol”, *ACS Sustain. Chem. Eng.* **2014**, *2*, 2081–2089.

3) **Bobbink, F. D.***; Zhang, J.*; Pierson, Y.; Chen, X.; Yan, N., “Conversion of chitin derived N-acetyl- D-glucosamine (NAG) into polyols over transition metal catalysts and hydrogen in water”, *Green Chem.* **2015**, *17*, 1024–1031.

* = equal contribution

4) Das, S.; **Bobbink, F. D.**; Laurenczy, G.; Dyson, P. J., "Metal-Free Catalyst for the Chemoselective Methylation of Amines Using Carbon Dioxide as a Carbon Source" *Angew. Chemie Int. Ed.* **2014**, *53*, 12876–12879.

2015:

5) Das, S.; **Bobbink, F. D.**; Gopakumar, A.; Dyson, P. J., "Soft Approaches to CO₂ Activation", *Chimia*, **2015**, *69*, 765-768.

6) Fei, Z.; **Bobbink, F. D.**; Paunescu, E.; Scopelliti R.; Dyson, P. J., "Influence of Elemental Iodine on Imidazolium-Based Ionic Liquids: Solution and Solid-State Effects" *Inorganic Chemistry*, **2015**, *54* (21), 10504-10512.

7) Das, S, **Bobbink, F. D.**; Soudani, M.; Bulut, S.; Dyson, P. J., "Thiazolium carbene catalysts for the fixation of CO₂ onto amines" *Chem. Comm.*, **2016**, *52*, 2497-2500.

2016:

8) **Bobbink, F. D.**; Paul J. Dyson; "Synthesis of carbonates and related compounds incorporating CO₂ using ionic liquid-type catalysts: State-of-the-art and beyond" *J. Cat.*, **2016**, *343*, 52-61.

9) **Bobbink, F. D.**; Fei Z.; Scopelliti, R.; Das, S.; Dyson, P. J., "Functionalized Ionic (Poly)Styrenes and their Application as Catalysts in the Cycloaddition of CO₂ to Epoxides" *Helv. Chim. Acta.*, **2016**, *99*, 1-9.

10) **Bobbink, F. D.***; Gruszka, W.*; Hulla, M.; Das, S.; Dyson, P. J.; "Synthesis of cyclic carbonates from diols and CO₂ catalyzed by carbenes" *Chem. Commun.*, **2016**, *52*, 10787-10790.

*equal contribution

11) Hulla, M; **Bobbink, F. D.**; Das, S.; Dyson, P. J., "Carbon Dioxide Based N-Formylation of Amines Catalyzed by Fluoride and Hydroxide Anions", *ChemCatChem*, **2016**, *8*, 3338-3342.

2017:

12) **Bobbink, F. D.***; Van Muyden, A. P.; Gopakumar, A.; Fei Z.; Dyson, P. J., "Synthesis of Cross-linked Ionic Poly(styrenes) and their Application as Catalysts for the Synthesis of Carbonates from CO₂ and Epoxides" *ChemPlusChem*, **2017**, *82*, 144-151.

*equal contribution

13) **Bobbink, F.D.**; Das, S.; Dyson, P. J.; "N-formylation and N-methylation of amines using metal-free N-heterocyclic carbene catalysts and CO₂ as carbon source", *Nature Protocols*, **2017**, *12*, 417-428.

14) **Bobbink, F. D.***; Wei, Z.*; Fei, Z.; Dyson, P.J., "Polyimidazolium Salts: Robust Catalysts for the Cycloaddition of Carbon Dioxide into Carbonates in Solvent-Free Conditions", *ChemSusChem*, **2017**, *10*, 2728-2735.

*equal contribution

2018:

15) Perrin, F. G.; **Bobbink, F. D.**; Paunescu, E.; Fei, Z.; Scopelliti R.; Laurenczy, G.; Katsyuba, S.; Dyson, P. J., "Towards a frustrated Lewis pair-ionic liquid system Florian", *Inorg. Chimica Acta*, **2018**, *470*, 270-274.

16) Izak, P.; **Bobbink, F. D.**; Hulla, M.; Klepic, M; Friess, K; Hovorka, S; Dyson, P. J., "Catalytic Ionic-Liquid Membranes: The Convergence of Ionic-Liquid Catalysis and Ionic-Liquid Membrane Separation Technologies", *ChemPlusChem*, **2018**, *83*, 7-18.

17) Siankevich, S.; Mozzettini, S.; **Bobbink, F. D.**; Ding, S.; Fei, Z.; Yan, N.; Dyson, P. J., "Influence of the Anion on the Oxidation of 5-Hydroxy-methylfurfural by Using Ionic-Polymer-Supported Platinum Nanoparticle Catalysts", *ChemPlusChem*, **2018**, *83*, 19-23

18) **Bobbink, F. D.**; Vasilyev, D.; Hulla, M.; Chamam, M., Menoud, F., Laurency, G., Katsyuba, S., Dyson, P. J., "Intricacies of Cation–Anion Combinations in Imidazolium Salt Catalyzed Cycloaddition of CO₂ Into Epoxides" *ACS Catal.*, **2018**, *8*, 2589-2594.

19) **Bobbink, F. D.**; Menoud, F.; Dyson, P. J.; **2018**, *manuscript submitted*.

Posters:

1) **SCS Fall meeting** – Zürich, September 2014: "*Towards Ocean Based Biorefinery: N-Acetyl-D-Glucosamine (NAG) to Value-Added Polyols.*"

2) **World Gas Congress** – Paris, June 2015: "*Capture of CO₂ and Manufacturing of Products From CO₂*"

3) **SCS Fall meeting** – Lausanne, September 2015: "*Synthesis, Characterization and Application of Styrene-Functionalized Imidazolium Salts.*"

4) **SSS meeting** – Saas-Fee, January 2016

5) **SCS Fall meeting** – Zürich, September 2016

Presentations:

1) **SCCER meeting**, Villars, January 2015 : "*Formation of Methanol from Carbon Dioxide Via Carbonates*"

2) **e-COST meeting**, Prague, Czech Republic, April 2015: "*Synthesis, Characterization and Application of Task-Specific Ionic Styrenes.*"

3) "**My Thesis in 3 minutes**" contest, EPFL, October 2015 (3rd place)

4) **SCCER meeting**, Les Diablerets, January 2016

5) "**My thesis in 180 seconds**" contest, first Swiss National Final, June 2016 (Broadcasted on RTS on 14th October 2016 on RTS 1 and RTS 2)

6) "**Swiss Snow Symposium**", Saas-Fee, January 2017, runner-up prize.

7) "**SCS Fall Meeting**", Bern, August 22 2017

Prizes:

1) Prize for excellent contribution as a teaching-assistant (received 27.10.16)

2) SCNAT travel award 2017

Languages

Dutch Mother tongue

French Fluent

English Fluent (CAE)

German Basic knowledge (level B2)

Extra-curricular activities

1996-present Football player at Football Sud Gessien (France)

Leadership, competition

1996-2009 Competition swimming at Meyrin Natation (Switzerland)

Competition

1996-2005 Competition skiing at Ski Club Thoiry (France)

Competition